

Elucidating mechanisms of protection conferred by a primary *Mycobacterium tuberculosis* (Mtb) infection to a secondary Mtb infection in non-human primates

by

Sharie Keanne Chua Ganchua

B.S., University of the Philippines Manila, 2007

Submitted to the Graduate Faculty of the
School of Medicine in partial fulfillment
of the requirements for the degree of
Doctor of Philosophy

University of Pittsburgh

2020

UNIVERSITY OF PITTSBURGH

SCHOOL OF MEDICINE

This dissertation was presented

by

Sharie Keanne Chua Ganchua

It was defended on

July 10, 2020

and approved by

Simon M. Barratt-Boyes, PhD, Professor of Immunology and Infection Diseases and
Microbiology

Jennifer Bomberger, PhD, Associate Professor of Microbiology and Molecular Genetics

Timothy Hand, PhD, Assistant Professor of Immunology and Pediatrics

John V. Williams, MD, Professor of Pediatrics

Dissertation Director: JoAnne L. Flynn, PhD, Professor of Microbiology and Molecular
Genetics, Medicine and Immunology

Copyright © by Sharie Keanne Chua Ganchua

2020

Elucidating mechanisms of protection conferred by a primary *Mycobacterium tuberculosis* (Mtb) infection to a secondary Mtb infection in non-human primates

Sharie Keanne Chua Ganchua, PhD

University of Pittsburgh, 2020

Mycobacterium tuberculosis (Mtb), the causative agent of tuberculosis (TB), has lived with man for thousands of years. Yet, TB is still a major global health problem killing more than a million people every year. Bacille Calmette-Guerin was developed almost a hundred years ago and is still the only licensed vaccine for TB. The main hindrance to current vaccine development is the lack of correlates and immune targets of protection. Early published data suggest that individuals with latent TB have a lower risk of developing active TB disease after Mtb re-exposure. A more recent study showed that macaques with an ongoing primary Mtb infection are protected against establishment of granulomas and bacterial growth from a secondary Mtb challenge. The precise immune mechanisms of this protection are largely unknown. The main goal of this dissertation is to investigate the importance of bacterial viability and CD4 T cells in the protection against Mtb reinfection using DNA-barcoded Mtb strains. Eliminating live Mtb bacilli by drug treatment reduced but did not abolish the protection against the establishment of and bacterial growth in granulomas arising from the second infection; although the effect of long term primary Mtb infection against a second infection needs to be further studied. Depletion of CD4 T cells in macaques before reinfection resulted in increased bacterial burden in secondary granulomas, however it only increased the number of secondary granulomas in some macaques showing heterogeneity in these animals. Moreover, we showed that CD4 T cells are important in preventing Mtb dissemination to the lymph nodes. Bacterial burden in secondary granulomas, lungs and lymph nodes in the CD4 T cell-depleted macaques did not reach the level of bacterial burden in the naïve controls suggesting protection is multifactorial. Lastly, we showed

that lymph nodes are more than just sites of antigen presentation and immune activation; rather, they are sites of Mtb persistence and growth. Overall, this dissertation provided elements to consider and target in the design and testing of vaccines and therapeutics.

Table of Contents

Acknowledgements xviii

1.0 Introduction..... 1

1.1 Epidemiology of tuberculosis..... 1

1.2 Mycobacterium tuberculosis 1

1.3 Clinical aspects of TB – diagnosis, vaccine and treatment 3

1.4 Granuloma – the hallmark of tuberculosis 10

1.5 Immune response to tuberculosis..... 12

1.6 Non-human primate model of tuberculosis..... 19

1.7 Lymph nodes – the neglected battlefield of tuberculosis 22

1.8 Reinfection in TB..... 27

2.0 Gaps in knowledge and specific aims 29

3.0 Drug treatment does not abolish the protection against Mtb reinfection..... 32

3.1 Introduction 32

3.2 Methodology..... 34

3.2.1 Ethics Statement.....34

3.2.2 Animals, infections, drug treatment and disease tracking by PET CT36

3.2.3 Bronchoalveolar lavage (BAL)37

3.2.4 Necropsy Procedures38

3.2.5 Isolation of genomic DNA from bacteria38

3.2.6 Library identification39

3.2.7 Intracellular cytokine staining and flow cytometry39

| | |
|-----------------------------------------------------------------------------------------------------------------------------|----|
| 3.2.8 Luminex on BAL samples | 41 |
| 3.2.9 Statistical Analysis | 41 |
| 3.3 Results..... | 42 |
| 3.3.1 Drug treatment sterilized most macaques | 42 |
| 3.3.2 Drug treatment does not abolish protection from second infection | 45 |
| 3.3.3 Drug treatment does not change lymphocyte populations and cytokine response in airways | 48 |
| 3.3.4 Similar immunological environment in new granulomas, involved lymph nodes and uninvolved lungs in both groups..... | 57 |
| 3.4 Discussion | 64 |
| 4.0 CD4 T cells are important in protecting against Mtb reinfection | 70 |
| 4.1 Introduction | 70 |
| 4.2 Methodology..... | 71 |
| 4.2.1 Ethics Statement..... | 71 |
| 4.2.2 Animals, infections, CD4 T cell depletion and disease tracking by PET CT73 | |
| 4.2.3 Antibody validation..... | 76 |
| 4.2.4 Bronchoalveolar lavage | 76 |
| 4.2.5 Necropsy Procedures | 77 |
| 4.2.6 Isolation of genomic DNA from bacteria | 79 |
| 4.2.7 Library and barcode identification | 79 |
| 4.2.8 Intracellular cytokine staining and flow cytometry | 80 |
| 4.2.9 Luminex on lung homogenates | 81 |
| 4.2.10 3D rendering of Mtb barcodes in macaque lungs | 82 |

| | |
|----------------------------------------------------------------------------------------------------------------------------------------------------------------|-----|
| 4.2.11 Statistical analysis | 82 |
| 4.3 Results..... | 83 |
| 4.3.1 Experimental Design..... | 83 |
| 4.3.2 CD4 T cell depleting antibody does not mask CD4 receptors..... | 85 |
| 4.3.3 Macaques with primary Mtb infection, regardless of drug treatment, have significantly higher T cell counts and cytokine-producing CD4 T cells in BAL ... | 87 |
| 4.3.4 Robust CD4 T cell depletion in blood and tissues | 90 |
| 4.3.5 CD4 T cell depletion diminishes the protection a primary Mtb infection confers against a secondary Mtb challenge | 96 |
| 4.3.6 Number of CD4 and CD8 T cells in the airways negatively correlate with new granuloma formation and total lung CFU | 99 |
| 4.3.7 CD4 T cell numbers in the blood and lungs do not correlate with new granuloma formation and bacterial burden in lungs and lymph nodes | 105 |
| 4.3.8 CD4 T cell depletion did not affect CD8 T cell function in tissues during second infection | 109 |
| 4.3.9 Cytokine production in uninvolved lung lobes..... | 115 |
| 4.3.10 CD4 T cell depletion results in dissemination of second infection to lymph nodes..... | 118 |
| 4.4 Discussion | 127 |
| 4.5 Acknowledgements | 134 |
| 5.0 Lymph nodes are sites of prolonged bacterial persistence during <i>Mycobacterium tuberculosis</i> infection in macaques | 135 |
| 5.1 Introduction | 135 |

| | |
|----------------------------------------------------------------------------------------------------------------------------------------|------------|
| 5.2 Methodology | 139 |
| 5.2.1 Animals | 139 |
| 5.2.2 Ethics Statement | 141 |
| 5.2.3 FDG PET-CT imaging | 142 |
| 5.2.4 Necropsy Procedures | 143 |
| 5.2.5 Intracellular cytokine staining and flow cytometry | 144 |
| 5.2.6 Histology | 145 |
| 5.2.7 Immunohistochemistry | 146 |
| 5.2.8 Isolation of genomic DNA from bacteria | 146 |
| 5.2.9 Statistical Analysis | 147 |
| 5.3 Results | 148 |
| 5.3.1 ¹⁸F-FDG PET CT imaging can identify Mtb-infected thoracic lymph nodes | 148 |
| 5.3.2 Thoracic lymph nodes of rhesus macaques have reduced killing capacity for Mtb compared to cynomolgus macaques | 151 |
| 5.3.3 Low Mtb burden and better killing in peripheral lymph nodes | 163 |
| 5.3.4 Lymph node effacement is associated with higher bacterial burden | 166 |
| 5.3.5 Bacterial burden is associated with decreased capacity to induce cytokine production in lymph nodes with granulomas | 172 |
| 5.3.6 Short course drug treatment is more effective in lung granulomas than in thoracic lymph nodes | 181 |
| 5.4 Discussion | 183 |
| 6.0 Summary, implications and future directions | 189 |

| | |
|----------------------------------------------------------------------------------------------------------------------|-----|
| 6.1 Bacterial viability is not essential but CD4 T cells are important in protection against a second infection..... | 189 |
| 6.2 Lymph nodes are sites of Mtb persistence and growth..... | 198 |
| 7.0 Publication record..... | 204 |
| 8.0 Lymph nodes – the neglected battlefield in tuberculosis..... | 205 |
| 8.1 Introduction | 205 |
| 8.2 From the air to the lymph nodes | 206 |
| 8.3 Bacterial dynamics in the lymph nodes | 212 |
| 8.4 Immune response of lymph nodes to Mtb | 215 |
| 8.5 Mtb remodels lymph node structure | 217 |
| 8.6 Mtb disseminates ipsilaterally from lungs to lymph nodes | 220 |
| 8.7 Lymph nodes are sites of TB reactivation | 221 |
| 8.8 Lymph nodes influence effectiveness of BCG vaccine | 225 |
| 8.9 Lower drug penetration in lymph nodes | 227 |
| 8.10 Concluding Remarks..... | 229 |
| 8.11 Methodology..... | 230 |
| 8.11.1 Mtb dissemination from lungs to lymph nodes analysis..... | 230 |
| 8.11.2 Histology | 230 |
| 8.11.3 Ethics Statement..... | 230 |
| 8.12 Acknowledgements | 232 |
| Bibliography | 233 |

List of Tables

| | |
|---------------------------------------------------------------------------------------------------------------------------------------|------------|
| Table 1. Granuloma classification scheme..... | 39 |
| Table 2. Animals used in CD4 T cell depletion study. | 75 |
| Table 3. Granuloma classification scheme..... | 80 |
| Table 4. Animals used in the CFU, CEQ, histological studies. | 139 |
| Table 5. List of macaques used in this study (CFU, CEQ, CFU/CEQ)..... | 140 |
| Table 6. List of macaques used for immunological assays..... | 145 |
| Table 7. Cytokine responses in CFU+ and CFU- thoracic LNs..... | 173 |
| Table 8. T cell cytokines and proliferative capacity in response to PDBu and ionomycin in thoracic and peripheral LNs..... | 178 |
| Table 9. T cell cytokines in response to Mtb-specific antigens (ESAT-6 and CFP-10) in differentially effaced LNs..... | 180 |

List of Figures

| | |
|----------------------------------------------------------------------------------------------------------------------------------------------|-----------|
| Figure 1. The spectrum of tuberculosis..... | 6 |
| Figure 2. The structure of a granuloma..... | 11 |
| Figure 3. Serial PET CT imaging allows tracking of inflammation and formation of new granulomas. | 22 |
| Figure 4. Drug treatment reduced metabolic activity in lung granulomas and lymph nodes of macaques. | 43 |
| Figure 5. Drug treatment sterilized majority of the drug-treated macaques..... | 44 |
| Figure 6. Drug treatment does not abolish protection from second infection..... | 48 |
| Figure 7. No significant difference in lymphocyte populations in airways of the 2 groups from pre- to post-drug treatment..... | 49 |
| Figure 8. Similar changes in cytokine response of CD4 T cells to Mtb-specific antigens from pre- to post-drug treatment..... | 50 |
| Figure 9. Similar changes in cytokine response of CD8 T cells to Mtb-specific antigens from pre- to post-drug treatment..... | 51 |
| Figure 10. Similar counts of lymphocytes, CD4 T cells and CD8 T cells in BAL pre-second infection in both groups..... | 52 |
| Figure 11. No difference in CD4 T cell cytokine response against Mtb-specific antigens pre-second infection between the 2 groups..... | 53 |
| Figure 12. No difference in CD8 T cell cytokine response against Mtb-specific antigens pre-second infection between the 2 groups..... | 54 |

| | |
|------------------------------------------------------------------------------------------------------------------------------------|-----------|
| Figure 13. Non-drug treated group had higher levels of proinflammatory chemokines and cytokine. | 55 |
| Figure 14. Cytokines and chemokines measured in BAL pre-second infection. | 57 |
| Figure 15. Similar levels of lymphocytes in new granulomas of both groups. | 58 |
| Figure 16. Similar CD4 T cell cytokine response in new granulomas from drug-treated and non-drug treated groups. | 59 |
| Figure 17. Similar CD8 T cell cytokine response in new granulomas from drug-treated and non-drug treated groups. | 60 |
| Figure 18. Similar CD4 T cell cytokine response in involved lymph nodes from drug-treated and non-drug treated groups. | 61 |
| Figure 19. Similar CD8 T cell cytokine response in involved lymph nodes from drug-treated and non-drug treated groups. | 62 |
| Figure 20. Similar CD4 T cell cytokine response in uninvolved lungs from drug-treated and non-drug treated groups. | 63 |
| Figure 21. Similar CD8 T cell cytokine response in uninvolved lungs from drug-treated and non-drug treated groups. | 64 |
| Figure 22. Cross-sectional PET CT scans of a macaque in each group pre- and post-second infection. | 79 |
| Figure 23. Experimental Design. | 84 |
| Figure 24. Total lung FDG activity in α-CD4 and IgG groups pre- and post-drug treatment. | 85 |
| Figure 25. Anti-CD4 T cell depleting antibody does not mask CD4 receptors. | 86 |
| Figure 26. Greater T cell counts in BAL of macaques with primary Mtb infection. | 88 |

| | |
|----------------------------------------------------------------------------------------------------------------------------------------------------------------------------------|------------|
| Figure 27. Greater CD4 T cell counts producing cytokines in BAL of macaques with primary Mtb infection. | 89 |
| Figure 28. No difference in the numbers of functional CD8 T cells between naïve and primary-infected drug treated macaques. | 90 |
| Figure 29. CD4 T cell depletion in the blood. | 91 |
| Figure 30. Frequency of CD4 T cells in tissues at necropsy. | 93 |
| Figure 31. CD4 T cell counts in tissues at necropsy. | 94 |
| Figure 32. CD8 T cell counts in tissues at necropsy. | 95 |
| Figure 33. B cell counts in tissues at necropsy. | 96 |
| Figure 34. CD4 T cell depletion diminished protection a primary Mtb infection confers to a secondary Mtb challenge. | 98 |
| Figure 35. Correlation between CD4 T cell counts in the BAL and various disease outcome measures at necropsy. | 101 |
| Figure 36. Correlation between number of IFNγ-producing CD4 T cells in the BAL and various disease outcome measures at necropsy. | 102 |
| Figure 37. Correlation between number of TNFα-producing CD4 T cells in the BAL and various disease outcome measures at necropsy. | 103 |
| Figure 38. Correlation between CD8 T cell counts in the BAL and various disease outcome measures at necropsy. | 104 |
| Figure 39. Correlation between the number of CD4 T cells in the blood at second infection and various disease outcome measures in the α-CD4 group. | 106 |
| Figure 40. Correlation between the number of CD4 T cells in the blood at necropsy and various disease outcome measures in the α-CD4 group. | 107 |

| | |
|-------------------------------------------------------------------------------------------------------------------------------------------------------------------------|------------|
| Figure 41. Correlation between the number of CD4 T cells in the lungs at necropsy and various disease outcome measures in the α-CD4 group..... | 108 |
| Figure 42. CD4 T cell counts producing various cytokines in new granulomas. | 110 |
| Figure 43. CD8 T cell counts producing various cytokines in new granulomas. | 111 |
| Figure 44. CD4 T cell counts producing various cytokines in CFU+ thoracic lymph nodes. | 112 |
| Figure 45. CD8 T cell counts producing various cytokines in CFU+ thoracic lymph nodes. | 113 |
| Figure 46. CD4 T cell counts producing various cytokines in uninvolved lung lobes. | 114 |
| Figure 47. CD8 T cell counts producing various cytokines in uninvolved lung lobes. | 115 |
| Figure 48. Cytokine levels in uninvolved lung lobes..... | 116 |
| Figure 49. Cytokine levels in uninvolved lung lobes..... | 118 |
| Figure 50. Barcode heatmaps of naive controls. | 121 |
| Figure 51. Barcode heatmaps of IgG controls..... | 123 |
| Figure 52. Barcode heatmaps of α-CD4 group. | 125 |
| Figure 53. The number of unique barcodes in each animal, granulomas and lymph nodes. | 125 |
| Figure 54. 3D rendering of thoracic cavity of “best” and “worst” macaques from each group. | 126 |
| Figure 55. FDG PET CT analysis of Mtb infection in lymph nodes of cynomolgus and rhesus macaques..... | 150 |
| Figure 56. Modest positive correlation between LN SUVr and live bacterial burden at necropsy. | 151 |

| | |
|--------------------------------------------------------------------------------------------------------------------------------------------------------------|------------|
| Figure 57. Mtb burden and killing in lymph nodes of cynomolgus and rhesus macaques. | 153 |
| Figure 58. Comparison of CFU, CEQ and killing (CFU/CEQ) between cynomolgus and rhesus macaques at similar time points post infection. | 155 |
| Figure 59. LN CFU and CFU/CEQ of cynomolgus macaques with active disease, controlling disease and rhesus macaques at 16-29 weeks post-infection. | 157 |
| Figure 60. Isoniazid treatment for 2 months does not significantly change CEQ in lymph nodes. | 158 |
| Figure 61. Proportion of thoracic lymph nodes infected with Mtb in cynomolgus and rhesus macaques at necropsy. | 162 |
| Figure 62. Proportion of thoracic lymph nodes that had granuloma by gross and microscopic examination at necropsy. | 163 |
| Figure 63. Most peripheral lymph nodes that had detectable Mtb genome were sterile. .. | 165 |
| Figure 64. Mtb infection results in granuloma formation and in some instances lymph node effacement. | 167 |
| Figure 65. Histologic and immunohistochemical characterization of Mtb-infected macaque lymph nodes with varying levels of disease. | 169 |
| Figure 66. Lymph node effacement promotes Mtb growth. | 171 |
| Figure 67. Immune response in thoracic LNs of cynomolgus macaques with granulomas. | 176 |
| Figure 68. Comparison of immune responses in peripheral and thoracic LNs. | 179 |
| Figure 69. Correlation between extrapulmonary score (extent of extrapulmonary disease at necropsy) and LN necropsy score and bacterial burden. | 182 |

Figure 70. Reduction of bacterial burden in lymph nodes and lung granulomas of cynomolgus macaques after 2 months of linezolid (LZD) therapy (data from study [338]).
..... 183

Figure 71. Drug treatment does not abolish protection to secondary Mtb infection..... 193

Figure 72. CD4 T cell depletion reduces protection against Mtb reinfection..... 197

Figure 73. Role of CD4 T cells in Mtb reinfection. 198

Figure 74. *M. tuberculosis* infection in lymph nodes..... 202

Figure 75. *Mycobacterium tuberculosis* travels to the thoracic lymph nodes from the lungs.
..... 209

Figure 76. Mtb infection results in granuloma formation that disrupts the normal lymph node architecture. 219

Figure 77. Mtb is spread ipsilaterally from the lungs to the thoracic lymph nodes in macaques..... 221

Figure 78. Latent TB reactivation can start in the lymph nodes..... 224

Acknowledgements

This dissertation is dedicated to my parents.

Thank you for your unconditional love and support.

My PhD journey was everything that I had imagined and so much more. There were many highs but there were also many lows. I could not have made it without the help and support of many wonderful people of which I am taking the time to thank in this section.

First and foremost, I would like to thank my mentor, Dr. JoAnne L. Flynn, for taking me under her wing and pushing me not only to my limits but to break through my limits. She believed in me in times when I didn't believe in myself. I will not be the scientist that I am today without her. Her continuous support has been with me from the start to finish and even beyond as I start my job search. It truly is an honor and a joy to work with JoAnne and her lab. I could not have asked for a better mentor.

Second, I would like to thank the members of my dissertation committee for their kindness, understanding and support and for their thoughtful insights and critiques that helped make this dissertation better. It is a privilege to learn from the minds of such exceptional scientists.

Third, I would like to thank our collaborators in the Sarah Fortune lab without which this dissertation would not have been possible. I would like to especially thank Forrest Hopkins for untiringly processing my samples to identify Mtb libraries and barcodes and for creating the heatmaps that I included in this dissertation.

Fourth, I would like to thank the members (past and present) of the Flynn, Lin, Scanga, Mattila and Gideon labs for their support in my projects. I am grateful for the vet techs for taking such good care of our animals and for obtaining blood, lymph node and BAL samples. I also want to express my gratitude to the research techs in the lab for their help in processing the samples specially during necropsies. My heartfelt thanks to Hannah Gideon for teaching me flow cytometry and for her support and helpful advice in my studies. To Pauline Maiello, thank you for teaching me statistics and for quelling my panic attacks when faced with “not significantly different” data. Everyone in the lab is like a family to me. I could not have made it without their support. They are a bunch of quirky individuals always ready to help, always willing to listen, always making jokes, always ready for a trip to Everyday Noodles or to a karaoke party at KBOX and always making delicious food that they readily share with everyone.

Fifth, I would like to thank my friends and family in the Philippines and the US for their unending love and support throughout my PhD journey.

Last but not the least, I would like to thank God for orchestrating everything that resulted in my coming to the University of Pittsburgh and joining the Flynn lab. He was the rock I clung to in the lowest points of my PhD journey. He gave me hope when I was in despair. He gave me strength when I felt weak. He gave me peace in the face of fear.

1.0 Introduction

“Where youth grows pale, and spectre-thin, and dies.”

John Keats, Ode to a Nightingale, 1819

1.1 Epidemiology of tuberculosis

Tuberculosis (TB) is the leading cause of death from a single infectious microbe in the world. In 2018 alone, an estimated 10 million people developed the active form of TB and 1.45 million people died from TB [2]. Approximately 1/4 of the world’s population (~2 billion people) is currently infected with *Mycobacterium tuberculosis* [3], the bacteria that causes TB, however, most of these infected individuals reside in developing countries in Asia and Africa [2]. While a diagnosis of TB does not necessarily mean a death sentence in the modern world because of the discovery of antibiotics, emergence of drug resistance is becoming an important public health problem. In 2018, an estimated 390,000 of new cases were multidrug-resistant TB (MDR-TB; ie. resistant to two first-line anti-TB drugs – rifampicin and isoniazid) [2].

1.2 *Mycobacterium tuberculosis*

Mycobacterium tuberculosis (Mtb) is a member of the *Mycobacterium tuberculosis* complex (MTBC) which is comprised of *M. tuberculosis* (humans), *M. bovis* (cattle), *M. africanum* (humans), *M. caprae* (sheep and goats), *M. microti* (voles) and *M. pinnipedii* (sea lions and seals)

[4]. Despite the differences in host specificity and pathogenicity, members of the MTBC share a 99.9% similarity in their genomic sequences [5, 6]. *M. tuberculosis* has 4.4 million base pairs with a high GC content of 65.9% encoding ~4,000 genes [7, 8]. *M. tuberculosis* and *M. africanum* form 7 lineages based on large sequence polymorphism, single nucleotide polymorphism markers and geographical location where each lineage is endemic. Some lineages can be found worldwide (eg. Lineage 2 which includes the Beijing strain and Lineage 4 which includes Erdman and H37Rv strains) while some are geographically restricted (eg. Lineages 5 and 6 in West Africa and Lineage 7 in Ethiopia) [9, 10].

Mtb are slow-growing, non-motile, non-spore forming aerobic bacilli. They have a 24 hour doubling time at 37°C in a laboratory setting, taking approximately 3 weeks to form rough colonies on a 7H11 agar plate [8]. One notable feature of Mtb is its thick cell wall. It is rich in lipids such that the cell wall lipid component comprises ~40% of the cell dry mass [11]. Like Gram-negative bacteria, it has an outer membrane, however this is composed mainly of long-chain fatty acids called mycolic acids. The mycolic acids are attached to an arabinogalactan layer which in turn is linked to a peptidoglycan layer which sits right above a typical lipid bilayer inner membrane [8, 11-13]. The mycobacterial cell wall serves as a relatively impenetrable layer to antibiotics and is the site of several virulence factors such as phenolic glycolipids, lipoarabinomannan (LAM), sulpholipids, cord factor (trehalose dimycolate), and phthiocerol dimycocerosate [8, 14, 15]. Gram staining is not effective to visualize mycobacteria under the microscope because of the high lipid content of their cell wall. Mycobacteria in samples can be detected by using the Ziehl-Neelsen (or other similar) staining method with the Mtb cell wall retaining the carbol fuchsin stain after acid-alcohol washes [16, 17]. Thus, mycobacteria are referred to as “acid-fast bacilli”.

Bacille Calmette-Guerin (BCG) is an attenuated form of *M. bovis* obtained through 230 serial in vitro passages in ox bile-soaked glycerinated potato slices over 13 years [18]. It is the only licensed vaccine for TB. BCG can protect infants and children from serious and disseminated disease (e.g. miliary TB, skeletal TB, and meningitis) but has variable efficacy in protecting adults from the more common form of disease, pulmonary TB [19]. An important genetic difference between BCG and Mtb is the deletion of region of difference 1 (RD1) which is in part responsible for BCG's attenuation [20-22]. RD1 forms part of the 6 kDa early secretory antigenic target (ESAT-6) secretion system (ESX-1), a Type VII secretion system, and encodes 2 major highly immunogenic secreted proteins, ESAT-6 and culture filtrate protein-10 (CFP-10) [7, 23, 24]. ESX-1 is a major virulence factor responsible for the lysis of the phagosome membrane in macrophages allowing Mtb or, more likely antigens, to escape into the cytosol [25-28]. ESAT-6 and CFP-10 have been shown to prevent phagosome and lysosome fusion [29], inhibit toll-like receptor signaling [30] and induce necrosis in macrophages promoting cell-to-cell spread of Mtb [31, 32]. ESAT-6 also inhibits T cell proliferation and IFN γ , IL-17 and TNF production in T cells [33].

1.3 Clinical aspects of TB – diagnosis, vaccine and treatment

A person gets infected with Mtb when it enters the airways in the form of inhaled droplet nuclei expelled from individuals with active TB disease [34]. About 30% of individuals exposed to Mtb will become infected. The most widely used method for detecting Mtb infection is the tuberculin skin test (TST). The TST involves purified protein derivative (PPD) injected intradermally into the forearm. A delayed type hypersensitivity response (due to cell-mediated immunity) results in induration at the site and is measured 48 to 72 hours post-injection. PPD was

developed by repeated precipitation of proteins from steamed cultures of Mtb [35]. Individuals who were BCG-vaccinated or infected with nontuberculous mycobacteria (NTM), however, can present as false positives using this method [36], although the epidemiology suggests that the TST response due to BCG vaccination wanes ≥ 10 years after vaccination [37, 38]. Thus, a more specific method should be used for individuals known to have been vaccinated by BCG and in settings with high incidence of NTM infections. Interferon gamma (IFN γ) release assays (IGRAs) measure the T cell response to Mtb specific antigens, ESAT-6 and CFP-10, which are encoded by RD1. Only a few NTM species have RD1 and it is absent in BCG [20, 39]. Both TST and IGRAs are widely used for the diagnosis of Mtb infection, but neither is diagnostic for whether a person has active or latent TB [40-43].

The gold standard for TB diagnosis is still bacterial culture from sputum or bronchoalveolar lavage. However, because of the slow-growing nature of Mtb, it can take up to 8 weeks before results become available; the use of liquid media can shorten this time to 1-3 weeks [44]. Aside from being slow, culture can be expensive and requires specialized laboratories to perform [45]. Smear microscopy using the Ziehl-Neelsen staining method, on the other hand, is inexpensive and is the most widely used diagnostic technique in developing countries where most of the TB cases occur [45]. Although smear microscopy is highly specific its sensitivity is limited [46]. The World Health Organization has recommended the use of LED microscopy because of increased sensitivity, similar specificity, cost-effectiveness and quicker results compared to normal light smear microscopy [47]. Other techniques of TB diagnosis include chest X-ray and nucleic acid-based diagnostic assays, such as Xpert Mtb/Rif developed by Cepheid which can provide a diagnosis of active TB and drug resistance data in just 2 hours [45, 48].

Once infected, approximately 5-10% of individuals develop active TB disease. The symptoms of active TB are cough that lasts 3 weeks or longer, fever, night sweats, chills, loss of appetite and weight loss, signs of disease on chest x-ray or CT, TST or IGRA positivity, and confirmed by culture if possible. The majority of the Mtb-infected population (90-95%) control Mtb but does not completely eliminate it. These individuals are considered to be latently infected with Mtb (known as LTBI) and do not exhibit any symptoms but have evidence of Mtb infection. Around 10% of LTBI individuals will reactivate in their lifetime and will develop active TB disease [49, 50]. HIV co-infection increases the risk of reactivation TB to 10% per year [51, 52].

The classical dogma of binary states of Mtb infection, that is active TB vs. latent infection, is now obsolete. A new paradigm shift has occurred pushing towards Mtb infection as a spectrum (Figure 1) [1, 53, 54]. On one end of the spectrum, there are people who have naturally cleared Mtb infection. They may be positive or negative by TST and IGRA, exhibit no symptoms, have negative sputum smear and culture and normal chest x-ray [1, 42, 54]. Some of these people might be “resisters”, those who despite documented extended exposure to a confirmed TB case remain TST and IGRA negative, and “reverters”, people who were TST and IGRA positive and revert back to being negative to both tests [54-59]. Next on the spectrum are people who are TST and IGRA positive, have intermittent positive sputum culture but are smear negative, may exhibit mild to no symptoms and have a normal chest x-ray [1, 42, 54]. Individuals with active TB disease are positive for TST and IGRA, sputum culture positive, smear positive or negative, chest x-rays will show a range of disease and symptoms will range from mild to severe [1, 42, 54].

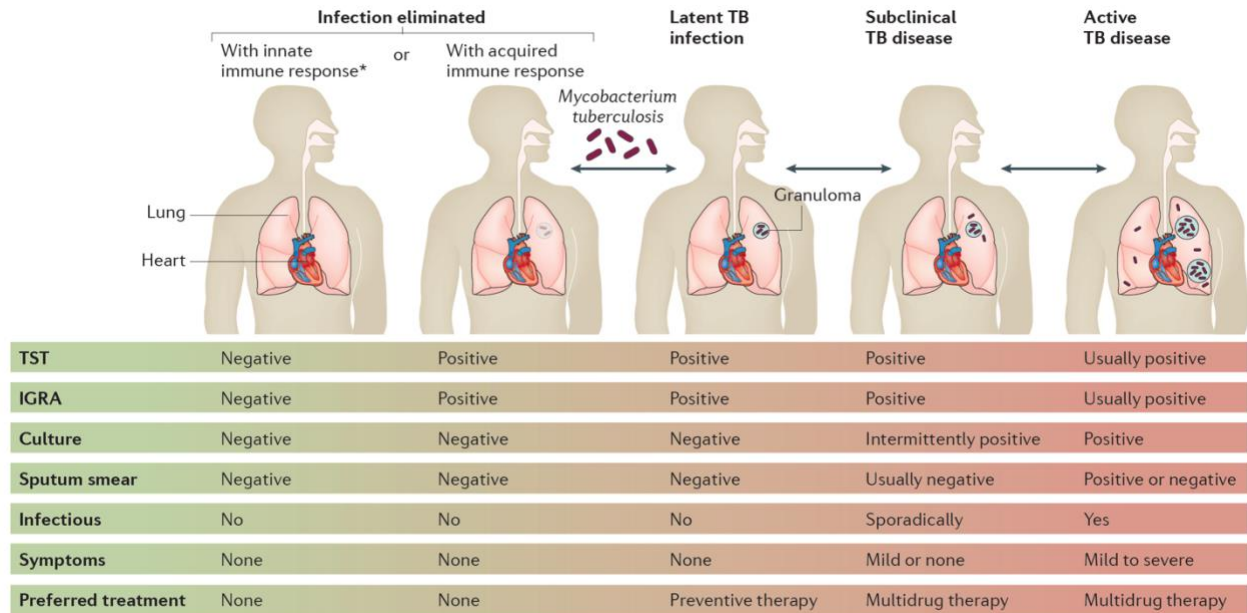


Figure 1. The spectrum of tuberculosis

Some people naturally clear Mtb infection either by their innate or adaptive immune system. People who remain infected with Mtb can present a range of results in various diagnostic tests and a wide range of symptoms. Reproduced with permission from Springer Nature, Pai et al., 2016 [1].

BCG, the only licensed TB vaccine used since the early 1920s, has variable efficacy in protecting adults from pulmonary TB [19]. However, there have been exciting recent developments in TB vaccines. In December of 2019, Tait and colleagues published the final results of a Phase 2b clinical trial of the subunit vaccine, M72:AS01E, which enrolled 3289 HIV-negative individuals with LTBI divided into 2 cohorts, one of which received the vaccine and the other a placebo. After 3 years of follow-up, M72:AS01E was shown to reduce the progression of LTBI to active TB by 49.7% [60]. A phase 2 clinical trial enrolling 990 BCG-vaccinated but IGRA negative adolescents (i.e. not Mtb infected) sought to evaluate the efficacy of H4:IC31 vaccine and BCG revaccination in preventing Mtb infection (conversion of IGRA to positive) and disrupting

continued Mtb infection (reversion of positive IGRA to negative) compared to placebo. While neither vaccine was effective in preventing Mtb infection (IGRA conversion), BCG revaccination reduced the rate of sustained IGRA conversion with 45.4% efficacy compared to placebo [61]. The most recent promising vaccination studies in macaques are with the use of a rhesus cytomegalovirus vector expressing Mtb-specific antigens (RhCMV-Mtb Ag) [62] and intravenous BCG vaccination (IV-BCG) [63]. Fourteen out of 34 (41%) rhesus macaques vaccinated with RhCMV-Mtb Ag did not develop any TB disease by CT scan nor at necropsy compared to 0 of the 17 unvaccinated controls. In addition, 10 out of these 14 did not grow any Mtb in any of the tissues examined. The disease of the remaining vaccinated animals was significantly reduced compared to unvaccinated controls [62]. Most recently, our group showed remarkable results with administering BCG intravenously in rhesus macaques. Six out of 10 IV-BCG vaccinated macaques did not form any lung granulomas after Mtb infection. Three of the remaining IV-BCG vaccinated macaques were protected with ≤ 3 granulomas and < 50 Mtb CFU in the entire animal. Overall, IV-BCG macaques had a 100,000-fold reduction in thoracic bacterial burden compared to the ID BCG group [63].

A review of studies from the pre-chemotherapy era showed a 10-year case fatality ratio of 70% in untreated smear-positive HIV-negative individuals, with the ratio being 20% in culture-positive smear-negative individuals. The duration from TB disease onset to death is approximately 3 years [64]. Current TB treatment regimen consists of 2 months of rifampicin (RIF), isoniazid (INH), pyrazinamide (PZA) and ethambutol (EMB) followed by 4 months of RIF and INH [65]. Drug resistant TB requires second line antibiotics, and there are several potential regimens. According to the 2019 WHO Global Tuberculosis report [2], treatment success is at least 85% for drug-susceptible cases and 56% for MDR-TB globally.

The first drug proven to have activity against Mtb, streptomycin, was discovered by Schatz and Waksman in 1944. It was rapidly tested in guinea pigs and within 3 years a randomized controlled clinical trial was started by the Medical Research Council in Britain. This trial showed that patients who received streptomycin and bed rest showed significant clinical improvement compared to patients who had bed rest alone. Unfortunately, this clinical trial also recorded the rapid development of streptomycin resistance in some patients with a median of 45 days after treatment initiation [66-68]. Around the same time, a Swedish scientist named Jörger Lehmann discovered para-aminosalicylic acid (PAS) which was also active against Mtb [69]. In 1950, the British Medical Research Council published a monumental study that showed combination drug therapy reduced the rate of the emergence of drug resistant Mtb compared to using streptomycin or PAS alone [70].

Of the current first line anti-TB drugs, isoniazid was the first to be discovered in 1912 and has been part of the anti-TB drug regimen since 1952 [71]. It is a pro-drug that enters the cell by passive diffusion and is activated by the mycobacterial catalase-peroxidase enzyme, KatG [72-74]. It only kills actively dividing mycobacteria by disrupting mycolic acid synthesis, which is a major component of the Mtb cell wall, inhibiting nucleic acid synthesis and producing nitric oxide free radicals [71, 74-77]. There are many genes thought to be involved in the development of INH resistance, the main of which are *katG inhA*, and *ahpC* [71, 78, 79]. Pyrazinamide was next to be discovered and was shown to be effective against Mtb in mice and humans in 1952 [80, 81]. PZA is a pro-drug that becomes its active form, pyrazinoic acid (POA), after conversion by the Mtb cytoplasmic enzyme, nicotinamidase/pyrazinamidase [82]. Although there is much debate on its mode of action, the most recently proposed is that POA binds and promotes degradation of aspartate decarboxylase (PanD) inhibiting Coenzyme A biosynthesis [80, 83, 84]. Coenzyme A

functions as a co-factor for many enzymes involved in fatty acid and nonribosomal peptide synthesis [85]. Mutations in the *pncA* (encodes pyrazinamidase) gene have been associated with PZA resistance [86-89]. Ethambutol was first described in 1961 and was included in the anti-TB regimen in 1966 [90]. Similar to INH, EMB inhibits actively replicating bacteria by disrupting arabinogalactan synthesis, depleting the molecules that anchor mycolic acids thus disrupting cell wall synthesis and increasing cell wall permeability [90-93]. EMB resistance is primarily associated with mutations in genes encoding arabinosyltransferases, *embB* and *embC* [90, 94-96]. The last to be included as a first line anti-TB drug is rifampicin. Rifampicin was discovered by Piero Sensi and was introduced as an anti-TB drug in 1968. It is one of the most potent anti-TB drugs currently available [97]. The introduction of rifampicin shortened chemotherapy from 1-2 years to 9 months and when used with PZA to 6 months [98, 99]. Rifampicin binds and inhibits the RNA polymerase β subunit of Mtb. Consequently, mutations in the *rpoB* gene confer rifampicin resistance [97, 100, 101]. Side effects from first line anti-TB drugs range from mild (eg. nausea, abdominal pain, drowsiness) to severe (eg. liver and kidney damage, joint pain, blurred vision) [102]. A number of second-line anti-TB drugs, which include fluoroquinolones, injectables (eg. amikacin, kanamycin), carbapenems, linezolid, and bedaquiline among others, are available for use if Mtb develops resistance to the first-line drugs, specially RIF and INH, but side effects can also be severe (eg. renal, liver and auditory dysfunction, psychosis, peripheral neuropathy) [103, 104].

1.4 Granuloma – the hallmark of tuberculosis

Once Mtb enters the airways and lodges in the alveoli, it is phagocytosed by alveolar macrophages, dendritic cells (DC) and neutrophils which carry it to the lungs [105]. Mtb-infected DCs then migrate to the lymph nodes to activate the adaptive immune system 9-11 days post-infection [106-108]. Activated lymphocytes then migrate from the lymph nodes to the site of lung infection aggregating with the innate immune cells forming a granuloma [109-111]. Granuloma formation is dependent on TNF production and the maintenance of chemokine concentrations to recruit and retain immune cells [112, 113]. As shown in Figure 2, Mtb is found at the center with cell debris and infecting macrophages at the periphery. Epithelioid macrophages dominate the “macrophage layer” although neutrophils, giant cells and foam cells can also be found interspersed. Surrounding the “macrophage layer” is the lymphocytic cuff composed of T cells, B cells and natural killer (NK) cells [109]; there are also types of macrophages in the lymphocyte cuff. Although granulomas serve as protective encasements to control or kill Mtb and prevent dissemination of the bacilli, they also serve as niches where Mtb can survive and persist. Granulomas can reactivate and become sources of bacterial dissemination [109, 114, 115].

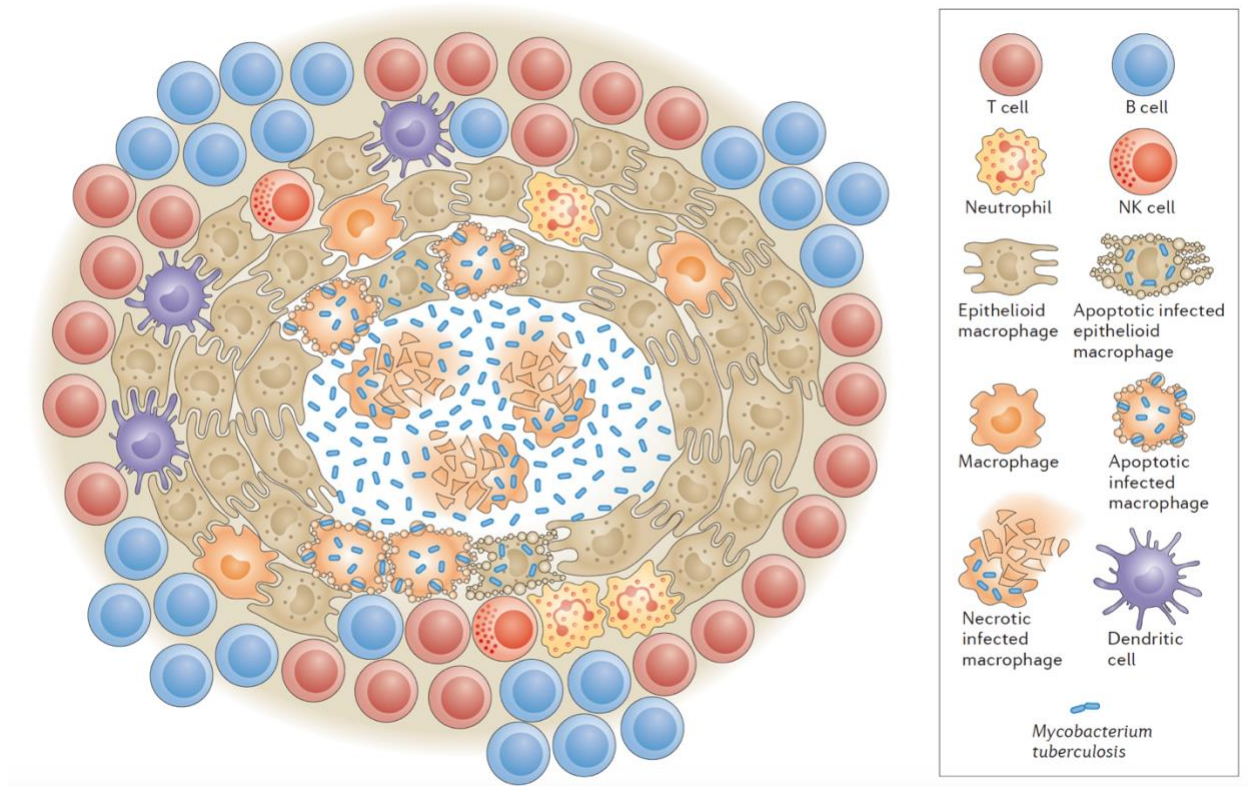


Figure 2. The structure of a granuloma.

A granuloma is an aggregation of host immune cells and Mtb bacilli. The center of a granuloma contains Mtb and cell debris surrounded by a “macrophage layer” containing epithelioid macrophages, giant cells, foam cells, dendritic cells and neutrophils. Enclosing the macrophage layer is the lymphocyte cuff which contains T cells, B cells, NK cells and macrophages. Reproduced with permission from Springer Nature, Cadena et al, 2017 [116].

Even within an animal, granulomas have independent trajectories, distinct local immune environment, killing ability and present as a spectrum that can influence host outcome. In a given animal, granulomas can range from sterilized to uncontrolled or disseminating based on a variety of host and bacterial factors [116]. Granulomas can be nonnecrotizing (with epithelioid macrophages and giant cells in the center), caseous (with necrotic center), suppurative (with

granulocytic center) and fibrocalcific (mineralized center surrounded by fibrosis). A macaque can have a combination of these granuloma types. Nonnecrotizing and suppurative granulomas are generally associated with high bacterial burden while fibrocalcific granulomas are associated with low bacterial burden and healing. Caseous granulomas can also be associated with poor Mtb control, however, over time bacterial killing increases and caseous granulomas evolve into fibrocalcific granulomas [117, 118]. In macaques, granuloma characteristics early in infection affect the progression of the disease as a whole. A significant increase in metabolic activity as measured by positron emission tomography (PET) in granulomas was associated with developing active TB disease [119]. Granulomas that would later disseminate and form new granulomas were significantly bigger in size (at 4-5 weeks post-infection) compared to contained granulomas and dissemination early during infection (3-6 weeks) is associated with developing active TB disease [119, 120]. Granulomas varied greatly in cell numbers, proportion of T cells, cytokine response and bacterial burden within and among animals and a spectrum of these parameters are present irrespective of the host's clinical status. Importantly, systemic immune responses do not reflect the local immune response in granulomas [121].

1.5 Immune response to tuberculosis

The first host cell Mtb encounters are the airway epithelial cells (AEC). These cells recognize pathogen-associated molecular patterns and danger-associated molecular patterns through their widely expressed toll-like receptors (TLRs) and nod-like receptors [122, 123]. During Mtb infection, airway epithelial cells produce a myriad of molecules that can regulate the host immune system. These include complement proteins, antimicrobial peptides, surfactants,

enzymes, reactive oxygen species (ROS), nitric oxide (NO), proinflammatory cytokines and chemokines which enhance host immune cell recruitment, increase inflammation and promote phagocytosis and microbial killing [123, 124]. However, in vitro evidence suggests that AECs can serve as niches for Mtb growth and replication [125, 126], although there is little in vivo evidence to support this. Mtb replicates >55-fold 7 days post-infection in A549 cells, a type II airway epithelial carcinoma cell line, compared to only 4-fold and 3-fold in murine macrophage cell line (J774) and fresh human monocyte-derived macrophages, respectively [127]. Transcriptome analysis of Mtb in A549 cells also showed an actively replicating state with enhanced virulence. Mtb genes associated with replication, mycolic acid synthesis, aerobic respiration and ESAT-6 were all upregulated, while, stress response and hypoxia-induced genes in AECs were downregulated [128].

Macrophages are the first immune cells that Mtb encounters [129]. Macrophages phagocytose Mtb and contain the bacteria inside a phagosome that undergoes a sequence of fusion events which are bactericidal to Mtb. Acidification of the phagosome is essential for bacterial clearance as it provides the optimum environment for lysosomal enzymes and ROS production [110, 130]. Mtb, however, has in its arsenal cell wall components such as trehalose dimycolate and lipoarabinomannan, and secreted proteins (eg. lipid phosphatase [SapM], tyrosine phosphatase [PtpA], a Zn²⁺ metalloprotease [Zmp1] among others) that prevent phagosomal maturation [131-133]. Activation of macrophages with IFN γ bypasses the phagosome maturation block by stimulation of autophagic pathways and inducing apoptosis in a NO dependent manner [134, 135]. In addition to phagosome acidification, macrophages also bombard the Mtb inside the phagosome with copper and zinc, which are toxic in large quantities, and deprive Mtb with iron and manganese which are essential micronutrients for bacterial survival [136].

Macrophages are armed with multiple receptors that can recognize Mtb such as TLRs, C-type lectin receptors (CLR), Fc receptors, scavenger receptors, mannose receptors and cytosolic DNA sensors [137]. Stimulation of these receptors result in enhanced antigen presentation, phagocytosis, apoptosis, autophagy, cytokine secretion and nitric oxide production [138, 139]. TLRs 2, 4 and 9 are key in recognizing Mtb [140]. Activation of TLR2 leads to production of NO, TNF α and IL-12 in murine and human monocytes and macrophages [141, 142]. Production of an antimicrobial peptide, cathelicidin, is induced by the upregulation of vitamin D receptor and vitamin D-1-hydroxylase genes caused by TLR2 activation [143]. Activation of TLR4 predominantly leads to TNF production, along with IL-6 and monocyte chemoattractant protein-1 (MCP-1), in murine macrophages and human monocytes [144-146]. TLR9 $-/-$ mice exhibited reduced IL12p40 and IFN γ production but there was no effect on bacterial burden. However, a TLR2/9 $-/-$ mice displayed enhanced susceptibility to Mtb infection suggesting a redundant role between TLR 2 and 9 [147]. In addition to TLRs, macrophages have complement receptors (CR) that recognize complement proteins and promote phagocytosis [148]. One of particular interest is CR3 as blocking of this receptor by monoclonal antibodies inhibited adherence of Mtb to human monocytes in vitro by up to 81% [149]. Mannose receptors are one mechanism used by Mtb to gain entry to macrophages without prior opsonization and promote survival and growth. Mannose receptors recognize LAM which blocks phagosome maturation [150]; there is a report that mannose receptors only recognizes virulent Mtb strains [151].

Neutrophils are also one of the first responders to Mtb infection [110]. Their role in TB is controversial, with the potential to be both beneficial and harmful. They have been shown to be important early in infection in mice [152-155] but also correlated to active TB disease, increased bacterial burden, host tissue destruction and even respiratory failure and death in several models

and humans [156-161]. Early recruitment of neutrophils by LPS administration in rats at the time of infection resulted in a 650-fold decrease in lung Mtb CFU (No LPS - 1.3×10^5 CFU vs with LPS - 200 CFU). This protection progressively waned as LPS was administered 1-10 days after Mtb infection [153]. Similar results were shown in other studies [152, 154, 155]. Proposed mechanisms by which neutrophils kill Mtb include phagocytosis, either directly or by phagocytosing Mtb-infected cells, producing reactive oxygen/nitrogen intermediates, degranulation of bactericidal molecules (eg. cathelicidins, defensins, elastase) and forming neutrophil extracellular traps (NETs) [162, 163]. In contrast, some studies showed poor Mtb killing in neutrophils even when stimulated with $\text{IFN}\gamma$ and $\text{TNF}\alpha$ making it a “trojan horse” harboring Mtb and hiding them from potentially bactericidal macrophages [156, 164, 165]. In macaques, granzyme B-expressing neutrophils were correlated with increased bacterial burden in granulomas [160]. Neutrophils have also been shown to produce cytokines such as TNF, IL-4, IL-10 and $\text{IFN}\gamma$ in macaque lung granulomas, however, cytokine secretion was not correlated with bacterial load [166].

Dendritic cells are the most effective antigen presenting cells and also important sources of IL-12 which promotes Th1 differentiation [167]. Although the host need Mtb-infected DCs to migrate to the lymph nodes to activate the adaptive immune system [105, 107], Mtb also uses DCs to dampen the immune response. CD209, also called DC-specific intracellular adhesion molecule 3-grabbing non-integrin receptor (DC-SIGN), binds to CD54, an intercellular adhesion molecule 1 (ICAM-1) found in endothelial cells that facilitate DC migration [129]. Interaction of CD209 with Mtb LAM mannose promotes internalization of Mtb, increased production of IL-10 and decreased production of IL-12 modulating T cell activity [168]. In contrast, studies have also shown that DCs infected with Mtb becomes activated upregulating expression of activation

markers (eg. MHC II, CD40, CD80) and increased production of inflammatory cytokines such as TNF α , IL-12, IL-1 and IL-6 promoting DC maturation and antigen presentation [169, 170].

Natural killer (NK) cells have been proposed to play a role during Mtb infection by lysing Mtb-infected macrophages [171, 172], producing IFN γ and IL-22, which enhances phagolysosomal infusion [173], stimulating IFN γ production by CD8 T cells [174], and limiting regulatory T cell (Treg) expansion [175].

Protection during Mtb infection is mostly attributed to the cellular adaptive immune response [176, 177]. The importance of CD4 T cells in TB was demonstrated by the increased susceptibility of HIV+ patients to Mtb infection and disease [178]. This was further supported by CD4 T cell depletion studies in mice [179-181] and non-human primates (NHP) [182, 183] where animals showed increased pathology, bacterial burden and reactivation of some macaques with LTBI. CD4 T cells producing IFN γ are key players in Mtb clearance by promoting phagosome-lysosome fusion and ROS production in macrophages [134, 176, 184, 185]. The importance of CD8 T cells was not readily apparent until studies in mice deficient in molecules necessary for antigen presentation through major histocompatibility complex (MHC) class I resulted in greater bacterial burden, severe pathology and accelerated death [186, 187]. CD8 T cells control Mtb infection by producing cytokines (eg. IL-2, TNF, IFN γ), and inducing apoptosis either by degranulation (perforin, granzymes and granulysin) or Fas-Fas ligand interaction in Mtb-infected cells [50, 188]. In BCG-vaccinated rhesus macaques, CD8 depletion prior to high-dose challenge resulted in higher bacterial burden, more severe lung pathology and more extensive dissemination compared to macaques given IgG control [189]. Our unpublished data also support a critical role for CD8 T cells in control of initial Mtb infection in macaques.

Studies in genetic knockout mouse strains were instrumental in demonstrating the importance of IFN γ [190, 191], IL-12 [192] and T-bet [193], a transcription factor regulating Th1 cell development, all of which were unable to control bacterial growth. The importance of IFN γ in TB is further supported by individuals with Mendelian susceptibility to mycobacterial disease (MSMD). MSMD is a rare genetic condition characterized by increased susceptibility to weakly virulent mycobacteria species, such as BCG and environmental mycobacteria, in an otherwise healthy person. Genes associated with MSMD diminishes the production or response to IFN γ [194, 195]. TNF α is also critical in TB infection as first shown in mice where TNF α neutralization and disruption of TNF receptor resulted in early death compared to controls [196]. This was validated in humans where latent TB subjects reactivated after administration of a TNF α -neutralizing antibody, infliximab [197], and in NHPs where TNF α neutralization resulted in disseminated TB disease and reactivation of ~50% of macaques with LTBI [198, 199]. The role of Th17 cells in humans is unclear. Low serum IL-17 level was associated with higher fatality 2 months after anti-TB treatment [200]. Humans with active TB disease had a lower frequency of CD4 T cells producing IL-17 in blood compared to healthy and LTBI individuals [201, 202]. However, one study did not find any significant difference in IL-17 mRNA levels in bronchoalveolar lavage and blood between patients with active TB and healthy controls [203]. In addition, high levels of CD4 T cells producing both IFN γ and IL-17 were associated with severe TB disease [204]. IL-17 has been shown to be protective in mice following primary infection with Mtb Beijing HN878 [205] or BCG vaccination [206]. IL-17 $^{-/-}$ mice exhibited greater lung pathology and bacterial burden after infection with Mtb Beijing HN878 [205]. BCG-induced protection in mice was dependent on the presence of IL-17 which leads to chemokine secretion and recruitment of IFN γ -producing CD4 T cells to the lungs [206]. IL-10 is widely regarded as detrimental to TB as it has been implicated

to arrest phagosomal maturation in Mtb-infected human macrophages [207] and downregulate protective Th1 responses in vitro [208, 209]. Increased IL-10 production in C57BL/6 mice, which are naturally resistant to Mtb infection, has no effect early during infection but resulted in 100-fold higher lung bacterial burden compared to untreated C57BL/6 mice during the chronic phase of the infection (100-200 days post-infection) [210]. Similarly, treatment of CBA/J mice, which are normally susceptible to Mtb infection, with anti-IL-10 resulted in stable lung bacterial burden and increased mice survival, and this was associated with T cell recruitment and IFN γ production [211]. In macaques, depleting IL-10 resulted in less lung inflammation and increased cytokine production at 3-4 weeks post-infection compared to control animals, but with no significant differences in bacterial burden during the early phase of infection [212]. Eliciting pro-inflammatory Th1 responses is assumed to be necessary during Mtb infection although several vaccines that elicit such responses are still not protective [213]. Indeed, a purely inflammatory response is destructive to the host causing widespread immunopathology, thus a balance between pro- and anti-inflammatory responses should be elicited to achieve optimal control of Mtb [121].

In contrast to T cells, the role of B cells and antibodies in TB has been uncertain and controversial. Serum therapy studies, that is the transfer of sera from animals infected with Mtb or immunized with Mtb products to other animals or humans, done in the early 1900s had inconsistent results [214]. Recently, however, with the improvement of technology and techniques, there have been studies that showed protective effect of passive transfer of antibodies to mycobacterial antigens in mice (reviewed by [215]). Humans with LTBI and active TB produced different antibody signatures. Antibodies from LTBI patients promoted phagosomal maturation, enhanced inflammasome activation and increased killing of intracellular Mtb in macrophages [216]. In NHPs, B cells can be found in clusters resembling germinal centers in granulomas and are actively

secreting Mtb-specific antibodies [217]. B cell depletion prior to infection did not result in increased overall susceptibility to TB disease, however, lung granulomas exhibited higher bacterial burden, less inflammation and altered cytokine levels [218]. Formation of iBALT was also associated with LTBI in NHPs [219].

1.6 Non-human primate model of tuberculosis

Many animal models have been developed to study TB. Mice are the most widely used and have contributed significantly in our current knowledge of TB. The commonly used mice (eg. C57BL/6 and BALB/c) are considered to be naturally resistant to Mtb infection; although they carry high bacterial burdens (10^5 - 10^6 CFU/lung) and cannot clear the infection, these strains can live for a year or more with TB. Some mouse strains are more susceptible (eg. C3H, CBA) developing progressively severe disease causing early death [220]. Although there is an abundance of available reagents to study mouse immunology and certain manipulations such as gene knock-outs and adoptive transfers are easily performed in this animal, it falls short in replicating some of the crucial aspects of human TB. Upon Mtb infection, murine lungs develop confluent collections of cells, termed granulomatous inflammation, but not organized granulomas as seen in humans, and do not have true latent and reactivation states [221-223]. Rabbits are resistant to Mtb but susceptible to *M. bovis*. Rabbits do form granulomas and develop cavities similar to humans [221, 224]. In contrast to rabbits, guinea pigs are susceptible to Mtb and a subset of their granulomas resemble those seen in humans. However, for both rabbits and guinea pigs, the lack of immunologic reagents is problematic, genetic manipulation is difficult and true latency and reactivation states have not been demonstrated [225-228]. Zebrafish infected with *M. marinum*, an

aquatic mycobacterial species, are good models to use for studying the dynamics of granuloma formation. Zebrafish develop human-like granulomas and as embryos they are transparent which is advantageous for real-time imaging. However, their anatomy and physiology are different from humans. For example, since zebrafish do not have lungs, granulomas form in the pancreas, liver, spleen, gonads and fatty tissue [225, 229]. Non-human primates (NHP) develop the full spectrum of TB disease including latency and reactivation, and form granulomas and other TB-associated pathologies identical to humans. Hindrances to NHP use, however, are high cost and large Biosafety Level 3 space required for housing and maintenance [225, 230].

The NHP model of TB is well established [231-234]. *Cynomolgus* macaques infected with a low dose inoculum (<25 CFU) of *Mtb* strain Erdman present with the full spectrum of infection outcomes seen in humans. Approximately 50% of macaques progress to active disease while ~50% develop latent TB infection showing no signs of disease. The clinical criteria used to classify active disease and latent TB are very similar to those used for humans [231-233]. Macaques are classified as having active TB disease if they present with clinical signs (eg. weight loss, cough), an elevated erythrocyte sedimentation rate (ESR >2mm), chest x-ray scan showing disease, and *Mtb* culture from gastric aspirate (GA) and/or bronchoalveolar lavage (BAL). Latent TB is defined as showing no clinical signs, negative *Mtb* culture from GA or BAL and normal ESR up to 6 months post-infection [198, 231, 233]. *Mtb*-infected macaques develop a range of granuloma types as seen in humans with caseous granulomas being predominant in the lungs [117]. Moreover, some macaques have extrapulmonary infection (eg. spleen, liver, lymph nodes) [233, 235].

In addition to exhibiting the full spectrum of *Mtb* infection, there are several other reasons that make NHPs superior in modeling TB compared to other animal models. Tracking disease progression such as granuloma formation and thoracic inflammation is possible in NHPs with the

use of serial imaging using positron emission tomography and computed tomography (PET CT) (Figure 3). CT provides a spatial map of the lungs where individual lesions and lymph nodes can be quantified for size and location. The use of the PET probe ^{18}F -fluorodeoxyglucose (FDG), which is taken up by metabolically active host cells, makes it possible to quantify overall lung inflammation as well as the FDG activity in individual granulomas. Combining PET and CT provides a structural and functional map of the lungs during Mtb infection [236]. In addition, thoracic lymph nodes (LNs) are also involved in TB disease in NHPs and humans, especially in children [234, 235, 237]. Individual granulomas and LNs can be excised and analyzed for bacterial burden, pathology and immune response. Lastly, NHPs can be used to study various interventions such as vaccines, drugs, and host-directed therapies as well as the importance of various immune factors using antibodies to deplete cell types or neutralize cytokines [234].

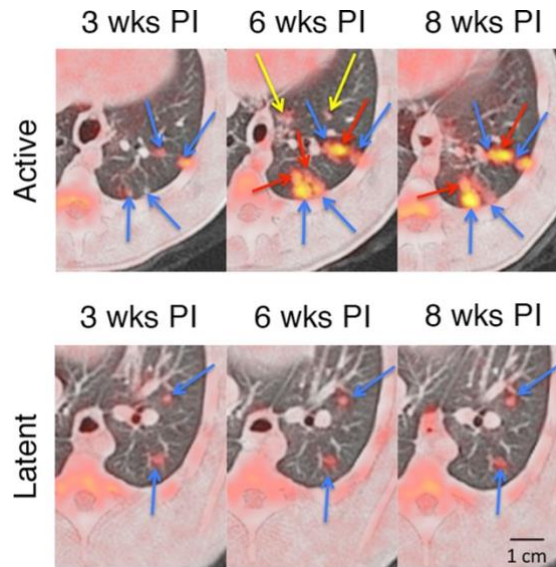


Figure 3. Serial PET CT imaging allows tracking of inflammation and formation of new granulomas.

Blue arrows = old granulomas; red arrows = new granulomas adjacent to old granulomas and yellow arrows = new granulomas forming at new sites far from initial granulomas. Reproduced from Coleman et al, 2014 [119].

1.7 Lymph nodes – the neglected battlefield of tuberculosis

This section is adapted from the original publication:

Ganchua SKC, White AG, Klein EC and Flynn JL. 2020. Lymph nodes – the neglected battlefield in tuberculosis. *PLoS Pathogens*. *In press*. (see Chapter 8 for full article)

Even though TB most commonly manifests as a pulmonary disease, extrapulmonary TB also occurs. In humans, *Mtb* infection usually results in a Ghon complex – a tuberculous lung lesion accompanied by a granuloma in a thoracic lymph node [238, 239]. Infected lymph nodes

are considered to be extrapulmonary, even if they are within the thoracic cavity, and are the most common sites of extrapulmonary Mtb infection [240, 241]. Early autopsy studies in humans found live Mtb in lymph nodes without signs of TB disease anywhere else in the body [242-244]. Even lymph nodes that appeared normal through gross inspection by a trained pathologist could harbor live Mtb [242]. In cattle, lymph nodes are the most common site of *M. bovis* infection [245]. In a small study of 15 cattle with evidence of bovine TB in lymph nodes, only 1 had identifiable pulmonary infection [246]. However, some authors as cited by Neill et al [245] believe that a more comprehensive inspection of the bovine lungs should be performed since TB lesions can be small. It is widely accepted that in bovine TB lymph nodes get infected first while pulmonary lesions develop later during the infection [245, 247]. In our experience working with non-human primates, lymph nodes are almost always infected with Mtb along with the lungs [235]. Occasionally, we find lymph nodes with no apparent granuloma also harboring live Mtb bacilli. Given these observations, it is understandable that Behr and Waters proposed TB as a lymphatic disease rather than strictly a pulmonary disease [248].

The involvement of lymph nodes during the first month of Mtb infection is well established in mouse models of TB. After aerosol infection, Mtb is phagocytosed by alveolar macrophages, myeloid dendritic cells (DC) and neutrophils in the lungs [105]. While other respiratory viral and bacterial pathogens induce DC migration to the lymph nodes to activate the adaptive immune system by 1-3 days post-infection [249-251], this important process is delayed in Mtb infection. Several studies have shown that Mtb-infected DCs do not migrate to the lymph node and prime T cells until 9-11 days post-infection [106-108]. This delay in the dissemination of Mtb bacteria to the lymph nodes is thought to play a role in the increased susceptibility of C3H/HeJ mice to Mtb compared to C57BL/6 mice [106]. Wolf and colleagues also showed that the migration of DCs

was transient, slowing down after peaking at 21 days post-infection, an interesting observation given the chronic nature of TB. Not only are DC migratory functions dysregulated, but DCs and interstitial macrophages that transport Mtb to the lymph nodes are relatively poor at stimulating T cell responses to Mtb antigens [107].

Based on human and macaque studies, lymph nodes can play a major role in reactivation of latent TB caused by immunosuppression. In NHPs, we define reactivation TB as a positive culture in bronchoalveolar lavage and/or gastric aspirate, increase in erythrocyte sedimentation rate, signs of disease such as coughing or weight loss, or the formation of a new granuloma by PET CT after latent Mtb infection was established [182, 183, 198, 199, 252]. In CD4 T cell-depleted cynomolgus macaques, lower CD4⁺ T cell levels in hilar lymph nodes was associated with reactivation [182]. In TNF-neutralized macaques, early signs of reactivation (ie. non-necrotizing granuloma formation adjacent to established and often mineralized granulomas) were observed microscopically in the lymph nodes [198]. Latently Mtb-infected macaques with a high risk of reactivating after TNF neutralization had a smaller proportion of sterile thoracic lymph nodes, highly metabolically active (by PET CT) lymph nodes and increased live Mtb burden in lymph nodes compared to low risk animals [199]. In a separate study [183], DNA barcoded Mtb bacteria, which allows for the discrimination of individual bacteria, was used to track Mtb dissemination during reactivation of latent TB in cynomolgus macaques induced by SIV co-infection. New lung granulomas that arose during reactivation were assessed for DNA barcodes and compared to the DNA barcoded bacilli found in old granulomas (those present prior to SIV infection) or in thoracic lymph nodes. Almost 50% of the DNA barcodes in new granulomas matched DNA barcodes from bacteria only found in lymph nodes and not in the old granulomas. Moreover, Mtb recovered from extrapulmonary sites (eg. liver and spleen) had the same barcodes

as Mtb from the lymph nodes. This suggests that Mtb dissemination during reactivation can originate from the lymph nodes dispersing to the lungs and other organs. In antiretroviral-naïve humans with latent TB co-infected with HIV, abnormal FDG uptake in lymph nodes was associated with reactivation. Ten participants determined to have subclinical TB pathology were more likely to develop abnormal uptake of FDG in thoracic lymph nodes compared to participants without subclinical TB disease. Participants with subclinical TB pathology were also significantly more likely to develop active TB disease (4/10) during the 6-month follow-up period compared the 25 participants with no subclinical pathology of which none developed active TB disease [253]. These data suggest that reactivation of latent TB, whether by SIV/HIV infection, CD4 depletion or TNF neutralization, can start in the lymph nodes and can be predicted by visualizing the metabolic activity of lymph nodes by PET CT.

For a vaccine to successfully elicit an immune response, it is required to reach secondary lymphoid organs such as the lymph nodes. A study in C57BL/6 mice compared the efficacy of three BCG vaccination routes [intradermal, subcutaneous (s.c.) and intralymphatic injection] in eliciting a robust immune response and protection from Mtb challenge [254]. Direct injection of BCG to the inguinal lymph nodes resulted in tremendous transient swelling of not just the injected lymph nodes but all the other lymph nodes as well (eg. mesenteric, axillary, brachial, thoracic and cervical nodes). This is in contrast to subcutaneous and intradermal vaccination which caused minimal swelling of any of the lymph nodes examined. Lymph nodes from intralymphatically vaccinated mice harbored greater numbers of BCG by Ziehl-Neelsen staining compared to s.c. vaccinated animals. Intralymphatic vaccination also elicited a more robust immune response compared to s.c. vaccinated animals. Significantly more proliferation and stronger TNF, IL-2, IL-17 and IFN γ responses up to 40 days post-vaccination were observed in PPD-stimulated

splenocytes from intralymphatic vaccinated animals compared to s.c. vaccinated animals. Direct vaccination of lymph nodes also resulted in significantly reduced Mtb burden (up to 12 weeks post-infection) against Mtb challenge in the lungs and spleen compared to s.c. and unvaccinated control mice [254]. These data suggest that direct vaccination of lymph nodes could improve the efficacy of BCG in eliciting an immune response and protection against Mtb challenge.

Lymph nodes are sites where Mtb can persist, disseminate and reactivate [182, 183, 198, 199, 253]. Therefore, it is imperative that anti-TB drugs be tested for their ability to eliminate Mtb bacteria in the lymph nodes. There is only one study I am aware of that examined concentrations of rifampicin (RIF) and isoniazid (INH) in the blood, lungs, granulomas and lymph nodes in humans [255, 256]. Rifampicin had the highest concentration in the blood (6.95 $\mu\text{g/ml}$) followed by tuberculous foci (2.43 $\mu\text{g/g}$) and healthy lung tissue (2.22 $\mu\text{g/g}$). Thoracic lymph nodes (1.41 $\mu\text{g/g}$) had lower RIF concentration compared to blood and lung granulomas. Interestingly, the lowest RIF concentration was found in caseous lymph nodes (0.03 $\mu\text{g/g}$). In contrast, although INH concentration was also highest in the blood (4.11 $\mu\text{g/ml}$), its concentration in healthy lungs (0.58 $\mu\text{g/g}$), bronchopulmonary lymph nodes (0.53 $\mu\text{g/g}$), cavities (0.59 $\mu\text{g/g}$), tuberculous foci (0.6 $\mu\text{g/g}$) and caseous lymph nodes (0.21 $\mu\text{g/g}$) were all relatively similar [255, 256]. Remarkably, caseous lymph nodes had once again the lowest INH concentration. No information about Mtb burden in the different tissues were provided. Although this is just one study, it provides a glimpse of lower RIF and INH penetration in lymph nodes compared to lung granulomas.

Lymph nodes are underappreciated in the study of TB. It is clear that aside from their main function of initiating and shaping adaptive immune responses, lymph nodes also play a role in Mtb persistence, TB reactivation, and vaccine efficacy and have impaired anti-TB drug penetration.

More attention should be paid to these organs when testing vaccines and drug candidates in the future.

1.8 Reinfection in TB

Most vaccines in use in humans are based on the idea that a previous infection with a microbe will induce an immune response that prevents infection or disease when the host encounters the microbe again. The vaccine mimics some part of the host response to infection and provides immunity against the pathogen. However, in TB, it is unclear whether an ongoing or previous Mtb infection confers protection to a secondary infection. This is a critical issue for vaccine development. Early human epidemiologic studies followed nursing and medical students by monitoring their TST status (indicating infection) and signs of TB disease (to distinguish latent vs active TB) throughout the course of their training and even many years after. Andrews and colleagues [257] did a meta-analysis of these and other epidemiologic studies and concluded that LTBI resulted in a 79% lower risk of developing active TB compared to an uninfected person. However, the timing of primary infection and even whether the subjects were exposed to or infected with Mtb during their training were not known. In addition, whether the protection against developing active TB disease seen in individuals with LTBI was due to their ongoing latent infection or their innate resistance to TB disease were also unknown. In humans, mixed infections (infected with ≥ 2 Mtb strains) could be present in 0.4-57% of active TB patients, although extent of disease and transmission in the community, specimen handling, contamination rate, strain typing method used, drug resistance and the patient's HIV status could all affect this number [258].

Several early reinfection studies also exist in animal models where Mtb reinfection can be assured although discrimination between the 2 infections can still be challenging. By using a drug-susceptible Mtb strain for the first infection and a streptomycin-resistant strain for the second infection, Kanai and Yanagisawa showed that for both guinea pigs and rats multiplication of Mtb bacilli from the second infection was significantly hindered while the Mtb from the first infection thrived [259, 260]. Similar results were obtained in rabbits where granulomas formed by the second infection had fewer Mtb bacilli. Although discrimination between the 2 infections relied on the size and histology of granulomas in one study, one study used Mtb for the first infection and *M. bovis* for the second infection [261, 262]. More recently, in mice that were drug treated before reinfected with Mtb, significantly fewer Mtb bacilli (1000-fold lower) were found in the lungs 30 days post-infection, however, this protection waned and the lung Mtb burden reached the level of control animals by 60 days post-infection [263]. By using serial PET CT scans and DNA-tagged Mtb strains, Cadena et al [264] showed that reinfected cynomolgus macaques formed significantly fewer granulomas from the second infection compared to controls (those that did not have primary infection) with 5/8 reinfected animals failing to form any CFU+ granulomas from the second infection. The granulomas that did grow Mtb had significantly fewer bacterial load compared to the controls. In addition, there was dissemination to the thoracic lymph nodes in only 1 of the 8 reinfected animals, compared to 5 of 6 of the control animals. Overall, there was a 10,000-fold reduction in bacterial burden from the second infection in macaques with ongoing primary infection.

2.0 Gaps in knowledge and specific aims

The main hindrance to current vaccine development is the lack of biomarkers or immune correlates for protection against TB. In fact, the immune responses to target in a protective vaccine are largely unknown. Published data suggest that individuals with latent TB have a lower risk of progressing to active TB after Mtb re-exposure [257]. However, the extent to which Mtb protects against actual reinfection (and not simply disease) is completely unknown and extremely challenging to assess in humans. In previous work in our lab, we showed that macaques with an ongoing primary Mtb infection presented with limited disease progression (fewer new granulomas and higher frequency of sterile lesions) after secondary challenge. This degree of protection is greater than most vaccines tested thus far and provides a model for protective immunity. The mechanisms and factors limiting disease progression during a secondary Mtb infection are currently unknown. In this dissertation, I investigated the protection provided by primary infection, focusing on the contribution of bacterial viability and CD4 T cells. ***I hypothesize that the resulting adaptive cellular immunity from an ongoing primary Mtb infection limits granuloma formation, bacterial burden and disease progression of a secondary Mtb infection.*** I also performed an extensive analysis of lymph nodes from Mtb-infected macaques to understand their role in Mtb infection, with the hypothesis that thoracic lymph nodes are a unique reservoir for Mtb.

The main hypothesis will be directly tested through these specific aims:

AIM 1. Determine the contribution of bacterial viability in the protection conferred by a primary Mtb infection to a secondary Mtb infection. Mtb-infected cynomolgus macaques will be drug treated to eliminate viable Mtb prior to reinfection. Infection and disease progression will be followed by PET CT, immunologic responses monitored by flow cytometry and disease outcome measures (number of secondary granulomas and bacterial burden) evaluated in all macaques. *I hypothesize that live Mtb is required to provide protection against a secondary Mtb infection.*

AIM 2. Determine the contribution of CD4 T cells in the protection conferred by a primary Mtb infection to a secondary Mtb infection. There will be 3 cohorts in this study: (1) CD4 T cell-depleted macaques, (2) macaques infused with IgG control, and (3) macaques infected with 2nd infection only. As in Aim 1, infection and disease progression, host immune response and disease outcome measures will be monitored. *I hypothesize that CD4 T cells are important in providing protection against a secondary Mtb infection.*

AIM 3. Determine the role of lymph nodes during a primary Mtb infection and reinfection. Lymph nodes from infected cynomolgus and rhesus macaques at different time points post-infection, as well as from reinfected cynomolgus macaques from Aims 1 and 2, will be assayed for bacterial burden, Mtb killing capability and immune response. Localization of Mtb and immune cells in infected lymph nodes will also be determined. *I hypothesize that*

thoracic lymph nodes serve as niches for bacterial replication during a primary Mtb infection while lymph nodes play a minimal role in the protection against a secondary Mtb infection.

The development of an effective TB vaccine that prevents establishment of infection and disease progression is crucial if we want to eradicate TB. The goals of this dissertation are to gain important insight into the immunologic mechanisms of protection and the different bacterial and host factors influencing them. This will lead to a more focused approach to effective TB vaccine design and development. Elucidating the role of lymph nodes in Mtb infection will also draw consideration of these tissues in effective drug treatment and vaccine design.

3.0 Drug treatment does not abolish the protection against Mtb reinfection

3.1 Introduction

A meta-analysis of early epidemiology studies showed that a person with latent *M. tuberculosis* (Mtb) infection (LTBI) has a 79% lower risk of developing active TB disease compared to an uninfected person [257]. However, in these early studies, the timing and whether or not the subjects were exposed to or reinfected with Mtb were unknown, since development of active TB was the outcome measure. This limitation was circumvented using small animal models which showed that an ongoing Mtb infection impaired bacterial growth from the second infection; although discrimination between the 2 infections was challenging [259-262]. These small animal studies were done in the early to mid-1900s and over time there have been significant improvements in technology. In our laboratory in collaboration with Sarah Fortune's lab at Harvard, Cadena and colleagues used serial PET CT scans to track the first and second infection in real time in cynomolgus macaques and used DNA-tagged Mtb strains to effectively discriminate granulomas that formed from the first infection vs. second infection. Similar to the early animal studies, macaques that had an ongoing Mtb infection formed significantly fewer granulomas from the second infection compared to naïve controls (i.e. those that did not have a first infection). In 5/8 reinfected animals, the few granulomas that formed from the second infection were sterile while the remaining 3 reinfected animals that did form CFU+ granulomas from the second infection had significantly lower (10,000-fold reduction) bacterial burden compared to the granulomas that formed in the control animals [264]. This demonstrated that an ongoing Mtb

infection, regardless of extent of disease, provided robust protection against a second Mtb infection.

The underlying mechanism of protection in Mtb reinfection studies is still largely unknown. When mice were drug treated before reinfected with Mtb, 1,000-fold fewer Mtb bacilli was found in the lungs 30 days post-infection, however, this protection waned and lung bacterial burden increased to the level of control animals by 60 days post-infection [263]. In humans, the incidence rate of recurrent TB disease, either by relapse or reinfection, after successful treatment was 18x (China, [265]) and 14.6x (Spain, [266]) more than the incidence rate of initial TB disease in the general population. A study in Cape Town, South Africa which used DNA fingerprinting methods to discriminate between relapse and reinfection showed the incidence rate of active TB disease attributed to Mtb reinfection after successful treatment was 4x more than the incidence rate of initial TB disease in the general population [267]. Three possible reasons that could explain these findings include: (1) selection bias – selection of individuals with predisposition to Mtb infection and TB disease; (2) TB disease increases susceptibility of an individual to succeeding Mtb infection and disease; and (3) elimination of live Mtb resulting from drug treatment increased susceptibility of these individuals to subsequent Mtb infection and disease. Human studies are vulnerable to confounding factors, such as, laboratory errors, lung damage, timing of reinfection, HIV status, socio-economic background and emergence of drug resistant Mtb strains which are not always included in the analysis.

Here, we sought to address whether eliminating live Mtb bacilli abolishes the protection an ongoing primary Mtb infection confers to a second Mtb challenge using the established NHP reinfection model [264]. NHPs faithfully model the full spectrum of human Mtb infection outcomes and granulomas without the confounding factors prevalent in human studies [230-233].

In addition, by using serial PET CT scans and DNA-tagged Mtb strains, we can track granuloma formation in real time and discriminate between granulomas formed by first vs. second infection [264]. Our findings indicate that drug treatment reduced but did not abolish the protection a primary Mtb infection conferred to a second infection. There was no significant difference in protection (measured as number of and Mtb burden in granulomas forming from the second infection) between the drug-treated and non-drug treated groups, although both drug treated and non-drug treated animals did not demonstrate as robust protection as in the original reinfection study [264].

3.2 Methodology

3.2.1 Ethics Statement

All experimental manipulations, protocols, and care of the animals were approved by the University of Pittsburgh School of Medicine Institutional Animal Care and Use Committee (IACUC). The protocol assurance number for our IACUC is A3187-01. Our specific protocol approval number for this project is 15066174. The IACUC adheres to national guidelines established in the Animal Welfare Act (7 U.S.C. Sections 2131–2159) and the Guide for the Care and Use of Laboratory Animals (8th Edition) as mandated by the U.S. Public Health Service Policy.

All macaques used in this study were housed at the University of Pittsburgh in rooms with autonomously controlled temperature, humidity, and lighting. Animals were singly housed in caging at least 2 square meters apart that allowed visual and tactile contact with neighboring conspecifics. The macaques were fed twice daily with biscuits formulated for nonhuman primates,

supplemented at least 4 days/week with large pieces of fresh fruits or vegetables. Animals had access to water *ad libitem*. Because our macaques were singly housed due to the infectious nature of these studies, an enhanced enrichment plan was designed and overseen by our nonhuman primate enrichment specialist. This plan has 3 components. First, species-specific behaviors are encouraged. All animals have access to toys and other manipulata, some of which will be filled with food treats (e.g. frozen fruit, peanut butter, etc.). These are rotated on a regular basis. Puzzle feeders foraging boards, and cardboard tubes containing small food items also are placed in the cage to stimulate foraging behaviors. Adjustable mirrors accessible to the animals stimulate interaction between animals. Second, routine interaction between humans and macaques are encouraged. These interactions occur daily and consist mainly of small food objects offered as enrichment and adhere to established safety protocols. Animal caretakers are encouraged to interact with the animals (by talking or with facial expressions) while performing tasks in the housing area. Routine procedures (e.g. feeding, cage cleaning, etc) are done on a strict schedule to allow the animals to acclimate to a routine daily schedule. Third, all macaques are provided with a variety of visual and auditory stimulation. Housing areas contain either radios or TV/video equipment that play cartoons or other formats designed for children for at least 3 hours each day. The videos and radios are rotated between animal rooms so that the same enrichment is not played repetitively for the same group of animals.

All animals are checked at least twice daily to assess appetite, attitude, activity level, hydration status, etc. Following *M. tuberculosis* infection, the animals are monitored closely for evidence of disease (e.g., anorexia, weight loss, tachypnea, dyspnea, coughing). Physical exams, including weights, are performed on a regular basis. Animals are sedated prior to all veterinary procedures (e.g. blood draws, etc.) using ketamine or other approved drugs. Regular PET CT

imaging is conducted on most of our macaques following infection and has proved very useful for monitoring disease progression. Our veterinary technicians monitor animals especially closely for any signs of pain or distress. If any are noted, appropriate supportive care (e.g. dietary supplementation, rehydration) and clinical treatments (analgesics) are given. Any animal considered to have advanced disease or intractable pain or distress from any cause is sedated with ketamine and then humanely euthanized using sodium pentobarbital.

3.2.2 Animals, infections, drug treatment and disease tracking by PET CT

Ten cynomolgus macaques (*Macaca fascicularis*) with age range of 6.5-9.6 years were obtained from Valley Biosystems (3 females, 7 males, Sacramento, California). Animals were placed in quarantine for 1 month where they were monitored to ensure good physical health and no prior Mtb infection. All animals were infected with DNA-tagged Mtb Erdman via bronchoscopic instillation as previously described [232, 233]. All 10 macaques received Mtb library A as the first infection. Granuloma formation, lung inflammation and overall disease was tracked using ¹⁸F-fluorodeoxyglucose (FDG) PET CT every 4 weeks. PET CT scans were analyzed using OsiriX viewer as previously described with a detection limit of 1mm [236]. The first infection was followed for 16 weeks before splitting the 10 macaques into 2 cohorts: drug treated (n=7) and non-drug treated (n=3). Because this study was scheduled to last for 9 months, we needed to choose macaques for the non-drug treated group that we predicted would survive until the end of the study without drug intervention. The 3 macaques were chosen based on minimal change in granuloma numbers from 4 to 12 weeks post-infection and reduced total lung inflammation measured by PET CT. We previously described that lack of new granuloma formation and a stable metabolic activity measured by FDG in granulomas and lymph nodes early

post-infection could predict which macaques will develop LTBI at 6 months post-infection [119]. Macaques in the drug-treated group were given anti-TB drugs orally once daily for ~3 months (80-97 days) (RIF 20mg/kg; INH 15mg/kg; ETH 50mg/kg; PZA 150mg/kg) [268]. Compliance ranged from 80-98% although one macaque had low compliance (30416, 62%). Macaques were taken off drug treatment 2-4 weeks before the second infection with Mtb library B and subsequently necropsied 4 weeks later. The macaques in the non-drug treated group followed the same timeline as the drug-treated group but without drug treatment. Macaques received 14-16 CFU of Mtb library A for the first infection and 8-9 CFU of Mtb library B for the second infection. Dose was calculated from colony counts after plating an aliquot of the infection inoculum on 7H11 agar plates and incubating for 3 weeks at 37°C/5% CO₂. Historical controls from a previous Mtb reinfection study [264] were used as comparison in some parameters.

3.2.3 Bronchoalveolar lavage (BAL)

BAL was obtained every 8 weeks as described previously [231, 233]. Briefly, a bronchoscope with a 2.5 mm outer diameter was inserted into the trachea of a sedated animal and placed in the right middle or lower lobe. A saline solution (40ml) was introduced briefly, suctioned and transferred to a 50ml conical tube. An aliquot was used to plate for CFU on 7H11 agar which was read after 3 weeks of incubation at 37°C/5% CO₂. BAL were centrifuged at 1,800 rpm for 8 minutes at 4°C. Cells were resuspended in 1ml PBS, counted using a hemocytometer and used for intracellular cytokine staining. Supernatants were filtered with 0.22µm syringe filter to remove Mtb bacteria and frozen at -80°C until use for Luminex.

3.2.4 Necropsy Procedures

Procedures done during necropsy have been previously described [231, 232]. Briefly, 1-3 days prior to necropsy, a PET CT scan was taken and used to identify the location and metabolic activity (FDG activity) of granulomas and lymph nodes; this scan was used as a map to aid in the individual identification and excision of these samples during necropsy. On the day of necropsy, macaques were humanely sacrificed with sodium pentobarbital injection and terminally bled. Individual granulomas, thoracic and peripheral lymph nodes, lung tissue, spleen and liver were all excised and homogenized separately into single cell suspensions. Homogenates were aliquoted for plating on 7H11 agar for bacterial burden, freezing for DNA extraction and staining for flow cytometry analysis. Any remaining samples were frozen for future use. Homogenates were plated in serial dilutions on 7H11 medium and incubated at 37°C/5% CO₂ for 3 weeks before enumeration of CFU.

3.2.5 Isolation of genomic DNA from bacteria

DNA extraction was performed on granuloma and lymph node homogenates, as well as their scrapates (scraped colonies that grew on 7H11 agar plates) for library identification as described previously [118]. Briefly, a small aliquot of the homogenate or scrapate were vortexed with 0.1mm zirconia-silica beads (BioSpec Products, Inc.) and subsequently extracted twice with phenol chloroform isoamyl alcohol (25:24:1, Sigma-Aldrich) before precipitating DNA with molecular grade 100% isopropanol (Sigma-Aldrich) and 3M sodium acetate (Sigma-Aldrich) and resuspending in nuclease-free water (Invitrogen).

3.2.6 Library identification

Identification of library DNA tags have been previously described [264]. Briefly, DNA was amplified by PCR for 24-36 cycles before using in the NanoString nCounter assay (NanoString Technologies) with custom designed probes. The scheme for labeling granulomas as old or new is found in Table 1.

Table 1. Granuloma classification scheme

| PET CT* | Library | Classification |
|---------|---------|----------------|
| old | A | old |
| old | B | new |
| new | A | old |
| new | B | new |
| old/new | A + B | new |
| unknown | A | old |
| unknown | B | new |
| old | No data | old |
| new | No data | new |

* granuloma was noted on PET CT scan during first infection (old) or only after second infection (new). Unknown: granuloma was not seen on PET CT scan, possibly due to size or inability to discriminate from other granulomas in close proximity.

3.2.7 Intracellular cytokine staining and flow cytometry

Intracellular cytokine staining was performed on BAL and individual granuloma samples, involved lymph nodes (with granuloma either by gross inspection or microscopy and/or CFU+) and uninvolved lung lobes (no granulomas and CFU-). BAL cells (250,000-1x10⁶) were stimulated with peptide pools of ESAT-6 and CFP-10 (10µg/ml of each peptide pool) in the presence of Brefeldin A (GolgiPlug, BD Biosciences) at 37°C/5% CO₂ for 3.5-4 hours prior to staining.

Unstimulated controls were always included, however, positive controls (phorbol dibutyrate [PdBu] and ionomycin [231]) were only included if there were enough cells. Cells were stained with a viability marker (LIVE/DEAD fixable blue dead cell stain kit, Invitrogen) and surface and intracellular markers. Surface markers for T cells include CD3 (clone SP34-2, BD Pharmingen), CD4 (Clone L200, BD Horizon) and CD8 (Clone SK1, BD Biosciences). Intracellular markers include IFN γ (Clone B27, BD Biosciences), TNF (Clone MAB11, BD Biosciences), IL-2 (Clone MQ1-17H12, Biolegend), IL-10 (Clone JES3-9D7, eBioscience) and Ki67 (Clone B56, BD Biosciences). Data was acquired using the LSR II (BD) and analyzed using FlowJo software v10.6.1 (BD).

Because of the abundance of Mtb antigens already present in granulomas and involved lymph nodes [121], these samples were not further stimulated with Mtb peptides. Due to low number of cells, uninvolved lung lobes were also not stimulated. All samples were incubated in the presence of Brefeldin A (GolgiPlug, BD Biosciences) at 37°C/5% CO₂ for 3.5-4 hours prior to staining. Cells were stained with a viability marker (LIVE/DEAD fixable blue dead cell stain kit, Invitrogen) and surface and intracellular markers. Surface markers include CD3 (clone SP34-2, BD Pharmingen), CD4 (Clone L200, BD Horizon), CD8 (Clone SK1, BD Biosciences) and CD20 (Clone 2H7, eBioscience). Intracellular markers include CD107a (Clone H4A3, Biolegend), IFN γ (Clone B27, BD Biosciences), TNF (Clone MAB11, BD Biosciences), IL-2 (Clone MQ1-17H12, Biolegend), IL-10 (Clone JES3-9D7, eBioscience) and IL-17 (Clone eBio64CAP17, eBioscience). Data was acquired using the LSR II (BD) and analyzed using FlowJo software v10.6.1 (BD).

3.2.8 Luminex on BAL samples

Frozen supernatants were thawed on ice and concentrated using a centrifugation filter unit (Amicon Ultra-4 Centrifugal Filter Unit, 3kDa cutoff, Millipore Sigma) following manufacturer's instructions. Samples were assayed in duplicates using the ProcartaPlex NHP multiplex immunoassay (Invitrogen) following manufacturer's instructions measuring levels of 30 cytokines and chemokines using the BioPlex reader (Biorad). An additional 2-fold dilution was performed on the supplied standards to extend its lower detection limit.

3.2.9 Statistical Analysis

We used D'Agostino & Pearson test to determine normality of data, but due to small sample sizes, nonparametric tests were used. The Mann-Whitney test was used to compare 2 groups. The Kruskal-Wallis test with Dunn's adjustment for multiple comparisons was used to compare 3 or more groups. P values < 0.05 were considered statistically significant. Data were graphed and analyzed using GraphPad Prism v8 (GraphPad Software). All CFU data in graphs with the y-axis in log scale were transformed by adding 1.

3.3 Results

3.3.1 Drug treatment sterilized most macaques

To determine whether live bacteria were necessary in the protection a primary Mtb infection confers to a second infection, 10 cynomolgus macaques were divided into 2 groups (Figure 4A). Sixteen weeks after initial infection with Mtb library A, one group (n=7) was treated with anti-TB drugs (RIF, INH, ETH, PZA) for ~3 months (80-97 days) before the second infection with Mtb library B. The control group (n=3) followed the same timeline but was not given any anti-TB drugs. By PET CT, drug treatment reduced metabolic activity in lung granulomas and lymph nodes (Fig 4B). Total lung inflammation decreased in majority of the animals during the drug treatment period (Fig 4C). Macaques in the non-drug treated group had stable lung metabolic activity throughout the study (Fig 4D). The y-axis is in log scale and a change from 100 to 0 and vice versa is not considered significant in FDG activity.

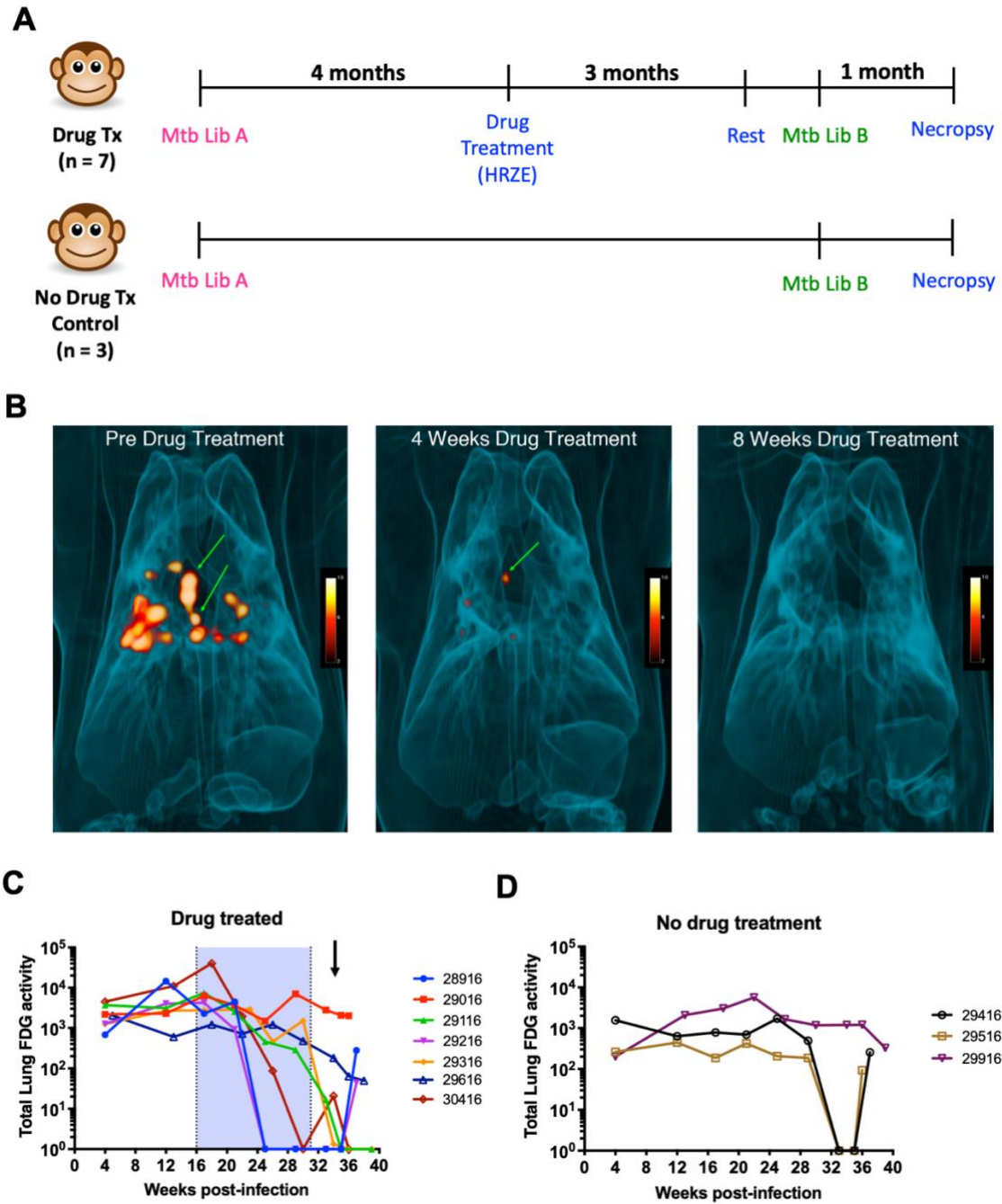


Figure 4. Drug treatment reduced metabolic activity in lung granulomas and lymph nodes of macaques.

A. Experimental plan. B. 3D rendering of the thoracic cavity of a macaque pre- and post-drug treatment. Green arrow points to lymph nodes. C. Total lung metabolic activity in drug-treated

macaques. Area shaded light blue indicates drug treatment period. Arrow indicates second infection. D. Total lung metabolic activity in non-drug treated macaques.

To evaluate the sterilizing efficacy of our drug regimen, we determined whether any of the scrapates (colonies scraped from 7H11 agar plates) from the drug treated monkeys were Mtb library A. Drug treatment sterilized 5 of 7 macaques. The remaining 2 macaques still had live Mtb library A, however, each monkey only had 1 CFU+ tissue and the CFU was very low (10 CFU in a lung granuloma of 29116 and 20 CFU in a lymph node of 29616) (Figure 5). Macaques that did not receive drug treatment also had live Mtb library A strains (Figure 5).

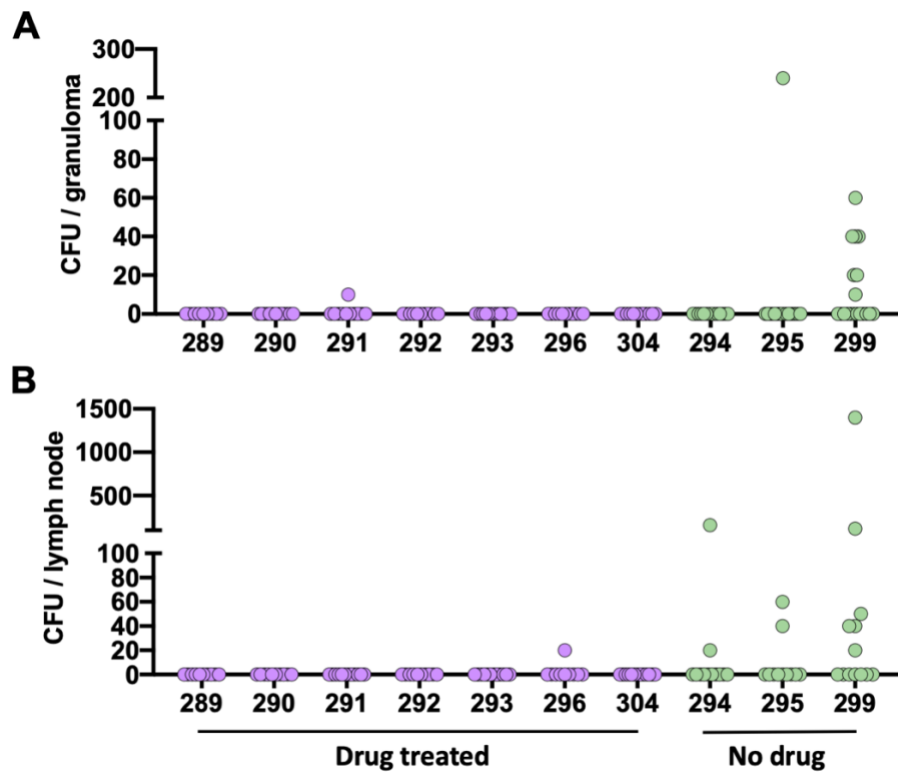


Figure 5. Drug treatment sterilized majority of the drug-treated macaques.

A. Bacterial burden of lung granulomas with Mtb library A. B. Bacterial burden of lymph nodes with Mtb library A.

3.3.2 Drug treatment does not abolish protection from second infection

Our primary outcome measures to determine whether a macaque was protected from the second infection are the number of and bacterial burden in granulomas attributed to the second infection (i.e. new granulomas) by PET CT and/or Mtb library B confirmation. Both groups formed fewer new granulomas 4 weeks after the second infection compared to 4 weeks after the initial infection using a similar dose (14-16 CFU – 1st dose, 8-9 CFU – 2nd dose) (Figure 6A). There was no significant difference in the reduction of the number of granulomas formed at 4 weeks post-second infection between the 2 groups (Figure 6A). The number of new granulomas (Figure 6B) and bacterial burden (Figure 6C) in both groups were not significantly different. Historical controls used in this study are naïve and 16-week reinfection controls from [264]. The naïve group only received Mtb library B infection and was necropsied 4 weeks after. The 16-week reinfection group received Mtb library A as the first infection followed by Mtb library B infection 16 weeks after. They were necropsied 4 weeks after Mtb library B infection. Even though the number of new granulomas formed in the drug treated and non-drug treated groups were similar with the 16-week reinfection group, the bacterial burden in the new granulomas of the 16-week reinfection group was lower. The median CFU of new granulomas of both drug- and non-drug treated groups was ~60-fold lower compared to the median CFU of the naïve controls, however this was not statistically significant (Figure 6C). The protection observed in both groups was not as robust as the historical 16-week reinfection control animals (Figure 6C). One animal (29416) in the non-drug treated group did not form any new granulomas. The CFU of new granulomas in each macaque is shown in Figure 3D. Similar to the 16-week reinfection animals, thoracic lymph nodes were protected from Mtb library B infection. Of 10 animals, only 4 (3 in drug-treated; 1 in non-drug treated) macaques had 1 lymph node CFU+ for Mtb library B (Figure 6E). These data suggest

that elimination of live Mtb by drug treatment does not abolish the protection a primary Mtb infection confers to a second infection. However, the protection in both drug treated and non-drug treated groups were not as robust as the protection seen in the 16-week reinfection animals.

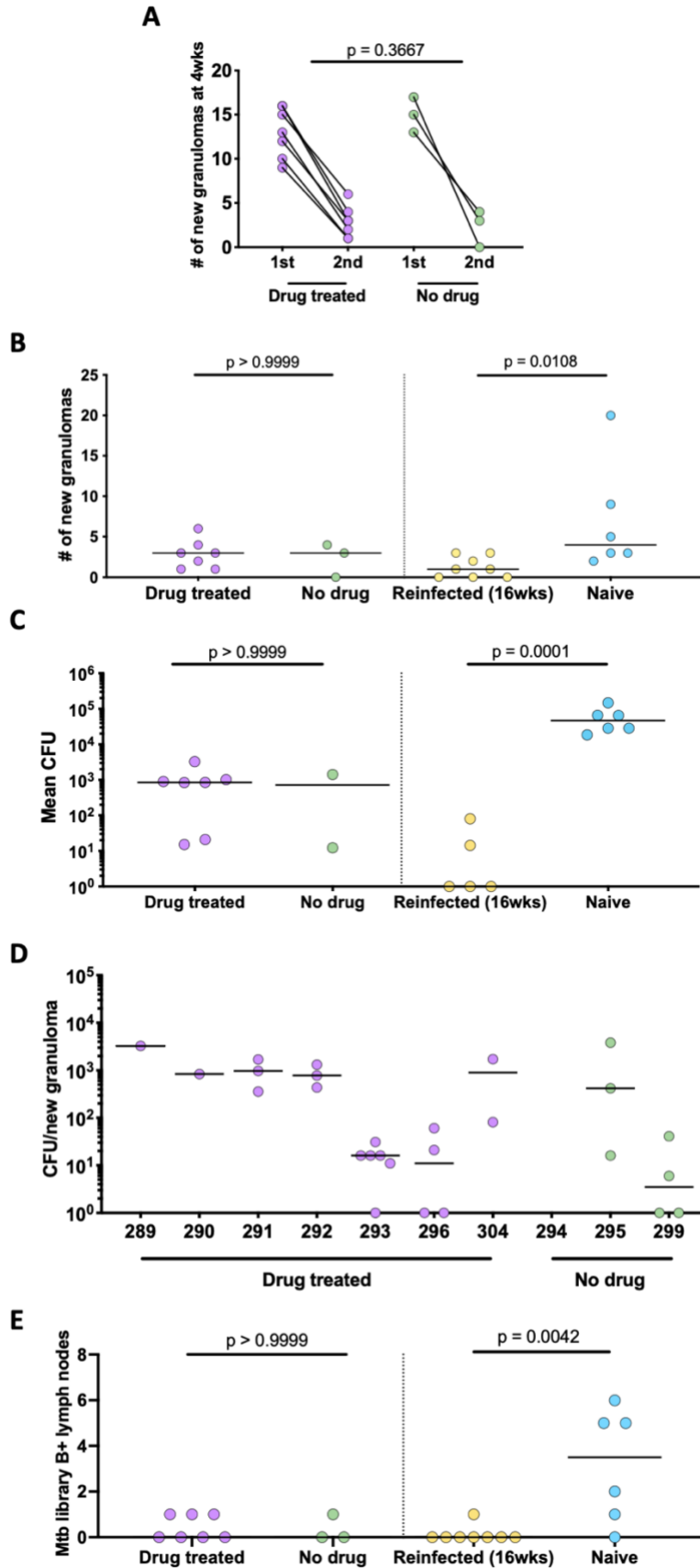


Figure 6. Drug treatment does not abolish protection from second infection.

A. Number of granulomas formed 4 weeks after the first and second infection. Each data point is a monkey. Mann-Whitney test was used to compare the change in number of granulomas formed from the first and second infection. B. Number of new granulomas that formed after the second infection. The reinfected (16wks) and naïve groups are historical controls from an earlier study [264] that were added for comparison. Each data point is a monkey. Kruskal-Wallis with Dunn's multiple comparison test was used to compare the groups. C. Mean total CFU of new granulomas formed after second infection. The reinfected (16wks) and naïve groups are historical controls from an earlier study [264] that were added for comparison. Each data point is a monkey. Kruskal-Wallis with Dunn's multiple comparison test was used to compare the groups. D. CFU of new granulomas per macaque in both groups. Each data point is a granuloma. E. Number of thoracic lymph nodes that were CFU+ for Mtb library B. The reinfected (16wks) and naïve groups are historical controls from an earlier study [264] that were added for comparison. Each data point is a monkey. Kruskal-Wallis with Dunn's multiple comparison test was used to compare the groups.

3.3.3 Drug treatment does not change lymphocyte populations and cytokine response in airways

We next investigated whether drug treatment changes the airway immune environment by interrogating lymphocyte populations, cytokine production and proliferation in response to Mtb-specific antigens ESAT-6 and CFP-10, pre- and post-drug treatment, using flow cytometry for surface markers with intracellular cytokine staining. There was no change in the number of lymphocytes per ml of BAL in both drug-treated and non-drug treated groups pre- and post-drug treatment (Figure 7A). Similarly, no changes occurred in the number of CD4 and CD8 T cells per

ml BAL from pre- to post-drug treatment (Figure 7B-C). When comparing between groups, we did not find any significant change in the frequency of lymphocytes, CD4 and CD8 T cells in the BAL that was due to drug treatment (Figure 7). Some macaques had a large decrease in the frequency of CD4 T cells producing $\text{IFN}\gamma$, IL-2 and $\text{TNF}\alpha$ in the drug treated group (Figure 8). However, overall, there was no significant difference in cytokine response and proliferation in CD4 (Figure 8) and CD8 T cells (Figure 9) in the BAL between the 2 groups indicating that drug treatment did not result in a significant change in the airway lymphocyte environment.

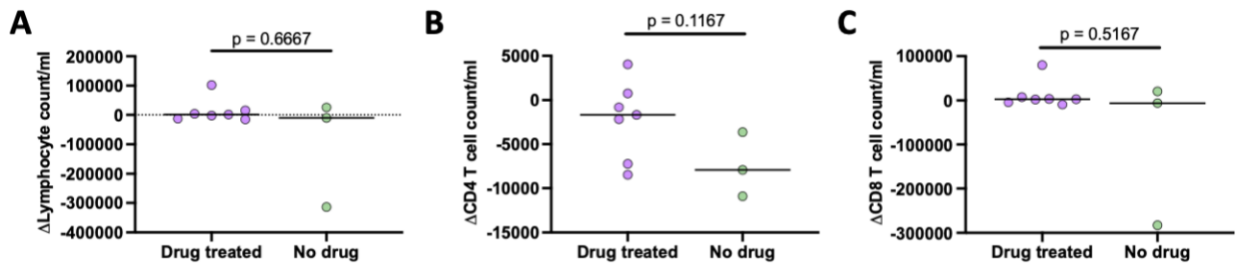


Figure 7. No significant difference in lymphocyte populations in airways of the 2 groups from pre- to post-drug treatment.

A. Change between the lymphocyte count/ml of BAL pre-drug treatment and post-drug treatment.

B. Change between the CD4 T cell count/ml of BAL pre-drug treatment and post-drug treatment.

C. Change between the CD8 T cell count/ml of BAL pre-drug treatment and post-drug treatment.

Each data point is a monkey. Lines at median. Mann-Whitney test was used to compare the groups.

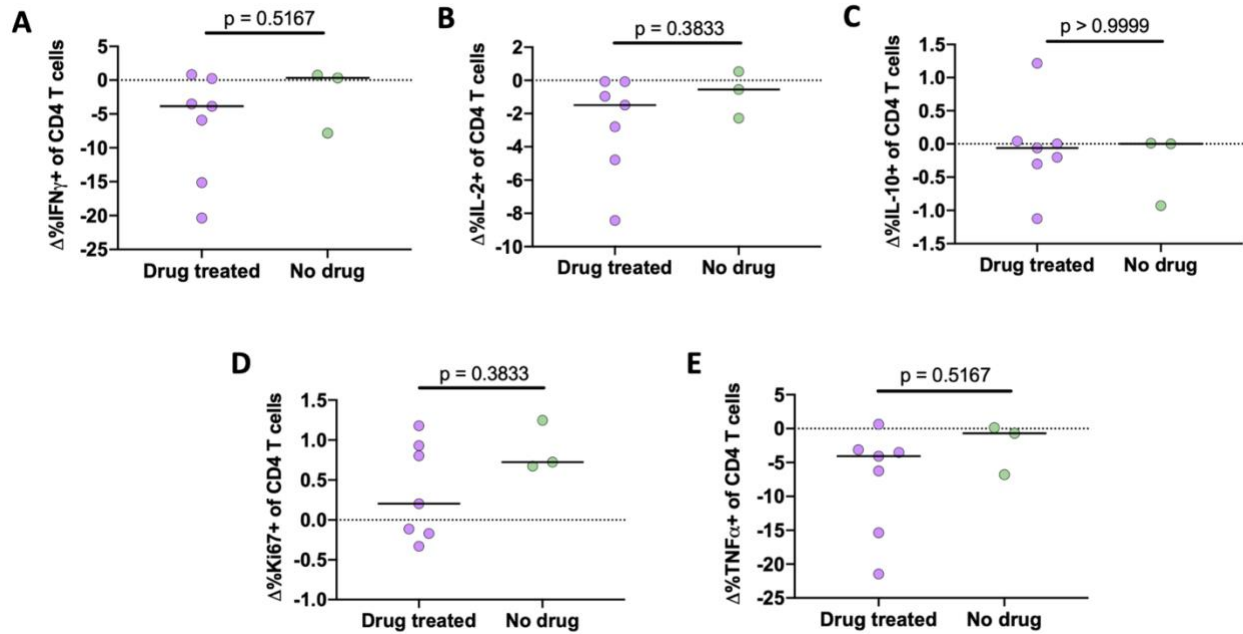


Figure 8. Similar changes in cytokine response of CD4 T cells to Mtb-specific antigens from pre- to post-drug treatment.

A. Change in frequency of $IFN\gamma^+$ CD4 T cells from pre- to post-drug treatment. B. Change in the frequency of $IL-2^+$ CD4 T cells from pre- to post-drug treatment. C. Change in the frequency of $IL-10^+$ CD4 T cells from pre- to post-drug treatment. D. Change in the frequency of $Ki67^+$ CD4 T cells from pre- to post-drug treatment. E. Change in the frequency of $TNF\alpha^+$ CD4 T cells from pre- to post-drug treatment. Each data point is a monkey. Lines at median. Media subtracted. Mann-Whitney test was used to compare the groups.

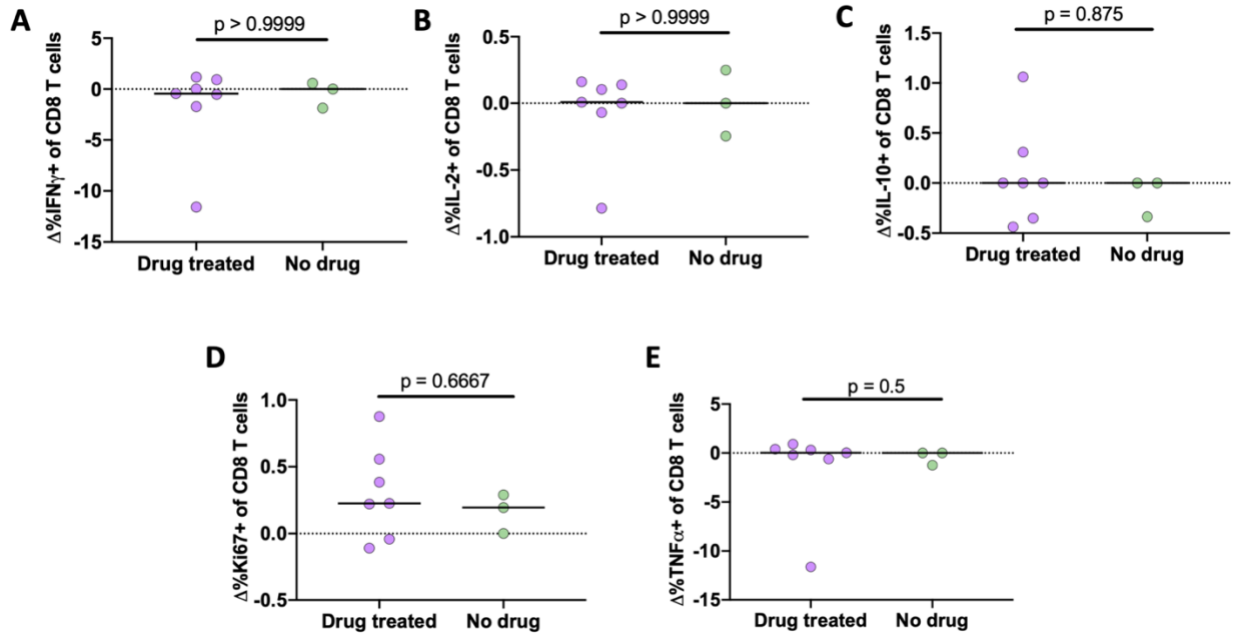


Figure 9. Similar changes in cytokine response of CD8 T cells to Mtb-specific antigens from pre- to post-drug treatment.

A. Change in the frequency of IFN γ + CD8 T cells from pre- to post-drug treatment. B. Change in the frequency of IL-2+ CD8 T cells from pre- to post-drug treatment. C. Change in the frequency of IL-10+ CD8 T cells from pre- to post-drug treatment. D. Change in the frequency of Ki67+ CD8 T cells from pre- to post-drug treatment. E. Change in the frequency of TNF α + CD8 T cells from pre- to post-drug treatment. Each data point is a monkey. Lines at median. Media subtracted. Mann-Whitney test was used to compare the groups.

To determine whether there was a difference in the airway immune environment pre-second infection in both groups, we examined lymphocyte populations, cytokine response and proliferation in response to ESAT-6 and CFP-10. In addition, we did a multiplex immunoassay (Luminex) on the BAL supernatants pre-second infection. There was no significant difference in the lymphocyte, CD4 and CD8 T cell counts between the two groups (Figure 10). There was also

no significant difference in the cytokine response and proliferation of CD4 (Figure 11) and CD8 T cells (Figure 12) between the two groups. Levels of two chemokines, B lymphocyte chemoattractant (BLC) and macrophage inflammatory protein-1 beta (MIP-1 β), and 1 cytokine, monokine induced by IFN γ (MIG), were significantly higher in the non-drug treated group (Figure 13 B-D). Levels of interferon-inducible T cell alpha chemoattractant (I-TAC) and IL-1 β also trended to be higher in the non-drug treated group albeit not statistically significant (Figure 13A and 13E). Data on other cytokines and chemokines tested that were not statistically different between the two groups is in Figure 14. These data suggest that the airway lymphocyte environment was similar in macaques regardless of drug treatment immediately prior to the second infection. Macaques in the non-drug treated group, however, had higher levels of proinflammatory chemokines and cytokine.

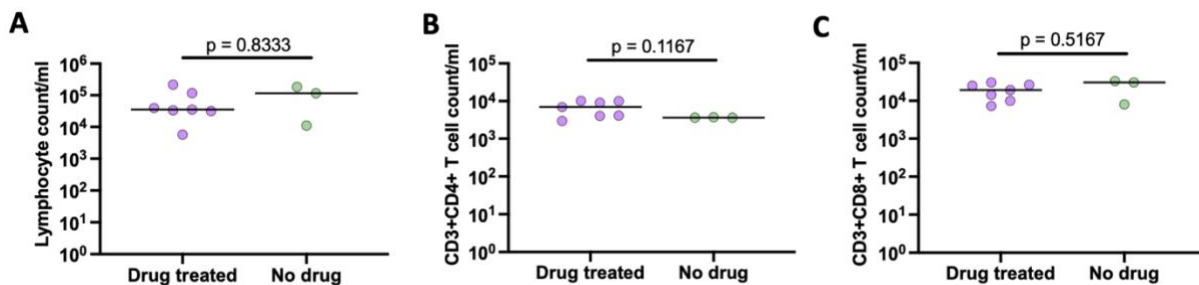


Figure 10. Similar counts of lymphocytes, CD4 T cells and CD8 T cells in BAL pre-second infection in both groups.

A. Lymphocyte count per ml of BAL. B. CD4 T cell count per ml of BAL. C. CD8 T cell count per ml of BAL. Each data point is a monkey. Lines at median. Mann-Whitney test was used to compare the groups.

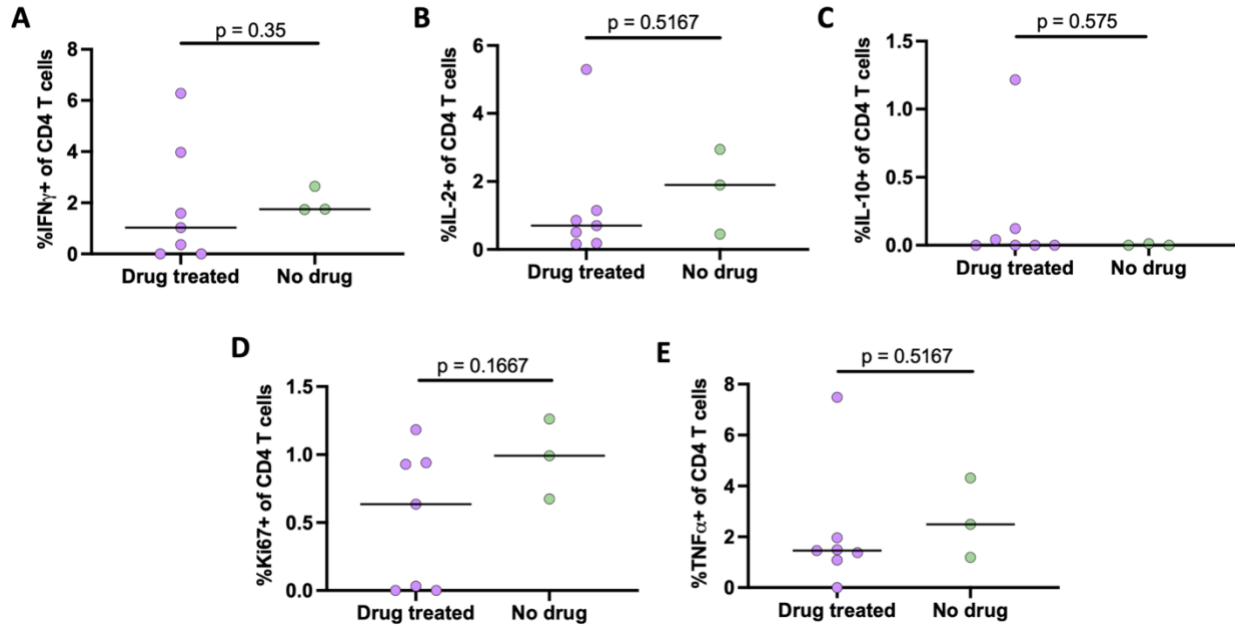


Figure 11. No difference in CD4 T cell cytokine response against Mtb-specific antigens pre-second infection between the 2 groups.

A. Frequency of IFN γ + CD4 T cells. B. Frequency of IL-2+ CD4 T cells. C. Frequency of IL-10+ CD4 T cells. D. Frequency of Ki67+ CD4 T cells. E. Frequency of TNF α + CD4 T cells. Each data point is a monkey. Lines at median. Mann-Whitney test was used to compare the groups.

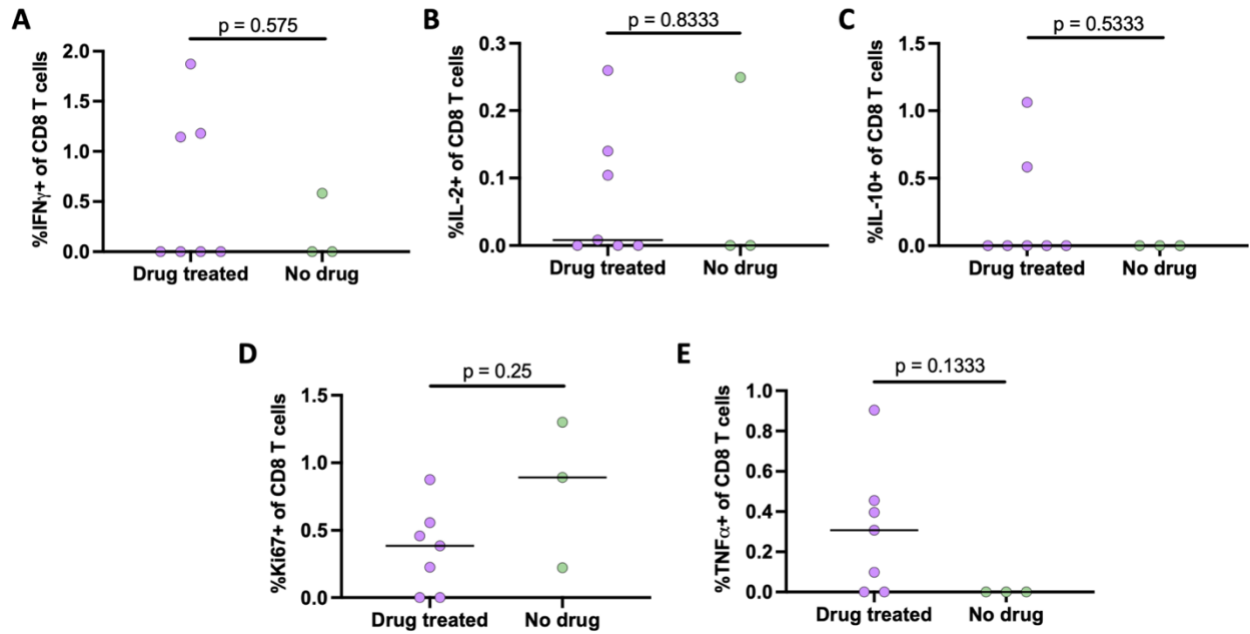


Figure 12. No difference in CD8 T cell cytokine response against Mtb-specific antigens pre-second infection between the 2 groups.

A. Frequency of IFN γ + CD8 T cells. B. Frequency of IL-2+ CD8 T cells. C. Frequency of IL-10+ CD8 T cells. D. Frequency of Ki67+ CD8 T cells. E. Frequency of TNF α + CD8 T cells. Each data point is a monkey. Lines at median. Mann-Whitney test was used to compare the groups.

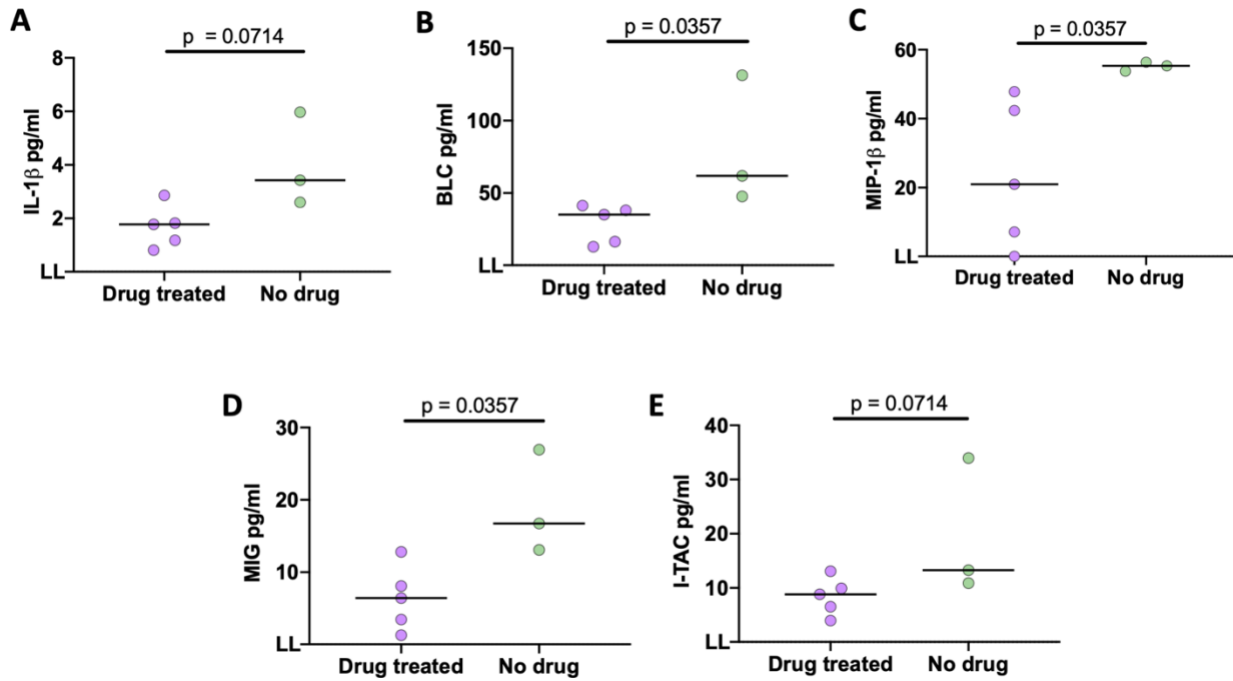


Figure 13. Non-drug treated group had higher levels of proinflammatory chemokines and cytokine.

A. IL-1 β . B. B lymphocyte chemoattractant (BLC). C. Macrophage inflammatory protein-1 beta (MIP-1 β). D. Monokine induced by IFN γ (MIG). E. Interferon-inducible T cell alpha chemoattractant (I-TAC). Each data point is a monkey. Lines at median. LL = lower limit of detection. Mann-Whitney test was used to compare the groups.

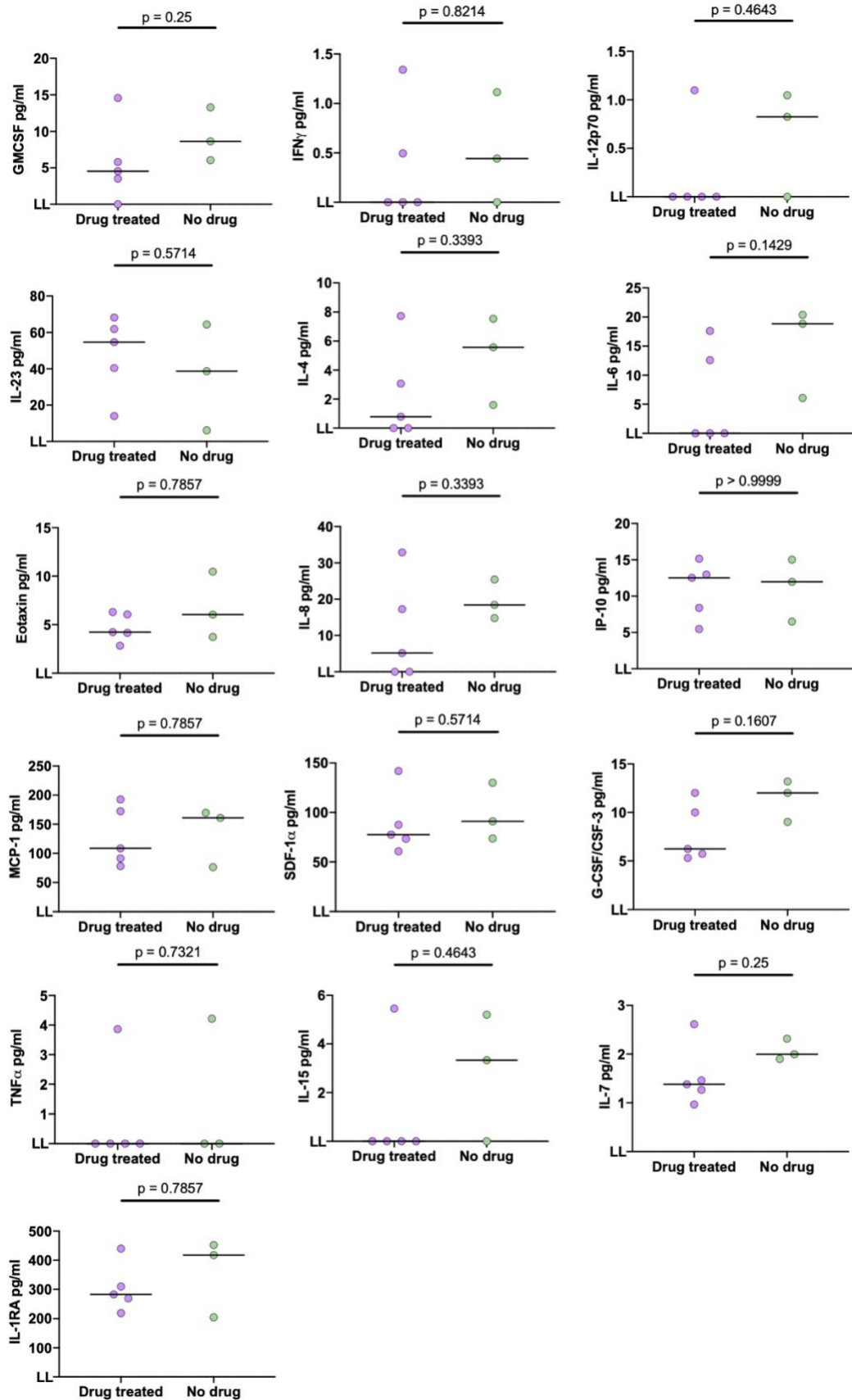


Figure 14. Cytokines and chemokines measured in BAL pre-second infection.

These were the analytes that were not significantly different between the groups. Each data point is a monkey. Lines at median. LL = lower limit of detection. Mann-Whitney test was used to compare the groups.

3.3.4 Similar immunological environment in new granulomas, involved lymph nodes and uninvolved lungs in both groups

To determine whether drug treatment affected the immune environment of new granulomas, involved lymph nodes (with granuloma either by gross inspection or microscopically and/or CFU+), and uninvolved lungs (no granuloma present in lobe and CFU-), we performed intracellular cytokine staining and flow cytometry after incubating them unstimulated for 3.5-4hrs at 37°C/5% CO₂. There was no difference in the frequencies of lymphocytes, CD3+ T cells, CD20+ B cells, CD4+ T cells and CD8+ T cells in the new granulomas (Figure 15). Similarly, no significant difference was found in the cytokine and cytotoxic response of CD4+ (Figure 16) and CD8+ T cells (Figure 17) in the new granulomas. Not all of the macaques had involved lymph nodes but comparing those that did have granuloma/s and/or were CFU+, we found no significant difference in the cytokine and cytotoxic response of CD4+ (Figure 18) and CD8+ T cells (Figure 19). Similar results were found in uninvolved lungs (Figure 20 and 21). The immune environment in new granulomas, involved lymph nodes and uninvolved lungs were similar in both groups suggesting that drug treatment had no effect on the immune environment in these tissues. One limitation is that the uninvolved lungs were not restimulated with peptides, which could have prevented us from measuring Mtb specific responses, as these lung lobes were not CFU+ at necropsy and therefore were not receiving endogenous stimulation.

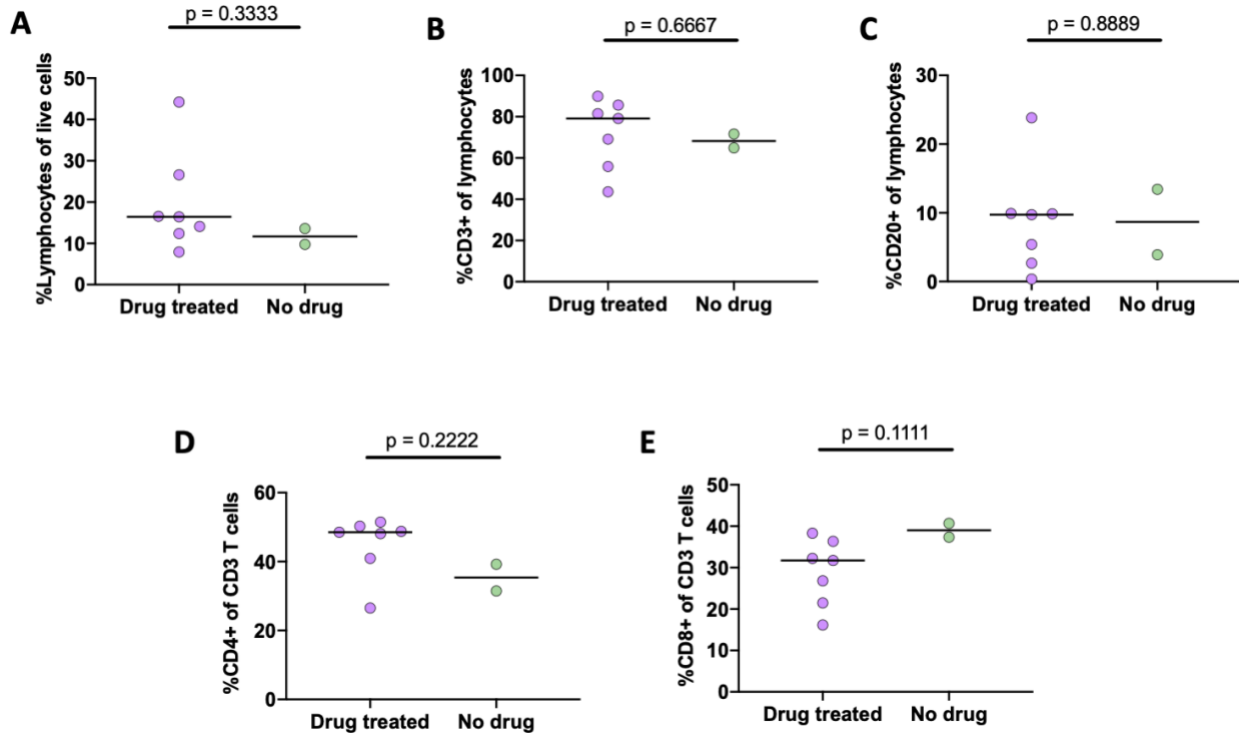


Figure 15. Similar levels of lymphocytes in new granulomas of both groups.

A. Frequency of lymphocytes of live cells. B. Frequency of CD3+ T cells of lymphocytes. C. Frequency of CD20+ B cells of lymphocytes. D. Frequency of CD4+ T cells of CD3+ T cells. E. Frequency of CD8+ T cells of CD3+ T cells. Each data point is a monkey. Lines at median. Mann-Whitney test was used to compare the groups.

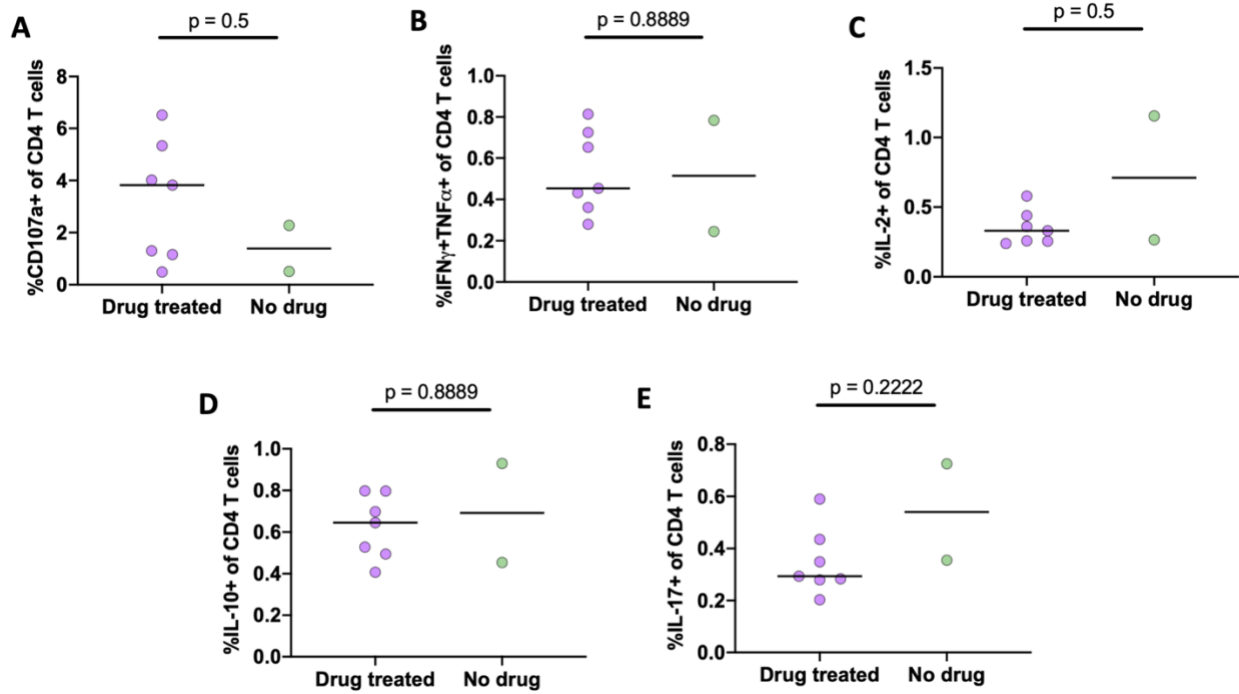


Figure 16. Similar CD4 T cell cytokine response in new granulomas from drug-treated and non-drug treated groups.

A. Frequency of CD107a+ CD4 T cells. B. Frequency of IFN γ + and/or TNF α + CD4 T cells. C. Frequency of IL-2+ CD4 T cells. D. Frequency of IL-10+ CD4 T cells. E. Frequency of IL-17+ CD4 T cells. Each data point is a monkey. Lines at median. Mann-Whitney test was used to compare the groups.

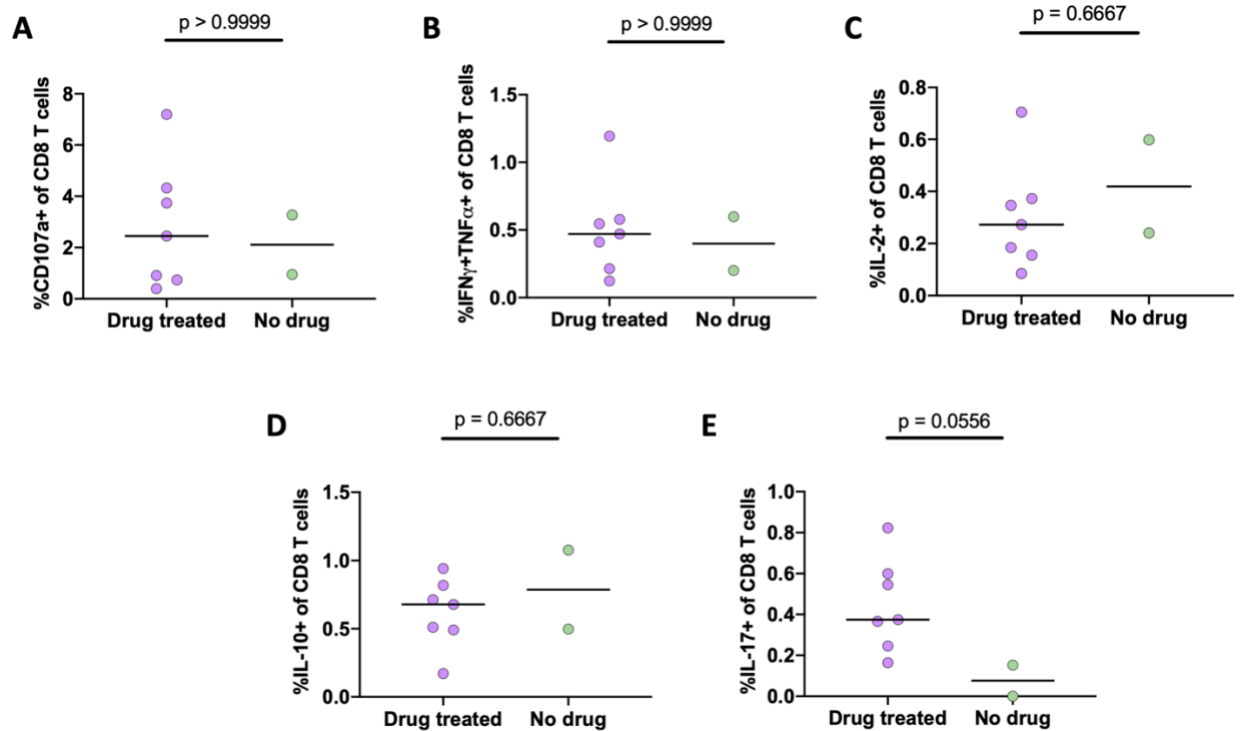


Figure 17. Similar CD8 T cell cytokine response in new granulomas from drug-treated and non-drug treated groups.

A. Frequency of CD107a+ CD8 T cells. B. Frequency of IFN γ + and/or TNF α + CD8 T cells. C. Frequency of IL-2+ CD8 T cells. D. Frequency of IL-10+ CD8 T cells. E. Frequency of IL-17+ CD8 T cells. Each data point is a monkey. Lines at median. Mann-Whitney test was used to compare the groups.

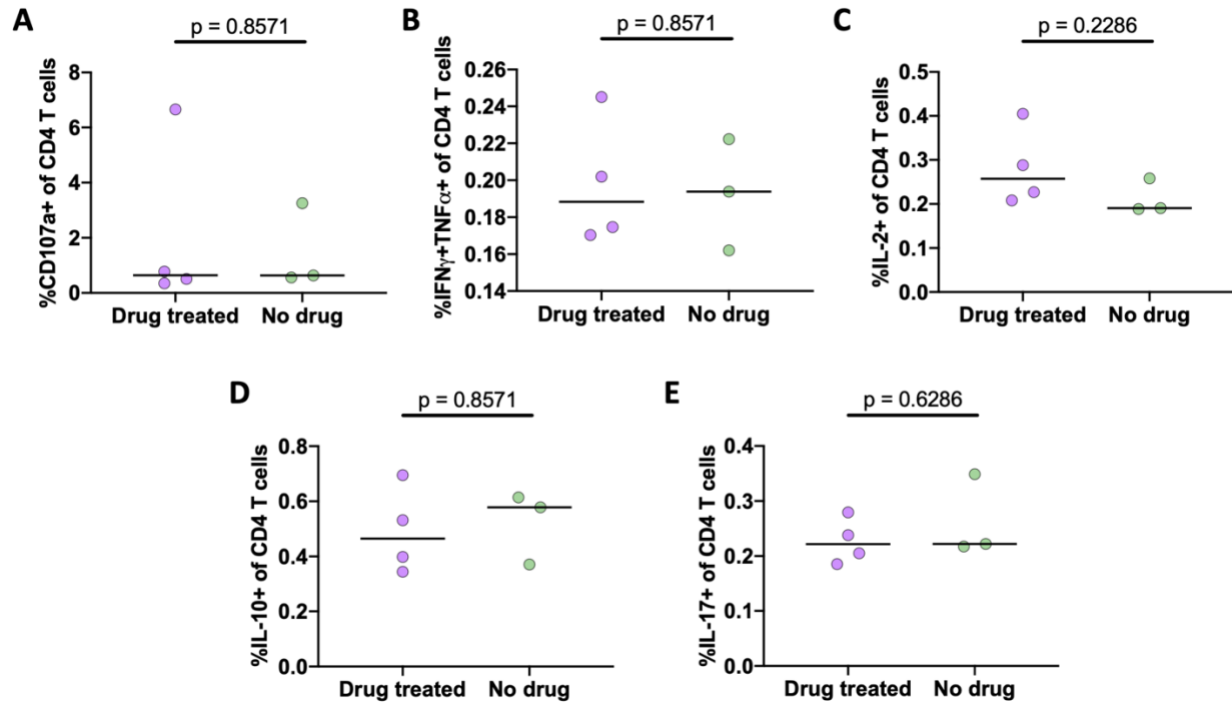


Figure 18. Similar CD4 T cell cytokine response in involved lymph nodes from drug-treated and non-drug treated groups.

A. Frequency of CD107a+ CD4 T cells. B. Frequency of IFN γ + and/or TNF α + CD4 T cells. C. Frequency of IL-2+ CD4 T cells. D. Frequency of IL-10+ CD4 T cells. E. Frequency of IL-17+ CD4 T cells. Each data point is a monkey. Lines at median. Mann-Whitney test was used to compare the groups.

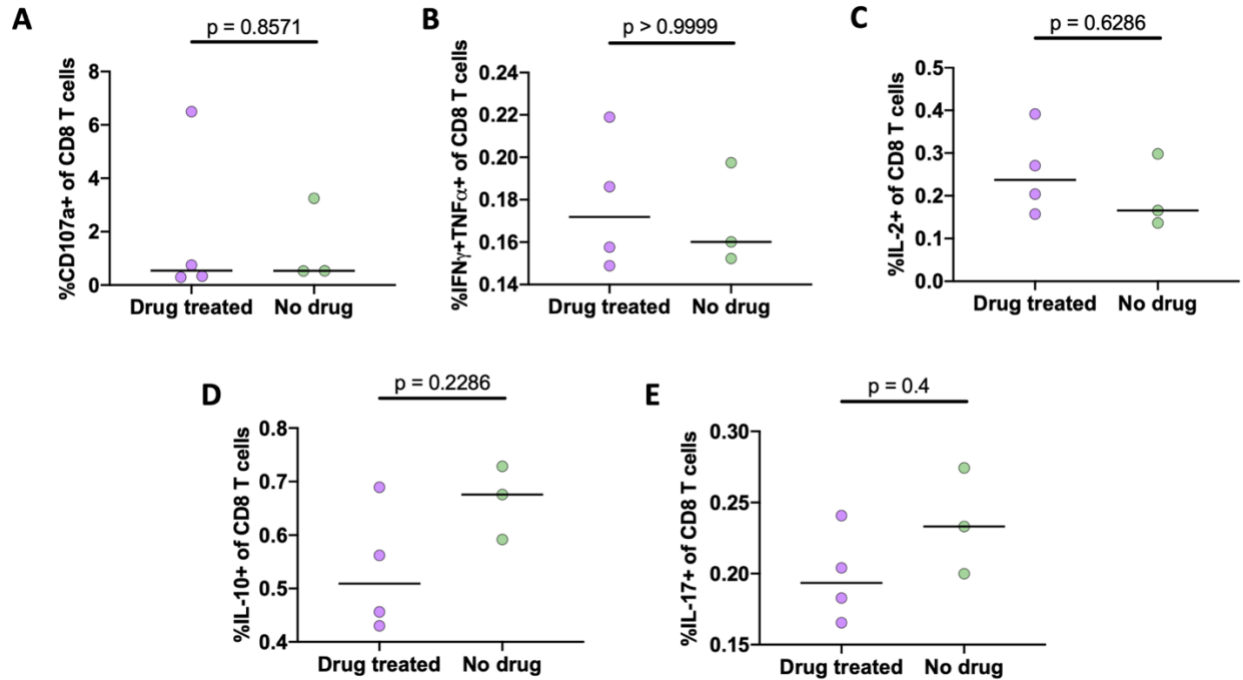


Figure 19. Similar CD8 T cell cytokine response in involved lymph nodes from drug-treated and non-drug treated groups.

A. CD107a+ CD8 T cells. B. IFN γ + and/or TNF α + CD8 T cells. C. IL-2+ CD8 T cells. D. IL-10+ CD8 T cells. E. IL-17+ CD8 T cells. Each data point is a monkey. Lines at median. Mann-Whitney test was used to compare treatment groups.

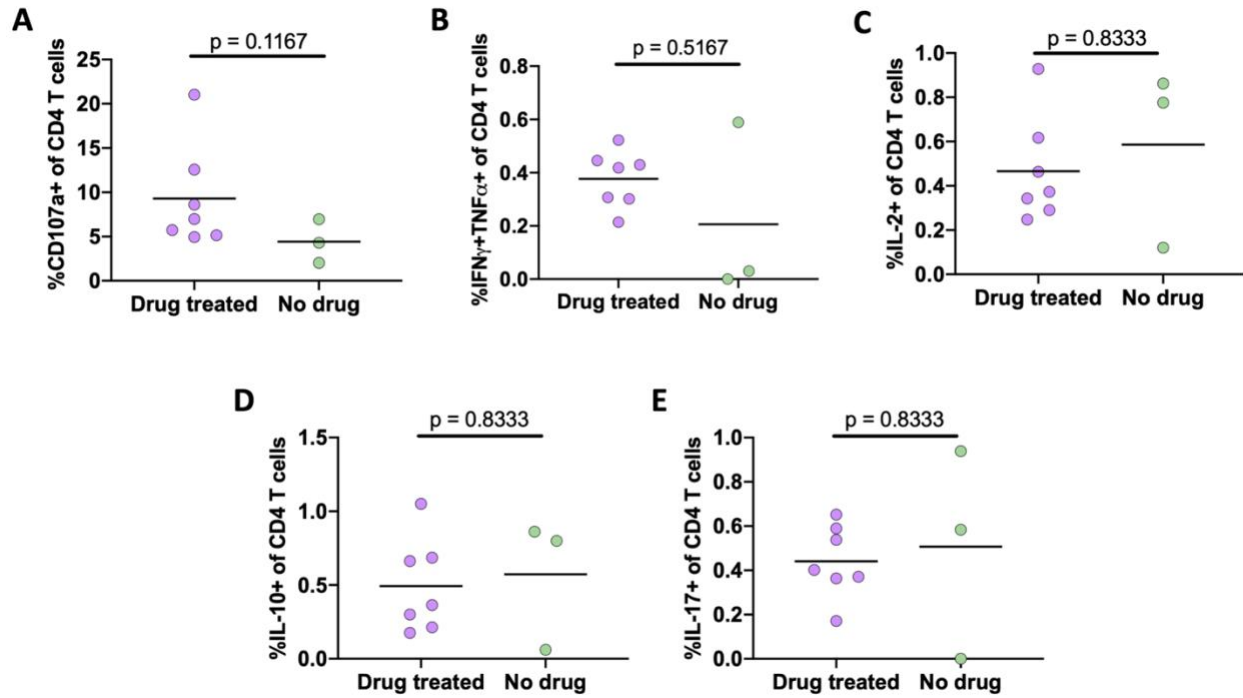


Figure 20. Similar CD4 T cell cytokine response in uninvolved lungs from drug-treated and non-drug treated groups.

A. CD107a+ CD4 T cells. B. IFN γ + and/or TNF α + CD4 T cells. C. IL-2+ CD4 T cells. D. IL-10+ CD4 T cells. E. IL-17+ CD4 T cells. Each data point is a monkey. Lines at median. Mann-Whitney test was used to compare treatment groups.

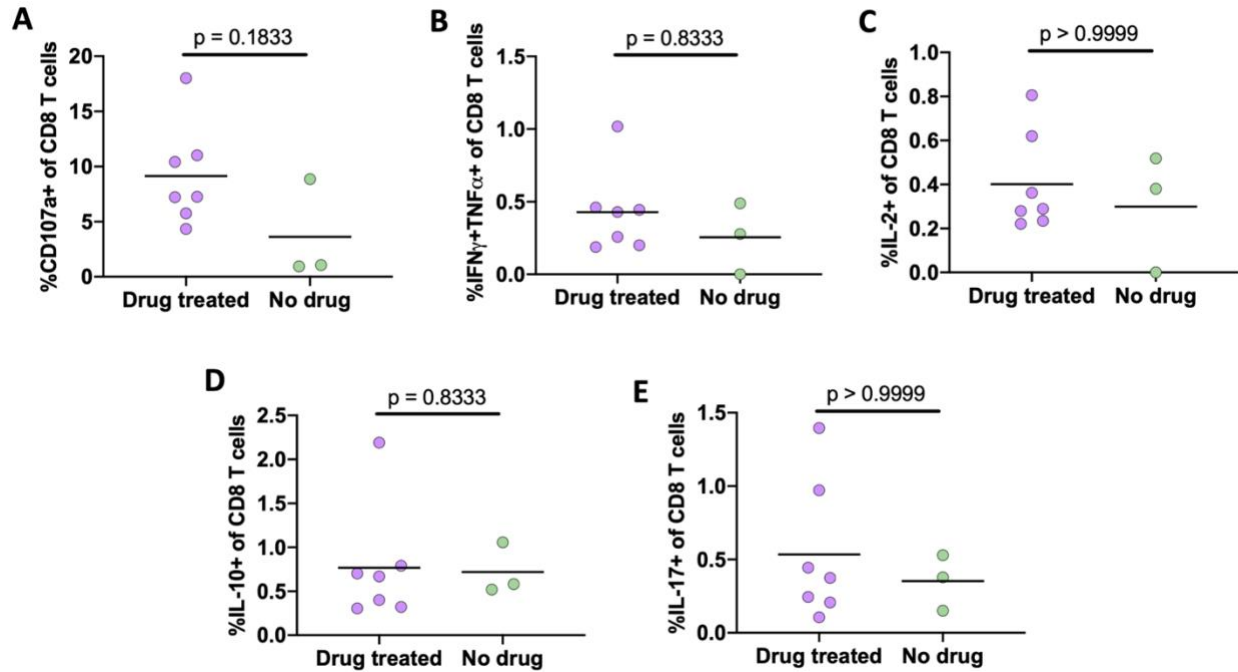


Figure 21. Similar CD8 T cell cytokine response in uninvolved lungs from drug-treated and non-drug treated groups.

A. CD107a+ CD8 T cells. B. IFN γ + and/or TNF α + CD8 T cells. C. IL-2+ CD8 T cells. D. IL-10+ CD8 T cells. E. IL-17+ CD8 T cells. Each data point is a monkey. Lines at median. Mann-Whitney test was used to compare treatment groups.

3.4 Discussion

Epidemiology studies on the incidence rate of recurrent TB disease in patients who were successfully drug treated begs the question of whether eliminating live Mtb bacilli by drug treatment somehow increases the risk of an individual to develop TB disease in succeeding exposures or infections. Here, we show that macaques that were drug treated had the same level

of protection as non-drug treated controls after second infection. Macaques from both groups developed fewer number of granulomas 4 weeks post-second infection compared to 4 weeks post-first infection when infected with a similar dose. The reduction in granuloma formation was similar in both groups. Macaques from both groups formed similar number and had similar bacterial burden in new granulomas. When compared to naïve controls, new granulomas from both drug and non-drug treated groups had ~60-fold lower CFU. However, the protection exhibited by the macaques in this study was not as robust as the 16-week reinfection controls.

One limitation of this study is the small number of animals in the non-drug treated controls. In addition, since we are testing protection, a macaque can be completely protected from the second infection (i.e. no new granuloma formation) like monkey 29416 in the non-drug treated group. Although that in itself is a result, it further reduces the number of data points from new granulomas that we can analyze. Even though 2 of 7 drug-treated macaques were not completely sterilized, it did not have an effect on the number of new granulomas formed and their bacterial burden compared to the macaques that were completely sterilized (Figure 3D). This study also focused on lymphocytes, especially T cells, which would cause us to miss any effect of drug treatment to the innate arm of the immune system, as well as the contribution of the innate immune cells to the protection we observed.

Similar to the 16-week reinfection controls, Mtb library B was not able to disseminate to and replicate in the lymph nodes of most animals in both drug-treated and non-drug treated groups. This suggests that Mtb library B was immediately killed or restricted when it entered the lungs. A recent NHP BCG vaccination study showed stunning protection when BCG was administered intravenously (IV-BCG) compared to intradermal or aerosol routes. Six of 10 IV-BCG vaccinated animals did not form any granulomas after Mtb infection with 3 of the remaining IV-BCG

vaccinated macaques forming ≤ 3 granulomas. The IV-BCG vaccinated group had an overall reduction of 100,000-fold in thoracic Mtb burden compared to animals vaccinated intradermally. Similar to the Mtb reinfection studies, 9 out of 10 rhesus macaques in the IV-BCG vaccinated group did not grow Mtb in any of their lymph nodes examined [63]. Based on the result of this study, the 16-week reinfection study [264], and the IV-BCG study [63], one characteristic of a successful vaccine is the ability to induce rapid killing of Mtb when it enters the lungs and to prevent Mtb from reaching the lymph nodes.

We have shown that lymph nodes serve as niches for Mtb persistence and growth during a primary infection (Chapter 5). These organs do not seem to play the same role during reinfection since Mtb library B rarely reaches the lymph nodes. T cell responses in involved lymph nodes were extremely low which could be explained by a large population of naïve T cells in these organs. However, even in lung granulomas, only a small proportion of T cells (~8%) produce cytokines [121]. Lymph nodes may not play an active role during the second infection, however, they are sources of Mtb-specific T cells primed during the first infection that home to the lungs which can also respond to the second infection. Lymph nodes have also been shown to be important in the development of protective immune responses against Mtb infection after BCG vaccination. Direct injection of BCG into lymph nodes of C57BL/6 mice generated significantly more proliferation and stronger TNF, IL-2, IL-17 and IFN γ responses in PPD-stimulated splenocytes compared to mice vaccinated subcutaneously. In addition, mice intralymphatically vaccinated had significantly reduced Mtb burden in the lungs and spleen up to 12 weeks after Mtb infection compared to subcutaneously vaccinated and unvaccinated mice [254]. IV-BCG vaccinated animals also had BCG infiltration and metabolic activity (probably activation of immune response) in thoracic lymph nodes and spleen which were not observed in animals

vaccinated via other routes (e.g. intradermal and aerosol). In both mice and NHP studies, BCG colonization of lung-draining lymph nodes is associated with protection from Mtb infection [63, 254].

We probed the immune environment of the airways since this is the first line of defense that Mtb will encounter and asked whether drug treatment changes this environment. In both drug-treated and non-drug treated groups, we did not observe any changes in the number of lymphocytes, CD4 and CD8 T cells in the BAL from pre- to post-drug treatment. We did not observe any significant change attributable to drug treatment in the frequency of lymphocytes, including CD4 and CD8 T cells, and T cell cytokine responses against Mtb-specific antigens, ESAT-6 and CFP-10, by flow cytometry. The lymphocyte populations investigated and their immune responses were similar in BALs of drug and non-drug treated groups before the second infection which could explain the similar protection observed in both groups. In a study by Condos and colleagues [269] of BAL immune responses in five patients with active TB, the level of IFN γ remained stable from baseline to 6 months post-drug treatment but increased after 12 months of drug treatment. TNF levels in 2 of 5 patients decreased from baseline to 6 months post-drug treatment while the remaining 3 patients had stable TNF levels. However, at 12 months after drug treatment, all patients had low levels of TNF in their BAL. Another study showed an increase in lymphocyte numbers in the BAL mostly due to an influx of CD4 T cells 8 weeks post-drug treatment in 5 patients with miliary TB. No cytokine response was recorded [270]. Studies comparing BAL responses before and after anti-TB drug treatment are fewer compared to studies comparing blood. However, blood responses do not necessarily correlate with local immune responses in the lungs [121]. Differences in the immune response to drug treatment in our study compared to the above-mentioned human studies could be explained by the following: (a) different

biological host (NHP vs human), (b) different treatment duration (3 months vs 2 months vs 6 and 12 months), (c) different instrumentation used (flow cytometry vs ELISA vs light microscopy for cell counting) and (d) low sample size.

Based on the results of this study, the increase in incidence of TB recurrence in successfully drug treated individuals in some studies [265-267] is most likely because of selection bias (i.e. selection of individuals with predisposition to Mtb infection and TB disease). However, there is one more important factor to consider as to why our study contradicts human epidemiology studies; and this is the timing of the second infection. In C57BL/6 mice, protection from the second infection after drug treatment only lasted for 30 days. On day 60, the protection waned resulting in the bacterial burden of reinfected mice matching those of the controls (one infection only) [263]. Human epidemiology studies also support the theory of waning protection after successful treatment. A study in Uganda showed that in both HIV-negative and HIV-positive individuals, TB recurrence due to relapse was more common and occurred early at 6.5 months after completion of drug treatment while TB recurrence due to reinfection occurred much later at 14.2 months post-drug treatment [271]. Similarly, in Cape Town, South Africa, reinfection accounted for only 20% (9/44) of recurrent cases in the first year after drug treatment completion. This increased to 66% (57/86) after the first year. This study found a strong association between relapse and earlier occurrence [272]. However, one study that analyzed extensive data from clinics in Cape Town, South Africa, found that the rate of Mtb reinfection and disease was highest in the first months after successful treatment. This rate rapidly declined by 2-3 years post-drug treatment and continued to decline until it reached the incidence rate of the general population at 10 years post-drug treatment [273]. In our study, we infected the macaques with Mtb library B (second infection) 2-4 weeks post-completion of drug treatment. We did not see any changes due to drug treatment

in the BAL lymphocyte compartment pre-second infection. However, we did observe higher levels of proinflammatory chemokines and cytokines in the BAL of non-drug treated macaques which could eventually influence recruitment of immune cells to the airways if given more time. Interestingly, the non-drug treated group appears to have diminished protection compared to the 16-week reinfection controls with the only difference being the longer time of the first infection in our study. Does this mean that the protection wanes from 16 weeks post-first infection to ~33 weeks post-first infection? However, due to our low sample size, we cannot make any solid conclusions. Questions about waning of protection and timing of second infection should be addressed in the future.

The hunt continues as to the mechanism of protection a first Mtb infection confers to a secondary challenge. Based on this study, live Mtb is not a requirement for this protection. However, the duration of this protection is currently unknown and needs to be studied. The role of immune cells, adaptive or innate, as well as antibodies, should also be examined. An unbiased approach like single cell RNA sequencing might prove useful in interrogating immune responses in different tissues. Whether this protection extends to different Mtb strains and different levels of virulence also remains to be investigated.

4.0 CD4 T cells are important in protecting against Mtb reinfection

4.1 Introduction

Protection against Mtb infection or disease is mostly attributed to the adaptive cellular immune response [176, 177]. HIV+ individuals have increased susceptibility to Mtb infection and disease highlighting the importance of CD4 T cells [178]. Indeed, in individuals with HIV infection, the incidence rate of TB increases as the peripheral CD4 T cell numbers decrease [274]. The importance of CD4 T cells was further reinforced by CD4 T cell depletion studies in mice [179-181] and non-human primates (NHP) [182, 183] where animals showed increased pathology, bacterial burden and reactivation of some macaques with LTBI. Reactivation in macaques was associated with greater CD4 T cell depletion in mediastinal lymph nodes [182], while greater CD4 T cell depletion in the blood was associated with early reactivation [252]. In addition, CD4 T cells producing IFN γ are key players in Mtb clearance by promoting phagosome-lysosome fusion and ROS production in macrophages [134, 176, 184, 185].

The mechanisms of protection against reinfection are not known. While the importance of CD4 T cells in TB have been demonstrated in humans with HIV/TB co-infection and animal models of CD4 T cell depletion, SIV infection and LTBI reactivation, their importance in protecting against Mtb reinfection has not been tested. Here, we show that CD4 T cells are important in the protection a primary drug treated Mtb infection confers to a secondary infection. CD4 T cell depleted macaques had higher Mtb burden in new granulomas compared to the IgG control animals. CD4 T cell depletion also promoted Mtb dissemination to the lymph nodes. However, our data supports that other factors are likely to be contributing to protection against

reinfection, as CD4 T cell-depleted reinfected macaques did not exhibit the same extent of Mtb burden as naïve animals.

4.2 Methodology

4.2.1 Ethics Statement

All experimental manipulations, protocols, and care of the animals were approved by the University of Pittsburgh School of Medicine Institutional Animal Care and Use Committee (IACUC). The protocol assurance number for our IACUC is A3187-01. Our specific protocol approval numbers for this project are 18063158 and 18124275. The IACUC adheres to national guidelines established in the Animal Welfare Act (7 U.S.C. Sections 2131–2159) and the Guide for the Care and Use of Laboratory Animals (8th Edition) as mandated by the U.S. Public Health Service Policy.

All macaques used in this study were housed at the University of Pittsburgh in rooms with autonomously controlled temperature, humidity, and lighting. Animals were singly housed in caging at least 2 square meters apart that allowed visual and tactile contact with neighboring conspecifics. The macaques were fed twice daily with biscuits formulated for nonhuman primates, supplemented at least 4 days/week with large pieces of fresh fruits or vegetables. Animals had access to water *ad libitem*. Because our macaques were singly housed due to the infectious nature of these studies, an enhanced enrichment plan was designed and overseen by our nonhuman primate enrichment specialist. This plan has 3 components. First, species-specific behaviors are encouraged. All animals have access to toys and other manipulata, some of which will be filled

with food treats (e.g. frozen fruit, peanut butter, etc.). These are rotated on a regular basis. Puzzle feeders, foraging boards, and cardboard tubes containing small food items also are placed in the cage to stimulate foraging behaviors. Adjustable mirrors accessible to the animals stimulate interaction between animals. Second, routine interaction between humans and macaques are encouraged. These interactions occur daily and consist mainly of small food objects offered as enrichment and adhere to established safety protocols. Animal caretakers are encouraged to interact with the animals (by talking or with facial expressions) while performing tasks in the housing area. Routine procedures (e.g. feeding, cage cleaning, etc) are done on a strict schedule to allow the animals to acclimate to a routine daily schedule. Third, all macaques are provided with a variety of visual and auditory stimulation. Housing areas contain either radios or TV/video equipment that play cartoons or other formats designed for children for at least 3 hours each day. The videos and radios are rotated between animal rooms so that the same enrichment is not played repetitively for the same group of animals.

All animals are checked at least twice daily to assess appetite, attitude, activity level, hydration status, etc. Following *M. tuberculosis* infection, the animals are monitored closely for evidence of disease (e.g., anorexia, weight loss, tachypnea, dyspnea, coughing). Physical exams, including weights, are performed on a regular basis. Animals are sedated prior to all veterinary procedures (e.g. blood draws, etc.) using ketamine or other approved drugs. Regular PET CT imaging is conducted on most of our macaques following infection and has proved very useful for monitoring disease progression. Our veterinary technicians monitor animals especially closely for any signs of pain or distress. If any are noted, appropriate supportive care (e.g. dietary supplementation, rehydration) and clinical treatments (analgesics) are given. Any animal

considered to have advanced disease or intractable pain or distress from any cause is sedated with ketamine and then humanely euthanized using sodium pentobarbital.

4.2.2 Animals, infections, CD4 T cell depletion and disease tracking by PET CT

Nineteen cynomolgus macaques (*Macaca fascicularis*) with age range of 5.8-9.1 years were obtained from Valley Biosystems (all males, Sacramento, California). Animals were placed in quarantine for 1 month where they were monitored to ensure good physical health and no prior Mtb infection. All animals were infected with DNA-tagged Mtb Erdman via bronchoscopic instillation as previously described [232, 233]. Thirteen macaques received Mtb library A as the first infection. Granuloma formation, lung inflammation and overall disease was tracked using ¹⁸F-fluorodeoxyglucose (FDG) PET CT every 4 weeks throughout infection. PET CT scans were analyzed using OsiriX viewer as previously described with a detection limit of 1mm [236]. The first infection was followed for 9 weeks before drug-treating all 13 macaques. Macaques were given anti-TB drugs orally once daily for 4-5 months (RIF 20mg/kg; INH 15mg/kg; ETH 50mg/kg; PZA 150mg/kg) [268]. Compliance ranged from 97-100%. The 13 macaques were matched by PET CT for disease status and randomized into 2 cohorts: CD4 T cell depletion (n=7) and IgG control (n=6). After resting for 4 weeks after drug treatment, CD4R1 (50mg/kg, NHP Reagent Resource), a rhesus recombinant CD4 T cell-depleting antibody, was administered subcutaneously in 4 animals and intravenously in 3 animals 1 week before the second infection with Mtb library B and then was administered intravenously every 2 weeks until necropsy. CD4 T cell depletion was monitored by flow cytometry in the blood and complete blood count weekly. To measure CD4 T cell depletion in tissues, a peripheral lymph node biopsy was performed before CD4 T cell depletion and the CD4 T cell level was compared with a peripheral lymph node from the same

macaque obtained at necropsy. Macaques from the IgG control group received rhesus recombinant IgG1 control antibody (50mg/kg, NHP Reagent Resource) following the same timeline of the CD4 T cell-depletion group. Six macaques were included as naïve controls infected with Mtb library B only.

Macaques received 4-12 CFU of Mtb library A for the first infection and 8-22 CFU of Mtb library B for the second infection (or the first infection for the naïve monkeys) (Table 2). Dose was calculated from colony counts after plating an aliquot of the infection inoculum on 7H11 agar plates and incubating for 3 weeks at 37°C/5% CO₂. Three macaques from a separate reinfection study (16 weeks Mtb library A followed by 4 weeks of Mtb library B, no drug treatment) were used as additional controls for some parameters, however, due to low sample size, they were not included in any statistical analyses.

Table 2. Animals used in CD4 T cell depletion study.

| Monkey ID | Group | Lib A infection date | Lib A dose | Drug start | Drug end | Antibody start | Lib B infection date | Lib B dose | New granuloma mean CFU | Total lung CFU | Total LN CFU |
|-----------|-------|----------------------|------------|------------|----------|----------------|----------------------|------------|------------------------|----------------|--------------|
| 12418 | IgG | 7/6/18 | 12 | 9/7/18 | 1/4/19 | 2/1/19 | 2/8/19 | 22 | 757 | 2750 | 320 |
| 12518 | IgG | 7/6/18 | 12 | 9/7/18 | 1/25/19 | 2/22/19 | 3/1/19 | 12 | 548 | 6060 | 105 |
| 12618 | IgG | 7/6/18 | 12 | 9/7/18 | 1/17/19 | 2/15/19 | 2/25/19 | 8 | 1584 | 17368 | 720 |
| 12718 | a-CD4 | 7/6/18 | 12 | 9/7/18 | 1/17/19 | 2/15/19 | 2/25/19 | 8 | 46707 | 195898 | 1800 |
| 12818 | a-CD4 | 7/6/18 | 4 | 9/7/18 | 1/25/19 | 2/22/19 | 3/1/19 | 12 | 6717 | 44350 | 210 |
| 12918 | Naïve | | | | | | 2/8/19 | 22 | 87529 | 615948 | 351020 |
| 13018 | Naïve | | | | | | 2/8/19 | 22 | 13550 | 110754 | 424000 |
| 13118 | Naïve | | | | | | 2/25/19 | 8 | 33935 | 543155 | 75425 |
| 13218 | a-CD4 | 7/6/18 | 12 | 9/7/18 | 1/4/19 | 2/1/19 | 2/8/19 | 22 | 4493 | 65040 | 4510 |
| 13318 | a-CD4 | 7/6/18 | 12 | 9/7/18 | 1/4/19 | 2/1/19 | 2/8/19 | 22 | 5275 | 30581 | 80 |
| 13418 | a-CD4 | 7/6/18 | 12 | 9/7/18 | 1/17/19 | 2/15/19 | 2/25/19 | 8 | 14003 | 159315 | 5895 |
| 13518 | a-CD4 | 7/6/18 | 12 | 9/7/18 | 1/25/19 | 2/22/19 | 3/1/19 | 12 | 32520 | 464550 | 5700 |
| 13618 | IgG | 7/6/18 | 4 | 9/7/18 | 1/17/19 | 2/15/19 | 2/25/19 | 8 | 1317 | 9220 | 0 |
| 13718 | Naïve | | | | | | 2/25/19 | 8 | 34882 | 352840 | 36000 |
| 13818 | Naïve | | | | | | 3/1/19 | 12 | 47026 | 848490 | 978980 |
| 13918 | Naïve | | | | | | 3/1/19 | 12 | 29404 | 329780 | 28295 |
| 14018 | IgG | 7/6/18 | 4 | 9/7/18 | 1/25/19 | 1/25/19 | 3/1/19 | 12 | 2131 | 12855 | 680 |
| 14118 | IgG | 7/6/18 | 4 | 9/7/18 | 1/4/19 | 2/1/19 | 2/8/19 | 22 | 2345 | 10800 | 30 |
| 14218 | a-CD4 | 7/6/18 | 4 | 9/7/18 | 1/25/19 | 2/22/19 | 3/1/19 | 12 | 5945 | 127550 | 33030 |

4.2.3 Antibody validation

To test whether the anti-CD4 depletion antibody masks CD4 receptors, peripheral blood mononuclear cells (PBMC) were incubated with 1X (0.77 mg/ml, the calculated concentration of α -CD4 antibodies in blood of macaques given a dose of 50mg/kg), 0.25X and 4X concentration of CD4 T cell-depleting antibody for 30 minutes at 37°C before surface staining with CD3 (clone SP34-2, BD Pharmingen), CD4 (Clone L200, BD Horizon) and CD8 (Clone RPA-T8, BD Biosciences) surface markers. PBMCs that were not incubated with the anti-CD4 antibody were included as a control. Data was acquired using the LSR II (BD) and analyzed using FlowJo software v10.6.1 (BD).

4.2.4 Bronchoalveolar lavage

BAL was obtained as described previously [231, 233]. Briefly, a bronchoscope with a 2.5 mm outer diameter was inserted into the trachea of a sedated animal and placed in the right middle or lower lobe. A saline solution (40ml) was introduced briefly, suctioned and transferred to a 50ml conical tube. An aliquot was used to plate for CFU on 7H11 agar which was read after 3 weeks of incubation at 37°C/5% CO₂. BAL were centrifuged at 1,800 rpm for 8 minutes at 4°C. Cells were resuspended in 1ml PBS, counted using a hemocytometer and used for intracellular cytokine staining.

4.2.5 Necropsy Procedures

Procedures done during necropsy have been previously described [231, 232]. Briefly, 1-3 days prior to necropsy, a pre-necropsy PET CT scan was taken and used to identify the location and metabolic activity (FDG activity) of granulomas and lymph nodes; this scan was used as a map to aid in the individual identification and excision of these samples during necropsy, including determination of old (post-first infection) and new (post-second infection) lesions (Figure 22). On the day of necropsy, macaques were humanely sacrificed with sodium pentobarbital and terminally bled. Individual granulomas, thoracic and peripheral lymph nodes, lung tissue, spleen and liver were all excised and homogenized separately into single cell suspensions. New granulomas determined by PET CT and uninvolved lung lobes (no granuloma present in the lobe) were enzymatically homogenized using a human tumor dissociation kit (Miltenyi Biotec) and a gentleMACS Dissociator (MiltenyiBiotec) following manufacturer's protocols. Homogenates were aliquoted for plating on 7H11 agar for bacterial burden, freezing for DNA extraction and staining for flow cytometry analysis. Any remaining samples were frozen for future use. Homogenates were plated in serial dilutions on 7H11 medium and incubated at 37°C/5% CO₂ for 3 weeks before enumeration of CFU. Lung homogenates physically homogenized were filtered with 0.22µm syringe filter to remove Mtb bacteria and frozen at -80°C until use for Luminex.

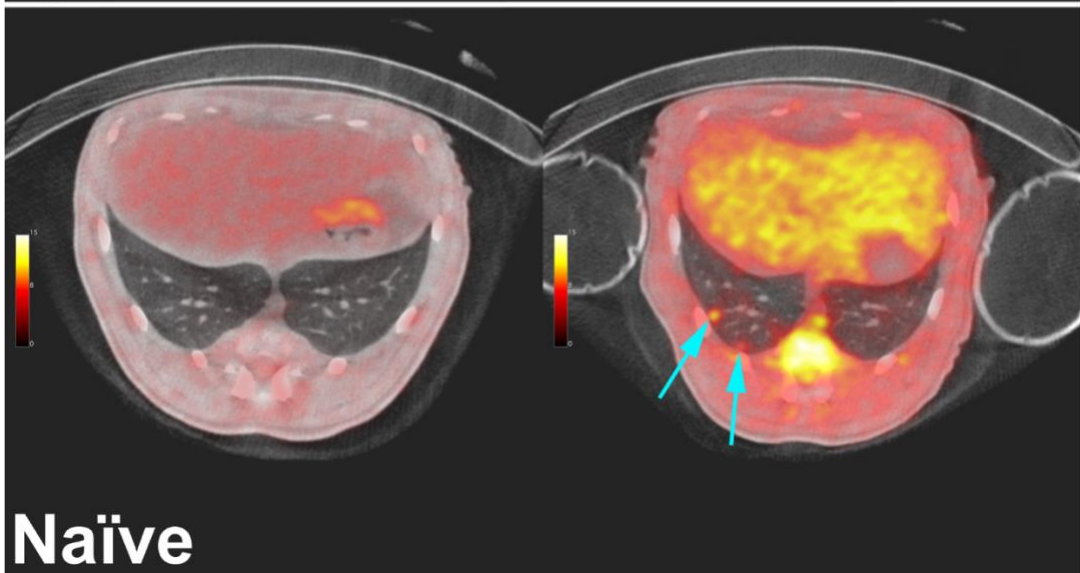
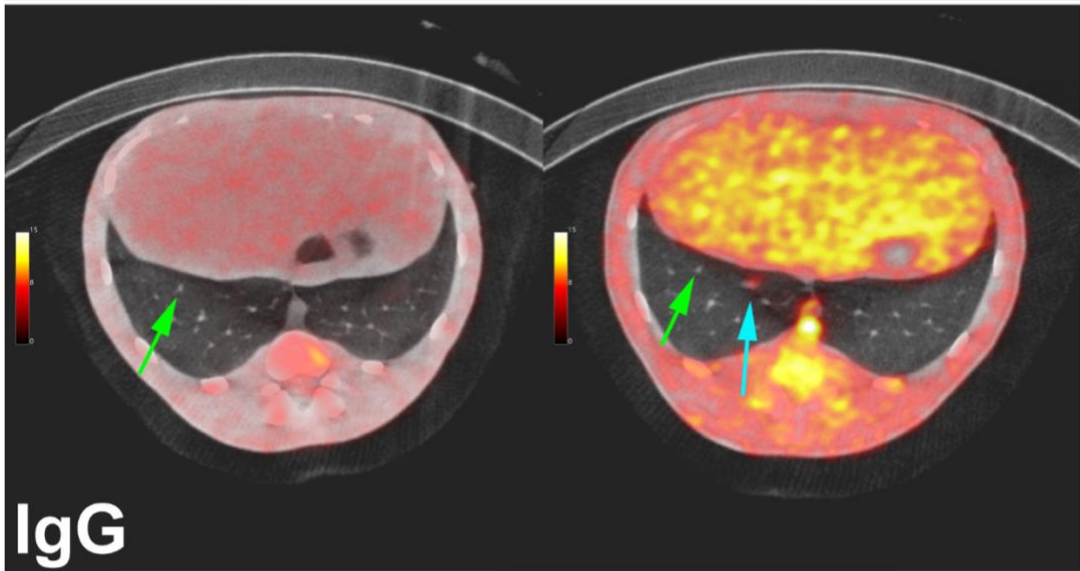
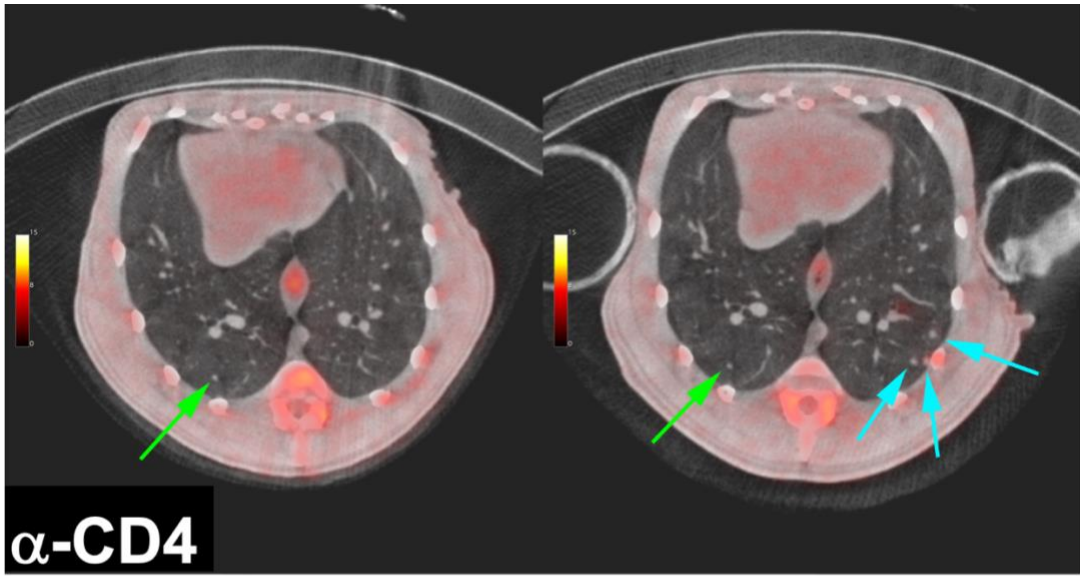


Figure 22. Cross-sectional PET CT scans of a macaque in each group pre- and post-second infection.

Left panel shows PET CT scan ~1 week before Mtb library B infection. Right panel shows PET CT scan 4 weeks after Mtb library B infection (1-3 days before necropsy). Green arrows point to “old” granulomas from Mtb library A. Blue arrows point to “new” granulomas formed after Mtb library B infection.

4.2.6 Isolation of genomic DNA from bacteria

DNA extraction was performed on granuloma and lymph node homogenates, as well as their scrapates (scraped colonies that grew on 7H11 agar plates) for library identification as described previously [118]. Briefly, a small aliquot of the homogenate or scrapate were vortexed with 0.1mm zirconia-silica beads (BioSpec Products, Inc.) and subsequently extracted twice with phenol chloroform isoamyl alcohol (25:24:1, Sigma-Aldrich) before precipitating DNA with molecular grade 100% isopropanol (Sigma-Aldrich) and 3M sodium acetate (Sigma-Aldrich) and resuspending in nuclease-free water (Invitrogen).

4.2.7 Library and barcode identification

Identification of library DNA tags have been previously described [264]. Briefly, DNA was amplified by PCR for 24-36 cycles before using in the NanoString nCounter assay (NanoString Technologies) with custom designed probes. Individual DNA barcodes were determined by sequencing using Illumina MiSeq and running custom bioinformatics scripts as previously described [120].

The scheme for labeling granulomas as old or new is found in Table 3.

Table 3. Granuloma classification scheme.

| PET CT* | Library | Classification |
|---------|---------|----------------|
| old | A | old |
| old | B | new |
| new | A | old |
| new | B | new |
| old/new | A + B | new |
| unknown | A | old |
| unknown | B | new |
| old | No data | old |
| new | No data | new |

* granuloma was noted on PET CT scan during first infection (old) or only after second infection (new). Unknown: granuloma was not seen on PET CT scan, possibly due to size or inability to discriminate from other granulomas in close proximity.

4.2.8 Intracellular cytokine staining and flow cytometry

Intracellular cytokine staining was performed on BAL and individual granulomas, CFU+ lymph nodes and uninvolved lung lobes (no granulomas and CFU-). BAL cells (250,000-1x10⁶) were stimulated with peptide pools of ESAT-6 and CFP-10 (10µg/ml of each peptide pool) in the presence of Brefeldin A (GolgiPlug, BD Biosciences) at 37°C/5% CO₂ for 6 hours prior to staining. Unstimulated controls were always included, however, positive controls (phorbol dibutyrate [PdBu] and ionomycin [231]) were only included if there were enough cells. Cells were stained with a viability marker (LIVE/DEAD fixable blue dead cell stain kit, Invitrogen) and surface and intracellular markers. Surface markers include CD3 (clone SP34-2, BD Pharmingen), CD4 (Clone L200, BD Horizon), CD8 (Clone RPA-T8, BD Biosciences) and CD206 (Clone 19.2, BD

Biosciences). Intracellular markers include IFN γ (Clone B27, BD Biosciences), TNF (Clone MAB11, BD Biosciences), IL-17 (Clone CZ8-23G1, Miltenyi Biotec), IL-10 (Clone JES3-9D7, Invitrogen), CD107a (eBioH4A3, Thermo Fisher Scientific) and IL-6 (Clone MQ2-13A5, Invitrogen). Data was acquired using the LSR II (BD) and analyzed using FlowJo software v10.6.1 (BD).

Because of the abundance of Mtb antigens already present [121], individual granulomas were not further stimulated before analysis by flow cytometry. Both CFU+ lymph nodes and uninvolved lung lobes were stimulated with peptide pools of Mtb-specific antigens, ESAT-6 and CFP-10 (10 μ g/ml of each peptide pool). All samples were incubated in the presence of Brefeldin A (GolgiPlug, BD Biosciences) at 37°C/5% CO₂ for 3.5-4 hours (granulomas) and 6 hours (lymph nodes and lung lobes) prior to staining. Cells were stained with a viability marker (LIVE/DEAD fixable blue dead cell stain kit, Invitrogen) and surface and intracellular markers. Surface markers include CD3 (clone SP34-2, BD Pharmingen), CD4 (Clone L200, BD Horizon), CD8 (Clone SK1, BD Biosciences), CD11b (Clone ICRF44, BD Biosciences) and CD20 (Clone 2H7, eBioscience). Intracellular markers include CD107a (Clone eBioH4A3, Thermo Fisher Scientific), IFN γ (Clone B27, BD Biosciences), TNF (Clone MAB11, BD Biosciences), Granzyme B (Clone GB11, BD Biosciences), IL-10 (Clone JES3-9D7, Biolegend), IL-17 (Clone CZ8-23G1, Miltenyi Biotec), calprotectin biotin (Clone 27E10, Invitrogen) and AF700 streptavidin (Invitrogen). Data was acquired using the LSR II (BD) and analyzed using FlowJo software v10.6.1 (BD).

4.2.9 Luminex on lung homogenates

Frozen supernatants were thawed on ice and concentrated using a centrifugation filter unit (Amicon Ultra-4 Centrifugal Filter Unit, 3kDa cutoff, Millipore Sigma) following manufacturer's

instructions. Samples were assayed in duplicates using the ProcartaPlex NHP multiplex immunoassay (Invitrogen) following manufacturer's instructions measuring levels of 30 cytokines and chemokines using the BioPlex reader (Biorad). An additional 2-fold dilution was performed on the supplied standards to extend its lower detection limit.

4.2.10 3D rendering of Mtb barcodes in macaque lungs

Three-dimensional plots illustrating the locations of excised barcoded granulomas and lymph nodes were constructed as previously described with minor modifications [275]. Briefly, these 3D images were built using a custom code written in Python. The outlines of the lung were displayed by using the terminal CT scan of each NHP to calculate a polygon mesh at the lung/soft tissue boundary defined by an image value of -400 Hounsfield Units. Pie chart markers were overlaid onto each rendering of the lung outlines. These markers represent the set of lesions and lymph nodes for which barcode percentages were also obtained.

4.2.11 Statistical analysis

We used D'Agostino & Pearson test to determine normality of data, but due to small sample sizes, nonparametric tests were used. The Mann-Whitney test was used to compare 2 groups. The Kruskal-Wallis test with Dunn's adjustment for multiple comparisons was used to compare 3 groups. The Wilcoxon matched pairs test was used for matching samples. The Spearman's test was used for correlation analyses. P values < 0.05 were considered statistically significant. Data were graphed and analyzed using GraphPad Prism v8 (GraphPad Software). All CFU data and cell

counts obtained from flow cytometry presented in graphs with the y-axis in log scale were transformed by adding 1.

4.3 Results

4.3.1 Experimental Design

We sought to determine whether CD4 T cells are important in the context of protection from Mtb reinfection. Since CD4 T cell depletion in macaques with acute or chronic Mtb infection results in exacerbation of disease [182], we chose to treat the macaques with primary Mtb Library A infection (N=13) in this study with anti-TB drugs for 4-5 months to eliminate the Library A bacteria prior to CD4 T cell depletion (Figure 23). Groups included (1) α -CD4 group (N=7): macaques treated with α CD4 Ab beginning 1 week prior to library B infection with infusions continuing up to 4 weeks post-library B infection; (2) IgG group (N=6): macaques following the same timeline as the α -CD4 group but infused with IgG control antibodies instead of α -CD4 antibodies; and (3) naïve group: macaques who only received Mtb library B infection and were not treated with antibodies. The macaques infected with library A and drug treated were matched based on the total lung FDG activity (the total amount of FDG retained in the infected lungs) post-drug treatment and randomized into α -CD4 and IgG groups. Total lung FDG activity is positively correlated with lung Mtb burden [235] and can be used to track response to drug treatment [276]. After randomization, there was no significant difference in the total lung FDG activity in both groups pre- and post-drug treatment (Figure 24). This indicates that macaques in the α -CD4 and

IgG groups had similar disease after the first infection and a similar response to drug treatment, and that our results are not influenced by selection bias.

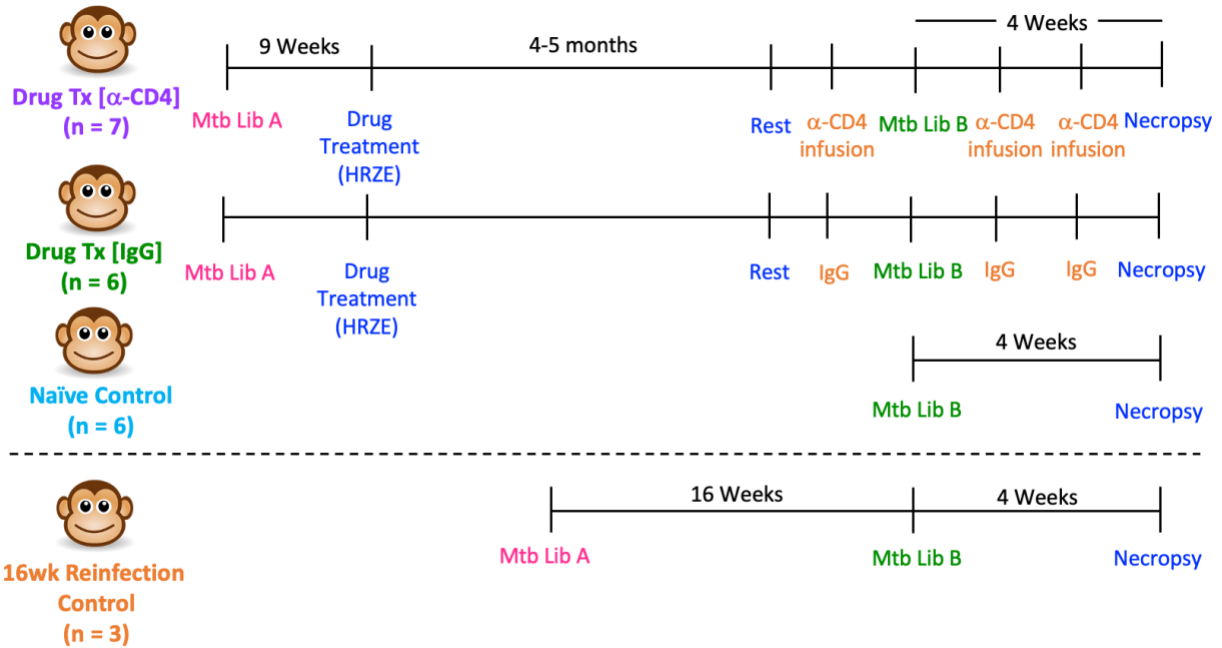


Figure 23. Experimental Design.

Both CD4 T cell-depleted (n=7) and IgG control (n=6) groups followed the same timeline of 9 weeks Mtb library A infection followed by 4-5 months of drug treatment before infusion with α -CD4 or IgG antibodies. Both groups were infected with Mtb library B 1 week after α -CD4 or IgG infusion and were necropsied after 4 weeks. The naïve controls only received Mtb library B infection and were also necropsied after 4 weeks. An additional 16-week reinfection control (n=3) from a different study was included for comparison.

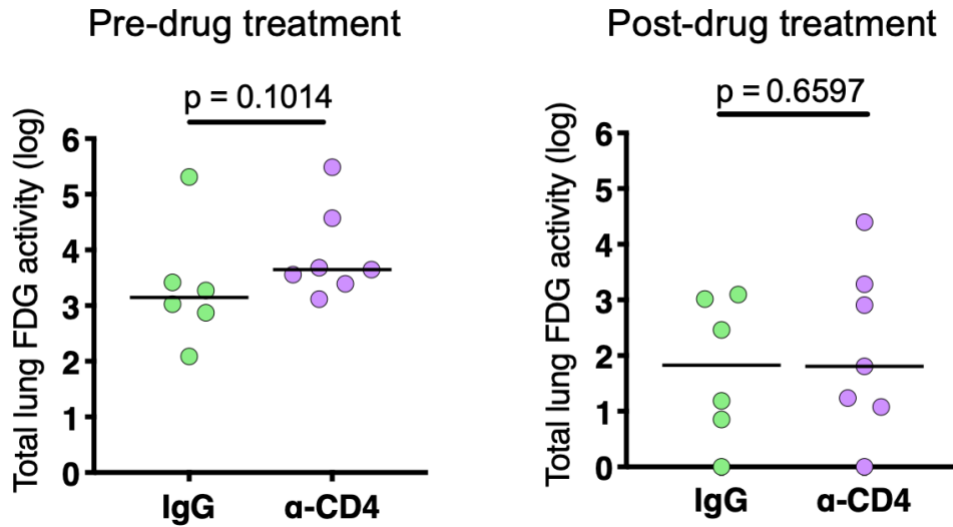


Figure 24. Total lung FDG activity in α -CD4 and IgG groups pre- and post-drug treatment.

Mann-Whitney test was used to compare the groups. Lines at median.

4.3.2 CD4 T cell depleting antibody does not mask CD4 receptors

To test whether the CD4 T cell depleting antibody masks CD4 receptors and thus could block binding of the anti-CD4 antibody for flow cytometry, we incubated PBMCs at 0.25X, 1X and 4X of the calculated blood concentration of the CD4 T cell-depleting antibody in macaques if given at 50mg/kg dose. No blocking of the CD4 receptor was observed in any of the concentrations tested when compared with the no CD4 T cell-depleting antibody control (Figure 25). This indicates that the CD4 T cell depletion in blood and tissues as measured by flow cytometry in this study is accurate and not confounded by blocking of the CD4 receptor by the CD4 T cell-depleting antibody.

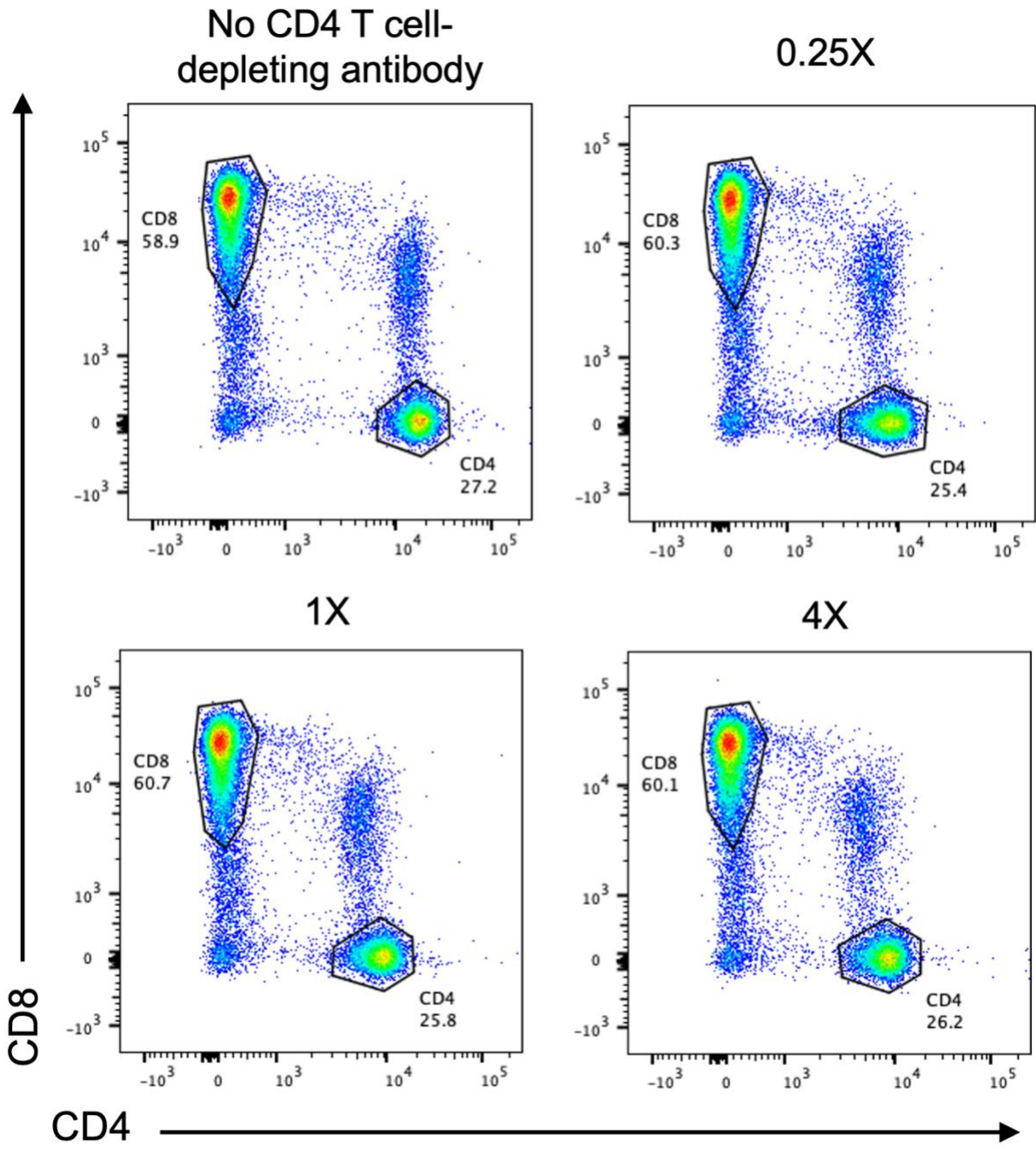


Figure 25. Anti-CD4 T cell depleting antibody does not mask CD4 receptors.

4.3.3 Macaques with primary Mtb infection, regardless of drug treatment, have significantly higher T cell counts and cytokine-producing CD4 T cells in BAL

The first site where Mtb encounters the immune system is in the airways. We tested whether the airway immune environment in primary infected drug treated and naïve macaques were significantly different 1 week before Mtb library B infection (prior to CD4 T cell depletion). The 16-week reinfection animals served as additional controls but were not included in statistical analyses. Macaques infected previously with Mtb library A, whether drug treated or not, had greater numbers of CD4 and CD8 T cells but similar levels of CD206+ alveolar macrophages in the airways compared to the naïve animals (Figure 26). In addition, macaques previously infected with Mtb library A, regardless of drug treatment, had a trending higher number of cytotoxic and IL-10-producing CD4 T cells and significantly greater number of CD4 T cells producing IFN γ and TNF α after ESAT-6/CFP-10 stimulation compared to the naïve group (Figure 27), although there was substantial variability across animals. There was no significant difference in the cytotoxic function and cytokine production of CD8 T cells in the BAL between drug treated and naïve groups (Figure 28). These data suggest that primary Mtb infection recruits T cells, especially IFN γ - and TNF α -producing CD4 T cells, to the airways and these cells remain in the airways even after drug treatment. This suggests that CD4 T cells may be important in protection against reinfection.

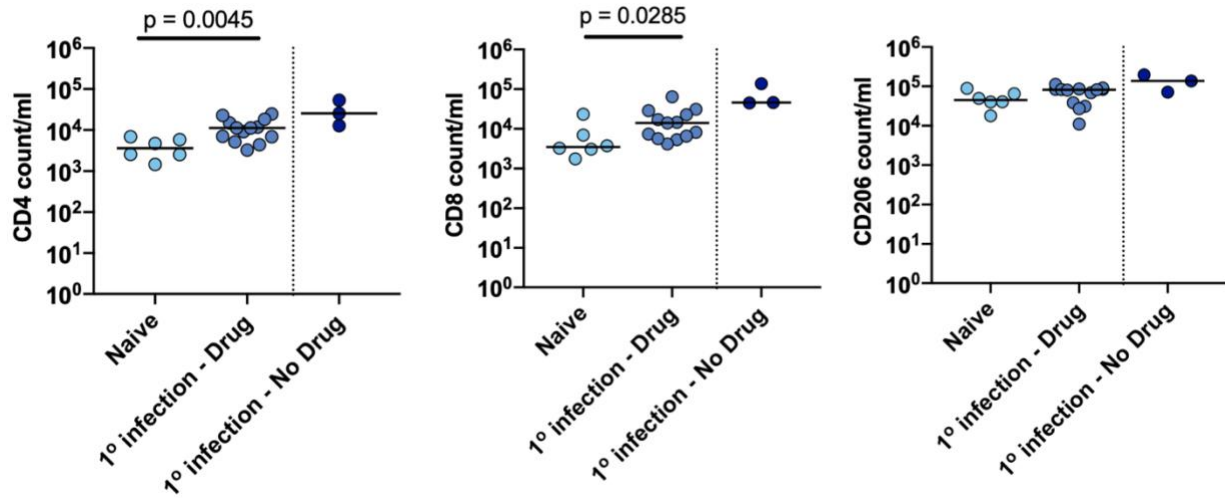


Figure 26. Greater T cell counts in BAL of macaques with primary Mtb infection.

Each data point is a monkey. Mann-Whitney test was used to compare the groups. Lines at median.

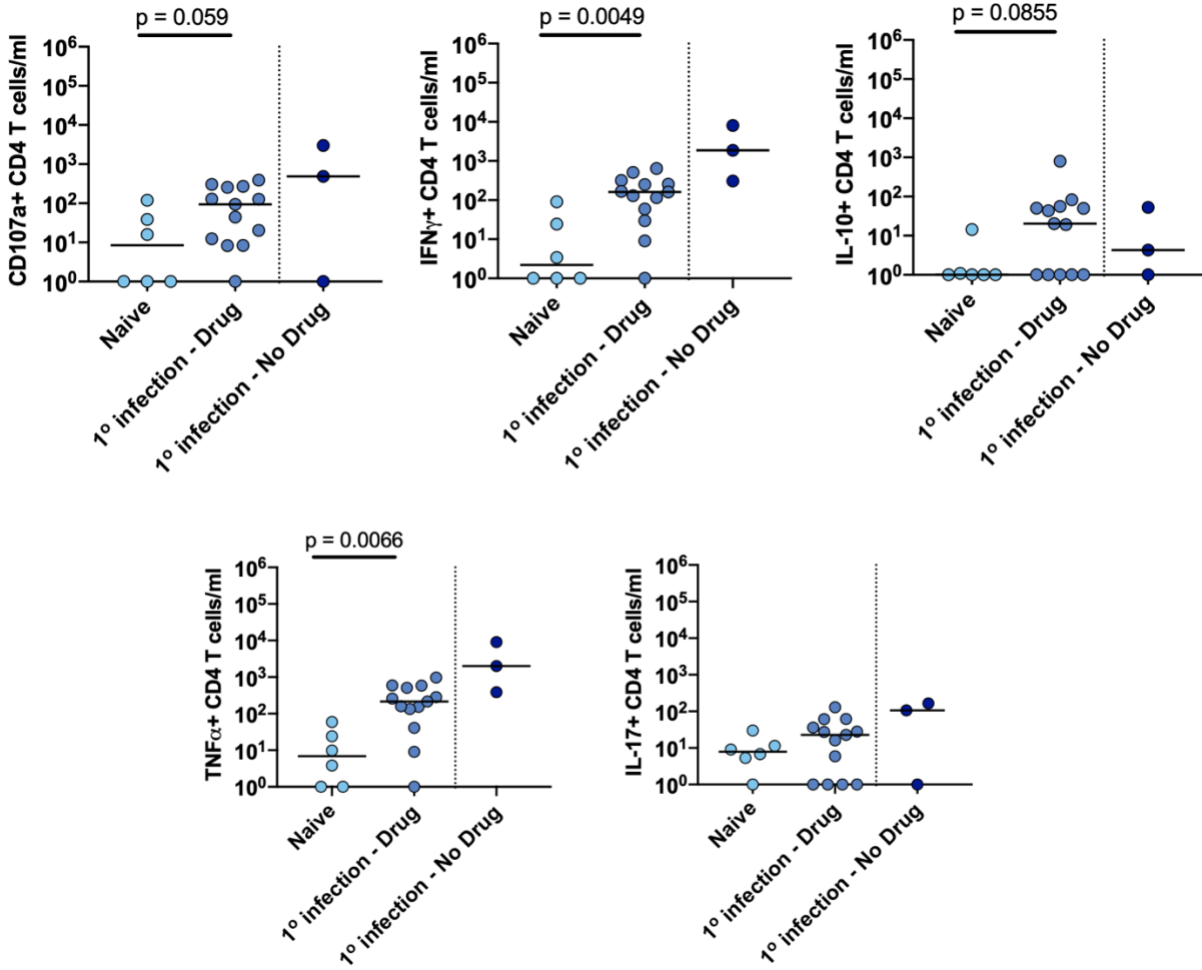


Figure 27. Greater CD4 T cell counts producing cytokines in BAL of macaques with primary Mtb infection.

Each data point is a monkey. Mann-Whitney test was used to compare the groups. Lines at median.

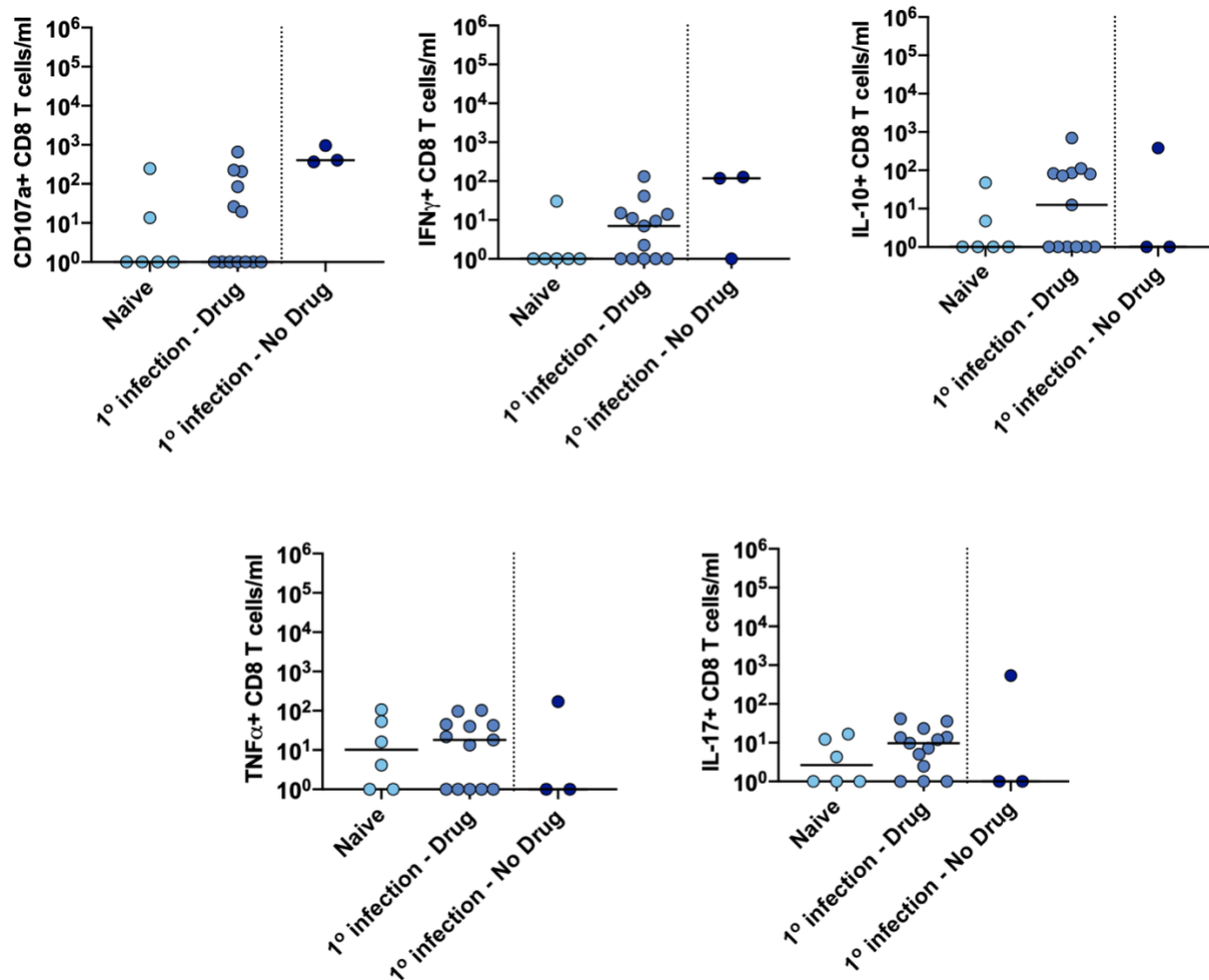


Figure 28. No difference in the numbers of functional CD8 T cells between naïve and primary-infected drug treated macaques.

Each data point is a monkey. Mann-Whitney test was used to compare the groups. Lines at median.

4.3.4 Robust CD4 T cell depletion in blood and tissues

To examine the effectiveness of CD4 T cell depletion in macaques, we measured the levels of CD4 T cells at time points pre- and post-infusion in the α -CD4, IgG and naïve groups. CD4 T cells were substantially depleted (10- to 1,000-fold compared to pre-infusion levels) in the blood

of macaques following α -CD4 antibody treatment, with some variability among animals, at the time of second infection and up to necropsy, while no change in CD4 T cell levels was observed in the IgG and naïve groups (Figure 29A). There was no difference in the cell counts of CD8 T cells, B cells, monocytes and neutrophils in the blood of all groups throughout the course of α -CD4 and IgG infusions (Figure 29B). Thus the α -CD4 antibody was successful at peripheral depletion of CD4 T cells with no effect to other cell populations in the blood.

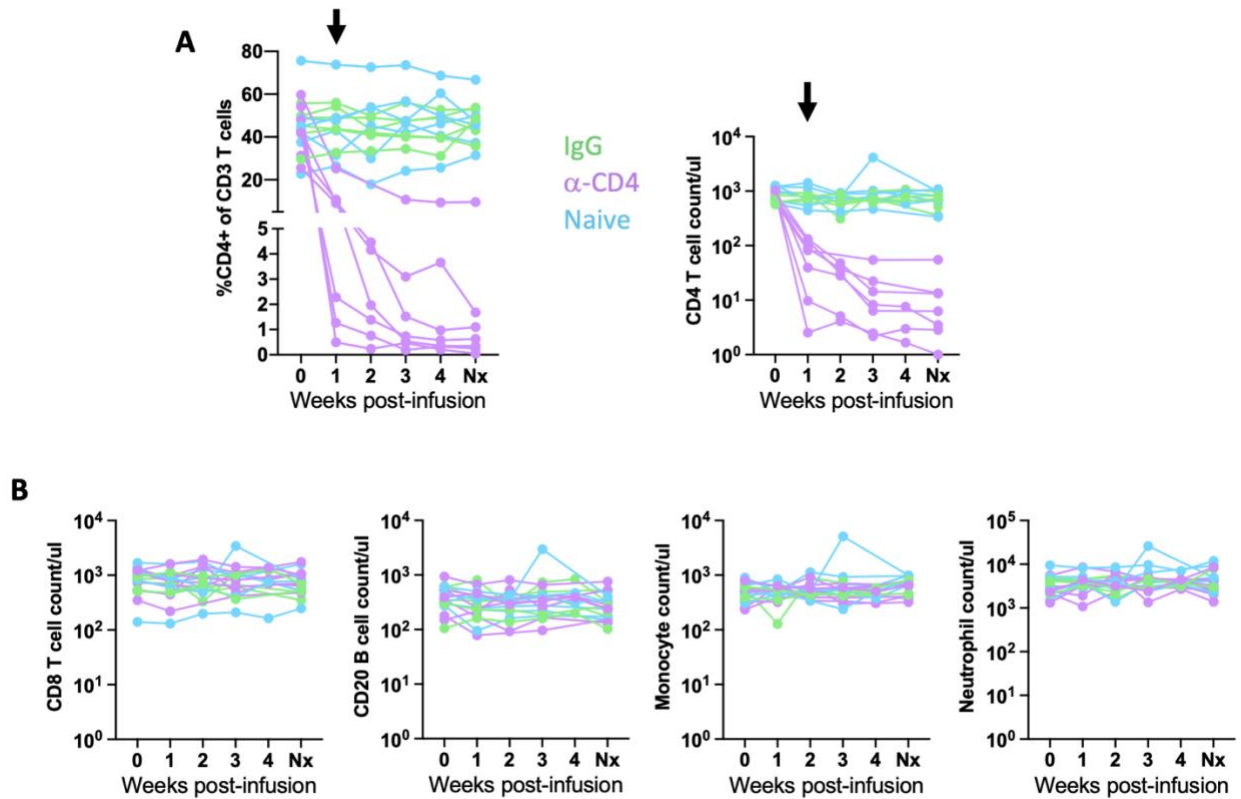


Figure 29. CD4 T cell depletion in the blood.

A. Frequency and cell count/ μ l of CD4+ T cells in the blood at different time points pre- and post-infusion. Arrow indicates time of second infection. B. Cell count/ μ l of CD8 T cells, CD20 B cells, monocytes and neutrophils in the blood at different time points pre- and post-infusion. The IgG group is shown in green, α -CD4 group in purple and the naïve controls are in blue.

Although depletion of CD4 T cells in blood appeared to be robust, it can be more difficult to deplete cells in tissues. We assessed the extent of CD4 T cell depletion in tissues at necropsy, 4 weeks after infection with Library B. The frequency of CD4 T cells in peripheral lymph nodes at necropsy was significantly lower compared to the peripheral lymph nodes biopsied pre-infusion in the CD4 T cell-depleted group ($p = 0.0156$, Wilcoxon-matched pairs test, Figure 30A) but not in the IgG group. The frequency of CD4 T cells was significantly reduced compared to the IgG and naïve groups in new granulomas (Figure 30B), uninvolved lung lobes (Figure 30C), thoracic and peripheral lymph nodes (Figure 30D, E) and spleen (Figure 30F). Similar results were found when the CD4 T cell counts per new granuloma or gram tissue were examined (Figure 31). Although we see a ~10-fold reduction in the number of CD4 T cells in the tissues examined during necropsy, there are still CD4 T cells remaining which could influence protection in the α -CD4 group.

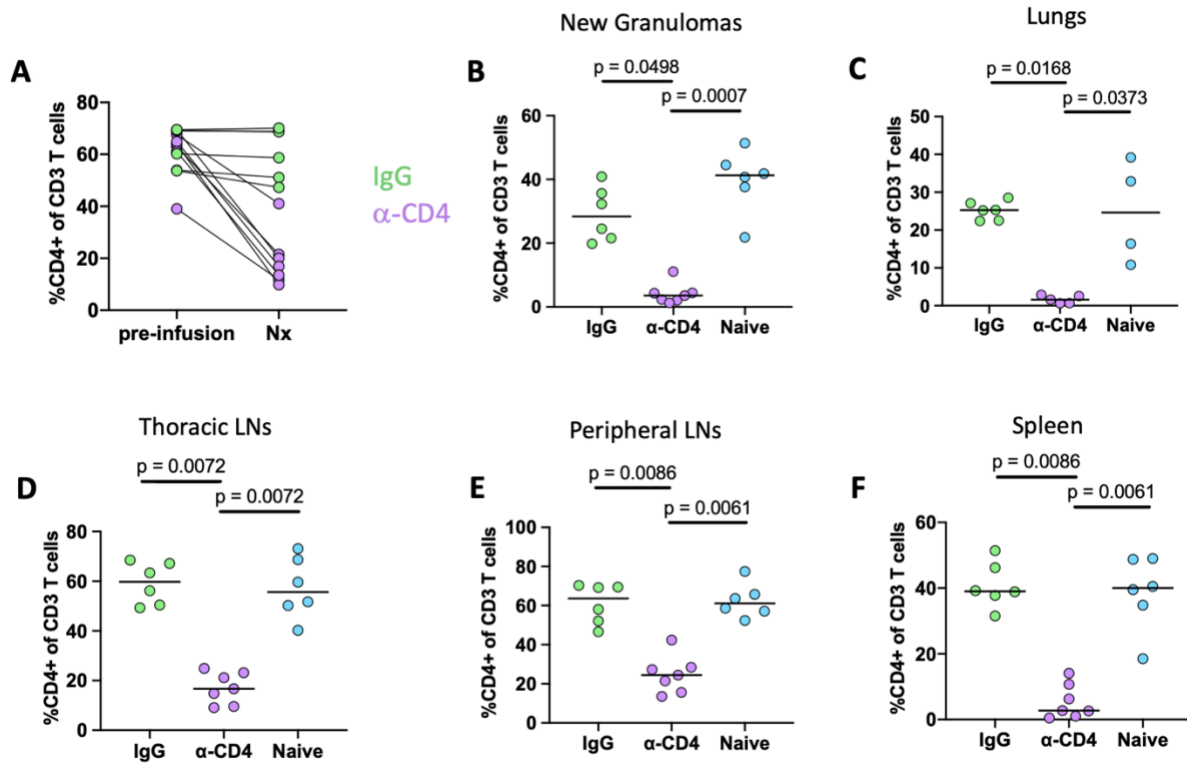


Figure 30. Frequency of CD4 T cells in tissues at necropsy.

A. Frequency of CD4 T cells in biopsied peripheral lymph nodes pre-infusion compared to peripheral lymph nodes at necropsy (Nx) in the IgG and α -CD4 groups. Frequency of CD4 T cells in all groups in new granulomas (B), uninvolvement lung lobes (2 macaques from α -CD4 and naïve groups did not have lung lobes processed via gentleMACS stained for flow cytometry) (C), thoracic lymph nodes (D), peripheral lymph nodes (E) and spleen (F). Each data point is a monkey. Kruskal-Wallis with Dunn's multiple comparison test was used to compare the groups. Lines at median.

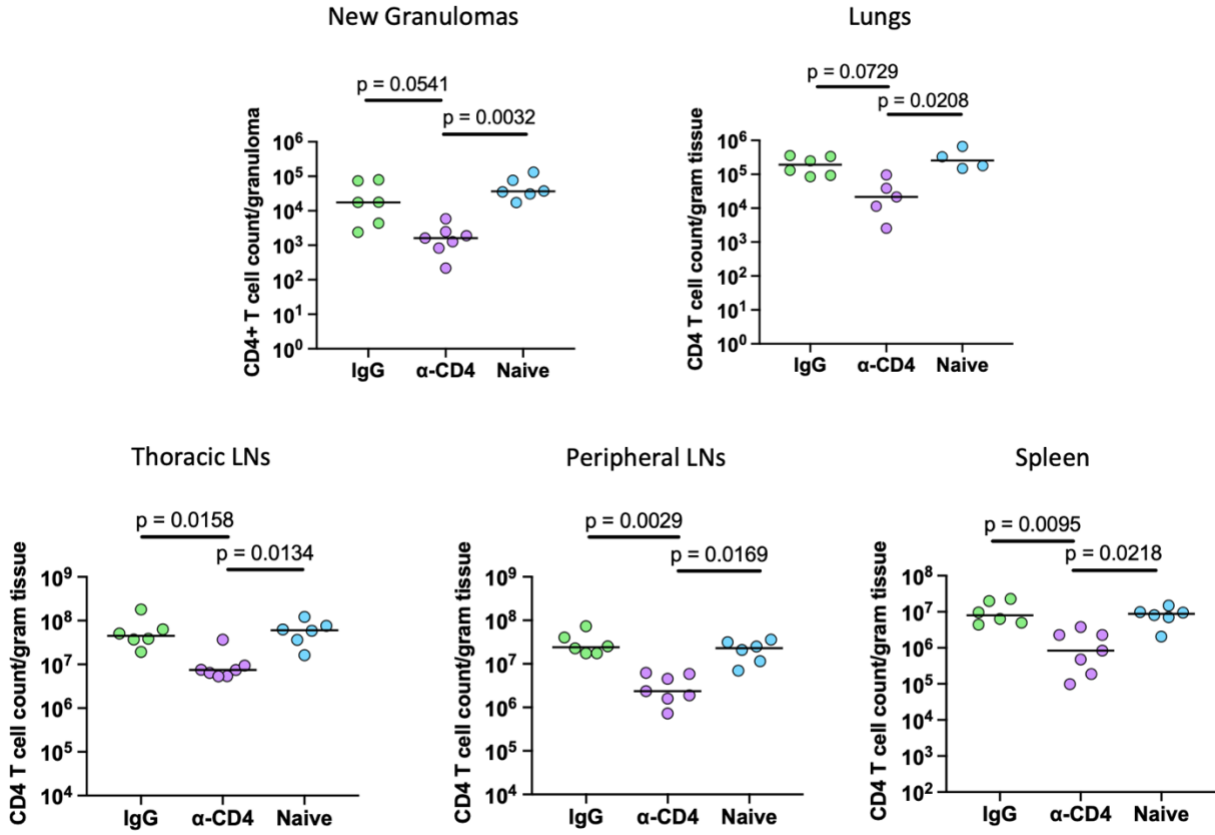


Figure 31. CD4 T cell counts in tissues at necropsy.

Two macaques from α -CD4 and naive groups did not have lung lobes processed via gentleMACS stained for flow cytometry. Each data point is a monkey. Kruskal-Wallis with Dunn's multiple comparison test was used to compare the groups. Lines at median.

We also examined the counts of CD8 T cells and B cells in tissues at necropsy and found no significant difference in almost all tissues between the 3 groups (Figure 32 and 33). The IgG group had significantly lower counts of B cells in new granulomas compared to the naive group, however it was not significantly different with the α -CD4 group. This indicates that depleting CD4 T cells does not affect the number of CD8 T cells and B cells in new granulomas, uninvolved lung lobes, thoracic and peripheral lymph nodes and spleen.

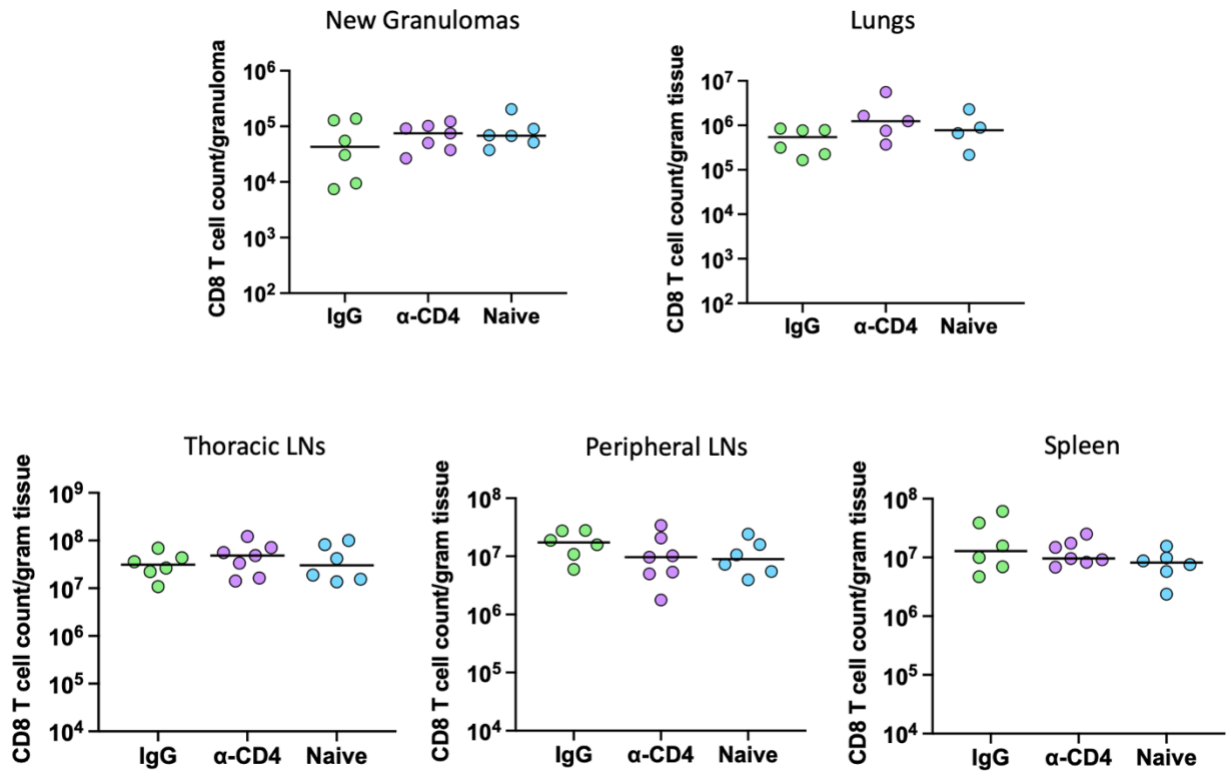


Figure 32. CD8 T cell counts in tissues at necropsy.

Two macaques from α-CD4 and naïve groups did not have lung lobes processed via gentleMACS.

Each data point is a monkey. Kruskal-Wallis with Dunn’s multiple comparison test was used to compare the groups. Lines at median.

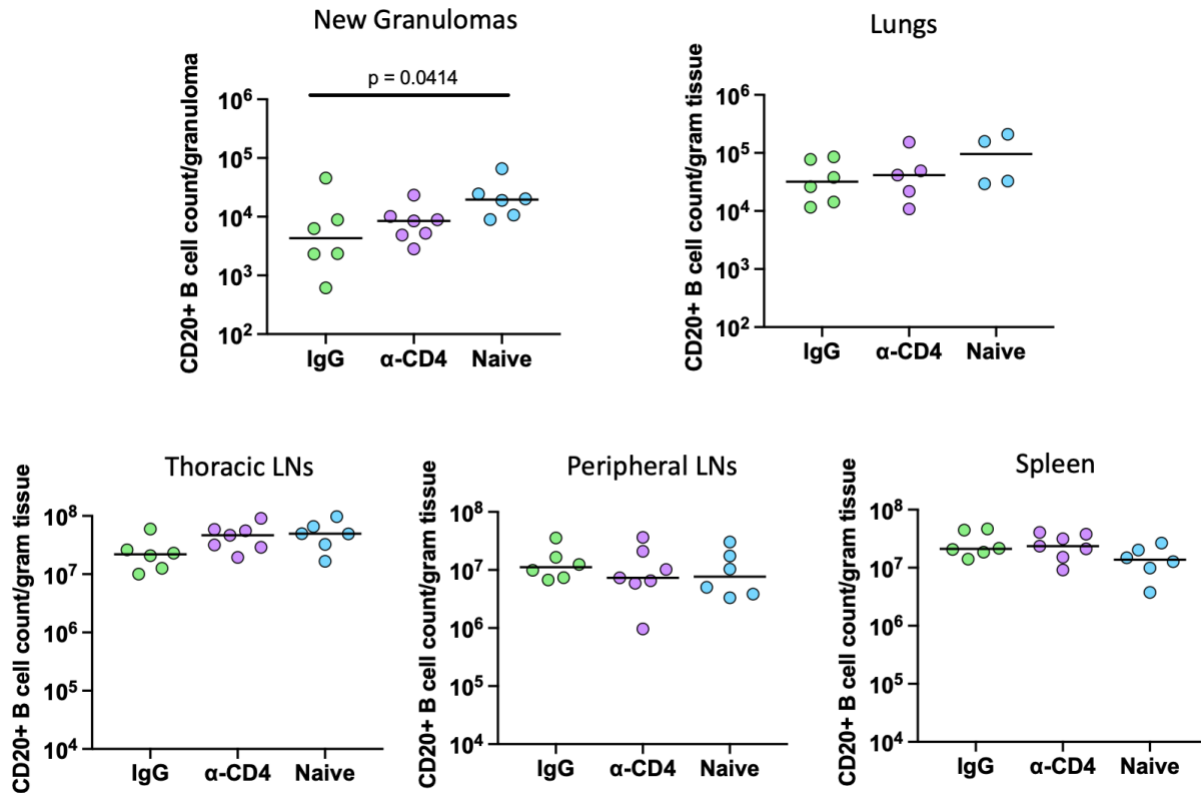


Figure 33. B cell counts in tissues at necropsy.

Two macaques from α-CD4 and naïve groups did not have lung lobes processed via gentleMACS. Each data point is a monkey. Kruskal-Wallis with Dunn's multiple comparison test was used to compare the groups. Lines at median.

4.3.5 CD4 T cell depletion diminishes the protection a primary Mtb infection confers against a secondary Mtb challenge

To determine the impact of CD4 T cell depletion in the protection a primary Mtb infection confers to a secondary Mtb challenge, we measured the number of new granulomas and Mtb burden in different tissues in each group. There was no significant difference in the number of new granulomas among the groups, however, the median number of new granulomas in the α-CD4 and

naïve groups was ~2x more compared to the IgG group (Figure 34A). In addition, the number of new granulomas in the α -CD4 and naïve groups were ~3x more than the 16-week reinfection control (Figure 34A). CD4 T cell depletion appears to result in an increase in new granulomas in some macaques but not all, suggesting heterogeneity among macaques. This heterogeneity could be related to extent of CD4 T cell depletion or to a stronger reliance on CD4 T cells for protection in some animals versus others [182]. Mtb burden in new granulomas was significantly higher in the α -CD4 group compared to the IgG group (Figure 34B). Mtb burden in new granulomas in the α -CD4 group was 5-fold lower compared to the naïve group, however it was not statistically significant (Figure 34B). The distribution of new granuloma CFU in each group is shown in Figure 34C. A similar pattern can be observed in total lung CFU (Figure 34D). The IgG group had significantly lower CFU in thoracic lymph nodes compared to naïve animals (998-fold lower), while α -CD4 group had trending lower CFU compared to the naïve group (47-fold lower) but not significantly higher compared to the IgG group (21-fold higher) (Figure 34E). These data suggest that while CD4 T cell depletion did not significantly increase the number of new granulomas in all CD4 T cell-depleted macaques, it resulted in significantly higher bacterial burden in new granulomas and lungs compared to IgG controls indicating a role for CD4 T cells in controlling bacterial burden resulting from the second infection. CD4 T cell depletion did not significantly increase Mtb burden in thoracic lymph nodes compared to the IgG group. Although CD4 T cells appear to be playing a role in control of reinfection, the bacterial burden in the α -CD4 group did not reach the same level as the naïve group. This suggests that protection was not completely abolished with CD4 T cell depletion, and that there are other factors that are contributing to this protection. However, the remaining CD4 T cells in the tissues could have also contributed to the residual protection.

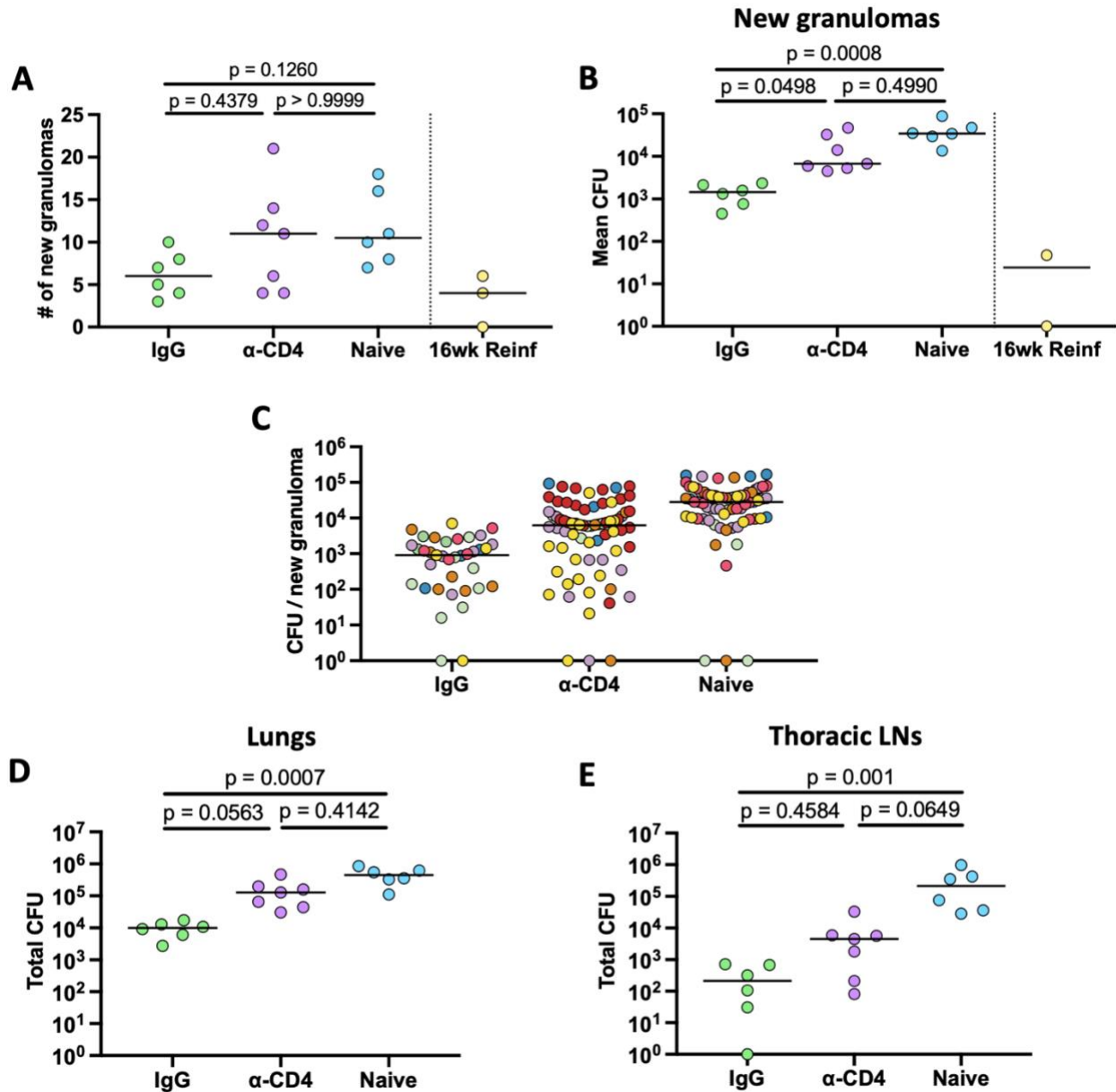


Figure 34. CD4 T cell depletion diminished protection a primary Mtb infection confers to a secondary Mtb challenge.

A. The number of new granulomas in each group. B. Mean total CFU in new granulomas in each group (note that there were no new granulomas in 1 of the 16-week reinfection animals, which is why there are only 2 points on this graph). C. Bacterial burden in new granulomas. Each data point is a granuloma. Each color is a monkey. D. Total CFU in uninvolved lungs in each group. E. Total

CFU in thoracic lymph nodes in each group. Each data point is a monkey for A-B and D-E. 16-week reinfection animals are not included in C and D, since these animals were not drug treated and are dominated by Library A bacteria. Kruskal-Wallis with Dunn's multiple comparison test was used to compare the groups. Lines at median.

4.3.6 Number of CD4 and CD8 T cells in the airways negatively correlate with new granuloma formation and total lung CFU

Since we observed greater numbers of CD4 and CD8 T cells in the BAL, as well as CD4 T cells producing IFN γ and TNF α , we wanted to test whether their numbers correlate with disease outcome measures. Including only the naïve and IgG macaques in the analysis (since this BAL is before CD4 T cell depletion), there was a moderate negative correlation between the number of CD4 T cells ($r = -0.6608$, $p = 0.0223$; Figure 35), number of IFN γ -producing CD4 T cells ($r = -0.7908$, $p = 0.0034$; Figure 36) and TNF α -producing CD4 T cells ($r = -0.6938$, $p = 0.0152$; Figure 37) and the number of new granulomas in the groups. There was also a moderate negative correlation between the number of CD4 T cells and the mean CFU of new granulomas ($r = -0.6294$, $p = 0.0323$), total lung CFU ($r = -0.7762$, $p = 0.0043$) and total thoracic lymph node CFU ($r = -0.7133$, $p = 0.0118$) (Figure 35). The number of IFN γ -producing CD4 T cells also moderately and negatively correlated with total lung CFU ($r = -0.6727$, $p = 0.0201$), but not with mean CFU of new granulomas ($r = -0.5232$, $p = 0.0836$) and total thoracic lymph node CFU ($r = -0.4983$, $p = 0.1014$) (Figure 36). The number of TNF α -producing CD4 T cells were moderately and negatively correlated with total lung CFU ($r = -0.7254$, $p = 0.0102$) and total thoracic lymph node CFU ($r = -0.662$, $p = 0.0229$) but not with mean CFU of new granulomas ($r = -0.5564$, $p = 0.0648$) (Figure 37). The number of CD8 T

cells were strongly and negatively correlated with the number of new granulomas ($r=-0.8049$, $p = 0.0024$), moderately and negatively correlated with total lung CFU ($r=-0.6573$, $p=0.0238$), but not correlated with mean CFU of new granulomas ($r=-0.5245$, $p=0.0839$) and total thoracic lymph node CFU ($r=-0.5455$, $p=0.0708$) (Figure 38). This suggests that the levels of CD4 and CD8 T cells, including IFN γ - and TNF α -producing CD4 T cells, in the airways before the second infection limit new granuloma formation and Mtb replication in the lungs. However, it is also possible that this relationship is a treatment effect (ie. negative correlation with new granuloma formation and total lung CFU is due to the macaques belonging to 2 different groups – naïve vs primary-infected and not due to the numbers of CD4 or CD8 T cells in the airways).

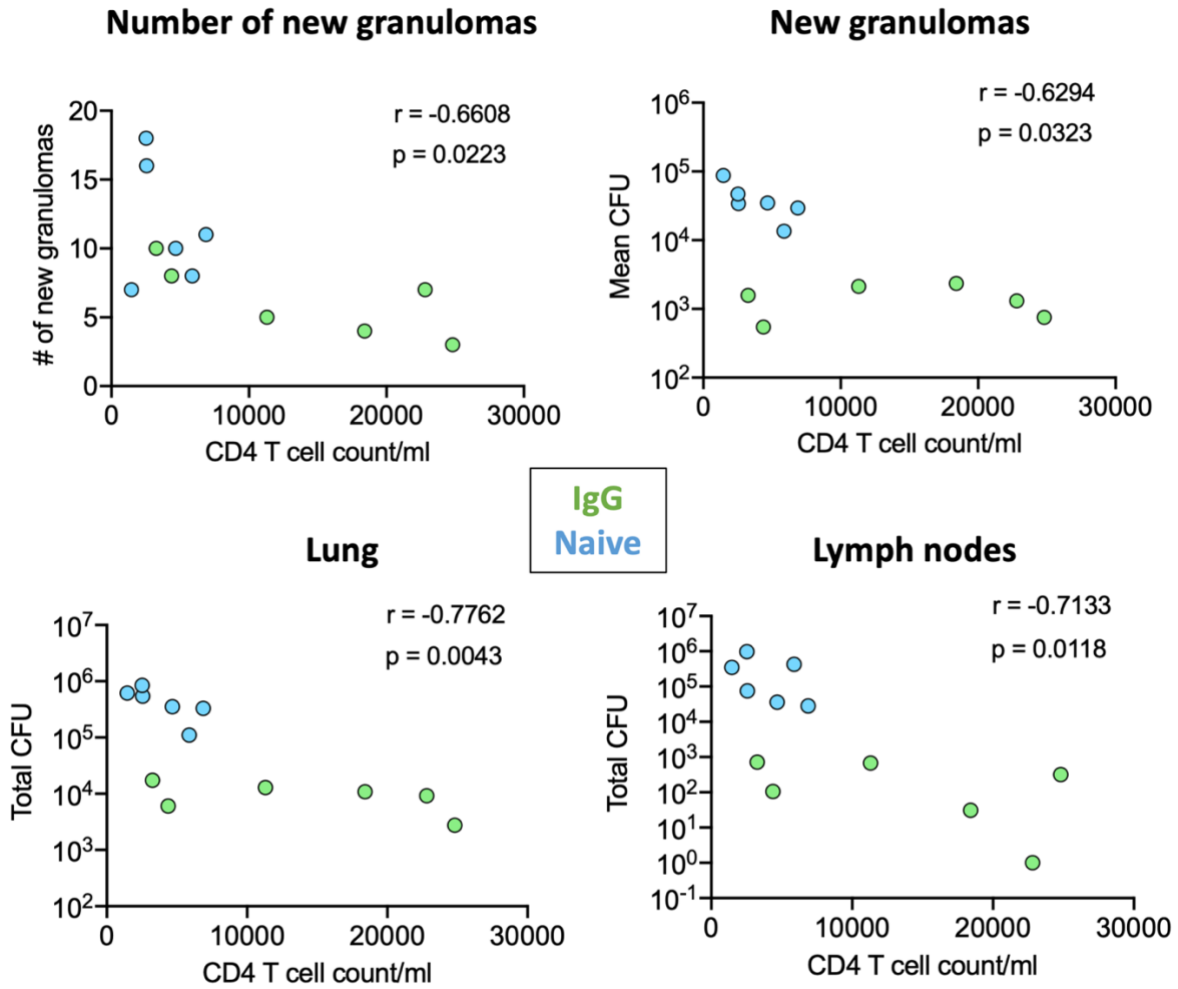


Figure 35. Correlation between CD4 T cell counts in the BAL and various disease outcome measures at necropsy.

Each data point is a monkey. Spearman correlation test was used to assess correlation between variables.

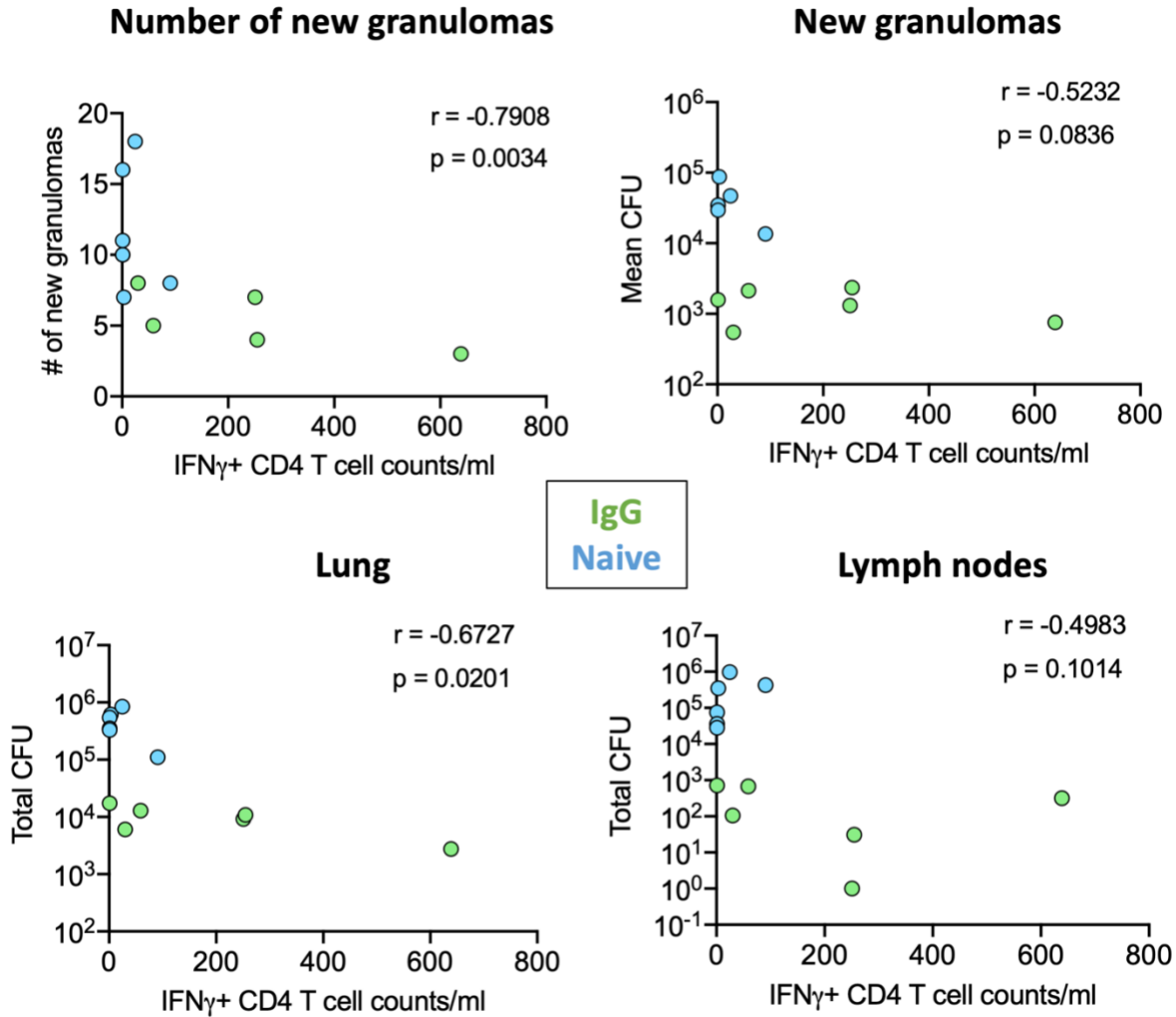


Figure 36. Correlation between number of IFN γ -producing CD4 T cells in the BAL and various disease outcome measures at necropsy.

Each data point is a monkey. Spearman correlation test was used to assess correlation between variables.

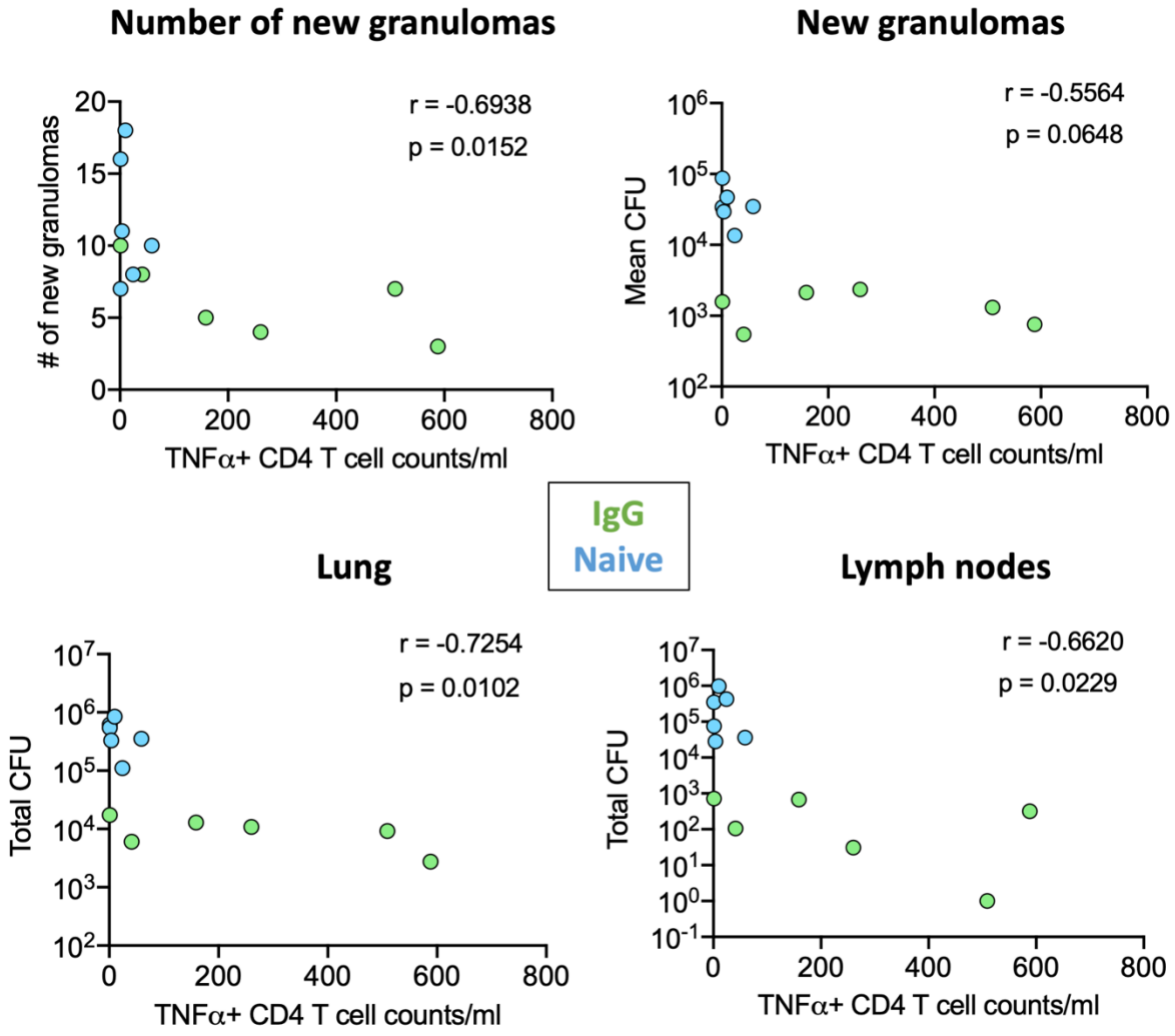


Figure 37. Correlation between number of TNFα-producing CD4 T cells in the BAL and various disease outcome measures at necropsy.

Each data point is a monkey. Spearman correlation test was used to assess correlation between variables.

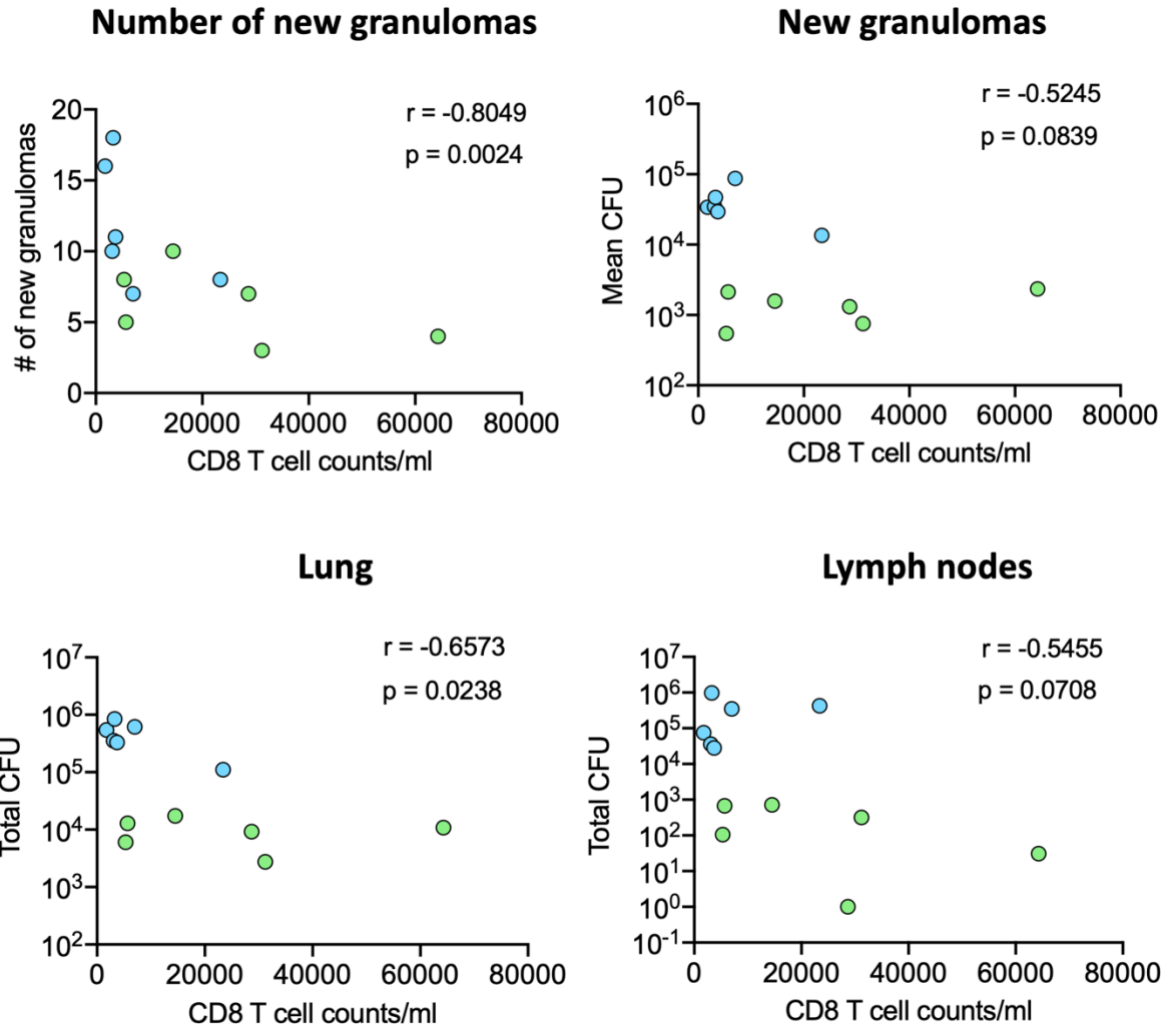


Figure 38. Correlation between CD8 T cell counts in the BAL and various disease outcome measures at necropsy.

Each data point is a monkey. Spearman correlation test was used to assess correlation between variables.

4.3.7 CD4 T cell numbers in the blood and lungs do not correlate with new granuloma formation and bacterial burden in lungs and lymph nodes

Because of the great variability in CD4 T cell numbers in the blood (range of 10-1000-fold reduction from pre-infusion levels) and the lungs (numbers range from ~2,500 cells to ~96,000 cells), we tested whether there was a correlation between the number of CD4 T cells in the blood and lungs and various disease outcome measures in the α -CD4 group. There was no correlation between the number of CD4 T cells in the blood at second infection (Figure 39) nor at necropsy (Figure 40), as well as the number of CD4 T cells in the lungs at necropsy (Figure 41), and new granuloma formation, mean CFU in new granulomas, total lung CFU and total thoracic lymph node CFU. This suggests heterogeneity in the response of macaques to CD4 T cell depletion, with some macaques relying more on CD4 T cells for protection. Since only the α -CD4 group was included in the correlation analyses, there is no treatment effect. However, one limitation of our correlation analyses is the low sample size.

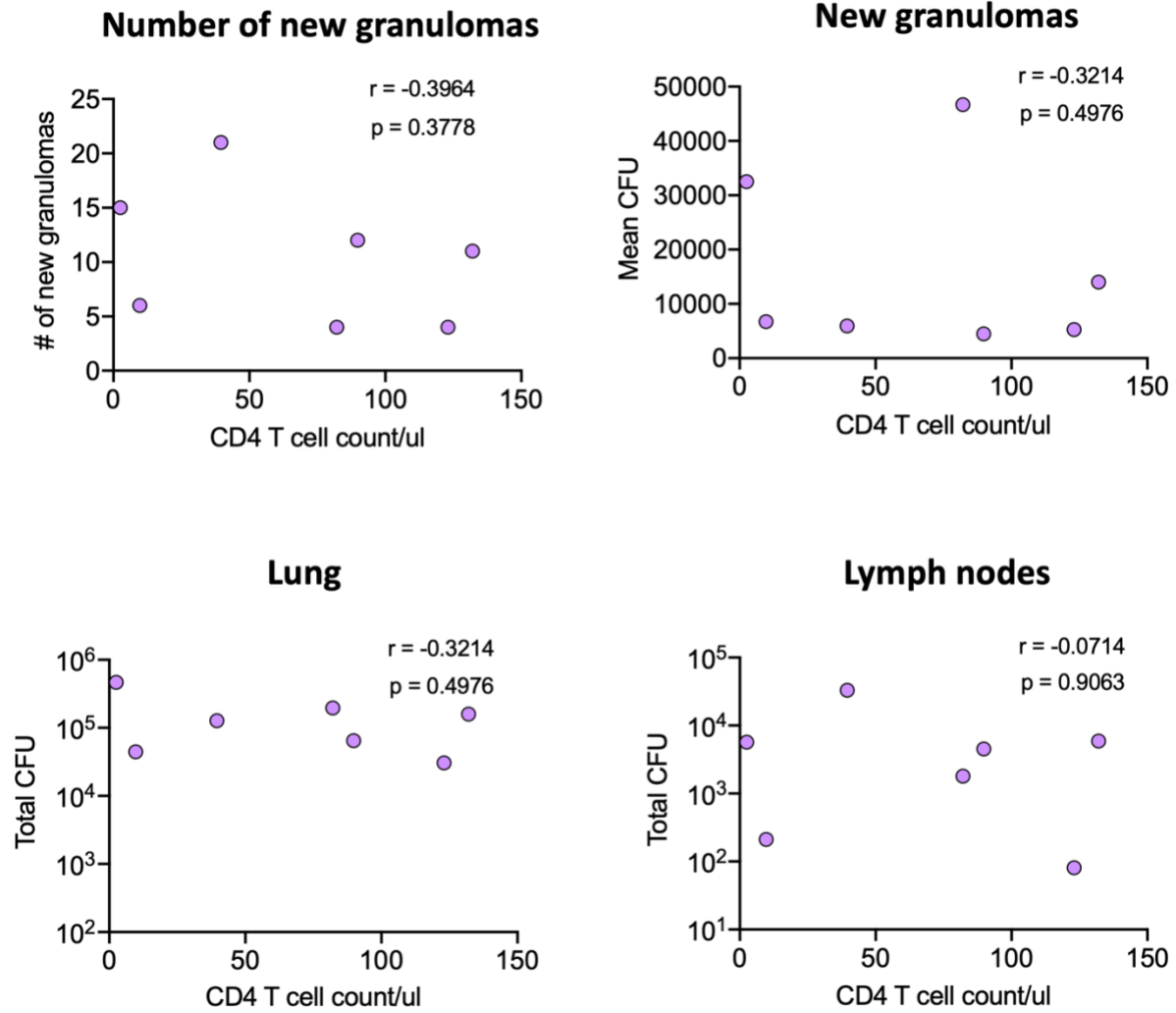


Figure 39. Correlation between the number of CD4 T cells in the blood at second infection and various disease outcome measures in the α -CD4 group.

Each data point is a monkey. Spearman correlation test was used to assess correlation between variables.

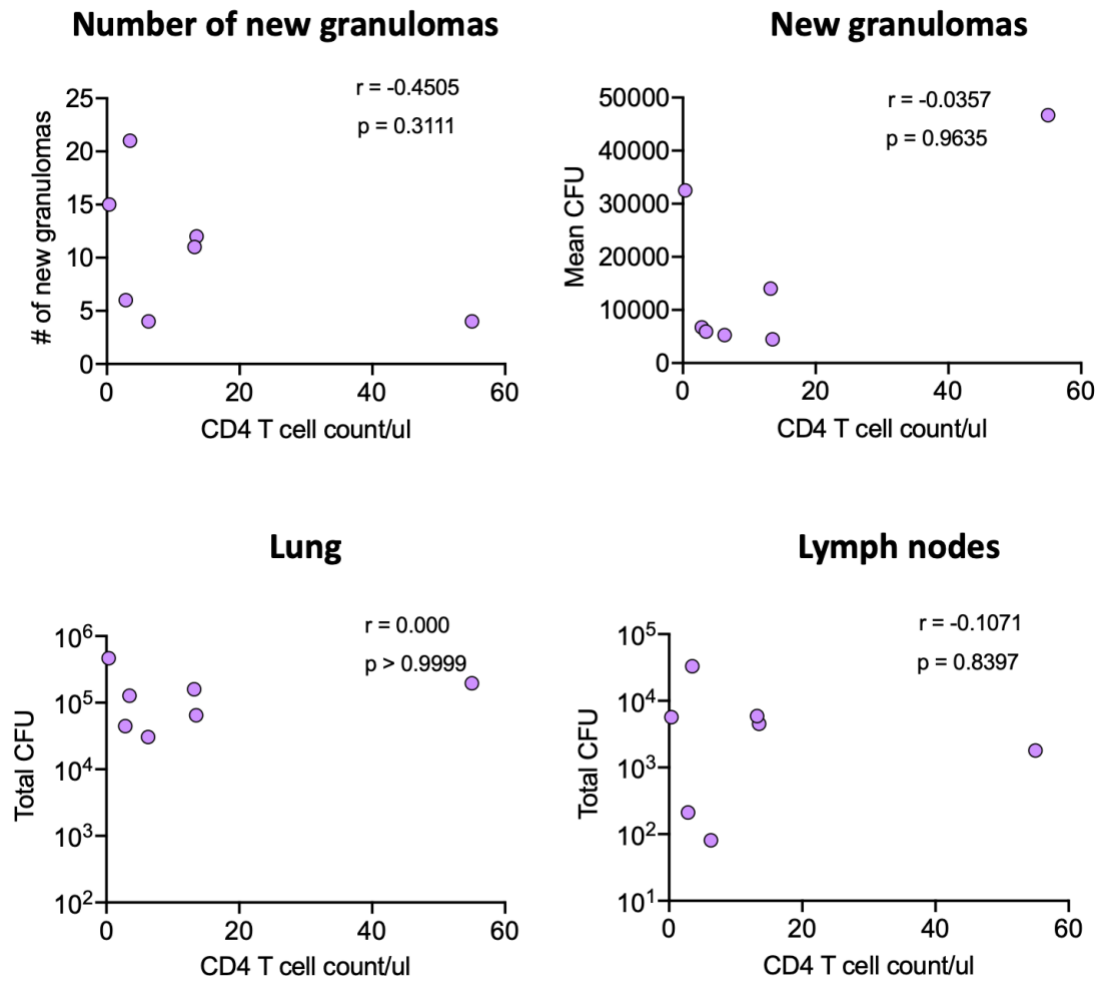


Figure 40. Correlation between the number of CD4 T cells in the blood at necropsy and various disease outcome measures in the α -CD4 group.

Each data point is a monkey. Spearman correlation test was used to assess correlation between variables.

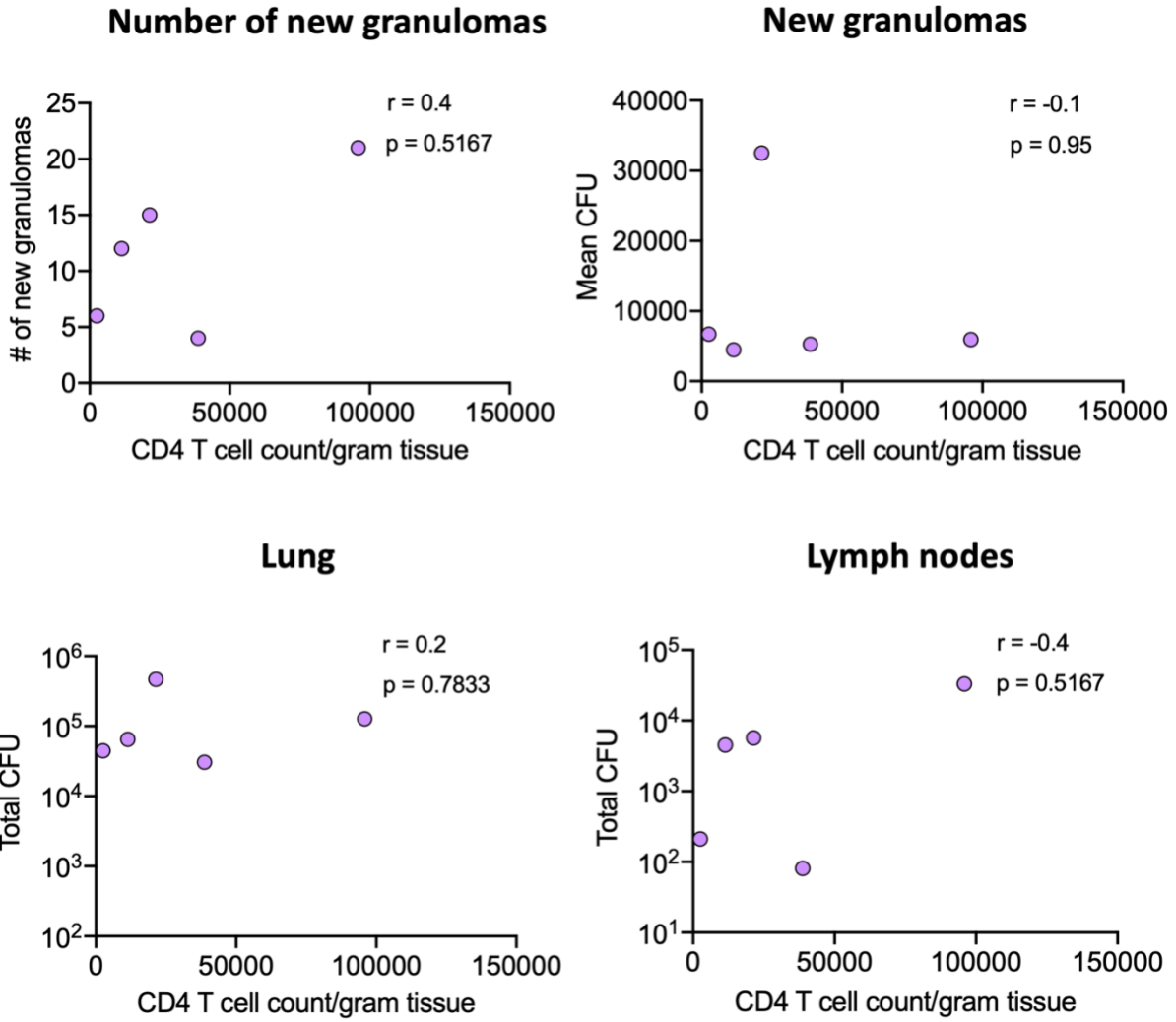


Figure 41. Correlation between the number of CD4 T cells in the lungs at necropsy and various disease outcome measures in the α -CD4 group.

Each data point is a monkey. Spearman correlation test was used to assess correlation between variables.

4.3.8 CD4 T cell depletion did not affect CD8 T cell function in tissues during second infection

Following CD4 T cell depletion, we examined CD4 T cell function in various tissues in the three groups. Unsurprisingly, the number of CD4 T cells producing cytokines and displaying cytotoxic function was significantly lower in new granulomas (Figure 42), CFU+ thoracic lymph nodes (Figure 44) and uninvolved lungs (Figure 46) in the α -CD4 group compared to the naive. Functional CD4 T cells were slightly lower in the α -CD4 group compared to the IgG group but this was not statistically significant. It appears that granulomas in the α -CD4 group had significantly lower numbers of CD4 T cells compared to the IgG group, however, the remaining CD4 T cells were still functional. CD4 T cells provide support in priming, development of cytotoxicity and generation of functional memory CD8 T cells [277-279]. To examine whether CD4 T cell depletion affected CD8 T cell cytotoxic function and cytokine production, we measured the levels of cytotoxic CD8 T cells and CD8 T cells producing various cytokines in tissues harvested at necropsy. There was no significant difference in CD8 T cell function among the 3 groups in new granulomas (Figure 43), CFU+ lymph nodes (Figure 45) and uninvolved lungs (Figure 47). This is likely because these cells were primed during the initial infection, and CD4 T cell depletion post-primary infection did not affect already primed CD8 T cells.

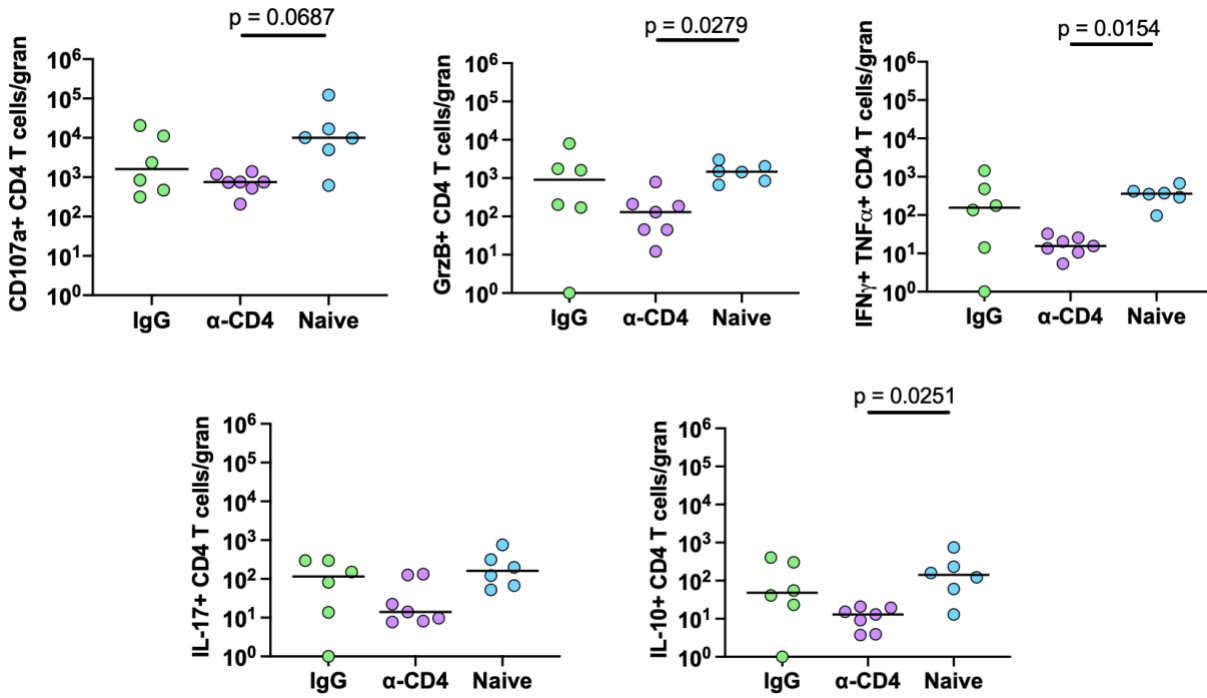


Figure 42. CD4 T cell counts producing various cytokines in new granulomas.

Each data point is a monkey. Kruskal-Wallis with Dunn's multiple comparison test was used to compare the groups. Lines at median.

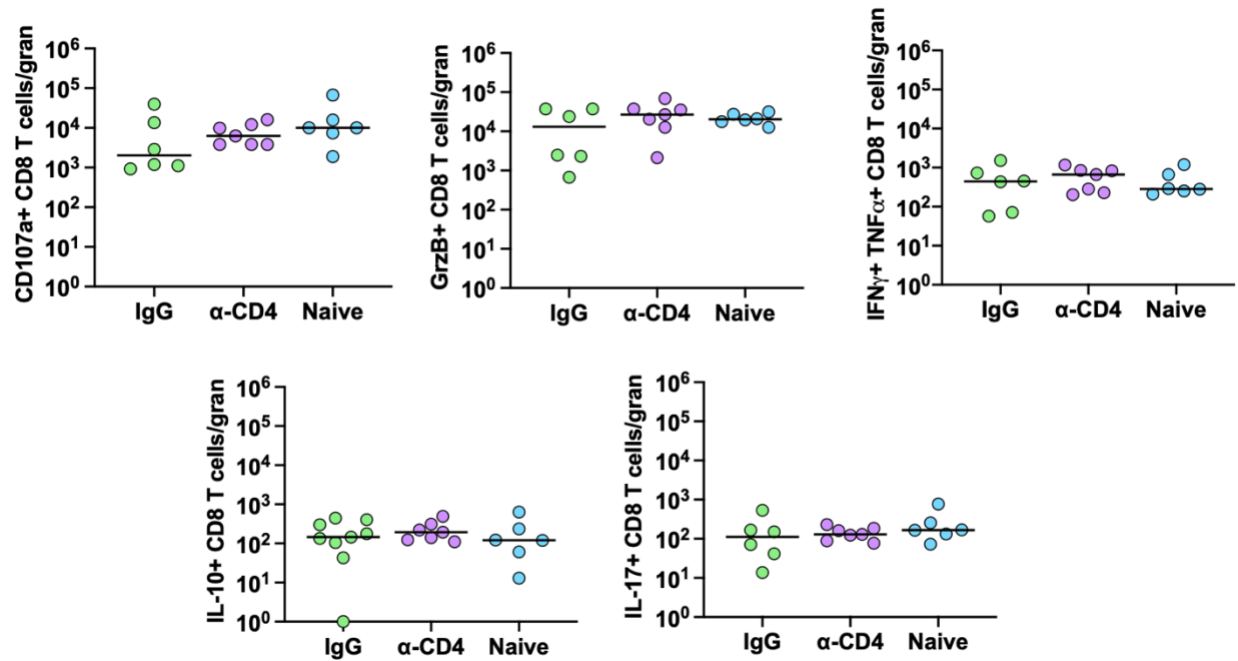


Figure 43. CD8 T cell counts producing various cytokines in new granulomas.

Each data point is a monkey. Kruskal-Wallis with Dunn's multiple comparison test was used to compare the groups. Lines at median.

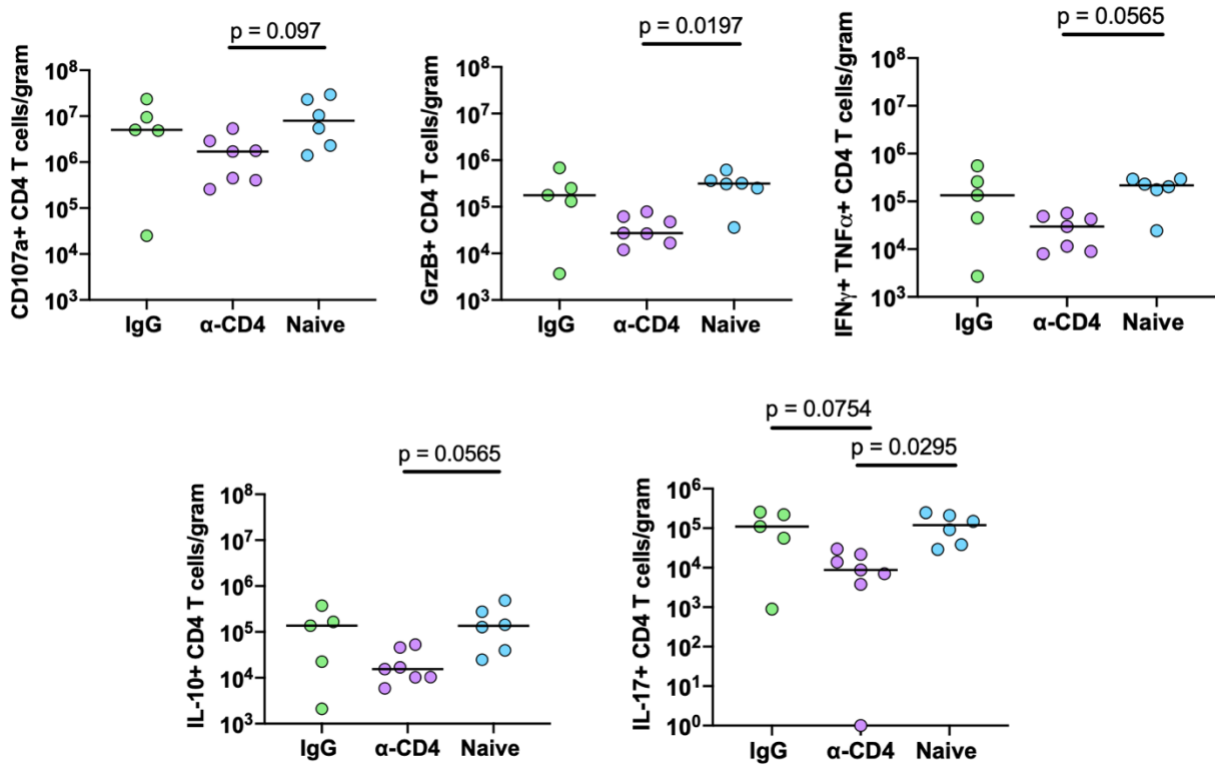


Figure 44. CD4 T cell counts producing various cytokines in CFU+ thoracic lymph nodes.

One macaque in the IgG group did not have a CFU+ thoracic lymph node. Each data point is a monkey. Kruskal-Wallis with Dunn's multiple comparison test was used to compare the groups.

Lines at median.

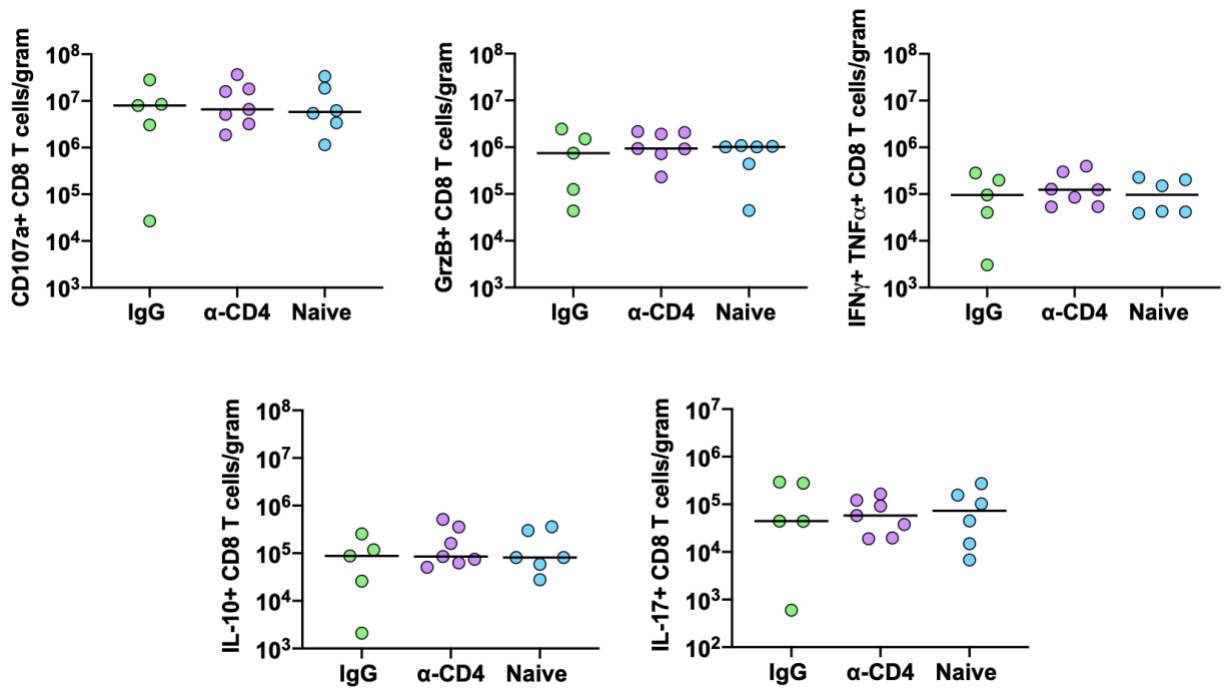


Figure 45. CD8 T cell counts producing various cytokines in CFU+ thoracic lymph nodes.

One macaque in the IgG group did not have a CFU+ thoracic lymph node. Each data point is a monkey. Kruskal-Wallis with Dunn's multiple comparison test was used to compare the groups. Lines at median.

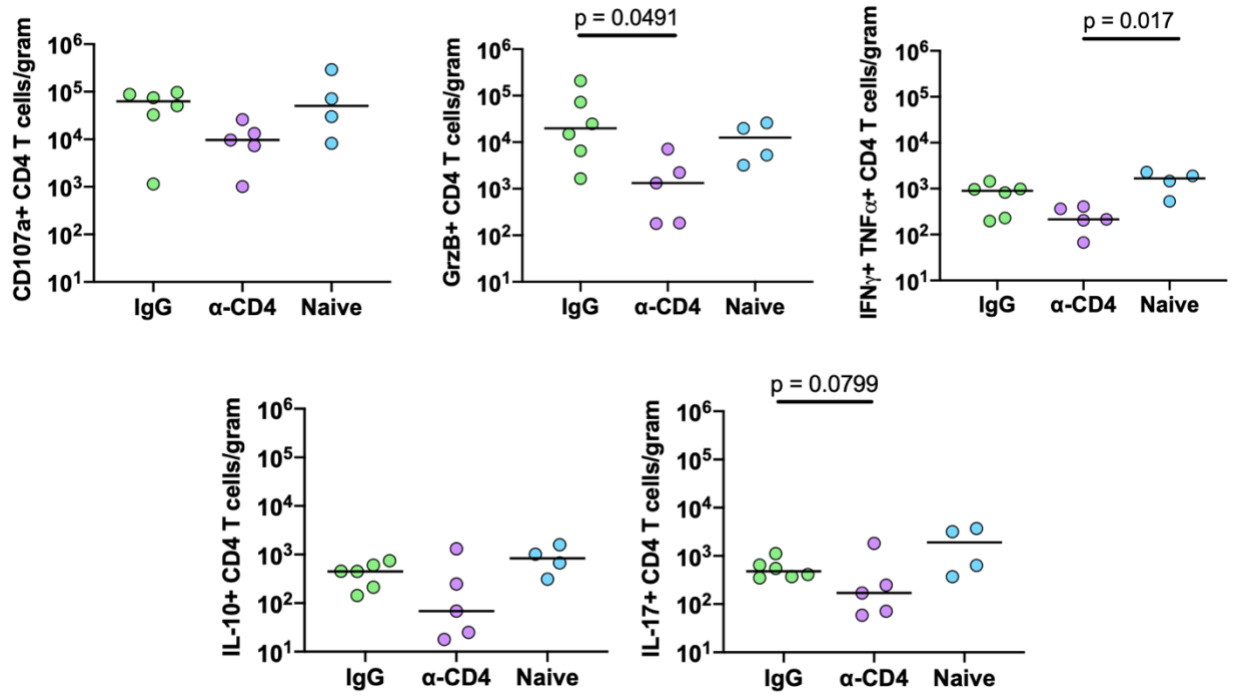


Figure 46. CD4 T cell counts producing various cytokines in uninjured lung lobes.

Two macaques from α-CD4 and naïve groups did not have lung lobes processed via gentleMACS stained by flow cytometry. Each data point is a monkey. Kruskal-Wallis with Dunn's multiple comparison test was used to compare the groups. Lines at median.

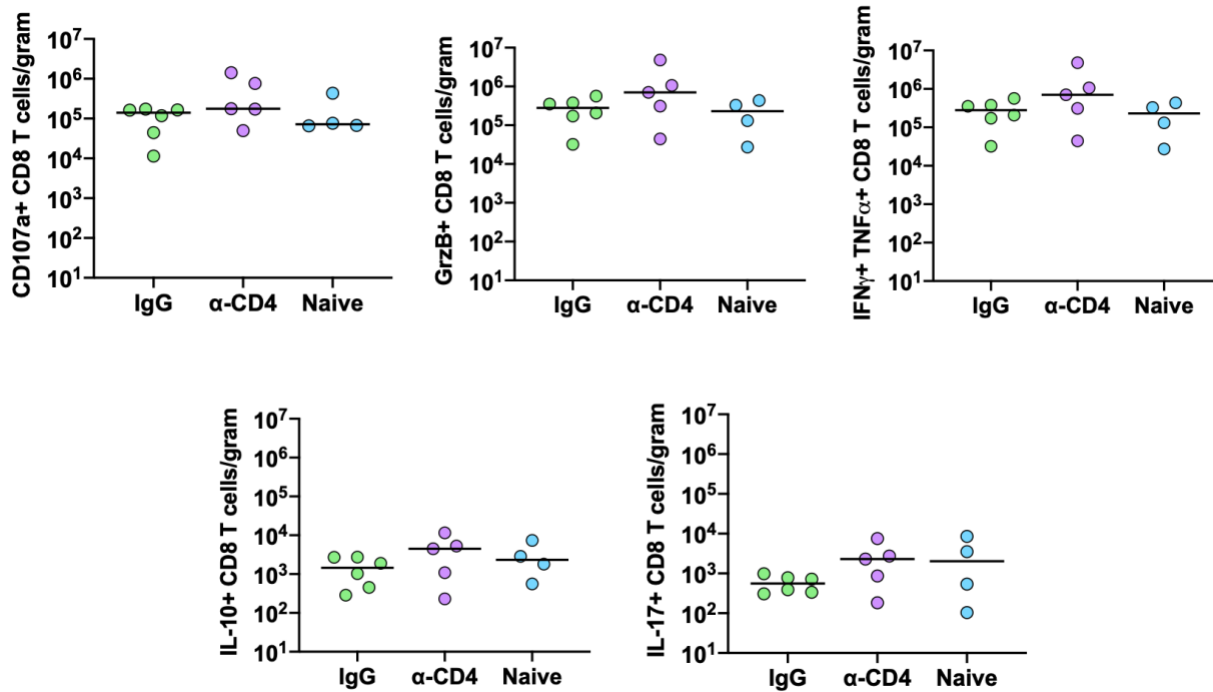


Figure 47. CD8 T cell counts producing various cytokines in uninvolved lung lobes.

Two macaques from α -CD4 and naïve groups did not have lung lobes processed via gentleMACS stained by flow cytometry. Each data point is a monkey. Kruskal-Wallis with Dunn's multiple comparison test was used to compare the groups. Lines at median.

4.3.9 Cytokine production in uninvolved lung lobes

The immune status of the lung tissue may play a role in restricting secondary infection. Using Luminex, we examined 30 cytokines and chemokines in uninvolved lung supernatants in the IgG, α -CD4, naïve and 16-week reinfection groups. Out of the 30 analytes tested, only 3 showed significant and trending differences among the groups (Figure 48). The α -CD4 group had trending lower IL-17A in the lungs compared to the naïve controls. The IgG group had significantly higher level of IL-23 compared to the α -CD4 group. Both IgG and α -CD4 groups

had lower TNF α levels compared to the naïve group. Other analytes tested but did not show any significant difference among the groups are shown in Figure 49. These data suggest that aside from IL-23, CD4 T cell depletion did not result in the alteration of the cytokine and chemokine environment in the lungs.

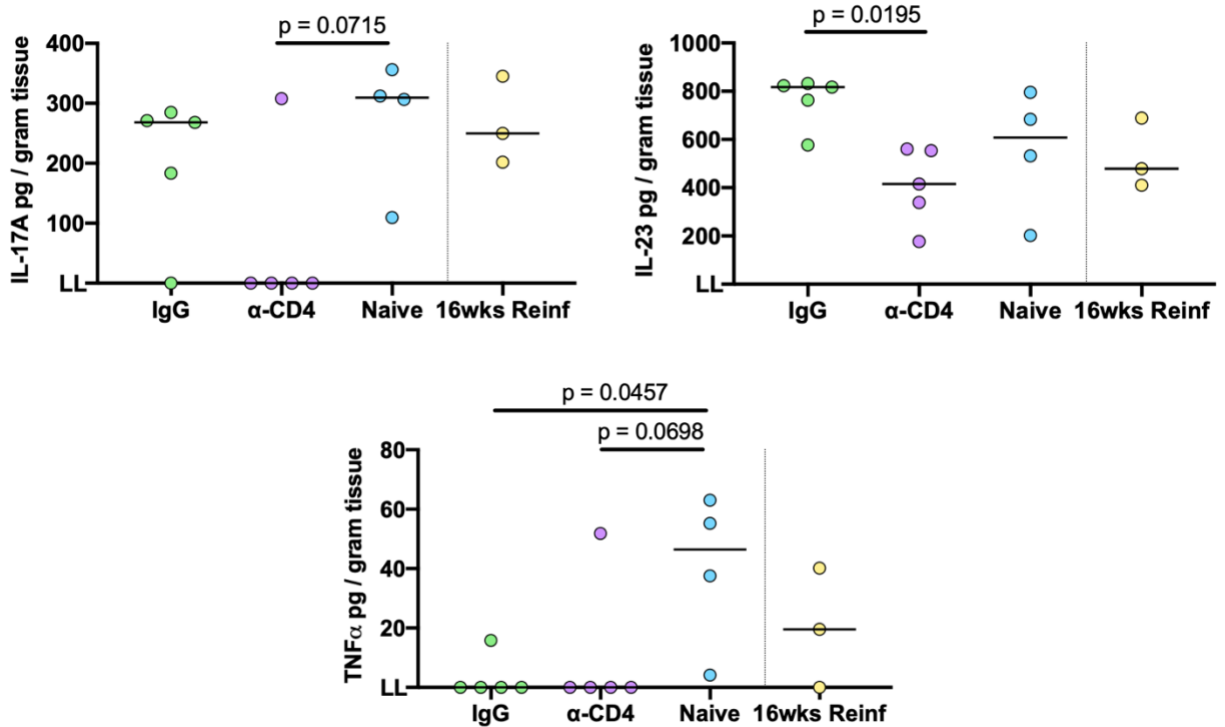


Figure 48. Cytokine levels in uninjured lung lobes.

Each data point is a monkey. Kruskal-Wallis with Dunn’s multiple comparison test was used to compare the groups. Lines at median.

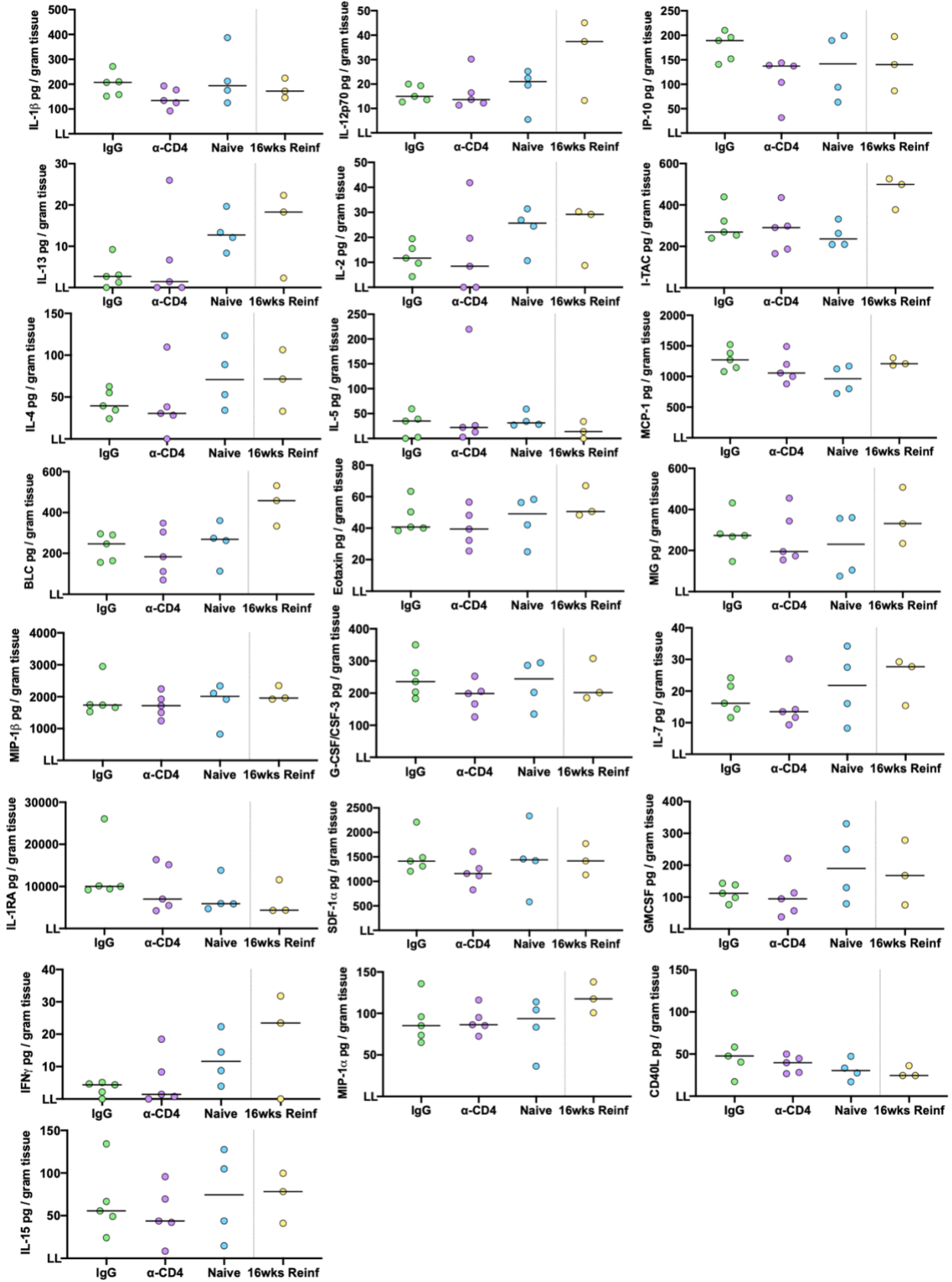


Figure 49. Cytokine levels in uninvolved lung lobes.

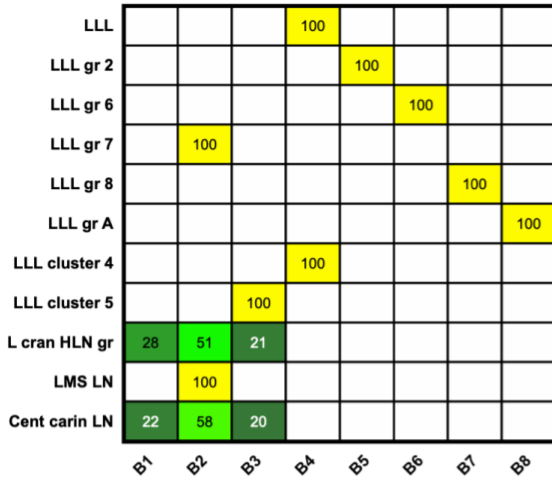
Shown are the analytes tested by Luminex that were not significantly different among groups. Each data point is a monkey. Kruskal-Wallis with Dunn's multiple comparison test was used to compare the groups. Lines at median.

4.3.10 CD4 T cell depletion results in dissemination of second infection to lymph nodes

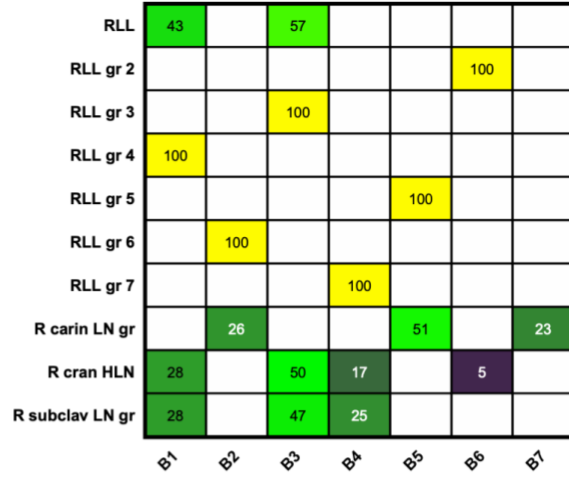
Aside from a DNA tag discriminating between libraries, each Mtb bacterium used in this study is also tagged with DNA barcodes that distinguish them individually [120]. A heatmap showing the list of samples that were CFU+ and had barcode data are shown in Figures 50 (naïve), 51 (IgG) and 52 (α -CD4). Most granulomas only grew 1 unique barcode while lymph nodes grew multiple barcodes which are consistent with our previous study [120]. Most of the CFU+ samples are from Mtb library B (except for 14218 in the α -CD4 group that had 2 granulomas with Mtb library A). We quantified the number of each unique barcode per animal and those found in granulomas and found no significant difference among the 3 groups (Figure 53). Interestingly, the number of unique barcodes in the lymph nodes of the α -CD4 group was significantly higher compared to the IgG group (Figure 53). We then mapped the location of unique barcodes from Mtb library B obtained from CFU+ granulomas and lymph nodes and made 3D renderings of the macaque's thoracic cavity using this data. The best (least dissemination) and the worst (greatest dissemination) are shown for each group in Figure 54. The "best" macaque in the IgG group had no dissemination either from the granuloma to the lymph nodes or granuloma to granuloma dissemination. The "best" macaques in the α -CD4 and naïve groups both had granuloma to lymph node dissemination. The "worst" macaque in the IgG group had granuloma to lymph node

dissemination, however, it was not as extensive as the “worst” macaques in the α -CD4 and naïve groups (solid color pie charts vs multi-colored pie charts). This suggests that CD4 T cell depletion results in an increase in Mtb dissemination to the lymph nodes.

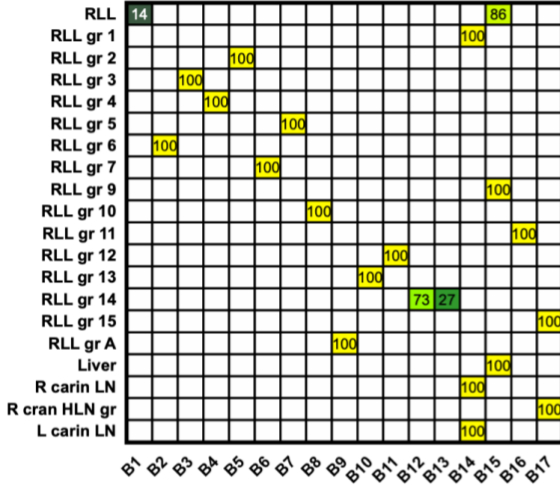
12918



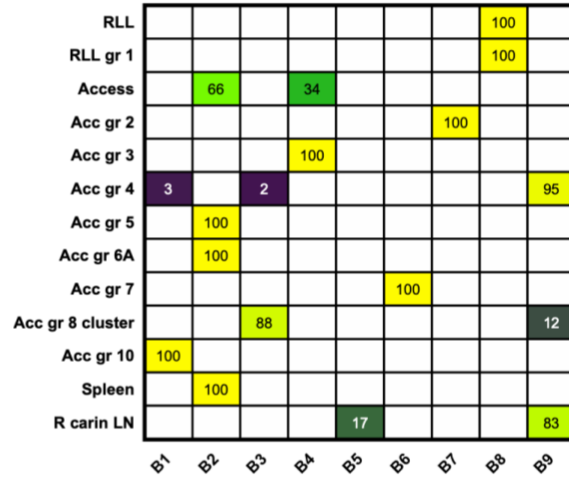
13018



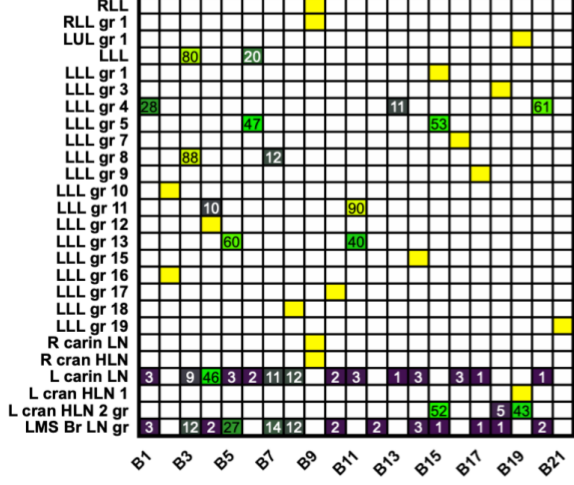
13118



13718



13818



13918

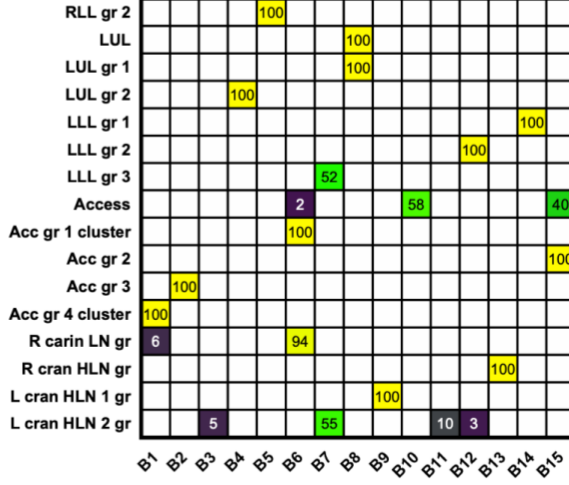
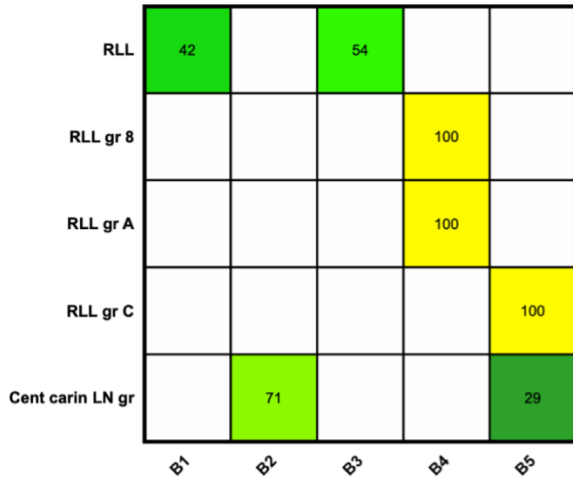


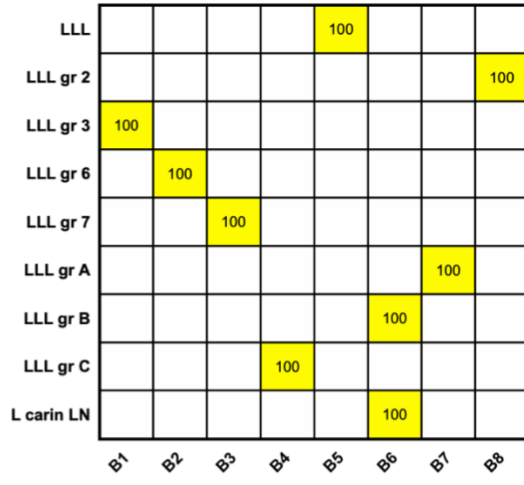
Figure 50. Barcode heatmaps of naive controls.

Samples can be divided into 4 groups: granulomas, lymph nodes, random lung lobe and extrapulmonary (eg. spleen and liver). Lung lobes are written using 3 letters which correspond to the side of the lungs (ie. left vs right), position of the lobe (ie. upper, middle or lower) and lobe. For example, right lower lobe is abbreviated as RLL, left upper lobe as LUL, and so on. The accessory lobe is written as Access. Granulomas are written as “lung lobe + granuloma number”, for example, RLL gr 1 or LUL gr 2. Lymph nodes are always written with the letters “LN” or “HLN” which means lymph node or hilar lymph node. The letters “gr” at the end of lymph node names means granuloma. The barcode IDs can be found at the bottom of each heatmap - A denotes Mtb library A and B denotes Mtb library B. Images courtesy of Forrest Hopkins, HSPH.

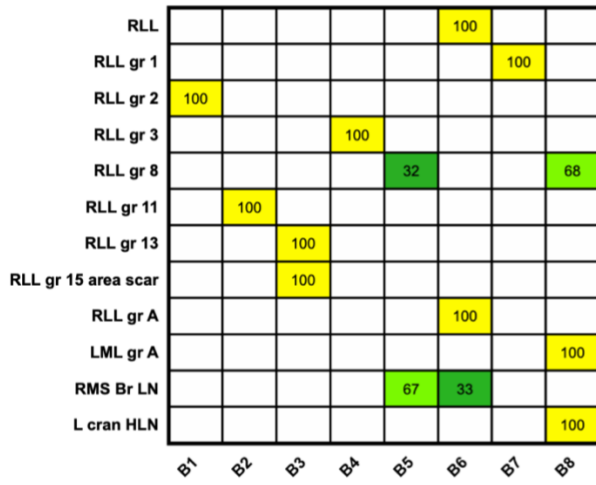
12418



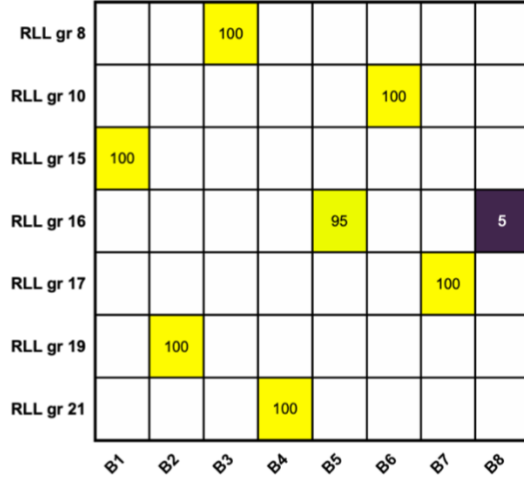
12518



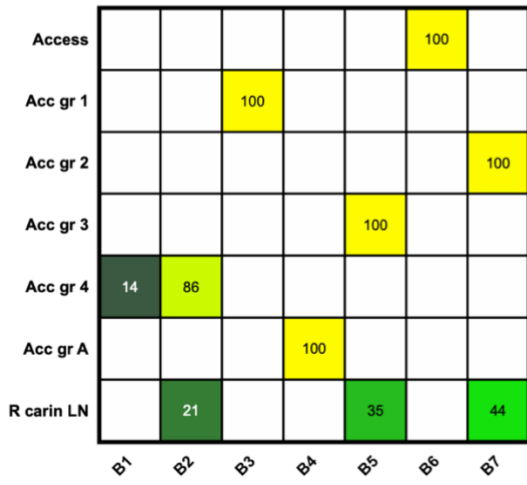
12618



13618



14018



14118

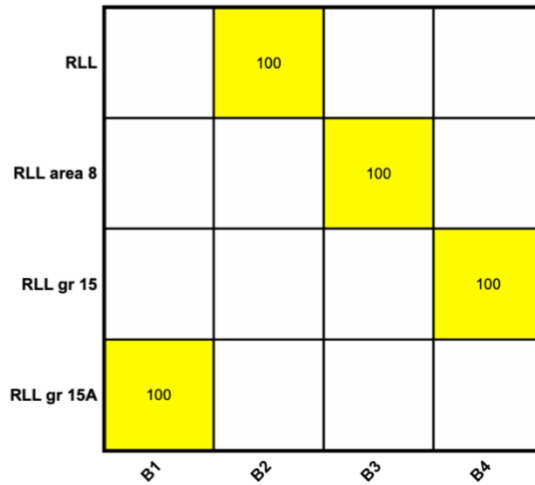


Figure 51. Barcode heatmaps of IgG controls.

Samples can be divided into 4 groups: granulomas, lymph nodes, random lung lobe and extrapulmonary (eg. spleen and liver). Lung lobes are written using 3 letters which correspond to the side of the lungs (ie. left vs right), position of the lobe (ie. upper, middle or lower) and lobe. For example, right lower lobe is abbreviated as RLL, left upper lobe as LUL, and so on. The accessory lobe is written as Access. Granulomas are written as “lung lobe + granuloma number”, for example, RLL gr 1 or LUL gr 2. Lymph nodes are always written with the letters “LN” or “HLN” which means lymph node or hilar lymph node. The letters “gr” at the end of lymph node names means granuloma. The barcode IDs can be found at the bottom of each heatmap - A denotes Mtb library A and B denotes Mtb library B. Images courtesy of Forrest Hopkins, HSPH.

Figure 52. Barcode heatmaps of α -CD4 group.

Samples can be divided into 4 groups: granulomas, lymph nodes, random lung lobe and extrapulmonary (eg. spleen and liver). Lung lobes are written using 3 letters which correspond to the side of the lungs (ie. left vs right), position of the lobe (ie. upper, middle or lower) and lobe. For example, right lower lobe is abbreviated as RLL, left upper lobe as LUL, and so on. The accessory lobe is written as Access. Granulomas are written as “lung lobe + granuloma number”, for example, RLL gr 1 or LUL gr 2. Lymph nodes are always written with the letters “LN” or “HLN” which means lymph node or hilar lymph node. The letters “gr” at the end of lymph node names means granuloma. The barcode IDs can be found at the bottom of each heatmap - A denotes Mtb library A and B denotes Mtb library B. Images courtesy of Forrest Hopkins, HSPH.

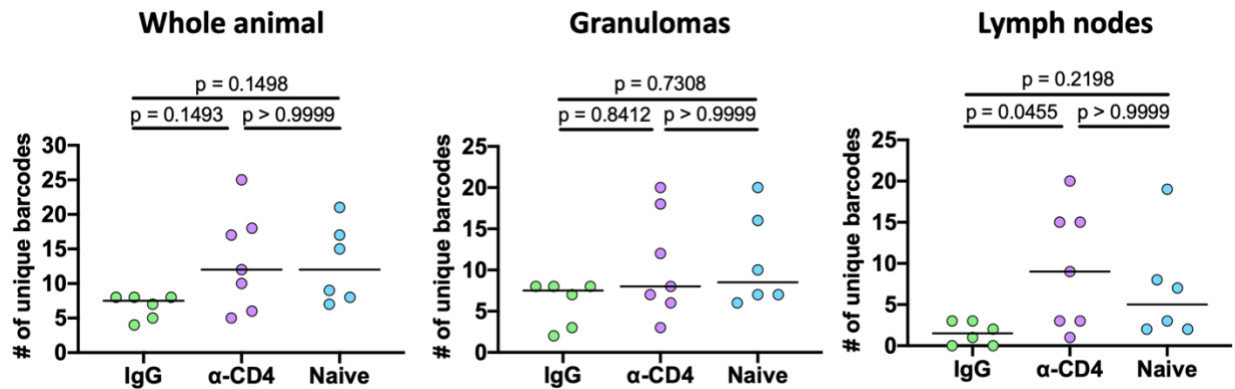


Figure 53. The number of unique barcodes in each animal, granulomas and lymph nodes.

Each data point is a monkey. Kruskal-Wallis with Dunn’s multiple comparison test was used to compare the groups. Lines at median.

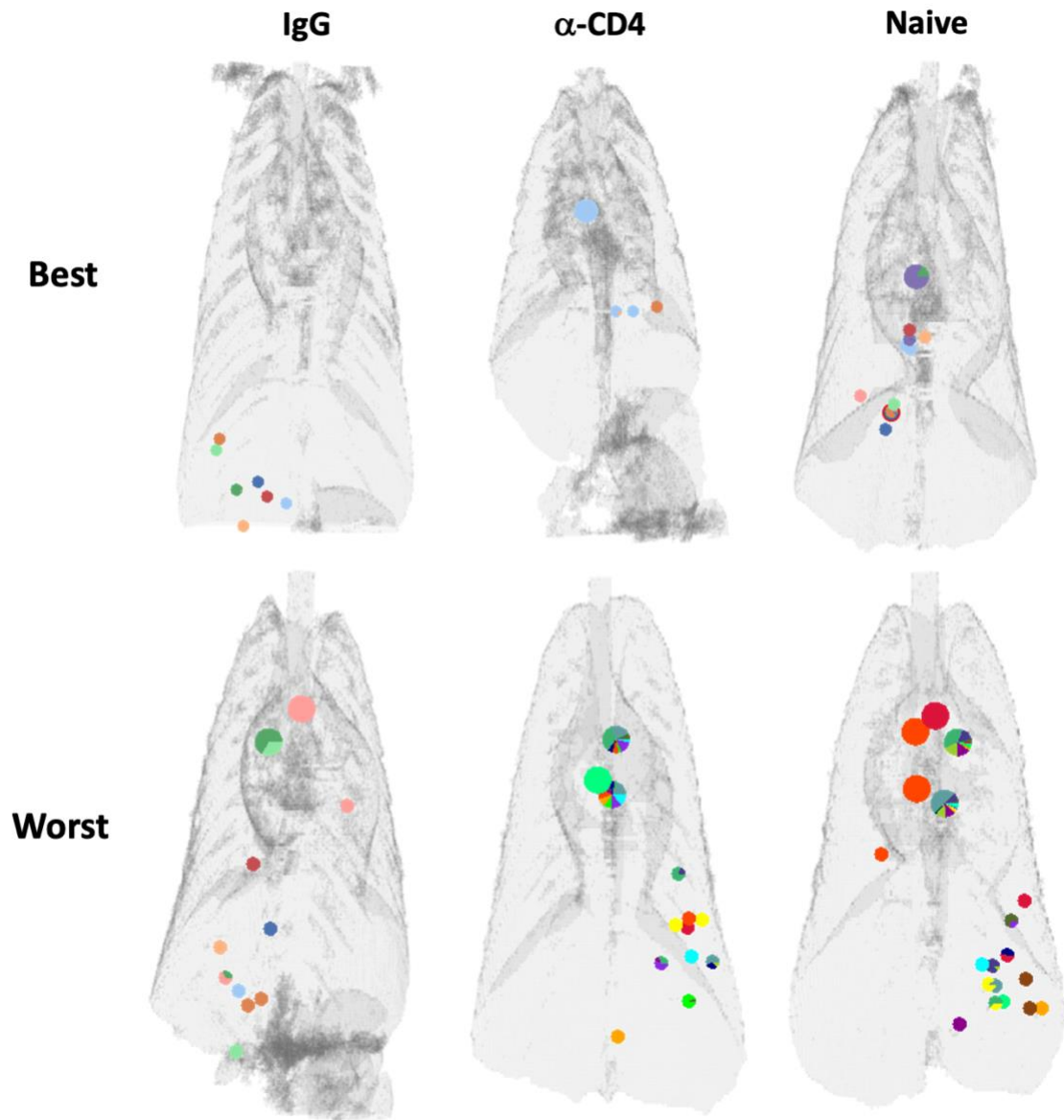


Figure 54. 3D rendering of thoracic cavity of “best” and “worst” macaques from each group.

Small markers represent pulmonary granulomas, while larger markers denote lymph nodes. Each color represents a unique barcode tag. Marker with red outer ring denotes a granuloma cluster.

Images courtesy of Henry J. Borish, Pitt MMG.

4.4 Discussion

The mechanisms of protection that a primary Mtb infection confers against a secondary Mtb challenge remains unknown. CD4 T cells have been shown to be important in protection against Mtb infection and disease in humans and animal studies [178-183, 252, 274], however the role of CD4 T cells in the context of Mtb reinfection remains to be elucidated. Here, we show that CD4 T cells are important in the protection a primary Mtb infection confers to a secondary Mtb challenge. Depleting CD4 T cells prior to second infection resulted in the formation of a greater number of new granulomas in some but not all macaques, which may point to the heterogeneity of response to CD4 T cell depletion, wherein some animals are more dependent on CD4 T cells for protection against secondary Mtb challenge while some animals are not. CD4 T cell depletion resulted in significantly higher Mtb burden in new granulomas and the lungs and increased dissemination of Mtb from the lungs to the lymph nodes. Protection against the second infection was not completely abolished with CD4 T cell depletion suggesting that other immune factors are likely to contribute to this protection.

We tested whether there was a difference in the airway immune environment of naïve and Mtb library A-infected but drug treated macaques before the antibody infusions and Mtb library B infection. Here, we show that eliminating live Mtb by drug treatment does not result in the reversion of the airway immune environment to pre-infection levels. Both drug treated and non-drug treated infected animals had higher numbers of CD4 and CD8 T cells in the airways before Mtb library B infection compared to the naïve controls, which have been negatively correlated with the number of new granulomas and bacterial burden in new granulomas, lungs and lymph nodes. Interestingly, macaques previously infected with Mtb library A, with or without drug treatment, had greater numbers of CD4 T cells producing IFN γ and TNF α in response to ESAT-

6/CFP-10 stimulation and this was also negatively correlated with the formation of new granulomas and bacterial burden in the lungs and thoracic lymph nodes. However, we cannot discount the fact that the correlations could also be because of the different treatments (naïve vs Mtb-library A-infected) and not necessarily because of the cells examined. Studies in IFN γ knockout mice which are unable to control Mtb infection [190, 191] and humans with increased susceptibility to weakly virulent mycobacteria such as BCG or environmental mycobacteria (Mendelian susceptibility to mycobacterial disease) [194, 195], demonstrate the importance of IFN γ in the control of Mtb infection. TNF is also vital in the control of Mtb infection as first shown in mice where TNF neutralization and disruption of TNF receptor resulted in early death and higher bacterial burden compared to control animals [196]. This was further supported by reactivation of LTBI in humans after administration of infliximab [197], a TNF-neutralizing antibody, and in NHPs [198, 199]. Increased numbers of CD8 and CD4 T cells and CD4 T cells producing IFN γ and TNF α in the airways where the host first encounters Mtb may be critical in the protection against a secondary Mtb infection. This supports our decision to target CD4 T cells in our initial assessment of the immune mechanisms of protection against reinfection. Unfortunately, we were not able to get BAL samples after IgG and anti-CD4 antibody infusions because we did not want to disturb the airway environment shortly before Mtb library B infection which could affect our primary outcome measures (formation of new granulomas and CFU). Nevertheless, it is an avenue worthy of additional study.

Since CD4 and CD8 T cells are inextricably linked [277, 280], we investigated whether CD4 T cell depletion affected the number and function of CD8 T cells during a second Mtb infection. In our study, CD8 T cell numbers, cytotoxic function and cytokine production were not affected by CD4 T cell depletion. This is in contrast to a study in Mtb-infected mice where optimal

IFN γ production by CD8 T cells requires the continuous presence of CD4 T cells after BCG vaccination [281]. In addition, the absence of CD4 T cells resulted in decreased cytokine production and cytotoxic activity in CD8 T cells in mice, however these are both in the context of a primary Mtb infection [185, 278]. In the context of a second Mtb infection, CD4 T cells seem to be dispensable for the proper function of CD8 T cells. Indeed, while CD4 T cell help is required for the generation of memory CD8 T cells able to proliferate and respond to a secondary antigen exposure, this help is only required during the initial stage of CD8 T cell priming and not after [282-284]. In our Mtb reinfection model, CD8 T cells were already primed with CD4 T cell help during the first infection, generating effector memory CD8 T cells which were independent from CD4 T cells when exposed to a secondary Mtb challenge.

Our results in the current study demonstrate that depleting CD4 T cells diminished the protection a primary Mtb infection confers to a secondary infection. However, the exact mechanism by which CD4 T cells are providing protection is still unclear. The prevailing hypothesis is that CD4 T cells protect against primary Mtb infection in mice through the production of IFN γ [185], although IFN γ -independent mechanisms have also been described [285]. In our study, CD4 T cell depletion reduced the number of CD4 T cells producing various cytokines including IFN γ , TNF and IL-17A in all tissues examined, all of which have been shown to be important in Mtb control [191, 196, 205].

Using Luminex to assess a wide variety of cytokines and chemokines in lung tissue, we observed significantly lower levels of IL-23 in CD4 T cell-depleted macaques compared to IgG controls. IL-23 is produced by activated dendritic cells after encountering Mtb and promotes the generation of Th17 cells during initial priming [286, 287]. IL-23 has also been shown to induce proliferation and IL-17A production in memory T cells [288, 289] and is important in maintaining

Th17 function [290]. It is therefore not surprising that we also observed a lower level of IL-17A in the lungs of the α -CD4 group compared to the naïve controls. This was corroborated by a reduction in IL-17-producing CD4 T cells in the lungs measured by flow cytometry. In mice, $\gamma\delta$ T cells have been shown to be the major producers of IL-17A during early Mtb infection [291], but in NHP granulomas, a small frequency of CD4 and CD8 T cells produce IL-17 [121]. Although Mtb is still controlled in IL-23-deficient mice [286, 292], IL-23 has been shown to contribute to Mtb control when present early in infection [293]. IL-23, when delivered in an adenovirus vector 72 hours prior to Mtb infection in mice, resulted in significantly lower Mtb burden in the lungs compared to empty vector and PBS only controls. Adenovirus-IL-23 pretreatment also resulted in elevated IL-17A and IFN γ mRNA levels in the lungs and increased numbers of activated CD4 T cells in lungs and lymph nodes [293]. IL-17A has been shown to be critical in protecting mice against Mtb Beijing HN878 infection [205]. IL-17 $^{-/-}$ mice exhibited greater lung pathology and bacterial burden after infection with Mtb Beijing HN878 and this effect was linked to the induction of the chemokine CXCL-13, which is required for T cell localization in lymphoid follicles in the lungs facilitating macrophage activation and control of Mtb [205]. IL-17A also contributes in controlling Mtb infection by promoting the formation of mature granulomas [294]. Lastly, IL-17A induces CXCL1 and CXCL5 production in the lungs which are critical in recruiting neutrophils [295]. Although neutrophils have been associated with increased pathology, bacterial burden, active TB disease, respiratory failure and death in several animal models and in humans [156-158, 160, 161], early recruitment of neutrophils in rats resulted in significantly lower (650-fold) bacterial burden in the lungs [153]. This protection progressively lessened as neutrophil recruitment to the lungs was delayed. The importance of neutrophils early in Mtb infection was also demonstrated in other studies [152, 154]. Increased bacterial load in lungs of CD4 T cell-

depleted macaques might have been caused by the reduction of activated CD4 T cell and neutrophil recruitment and homing of T cells to lymphoid follicles in the lungs resulting from a decrease in IL-23 and IL-17A levels. It is important to note that cytokine levels in lungs were assayed at necropsy which might not reflect the lung environment at the time of the second infection 4 weeks earlier. Reduced TNF levels in the lungs of IgG and α -CD4 groups may reflect the lack of disease in these macaques compared to the naïve controls.

One common characteristic in the robust protection from Mtb infection and disease demonstrated by the Mtb reinfection and intravenous BCG (IV-BCG) vaccination studies in macaques is the rapid control of Mtb infection in the lungs preventing its dissemination to thoracic lymph nodes. In the initial Mtb reinfection study [264], 5 out of 8 reinfected macaques failed to form CFU+ new granulomas. The new granulomas that did grow Mtb had significantly lower thoracic Mtb burden compared to granulomas formed in naïve controls. Overall, bacterial burden from the second infection was 10,000-fold lower in reinfected macaques compared to naïve controls. In that study, only 1 out of 8 reinfected animals had Mtb library B in their thoracic lymph nodes. Similarly, 6 out of 10 IV-BCG vaccinated macaques did not form any granulomas after Mtb infection, and 3 of 10 had <50 CFU in total in the lungs. Overall, IV-BCG macaques had 100,000-fold lower thoracic bacterial burden compared to macaques vaccinated intradermally with BCG. Interestingly, 9 out of 10 IV-BCG macaques did not grow Mtb in any of the thoracic lymph nodes examined [63]. Here, we showed that CD4 T cells are important in preventing Mtb dissemination to the lymph nodes. Interestingly, even though there was increased Mtb dissemination to the lymph nodes in the α -CD4 group, the bacterial burden was still lower compared to the naïve group. Several possible reasons for this are: (1) the replicative ability of Mtb reaching the lymph nodes has been compromised, (2) lymph nodes have increased killing

capacity during a second infection and (3) Mtb dissemination to the lymph nodes was delayed resulting in lower CFU in these tissues. Quantifying Mtb genomes in lymph nodes would help to determine whether this finding is due to the first 2 possibilities. Since we have shown that lymph nodes are sites of Mtb persistence and growth (Chapter 5), this further reinforces the importance of CD4 T cells in conferring protection against a second Mtb infection.

It was surprising that even though the number of CD4 T cells producing cytokines was not significantly lower in new granulomas of the α -CD4 group compared to the IgG group, there was still a significant increase in the bacterial burden in the new granulomas of the α -CD4 group. It suggests that a small perturbation in the number of functional CD4 T cells in granulomas could tip the scale favoring Mtb growth. However, we did not examine all of the possible cytokines produced by CD4 T cells, and it is possible that other CD4 T cell functions could be impaired. We found no correlation between the number of CD4 T cells in the blood at second infection and necropsy, as well as in the lungs, and the number of new granulomas and bacterial burden in new granulomas, lungs and thoracic lymph nodes. This supports the idea that only some macaques rely heavily in CD4 T cells for protection. However, one limitation in our correlation analyses is the low sample size.

The reduced number of B cells in new granulomas of the IgG group compared to the naïve group was unexpected. In NHPs, B cells can be found in granulomas as clusters resembling germinal centers and actively secreting antibodies [217]. In addition, granulomas with reduced number of B cells have higher bacterial burden [218]. The discrepancy in our results could have stemmed from a reduced recruitment of B cells in new granulomas due to the new granulomas in the IgG group quickly controlling Mtb. This needs to be further studied.

While CD4 T cell depletion resulted in an increase in Mtb burden in the lungs compared to the IgG group, the α -CD4 group still had lower bacterial burden in new granulomas and lungs than naïve controls, albeit not statistically significant. There was also a significantly lower total CFU in thoracic lymph nodes compared to the naïve control. Thus, CD4 T cell depletion did not fully abrogate the protection generated by the first Mtb infection suggesting other factors contributing to this protection. This was also seen in the context of LTBI reactivation by CD4 T cell depletion wherein only a subset of CD4 T cell-depleted macaques reactivated [182, 296]. In macaques with acute Mtb infection, 1 of 5 was still able to control the infection [182]. In addition, early during reactivation, CD4 T cell-depleted LTBI macaques formed fewer new granulomas and many of these new granulomas were sterile [183]. Although we cannot disregard the contribution of the remaining CD4 T cells, there are other factors that could have prevented complete abolishment of protection in the α -CD4 group. CD8 T cells have been shown to be important in Mtb control in mice [186] and in BCG-induced protection in rhesus macaques [189]. Antibodies from LTBI patients have been shown to promote phagosomal maturation, inflammasome activation and enhanced intracellular Mtb killing in macrophages [216]. Innate immune memory, such as increased production of ROS by macrophages or enhanced monocyte production of proinflammatory cytokines, induced by BCG vaccination have also been reported [297, 298]. Further studies on other factors contributing to the protection a primary infection confers to a secondary Mtb infection are needed.

4.5 Acknowledgements

I would like to thank Henry J. Borish, Pauline Maiello and Philana Ling Lin for developing the code that created the 3D rendering images and Forrest Hopkins for identifying the Mtb libraries and barcodes and generating the heat maps.

5.0 Lymph nodes are sites of prolonged bacterial persistence during *Mycobacterium tuberculosis* infection in macaques

This section is adapted from the original publication:

Ganchua SKC, Cadena AM, Maiello P, Gideon HP, Myers AJ, Junecko BF, Klein EC, Lin PL, Mattila JT and Flynn JL. 2018. Lymph nodes are sites of prolonged bacterial persistence during *Mycobacterium tuberculosis* infection in macaques

PLoS Pathogens. 14(11): e1007337.

5.1 Introduction

Tuberculosis (TB) is one of the significant causes of morbidity and mortality in the world. It is estimated that 2.3 billion people worldwide are infected with *Mycobacterium tuberculosis* (Mtb), the causative agent of TB. In 2016, there were an estimated 10.4 million new TB cases and 1.6 million deaths [299]. Although the most common site of infection and disease is the lungs, extrapulmonary TB also occurs, and lymph nodes (LN) are the most common sites of extrapulmonary Mtb infection [240, 241]. In humans, it has been classically observed that a tuberculous pulmonary lesion is almost always accompanied by a granulomatous thoracic LN; this is called a Ghon complex [238, 239]. Moreover, reports of TB-associated cervical lymphadenitis (scrofula) span from antiquity to the present [300-302]. Historically, it was not known whether scrofula was related to TB [300], but some individuals with scrofula eventually died from TB-associated disease including TB meningitis and pneumonia, suggesting a relationship between

these dissimilar-appearing pathologies [300-302] and this has been demonstrated by more modern techniques, including microscopy, culture and nucleic acid amplification tests [303, 304].

Lymph node infection occurs in people with active and clinically latent TB [253, 305-307] but the timing and frequency of LN infection, bacterial load in LNs, and the relationship between LN infection and disease outcome remain uncertain. Most studies on Mtb infection in LNs were in murine models and focused mainly on identifying the mechanisms and regulation of T cell priming in LNs [106-108, 308]. However, mice are different from humans in that they only have a single lung-draining mediastinal LN. Moreover, pathologic presentation and course of TB in mice is substantially different than that seen in humans [309], and there has been little emphasis on identifying the long-term consequences of Mtb infection in these lymphoid tissues. Guinea pigs have been shown to develop rapid and severe lymphadenopathy after Mtb infection with live bacteria and T cell influx demonstrable in LNs as early as 5 days post-infection [310-312]. In cattle, LNs are the most common site of *M. bovis* infection with microscopic lesions visible as early as 7 days post-infection [245, 247, 313]. In a small study examining the prevalence of lung and LN infections in bovine TB, all cattle had *M. bovis*-infected LNs while pulmonary infection was much less common (1 of 15 cattle) [246]. However, since tuberculous lung lesions can be small, some authors as cited by Neill et al, believe that without thorough examination these lesions are missed [245]. It is widely believed that LNs get infected with *M. bovis* first while lung lesions develop later during infection [245, 247].

Rhesus and cynomolgus macaques have been used as models of human TB, and represent the spectrum of pathology and disease outcome seen in human Mtb infection [116, 230, 232, 233]. Thoracic LNs are frequently infected in Mtb-infected macaques [231-233] and the first signs of reactivated TB assessed by microscopic histology can occur in thoracic LNs. We previously

showed that macaques considered high risk for reactivation after TNF neutralization had a greater proportion of thoracic LN with Mtb growth compared to those that were low risk [198]. Moreover, in studies where immune suppression was induced by anti-CD4 antibodies, reactivation was associated with macaques with greater depletion of CD4 T cells in thoracic LNs [182, 198], suggesting immune responses in these organs are important for overall protection. Anti-TNF induced reactivation can also present in thoracic LNs [198]. In BCG or BCG+H56 vaccinated cynomolgus macaques, protection against reactivation was associated with limited LN involvement [199]. Although closely related to cynomolgus macaques, rhesus macaques are more susceptible to TB owing in part to their more extensive LN pathology [235]. Rhesus macaques have increased numbers of Mtb-infected LNs, higher bacterial burden per LN, and greater LN pathology than cynomolgus macaques. Extensive LN disease can lead to enlargement of LNs such that they impinge on the macaque's airway, occasionally leading to lung lobe collapse. Enlarged and necrotic LNs have also been noted to erode into the airways leading to substantial dissemination [235].

Although it is clear that LNs are commonly infected, we know very little about how Mtb infection influences LN structure and function. Lymph nodes are highly-structured organs where T cells and B cells interact with dendritic cells (DCs) in spatially-distinct anatomic regions, and this delicately balanced organization facilitates priming and adaptive immunity [314-317]. Other elements in LNs that are required for proper function and are susceptible to disruption by Mtb infection include subcapsular macrophages and fibroblastic reticular cells [318, 319], conduit systems that mediate fluid flow and antigen entry into LNs, capillaries, and lymphatic vessels [320-322]. Lymphatic endothelial cells have also been shown to promote or restrict Mtb replication depending on their activation status, thus these cells may represent an underappreciated intra-

lymph node niche for Mtb [323, 324]. In addition to priming adaptive immunity, LNs have intrinsic antimicrobial capacities that limit dissemination of pathogens [325-327] although it is unknown whether they have this capacity in Mtb infection.

Studies on LNs in TB often focus on diagnosis [303, 328-331] or priming of adaptive immunity [107, 108, 308, 314, 332], and despite more than a century of TB research, there are many aspects of the infection that remain unclear. Basic questions including the dynamics of LN Mtb infection, whether LNs are sites of successful defense against Mtb growth, the proportion of LNs that get infected, and how Mtb infection affects LN structure and function remain unanswered. To address these questions, we performed a comprehensive study of thoracic LNs in Mtb-infected cynomolgus and rhesus macaques to identify how Mtb infection changes LNs. We found that LNs in Mtb-infected macaques increased in PET-CT-measured metabolic activity early during infection, and at necropsy, almost all of the FDG-avid LNs contained viable Mtb or persistent Mtb DNA. We show that Mtb grows to the same level in LNs of both macaque species, however, cynomolgus macaque LNs were better able to control the infection compared to rhesus macaque LNs. In comparison with granulomas in the lung [118], thoracic LNs had limited abilities to kill Mtb. Granulomas that form in Mtb-infected LNs disrupt LN structures and greater destruction of the LN structure is associated with higher Mtb burden. Our data support that LNs are a niche for persistent infection, and are likely to play a larger role in the pathogenesis of TB than previously appreciated. Moreover, identifying relationships between LNs, bacterial persistence, and disease progression may yield new insights into disease pathogenesis, improve TB treatment and limit reactivation of latent TB.

5.2 Methodology

5.2.1 Animals

Cynomolgus (*Macaca fascicularis*) (n=32) and rhesus macaques (*Macaca mulatta*) (n=19) that served as controls (no vaccine or drug treatment) for other studies from 2011 to 2016 were selected for this study. These macaques were infected with a low dose (~1-28 CFU, median=6 CFU) of Mtb strain Erdman using a bronchoscope. The animals used in this study are summarized in Table 4. The number of LNs examined per monkey ranged from 4-21, with the median being 12 per monkey. A detailed list of animals can be found in Table 5; other data from some monkeys have been previously published in other studies as noted in that table. All procedures and protocols were approved by the University of Pittsburgh's Institutional Animal Care and Use Committee.

Table 4. Animals used in the CFU, CEQ, histological studies.

| Cynomolgus Macaques | | | | |
|---------------------|----------------|---------------------|-----------------------|-----------|
| Time post-infection | No. of animals | No. of thoracic LNs | No. of peripheral LNs | Total No. |
| 4-6 weeks | 8 | 61 | 32 | 93 |
| 11-14 weeks | 9 | 70 | 34 | 104 |
| 16-29 weeks | 9 | 57 | 12 | 69 |
| 34-54 weeks | 6 | 49 | 23 | 72 |
| Rhesus Macaques | | | | |
| Time post-infection | No. of animals | No. of thoracic LNs | No. of peripheral LNs | Total No. |
| 4 weeks | 4 | 38 | 16 | 54 |
| 11-14 weeks | 7 | 59 | 26 | 85 |
| 16-28 weeks | 8 | 79 | 28 | 107 |

Table 5. List of macaques used in this study (CFU, CEQ, CFU/CEQ)

| Monkey ID | Species | Days post-infection | Wks post-infection | Date infected | Dose | Necropsy date | PET CT scans (wks pi) | Reference |
|-----------|---------|---------------------|--------------------|---------------|------|---------------|--------------------------------------|-------------|
| 1414 | Cyno | 26 | 4 | 18-Jun-14 | 4.7 | 14-Jul-14 | 3 | unpublished |
| 1014 | Cyno | 28 | 4 | 23-May-14 | 1 | 20-Jun-14 | 2, 4 | unpublished |
| 1514 | Cyno | 28 | 4 | 18-Jun-14 | 4.7 | 16-Jul-14 | 4 | unpublished |
| 19015 | Cyno | 29 | 4 | 17-Nov-15 | 6 | 16-Dec-15 | 2, 4 | [121] |
| 1214 | Cyno | 31 | 4 | 23-May-14 | 1 | 23-Jun-14 | 2, 4 | unpublished |
| 8715 | Cyno | 36 | 5 | 12-Jan-16 | 2 | 17-Feb-16 | 2, 3, 4 | unpublished |
| 8915 | Cyno | 36 | 5 | 12-Jan-16 | 2 | 17-Feb-16 | 2, 3, 5 | unpublished |
| 8815 | Cyno | 41 | 6 | 12-Jan-16 | 2 | 22-Feb-16 | 2, 3, 4, 5 | unpublished |
| 2116** | Cyno | 74 | 11 | 25-Feb-16 | 3 | 9-May-16 | 4, 6, 8, 10 | [235] |
| 9814 | Cyno | 78 | 11 | 26-Aug-14 | 6 | 12-Nov-14 | 3, 6, 11 | [235] |
| 1114 | Cyno | 81 | 12 | 28-Aug-14 | 2.7 | 17-Nov-14 | 2, 4, 6, 8, 10, 11 | unpublished |
| 1314 | Cyno | 81 | 12 | 28-Aug-14 | 2.7 | 17-Nov-14 | 2, 4, 6, 8, 10, 11 | unpublished |
| 17413 | Cyno | 83 | 12 | 28-Aug-14 | 2.7 | 19-Nov-14 | 2, 3, 4, 6, 8, 10, 12 | unpublished |
| 616 | Cyno | 88 | 13 | 18-Feb-16 | 11 | 16-May-16 | 4, 6, 8, 12 | [235] |
| 13716 | Cyno | 88 | 13 | 14-Jul-16 | 5 | 10-Oct-16 | 4, 6, 8, 12 | [235] |
| 1714 | Cyno | 91 | 13 | 18-Jun-14 | 4.7 | 17-Sep-14 | 4, 6, 8, 10, 13 | unpublished |
| 916 | Cyno | 95 | 14 | 18-Feb-16 | 11 | 23-May-16 | 4, 5, 8, 13 | [235] |
| 2016 | Cyno | 109 | 16 | 25-Feb-16 | 3 | 13-Jun-16 | 4, 6, 8, 15 | [235] |
| 21112 | Cyno | 133 | 19 | 7-Oct-13 | 12 | 17-Feb-14 | 2, 4, 5, 6, 9, 13, 17, 19 | [235] |
| 20512 | Cyno | 143 | 20 | 12-Jul-13 | 6 | 2-Dec-13 | 2, 3, 4, 8, 12, 16, 20 | [235] |
| 20712 | Cyno | 152 | 22 | 12-Jul-13 | 6 | 11-Dec-13 | 1, 3, 4, 8, 12, 16, 21 | [235] |
| 16213 | Cyno | 163 | 23 | 14-Apr-14 | 15.2 | 24-Sep-14 | 3, 4, 5, 7, 10, 15, 23 | [235] |
| 16013 | Cyno | 170 | 24 | 14-Apr-14 | 15.2 | 1-Oct-14 | 2, 3, 4, 6, 10, 15, 24 | [235] |
| 16113 | Cyno | 170 | 24 | 14-Apr-14 | 15.2 | 1-Oct-14 | 2, 3, 4, 6, 10, 15, 24 | [235] |
| 20715 | Cyno | 174 | 25 | 22-Dec-15 | 12.5 | 13-Jun-16 | 4, 9, 12, 20, 24 | unpublished |
| 20915 | Cyno | 202 | 29 | 22-Dec-14 | 12.5 | 11-Jul-16 | 4, 8, 12, 17, 20, 24, 28 | unpublished |
| 9811 | Cyno | 238 | 34 | 17-Oct-11 | 20 | 11-Jun-12 | 3, 6, 8, 12, 16, 20, 24, 28, 34 | [235] |
| 15712 | Cyno | 293 | 42 | 11-Dec-12 | 12 | 30-Sep-13 | 40 | unpublished |
| 17211 | Cyno | 328 | 47 | 31-Jul-12 | 6 | 24-Jun-13 | 46 | [121] |
| 2312 | Cyno | 330 | 47 | 31-Jul-12 | 6 | 26-Jun-13 | 47 | [121] |
| 15812 | Cyno | 336 | 48 | 11-Mar-13 | 28 | 10-Feb-14 | 31, 40, 46, 48 | unpublished |
| 2612 | Cyno | 379 | 54 | 21-Aug-12 | 8 | 4-Sep-13 | 54 | [276] |
| 5614 | Rhesus | 26 | 4 | 18-Jun-14 | 4.7 | 14-Jul-14 | 3 | unpublished |
| 5714 | Rhesus | 28 | 4 | 18-Jun-14 | 4.7 | 16-Jul-14 | 4 | unpublished |
| 17115 | Rhesus | 28 | 4 | 19-Oct-15 | 5.3 | 16-Nov-15 | 3, 4 | unpublished |
| 17215 | Rhesus | 30 | 4 | 19-Oct-15 | 5.3 | 18-Nov-15 | 3, 4 | unpublished |
| 915** | Rhesus | 78 | 11 | 7-Apr-15 | 8 | 24-Jun-15 | 3, 8, 11 | [235] |
| 6114 | Rhesus | 80 | 11 | 23-May-14 | 1 | 11-Aug-14 | 2, 4, 8, 10, 11 | unpublished |
| 16915 | Rhesus | 86 | 12 | 12-Oct-15 | 7 | 6-Jan-16 | 3, 7, 12 | [235] |
| 5414 | Rhesus | 89 | 13 | 18-Jun-14 | 4.7 | 15-Sep-14 | 4, 6, 8, 10, 12 | unpublished |
| 5814 | Rhesus | 91 | 13 | 18-Jun-14 | 4.7 | 17-Sep-14 | 4, 6, 8, 10, 13 | unpublished |
| 1415** | Rhesus | 98 | 14 | 16-Apr-15 | 15 | 23-Jul-15 | 4, 8, 9, 11, 14 | [235] |
| 7614** | Rhesus | 99 | 14 | 27-May-14 | 8 | 3-Sep-14 | 2, 4, 6, 8, 11, 14 | [235] |
| 613 | Rhesus | 110 | 16 | 13-Mar-13 | 18 | 1-Jul-13 | 2, 4, 6, 8, 12, 15 | [235] |
| 813 | Rhesus | 112 | 16 | 13-Mar-13 | 18 | 3-Jul-13 | 2, 4, 6, 8, 12, 16 | [235] |
| 713 | Rhesus | 117 | 17 | 13-Mar-13 | 18 | 8-Jul-13 | 2, 4, 7, 8, 12, 16 | [235] |
| 2315 | Rhesus | 151 | 22 | 16-Apr-15 | 15 | 5-Aug-15 | 4, 8, 13, 16, 19, 21 | [235] |
| 1215 | Rhesus | 154 | 22 | 7-Apr-15 | 8 | 8-Sep-15 | 4, 8, 12, 16, 20, 21 | [235] |
| 6914 | Rhesus | 181 | 26 | 27-May-14 | 8 | 24-Nov-14 | 2, 4, 7, 8, 12, 17, 20, 25 (CT only) | [235] |
| 8214 | Rhesus | 186 | 27 | 29-May-14 | 10 | 1-Dec-14 | 4, 6, 8, 12, 16, 20, 26 | [235] |
| 7114 | Rhesus | 195 | 28 | 27-May-14 | 8 | 8-Dec-14 | 2, 4, 7, 8, 12, 16, 20, 27 | [235] |

5.2.2 Ethics Statement

All experimental manipulations, protocols, and care of the animals were approved by the University of Pittsburgh School of Medicine Institutional Animal Care and Use Committee (IACUC). The protocol assurance number for our IACUC is A3187-01. Our specific protocol approval numbers for this project are: 13122856, 15066174, 12080653, 15126588, 11110045, 12060181, 14023305, 1105870, 11090030, 15015299, 12090832, 15066174, 1003622, and 1105870. The IACUC adheres to national guidelines established in the Animal Welfare Act (7 U.S.C. Sections 2131–2159) and the Guide for the Care and Use of Laboratory Animals (8th Edition) as mandated by the U.S. Public Health Service Policy.

All macaques used in this study were housed at the University of Pittsburgh in rooms with autonomously controlled temperature, humidity, and lighting. Animals were singly housed in caging at least 2 square meters apart that allowed visual and tactile contact with neighboring conspecifics. The macaques were fed twice daily with biscuits formulated for nonhuman primates, supplemented at least 4 days/week with large pieces of fresh fruits or vegetables. Animals had access to water *ad libitem*. Because our macaques were singly housed due to the infectious nature of these studies, an enhanced enrichment plan was designed and overseen by our nonhuman primate enrichment specialist. This plan has three components. First, species-specific behaviors are encouraged. All animals have access to toys and other manipulata, some of which will be filled with food treats (e.g. frozen fruit, peanut butter, etc.). These are rotated on a regular basis. Puzzle feeders, foraging boards, and cardboard tubes containing small food items also are placed in the cage to stimulate foraging behaviors. Adjustable mirrors accessible to the animals stimulate interaction between animals. Second, routine interaction between humans and macaques are encouraged. These interactions occur daily and consist mainly of small food objects offered as

enrichment and adhere to established safety protocols. Animal caretakers are encouraged to interact with the animals (by talking or with facial expressions) while performing tasks in the housing area. Routine procedures (e.g. feeding, cage cleaning, etc) are done on a strict schedule to allow the animals to acclimate to a routine daily schedule. Third, all macaques are provided with a variety of visual and auditory stimulation. Housing areas contain either radios or TV/video equipment that play cartoons or other formats designed for children for at least 3 hours each day. The videos and radios are rotated between animal rooms so that the same enrichment is not played repetitively for the same group of animals.

All animals are checked at least twice daily to assess appetite, attitude, activity level, hydration status, etc. Following *M. tuberculosis* infection, the animals are monitored closely for evidence of disease (e.g., anorexia, weight loss, tachypnea, dyspnea, coughing). Physical exams, including weights, are performed on a regular basis. Animals are sedated prior to all veterinary procedures (e.g. blood draws, etc.) using ketamine or other approved drugs. Regular PET/CT imaging is conducted on most of our macaques following infection and has proved very useful for monitoring disease progression. Our veterinary technicians monitor animals especially closely for any signs of pain or distress. If any are noted, appropriate supportive care (e.g. dietary supplementation, rehydration) and clinical treatments (analgesics) are given. Any animal considered to have advanced disease or intractable pain or distress from any cause is sedated with ketamine and then humanely euthanatized using sodium pentobarbital.

5.2.3 FDG PET-CT imaging

Serial 2-deoxy-2-[¹⁸F]-D-deoxyglucose (FDG) positron emission tomography (PET) with computed tomography (CT) imaging was performed in a biosafety level 3 facility as described

previously [276]. Lymph nodes were identified by our analyst (P. Maiello) and metabolic activity (FDG avidity) was measured [236]. Lymph nodes that were seen on scan had a maximum SUV (standard uptake value) greater than or equal to 2.3. SUVR (maximum standard uptake value ratio normalized to muscle to reduce variability between scans). Despite the fact that we can see LNs with $SUV \geq 2.3$ on the scans, we consider LNs with SUVR of ≥ 5 to be “hot.” Serial scans were performed ranging from 1 week to 54 weeks post-infection. The majority of the shorter term infection macaques (necropsied 14 weeks post-infection or earlier) were scanned every 2 weeks until necropsy. The longer term infection macaques (necropsied 15 weeks post-infection or longer) were scanned every 2 weeks until 8 weeks post-infection and every 4 weeks thereafter. Some of the latent monkeys (34-54 weeks) were only scanned immediately prior to necropsy.

5.2.4 Necropsy Procedures

Necropsy procedures were as previously described [231]. Briefly, one to three days prior to necropsy, macaques were imaged by FDG-PET/CT to ascertain which LNs were metabolically active and to measure their FDG avidity. Individual lung granulomas, thoracic, axillary and inguinal LNs were excised and cut into 2 sections. One section was homogenized into single cell suspension in PBS for immunology and aliquots made for both plating on 7H11 agar plates to obtain colony forming units (CFU) and DNA extraction for qPCR. The other section was placed in 10% normal buffered formalin and paraffin embedded for histologic examination. Bacterial burden (CFU) per LN was determined by accounting for the amount of sample plated compared to the entire LN sample. The LN necropsy score was determined based on the number of LNs with granulomas, the size of the lymph nodes and the degree of LN effacement. The extrapulmonary score was determined based on the presence, relative frequency and size of granulomas in other

areas of the body (eg. diaphragm, liver, spleen, other abdominal viscera) and the number of extrapulmonary sites (excluding lymph nodes) that had bacterial burden. Our necropsy scoring system is available in [235].

5.2.5 Intracellular cytokine staining and flow cytometry

Intracellular cytokine staining was performed on a random sampling of LNs with and without granuloma from each animal (n=4/animal). A total of 168 LNs (with and without granuloma) from 24 cynomolgus macaques that were part of other studies in our lab were included in this analysis and processed as previously described [121]. Single cell suspension of 96 LN's were stimulated with peptide pools of Mtb specific antigens ESAT-6 and CFP-10 (10 µg/ml of every peptide) in the presence of Brefeldin A (Golgiplug: BD biosciences) for 3.5 hours at 37°C with 5% CO₂ [121]. Positive control (n=72 LNs) included stimulation with phorbol dibutyrate (PDBu) and ionomycin [231]. An unstimulated control was included whenever additional cells were available. The cells were then stained for viability (Invitrogen), surface and intracellular cytokine markers according to standardized protocols. Flow cytometry panel for cell surface markers for T cells included CD3 (clone SP34-2; BD Pharmingen), CD4 (Clone L200, BD Horizon) and CD8 (clone SK1: BD biosciences). In addition, the B cell marker CD20 (clone 2H7; eBioscience) and myeloid cell marker CD11b (clone Mac-1, BD Pharmingen) were included as additional markers in certain samples. Intracellular cytokine staining panel included pro-inflammatory cytokines: Th1 [IFN-γ (clone B27), IL-2 (clone: MQ1-17H12), TNF (clone: MAB11)], Th17 [IL-17 (clone eBio64CAP17) and the anti-inflammatory cytokine IL-10 (clone JES3-9D7) markers. In addition, T cell proliferation marker Ki67 [clone B56] was included in the panel for a subset of samples. Data acquisition was performed using an LSR II (BD) and analyzed

using FlowJo Software v.9.7 (Treestar Inc, Ashland, OR). A detailed list of macaques included in the analysis can be found in Table 6.

Table 6. List of macaques used for immunological assays.

| Monkey ID | Species | Days post-infection | Wks post-infection | Date infected | Dose | Nx date | Reference |
|-----------|---------|---------------------|--------------------|---------------|------|-----------|----------------|
| 2312 | Cyno | 330 | 47 | 31-Jul-12 | 6 | 26-Jun-13 | [121, 333-335] |
| 2412 | Cyno | 83 | 12 | 8-May-12 | 4 | 30-Jul-12 | [121, 333-335] |
| 2512 | Cyno | 85 | 12 | 5-Jun-12 | 8 | 29-Aug-12 | [121, 333-335] |
| 2612 | Cyno | 379 | 54 | 21-Aug-12 | 8 | 4-Sep-13 | [121, 333-335] |
| 2712 | Cyno | 384 | 55 | 21-Aug-12 | 8 | 9-Sep-13 | [121, 333-335] |
| 5716 | Cyno | 30 | 4 | 29-Mar-16 | 10 | 28-Apr-16 | Unpublished |
| 6610 | Cyno | 601 | 86 | 24-Mar-11 | 45 | 14-Nov-12 | [65] |
| 9511 | Cyno | 198 | 28 | 24-Oct-11 | 12 | 9-May-12 | [121, 333-335] |
| 9711 | Cyno | 175 | 25 | 17-Oct-11 | 20 | 9-Apr-12 | [121, 333-335] |
| 15312 | Cyno | 124 | 18 | 8-Mar-13 | 40 | 10-Jul-13 | [335] |
| 15712 | Cyno | 293 | 42 | 11-Dec-12 | 12 | 30-Sep-13 | [335] |
| 16113 | Cyno | 170 | 24 | 14-Apr-14 | 15.2 | 1-Oct-14 | [235] |
| 16213 | Cyno | 163 | 23 | 14-Apr-14 | 15.2 | 24-Sep-14 | [235] |
| 17111 | Cyno | 84 | 12 | 1-May-12 | 8 | 24-Jul-12 | [121, 218] |
| 17211 | Cyno | 328 | 47 | 31-Jul-12 | 6 | 24-Jun-13 | [121, 218] |
| 19915 | Cyno | 28 | 4 | 14-Mar-16 | 5 | 11-Apr-16 | Unpublished |
| 20212 | Cyno | 72 | 10 | 18-Feb-13 | 4 | 1-May-13 | [121, 218] |
| 20612 | Cyno | 72 | 10 | 25-Feb-13 | 6 | 8-May-13 | [121, 218] |
| 20712 | Cyno | 152 | 22 | 12-Jul-13 | 6 | 11-Dec-13 | [121, 218] |
| 20912 | Cyno | 72 | 10 | 4-Mar-13 | 4 | 15-May-13 | [121, 218] |
| 22410 | Cyno | 580 | 83 | 26-Apr-11 | 46 | 26-Nov-12 | [121, 218] |
| 22510 | Cyno | 297 | 42 | 24-May-11 | 42 | 16-Mar-12 | [121, 218] |
| 22610 | Cyno | 538 | 77 | 26-Apr-11 | 46 | 15-Oct-12 | [121, 218] |
| 22810 | Cyno | 386 | 55 | 17-May-11 | 22 | 6-Jun-12 | [121, 218] |

5.2.6 Histology

Histological examination was performed by an experienced veterinary pathologist (E. Klein) as previously described [231]. Tissue samples were cut (4-6mm) and stained with hematoxylin and eosin. Characteristics of granulomas, such as, size, type (caseous, non-necrotizing, suppurative, or mixed), distribution pattern (focal, multifocal, coalescing, focally extensive and locally invasive), and cellular composition were noted.

5.2.7 Immunohistochemistry

Immunohistochemistry was performed as previously indicated [336, 337] on formalin-fixed paraffin-embedded (FFPE) LNs obtained at necropsy. Briefly, sections were deparaffinized and antigen retrieval was performed using a Retriever (Electron Microscopy Services, Hatfield, PA) in Tris-EDTA-Tween-80 buffer (REF). Sections were stained for Tcells/B cells/dendritic cells (polyclonal rabbit anti-CD3, Dako, Santa Clara, CA; polyclonal rabbit anti-CD20, Thermo Fisher Scientific, Pittsburgh, PA; mouse-anti-CD11c, Leica Microsystems, Buffalo Grove, IL), macrophage subsets (mouse anti-CD68, Thermo Fisher; rabbit anti-DC-SIGN, ProSci Inc, Poway, CA; mouse anti-CD163, Thermo Fisher), LN vascular and structural aspects (Goat anti-LYVE-1, R&D Systems, Minneapolis, MN; rat-anti PNAd, BioLegend, San Diego, CA), and LN conduit systems (visualized by staining for rabbit anti-collagen 1 [Abcam, Cambridge, MA]). Primary antibodies were visualized with species- and isotype-specific secondary antibodies purchased from Jackson ImmunoResearch (West Grove, PA). Auramine rhodamine was performed as previously indicated [336] using reagents from BD Biosciences (San Jose, CA). Images were acquired at 20x magnification with a Nikon e1000 widefield microscope (Nikon, Melville, NY) with Nikon Elements.

5.2.8 Isolation of genomic DNA from bacteria

DNA extraction and qPCR was performed with modifications as described previously [118]. Briefly, frozen aliquots were thawed and volumes recorded throughout the extraction process. Samples were transferred to tubes containing 150 μ l of 0.1mm zirconia-silica beads (Biospec Products) before adding 600 μ l of Tris-EDTA buffer, pH 8.0. Three hundred microliters

of 70°C phenol/chloroform/isoamyl alcohol (25:24:1, Sigma-Aldrich) were subsequently added and the samples incubated at room temperature for 10 minutes. The samples were then vortexed, the aqueous layer separated and supplemented with 50µl 5M NaCl and a second phenol chloroform extraction performed on the extracted aqueous layer. DNA was precipitated with the addition of one volume of 100% isopropanol and one-tenth volume of 3M sodium acetate and incubating at -20°C overnight. The DNA pellet was washed with 70% ethanol, dried and resuspended in nuclease-free water. Mtb genomes were then quantified using Taqman Universal Master Mix II (Life Technologies) and previously published sigF primer-probe combination [118]. Each sample was amplified in triplicate using an ABI Systems 7900HT machine. Chromosomal equivalents (CEQ) were quantified by comparing the samples with a standard curve derived from serial dilution of Mtb genomes prepared from liquid culture. Our detection limit for the standard curve was 10 copies per reaction. When we calculated the number of genomes for the whole lymph node, our detection limit was 1,000 copies per lymph node.

5.2.9 Statistical Analysis

D'Agostino & Pearson Omnibus normality test was performed on all data described in this manuscript. Since the data were not normally distributed, Nonparametric t-test was used when comparing two groups (Mann-Whitney test). Kruskal-Wallis test was used to compare more than two groups with post hoc analysis Dunn's multiple test comparisons. P values ≤ 0.05 were considered significant. Statistical analysis was performed using GraphPad Prism v7 (GraphPad Software, San Diego, CA). For multivariate analysis, JMP Pro v12 (SAS Institute Inc., NC, USA) package was used. Nonparametric Spearman's rho was calculated for correlations (multivariate

analysis) using JMP Pro v12. All CFU data and CEQ data used in CFU/CEQ graphs were transformed by adding 1 to reflect sterile LNs in log-scale graphs.

5.3 Results

5.3.1 ^{18}F -FDG PET CT imaging can identify Mtb-infected thoracic lymph nodes

Macaques have multiple thoracic LNs [232] that drain different lung regions, and variable numbers among animals. We previously described differences in the extent of LN disease between rhesus and cynomolgus macaques [235]. To address the overall question of LN infection dynamics and differences between species, we first used PET CT imaging to track inflammation in thoracic LNs following Mtb infection. Our PET probe was ^{18}F -fluorodeoxyglucose (FDG), a radiolabeled glucose analog that is taken up by metabolically active cells; we have demonstrated previously the FDG avidity is enhanced in Mtb-affected tissues and is a surrogate for inflammation in granulomas and lungs [119, 199, 235, 276, 338, 339]. In our study, LNs that were FDG avid and detectable by PET follow one of three courses of FDG uptake over the course of the infection: increased, maintained, or decreased FDG avidity (Figure 55A and 55B). In many macaques, one or more thoracic LNs had measurable FDG uptake by 2 weeks post-infection (examples shown in Figure 55B), and different thoracic LNs within an animal followed different trajectories (ie. increasing, decreasing, maintaining FDG uptake) such that one animal could have individual LNs with different uptake patterns (Figure 55B). To examine the relationship between FDG positivity and the presence of viable Mtb in a specific LN, we performed PET CT scans on animals 1-2 days prior to necropsy and cultured LN homogenates to measure bacterial burden. We found 90.65%

(194 of 214) of LNs visible on scan by PET at necropsy contained culturable Mtb at necropsy, while 83.33% (200 of 240) of undetectable LNs (SUVR = 0) were sterile. Of the “hot” lymph nodes (defined as $SUVR \geq 5$ [199]) on the pre-necropsy PET CT scan, 96.3% (181 of 188) of thoracic LNs contained culturable Mtb, while in thoracic LNs that were “warm” (detectable but with $SUVR < 5$), only 50% (13 of 26) contained culturable Mtb (Figure 55C). There was a modest correlation (Spearman’s $\rho = 0.4812$, $p < 0.001$) between SUVR and live bacterial burden in PET-detectable LNs at necropsy (Figure 56). These data suggest that mycobacterial involvement in thoracic LNs is a dynamic process and PET CT-detected FDG uptake is associated with bacterial infection in LNs.

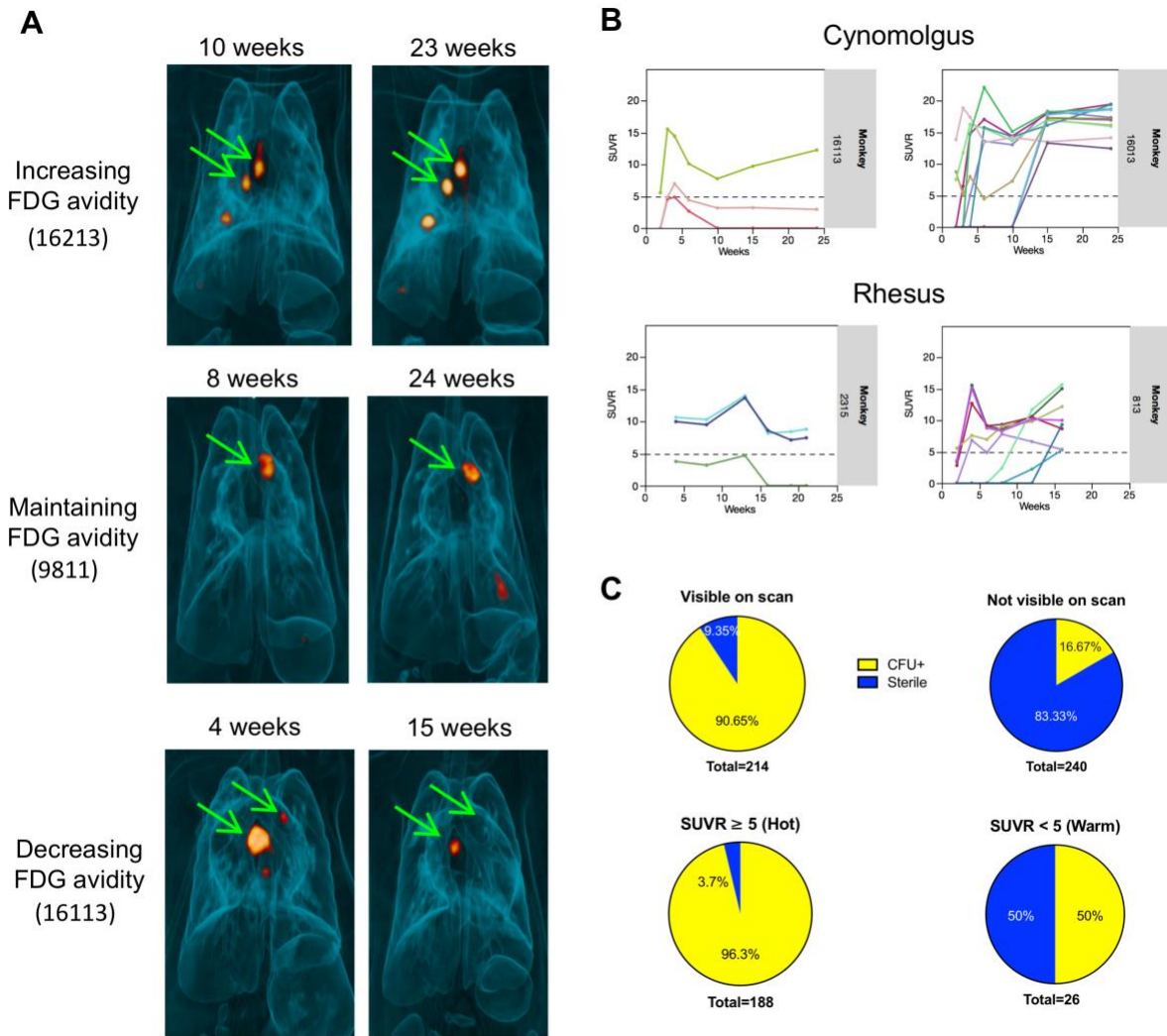


Figure 55. FDG PET CT analysis of Mtb infection in lymph nodes of cynomolgus and rhesus macaques.

A. PET/CT scans of 3 different macaques (monkey numbers 16213, 9811, 16113 showing different trajectories of thoracic lymph nodes at different time points post infection. B. Representative serial PET CT FDG SUVR plots showing several lymph nodes visible by PET at 2 weeks post infection in four different animals. Trajectories of individual lymph nodes in an animal is shown to be independent of each other. Each line is a lymph node. Dotted line represents the cut-off for calling FDG+ LNs “hot” (SUVR ≥ 5). C. Most lymph nodes visible (SUVR ≥ 2.3) on scan by PET 1-2 days

before necropsy harbor live Mtb (top left panel), while only a small proportion of those that are not seen by PET have live Mtb. Most "hot" lymph nodes ($SUVR \geq 5$) were CFU+ compared to only half of "warm" lymph nodes ($SUVR 2.3-4.99$) (bottom panels).

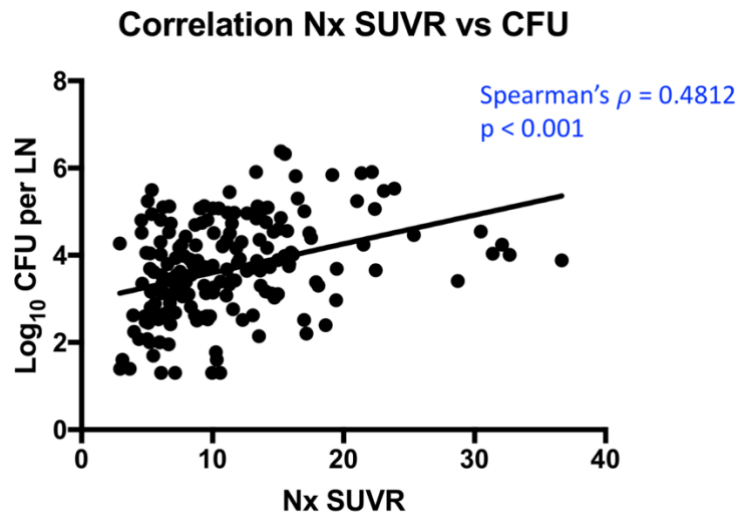


Figure 56. Modest positive correlation between LN SUVR and live bacterial burden at necropsy.

Each data point is a lymph node. Correlation was determined using Spearman's correlation test.

5.3.2 Thoracic lymph nodes of rhesus macaques have reduced killing capacity for Mtb compared to cynomolgus macaques

We previously determined that there is variation in the number of thoracic LNs that become infected with Mtb among macaques and differences in LN pathology and total LN bacterial burden between cynomolgus and rhesus macaques [235], however, we know little about bacterial dynamics in individual LNs. To address this, we first determined the number of viable Mtb per LN in both macaque species over time. In cynomolgus macaques, CFU peaked at 4-6 weeks (median

= 72001) post-infection which then greatly decreased by 11-14 weeks (median = 1226) and 16-29 weeks (median = 1021) post-infection (Figure 57A). Cynomolgus macaques with well-controlled (clinically latent, [232]) infection necropsied at 34-54 weeks post infection had the lowest median CFU (1 CFU per LN) (Figure 57A). Unlike cynomolgus macaques where CFU per LN decreased over the course of infection, rhesus macaques had relatively stable median CFU per LN (Figure 57B). At both early (4-6 weeks) and later (16-28 weeks) time points post-infection, there was no significant difference between the two species (Figure 58A). Of note, the 16-29 week post-infection group consisted of two animals with active disease (n=2; 15 LNs; median = 4901 CFU; green and orange circles) and six macaques that were controlling infection (n=6; 14 LNs; median = 101 CFU) (Figure 59A). A subanalysis showed that there was no significant difference between the LN CFU of the two cynomolgus macaques with active disease and the rhesus macaques at 16-29 weeks post-infection. However, median LN CFU of the six cynomolgus macaques controlling the infection was significantly lower compared to rhesus macaques at this time point (Figure 59A). Moreover, CFU of cynomolgus macaques at 11-14 weeks post infection was significantly lower than rhesus macaques, although the actual difference between medians was only 4-fold (Figure 58A). These data suggest that after reaching a peak in CFU, cynomolgus macaques are capable of reducing the bacterial burden in their LNs over the course of infection while rhesus macaques are not.

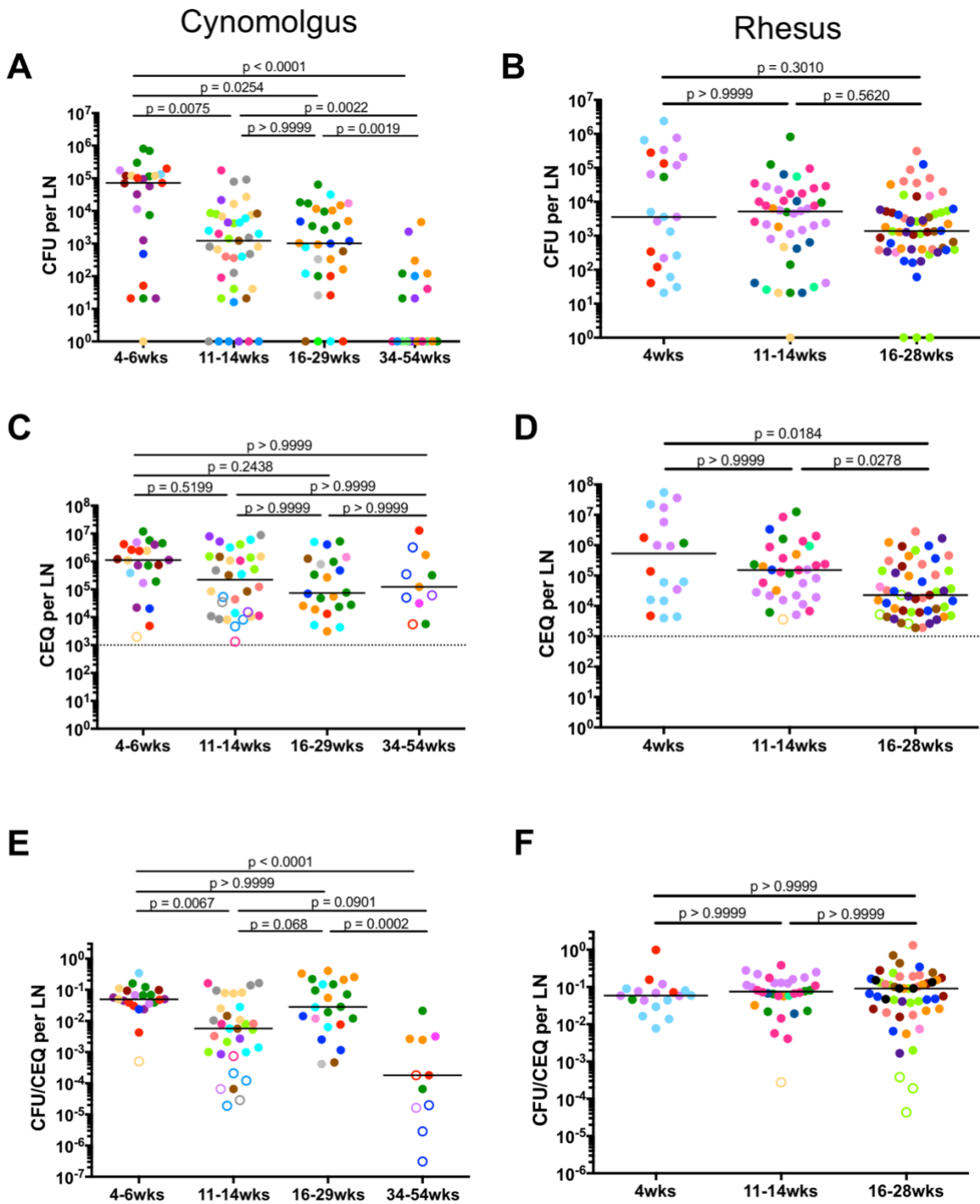


Figure 57. Mtb burden and killing in lymph nodes of cynomolgus and rhesus macaques.

A, B. Live Mtb burden (CFU) in thoracic LNs from cynomolgus (A) and rhesus (B) macaques at various time points post-infection (at necropsy). Lymph node CFU of cynomolgus macaques

decreases over the course of infection while rhesus macaques do not. C, D. Total (live+dead, CEQ) Mtb burden in cynomolgus (C) and rhesus (D) macaque LNs. There was no difference in the level of CEQ in cynomolgus macaque LNs over the course of infection, while a decline in CEQ was found in rhesus macaque LNs at later time points post-infection. E, F. Mtb killing in thoracic lymph nodes, as calculated as the ratio of live (CFU) compared to total (CEQ) bacteria. Cynomolgus macaque LNs (E) exhibit poor Mtb killing at 4 weeks post infection but improve over the course of infection. Highest Mtb killing capacity was observed in monkeys with latent infection (34-54 weeks post infection). Little killing was observed in rhesus macaque LNs (F). The CFU was transformed by adding 1 to reflect sterile LNs with CEQ and/or granulomas either by gross or microscopic examination. For C-F, only LNs in which CEQ were detected were included. Each macaque is shown in a different color. Each data point is one lymph node. Open symbols are sterile lymph nodes (CFU-). The number of macaques per time point post-infection is as follows: a.) 4-6 weeks (Cynos n=8, Rhesus n=4); b.) 11-14 weeks (Cynos n=9, Rhesus n=7); c.) 16-29 weeks (Cynos n=9, Rhesus n=8); d.) 34-54 weeks (Cynos n=6). The number of lymph nodes analyzed ranged from 4 to 13 per macaque. Dotted line represent the limit of detection of our qPCR assay. Statistics are Kruskal-Wallis with post-hoc Dunn's multiple test comparisons; p values are shown on figure.

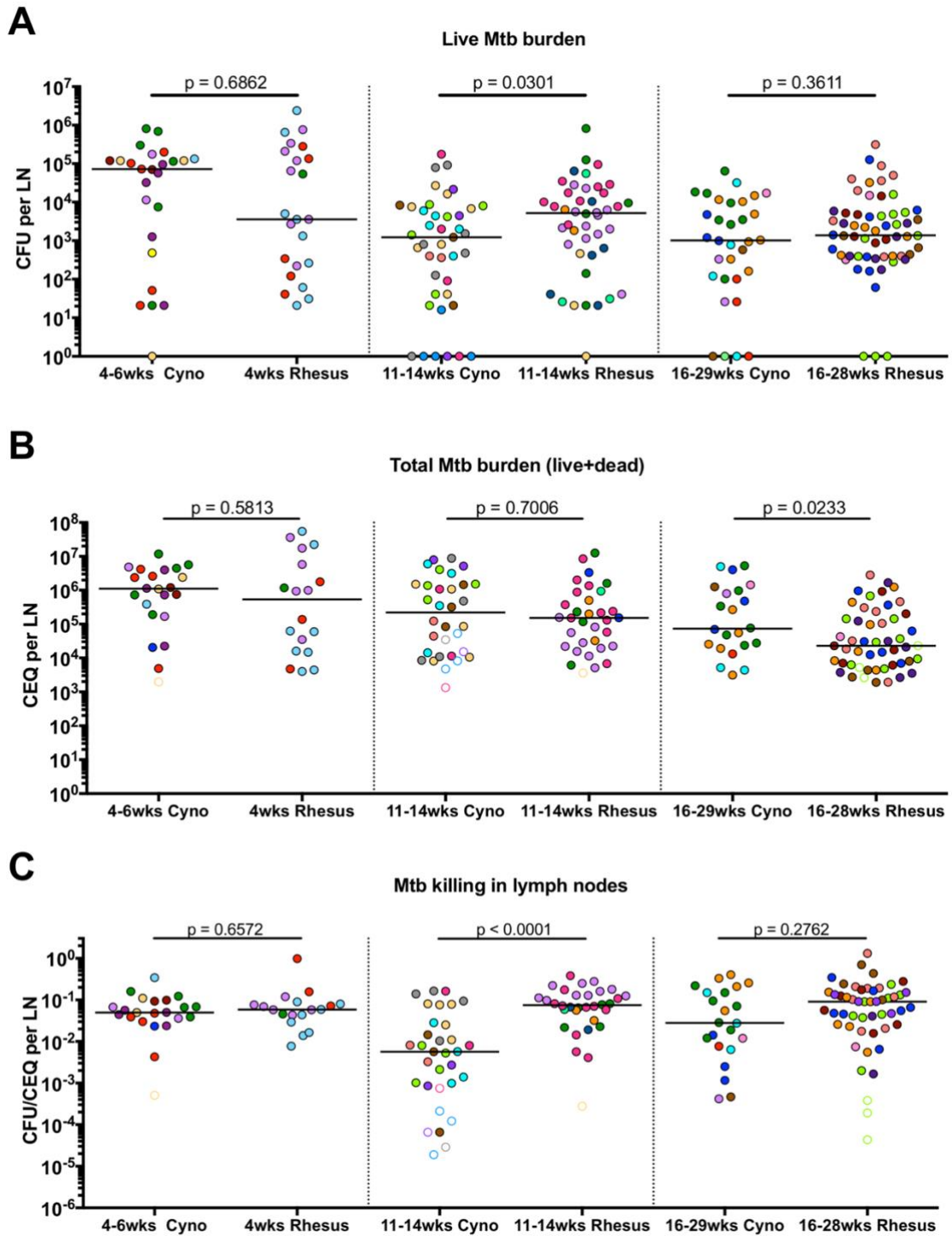


Figure 58. Comparison of CFU, CEQ and killing (CFU/CEQ) between cynomolgus and rhesus macaques at similar time points post infection.

A. Rhesus macaque lymph nodes have fewer live Mtb burden at 11-14 weeks post infection compared to cynomolgus macaques. B. Overall, there is little difference in the total (live+dead) Mtb burden in rhesus and cynomolgus macaque lymph nodes at the various time points post infection analyzed. C. Cynomolgus macaque lymph nodes are better at killing Mtb than rhesus macaque lymph nodes at 11-14 weeks post infection. Each data point is a lymph node. Each color is a macaque. Open symbols represent sterile lymph nodes. Statistics are Mann-Whitney.

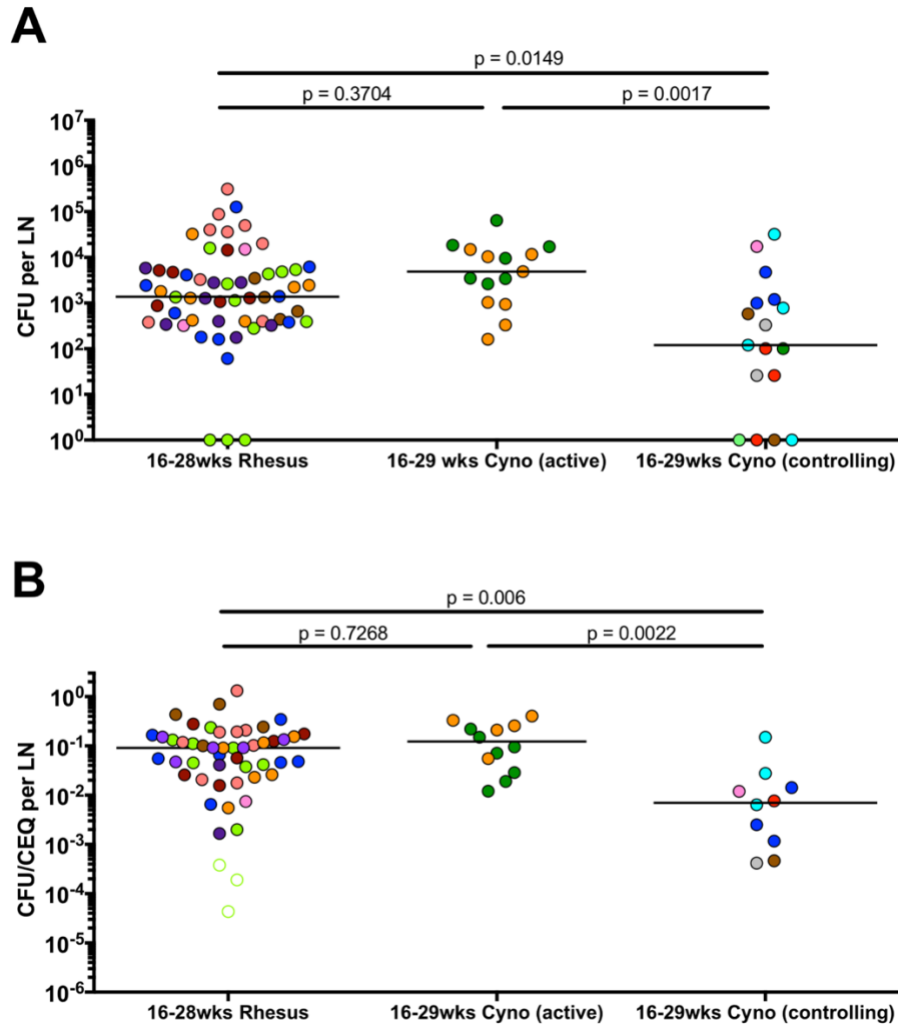


Figure 59. LN CFU and CFU/CEQ of cynomolgus macaques with active disease, controlling disease and rhesus macaques at 16-29 weeks post-infection.

A. CFU per lymph node. B. CFU/CEQ per lymph node. Statistical test is Kruskal Wallis with Dunn's multiple comparisons test.

To determine whether there were differences in the total (both live and dead) bacterial burden in these LNs, we used a qPCR-based technique amplifying *sigF*, a single-copy mycobacterial gene, to estimate the mycobacterial chromosomes per LN (expressed as chromosomal equivalents [CEQ]) [118]. Chromosomal DNA (CEQ) was first shown to persist in

mice lungs after killing Mtb with isoniazid treatment [340]. We previously assessed CEQ in macaque lung granulomas and demonstrated that CEQ persist after bacteria are killed by host responses or by isoniazid [118, 340]. To confirm this technique worked in LNs, we performed qPCR and bacterial culture on LN samples from isoniazid-treated macaques (n=4) and found similar CEQ numbers in the drug treated and control groups (Figure 60A). Moreover, similar levels of CEQ were found between CFU+ LNs and sterile LNs with granulomas from drug-treated macaques (Figure 60B). This shows that Mtb DNA persists in LNs even after Mtb is killed by isoniazid treatment. As a negative control and to confirm the specificity of our probes, we used LNs from an uninfected macaque and were unable to detect any Mtb genomes in these samples.

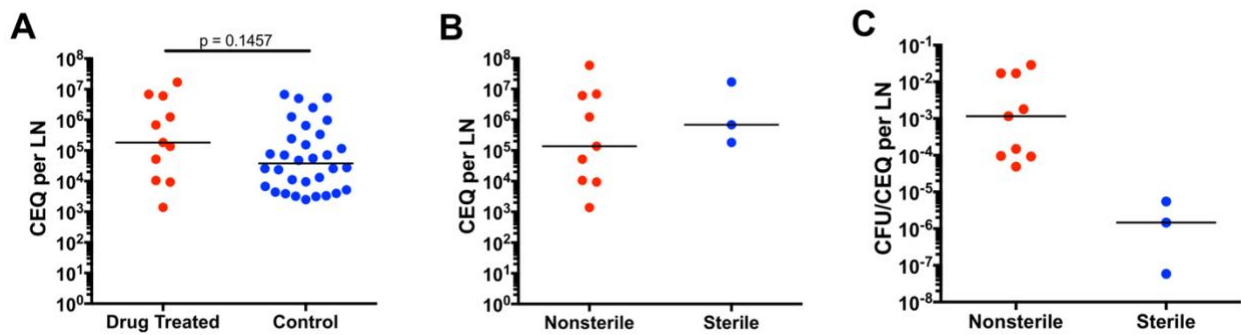


Figure 60. Isoniazid treatment for 2 months does not significantly change CEQ in lymph nodes.

A. CEQ is similar between INH-treated (N=4) and control (N=7) macaques. B. CEQ is similar between sterile and nonsterile lymph nodes with granulomas in INH-treated macaques. C. Greater killing capacity of sterile lymph nodes compared to nonsterile lymph nodes in INH-treated macaques. Each data point is a lymph node. Statistics are Mann-Whitney for A; there were insufficient samples for statistics in B and C.

We did not find significant differences in CEQ across different time points post-infection in cynomolgus macaques (Figure 57C). However, we saw a reduction in CEQ levels in rhesus macaques at later time points post-infection (4 weeks vs 16-28 weeks, 23.5-fold, $p = 0.0184$; 11-14 weeks vs 16-28 weeks, 6.7-fold, $p=0.0278$) (Figure 57D), which could be because the macaques that have severe disease and have deteriorated clinically are necropsied prior to this time point, and thus the samples are from those with less severe disease. Both species had similar levels of CEQ at 4-6 weeks and 11-14 weeks post-infection. Rhesus macaques at 16-28 weeks post-infection had lower CEQ compared to cynomolgus macaques (3.2-fold) (Figure 58B). These data suggest that Mtb replicates and grows to the same extent in LNs of both species and the lower viable Mtb burden in cynomolgus macaque LNs was not due to fewer Mtb in these tissues, but more likely to those LNs being better able to kill Mtb.

To estimate the ability of LNs to kill Mtb, we evaluated the ratio of live Mtb burden (CFU) and total (live+dead) Mtb burden (CEQ) per LN [118], as we previously described in macaque lung granulomas [118]. As validation of this technique in LNs, we estimated the CFU/CEQ killing ratio in sterile LNs (with evidence of previous infection, i.e. granuloma) compared to CFU+ LNs with granulomas following isoniazid treatment (Figure 60C). As expected, isoniazid treatment reduced the CFU/CEQ ratio (i.e. increased bacterial killing) in LNs. Thus, this technique can estimate Mtb killing in lymph nodes in the setting of drug treatment.

Cynomolgus macaque LNs showed little to no killing at 4 weeks post infection, but their ability to kill Mtb increased ~9-fold by 11-14 weeks post infection (Figure 57E). There was no significant difference in the killing capacity of LNs between 4 weeks and 16-29 weeks post-infection. Lymph nodes in the 16-29 weeks group represented macaques with a wide range of disease and the poor killing capacity is largely driven by samples from two monkeys with severe

disease at this time point (n=2; 12 LNs; median = 0.122; green and orange circles vs controlling animals n=6; 10 LNs; median = 0.0076). We found no significant difference between the killing capacity of cynomolgus macaque LNs who had active disease and rhesus macaque LNs at this time point. However, LNs from cynomolgus macaques who were controlling the infection had higher bacterial killing compared to rhesus macaques (Figure 59B). Lymph nodes from cynomolgus macaques with well-controlled infection sampled at 34-54 weeks had the highest level of bacterial killing (277-fold increase in killing capacity relative to macaques sampled at 4-6 weeks post infection) (Figure 57E). While the Mtb killing capacity of LNs from cynomolgus macaques who are controlling the infection improves over time, rhesus macaque LNs demonstrated little to no Mtb killing at any time point examined (Figure 57F). Cynomolgus macaque thoracic LNs were 13-fold ($p < 0.0001$) better at killing Mtb than rhesus macaque LNs at 11-14 weeks post-infection (Figure 58C), suggesting that rhesus macaque LN's reduced ability to kill Mtb may contribute to the more severe LN disease in rhesus macaques during Mtb infection [235].

Not all thoracic LNs in an individual macaque become infected with Mtb (Figure 61A, Figure 62). A significant proportion of thoracic LNs in individual macaques were CFU- (cynomolgus: 50-81%, rhesus: 26-40%, depending on time of necropsy) as supported by our PET CT data (Figure 55C). Although most CEQ+ LNs were also CFU+ (Figure 61B, pink bars), there were also CEQ+ LNs that were CFU- (Figure 61B, purple bars), suggesting that these LNs were able to completely sterilize the infection. Alternatively, it is possible that such LNs never have contained viable Mtb but we detected 'free-floating' Mtb genomes that were trapped by the LN; our limit of detection is 1000 CEQ per whole LN, so free floating DNA would have to be at reasonably high levels. These CFU-CEQ+ (purple bars) LNs were more prevalent in cynomolgus than rhesus macaques (Figure 61B). There were also LNs without detectable Mtb genomes but

contained culturable Mtb (CEQ-CFU+) (Figure 61B, yellow bars) which likely represent samples where the number of Mtb genomes were below the limit of our qPCR assay. Overall, these data indicate that although it is possible for immune responses in LNs to kill Mtb, viable bacteria can remain in LNs for extended periods of time, suggesting these organs represent sites of long-term bacterial persistence.

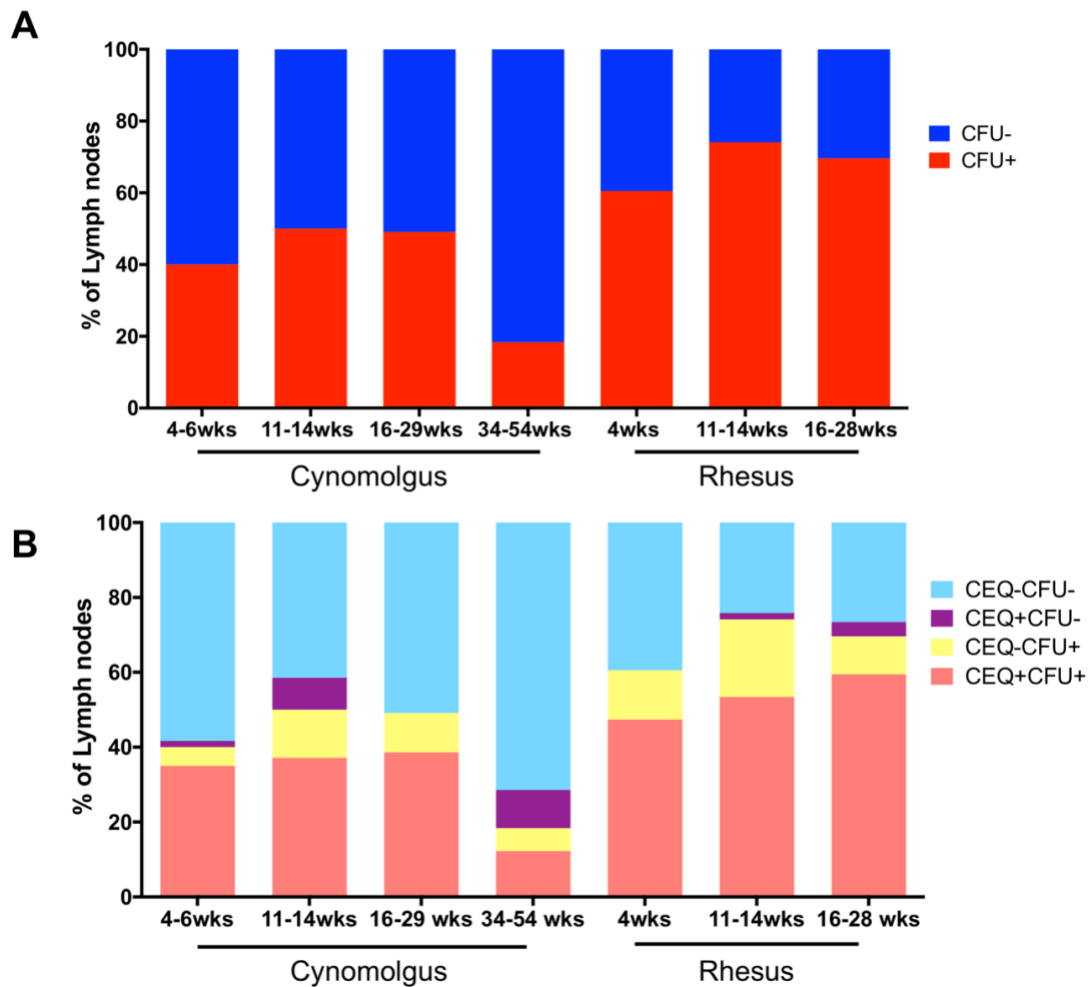


Figure 61. Proportion of thoracic lymph nodes infected with Mtb in cynomolgus and rhesus macaques at necropsy.

A. Percent of thoracic LNs that were CFU+ (red) or CFU- (blue) at necropsy. Rhesus macaques had higher proportion of Mtb-infected lymph nodes than cynomolgus macaques. B. Proportion of lymph nodes that were uninfected (CFU-/CEQ-, light blue), infected but were sterile (CEQ+/CFU-, purple), had culturable Mtb but no detected genome (CFU+/CEQ-, yellow) and with culturable Mtb and Mtb genome (CFU+/CEQ+, pink). Threshold for detection of CEQ is 1000 genomes/LN. CFU limit of detection is 20/LN. Number of macaques and lymph nodes at each time point is in Table 4.

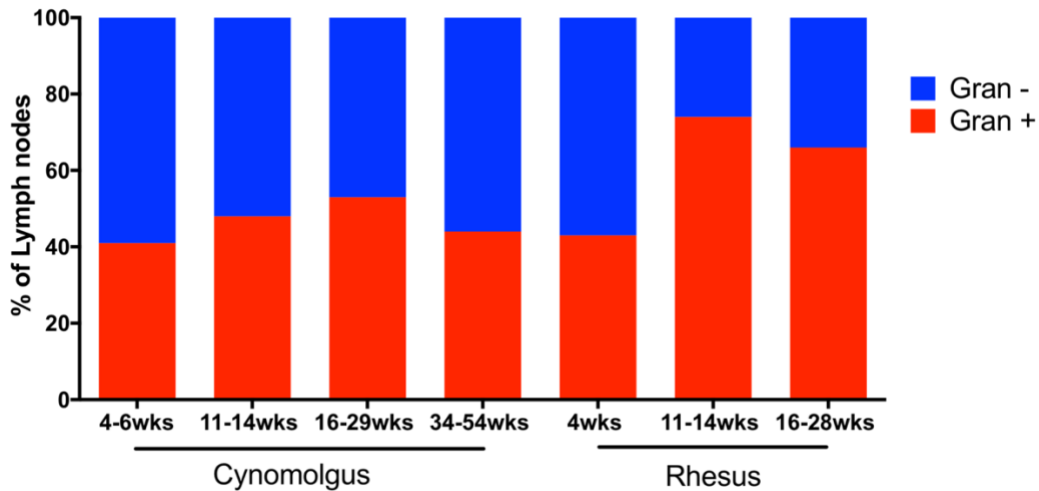


Figure 62. Proportion of thoracic lymph nodes that had granuloma by gross and microscopic examination at necropsy.

Time points shown are necropsy time points for cynomolgus and rhesus macaques.

5.3.3 Low Mtb burden and better killing in peripheral lymph nodes

Peripheral LNs, such as axillary and inguinal LNs, do not directly drain the lungs but may offer insight into extrapulmonary dissemination and immunity. To quantify mycobacterial dynamics in these organs, we sampled peripheral LNs for live Mtb and Mtb genomes from all macaques in this study and compared them to thoracic LNs. We found that only 8.2% (14 of 171) of the peripheral LNs we examined yielded Mtb genomes, and only 3.5% (6 of 171) contained viable Mtb, and these were at quite low levels (Figure 63A); this is not surprising since Mtb infection is generally confined to the thoracic cavity. Extrapulmonary disease, if present, is most frequently found in the liver, and occasionally the spleen, as noted in our previous publications [232, 233, 235]. We compared the live and total (live+dead) bacterial burden, as well as killing

capacity of LNs from ten macaques (n=5 cynomolgus, n=5 rhesus) that had CEQ from both thoracic and peripheral LNs. Peripheral LNs had significantly lower levels of CFU compared to thoracic LNs (Figure 63B). Because the CFU levels were so low, the majority of the CFU+ LNs were outside the CEQ assay's limit of detection. Here (Figure 63), we are only showing CFU, CEQ and CFU/CEQ data from CEQ+ LNs. The number of Mtb genomes recovered from peripheral LNs was significantly lower (29-fold, $p < 0.0001$) compared to thoracic LNs (Figure 63C). Since we found significantly more live Mtb in thoracic LNs and most of the peripheral LNs were sterile (Figure 63B), the killing capacity of peripheral LNs was significantly higher (168-fold, $p < 0.0001$) than thoracic LNs (Figure 63D). Our data suggest that Mtb infection of peripheral LNs can occur but is infrequent, and when it does occur, growth is to lower levels (CEQ) and these LNs are more likely to kill Mtb than thoracic LNs. However, trafficking of dead Mtb or Mtb genomes to peripheral LNs could also occur and should not be discounted.

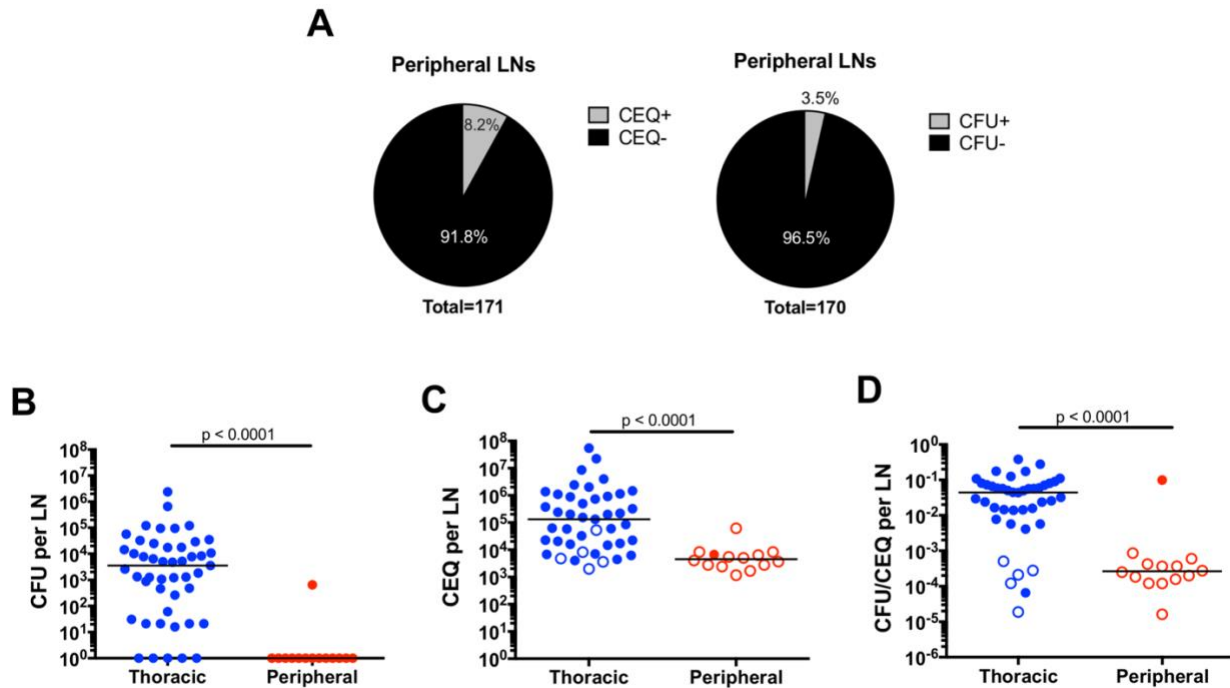


Figure 63. Most peripheral lymph nodes that had detectable Mtb genome were sterile.

A. The majority of peripheral lymph nodes assayed were CEQ- and CFU- (sterile). B, C. Live Mtb burden (CFU)(B) and total (live+dead, CEQ) Mtb burden (C) are significantly lower in peripheral lymph nodes than in thoracic lymph nodes. D. CFU/CEQ for thoracic and peripheral LNs. Killing capacity of peripheral lymph nodes is significantly higher (lower CFU/CEQ) compared to thoracic lymph nodes. These are data from 10 monkeys that had CEQ in both thoracic and peripheral lymph nodes. Each data point is one lymph node. Open symbols are sterile (CFU-) lymph nodes. The CFU was transformed by adding 1 to reflect sterile but CEQ+ LNs. Statistics are Mann-Whitney.

5.3.4 Lymph node effacement is associated with higher bacterial burden

Mtb infection leads to granuloma formation in thoracic LNs and these granulomas can be focal or coalescing lesions that grow in size and efface the LN (Figure 64A and 64B). We previously reported that bacilli from multiple granulomas can seed a single LN [118, 120], and this is supported by histologic evidence where multiple independent granulomas are observed in a single LN (Figure 64B). A LN's function is tightly linked to its physical structure and organization, and granulomas may physically disrupt LN architecture and impair their ability to function (ie. lymphatic filtration and immune cell trafficking to, from and within the LN). We performed IHC on cynomolgus macaque thoracic LNs with or without granulomas to investigate how granulomas influence the localization of cells, blood vessels, and the conduit systems that are important for normal LN function (Figure 65). We selected lymphocyte markers CD3 (T cells) and CD20 (B cells). Myeloid cell markers in lymph nodes are complex because dendritic cells (DCs) and epithelioid macrophages express both CD11c and DC-SIGN but can be distinguished by their different sizes and morphologies, while macrophages also express CD68 and can express CD163. For structural studies, we used markers defining vessels and conduit systems in LNs including LYVE-1 for lymphatic vessels, PNAd for high endothelial vessels (HEV), and collagen 1 (coll1) for conduit systems. We focused on LNs from cynomolgus macaques to capture LNs from the full range of infection outcomes. Uninfected thoracic LN organization is consistent with typical LN architecture with CD3+ T cells and CD11c+ DCs being abundant in paracortical regions, CD20+ B cell-rich germinal centers at the periphery, and CD68+ and CD163+ macrophages present in the subcapsular space and medullary region (Fig 6A). Mesh-like LYVE-1+ lymphatic vessels were present in the central LN region while PNAd+ HEV are distributed throughout the paracortex, and coll1+ conduits regularly-spaced through the T cell regions.

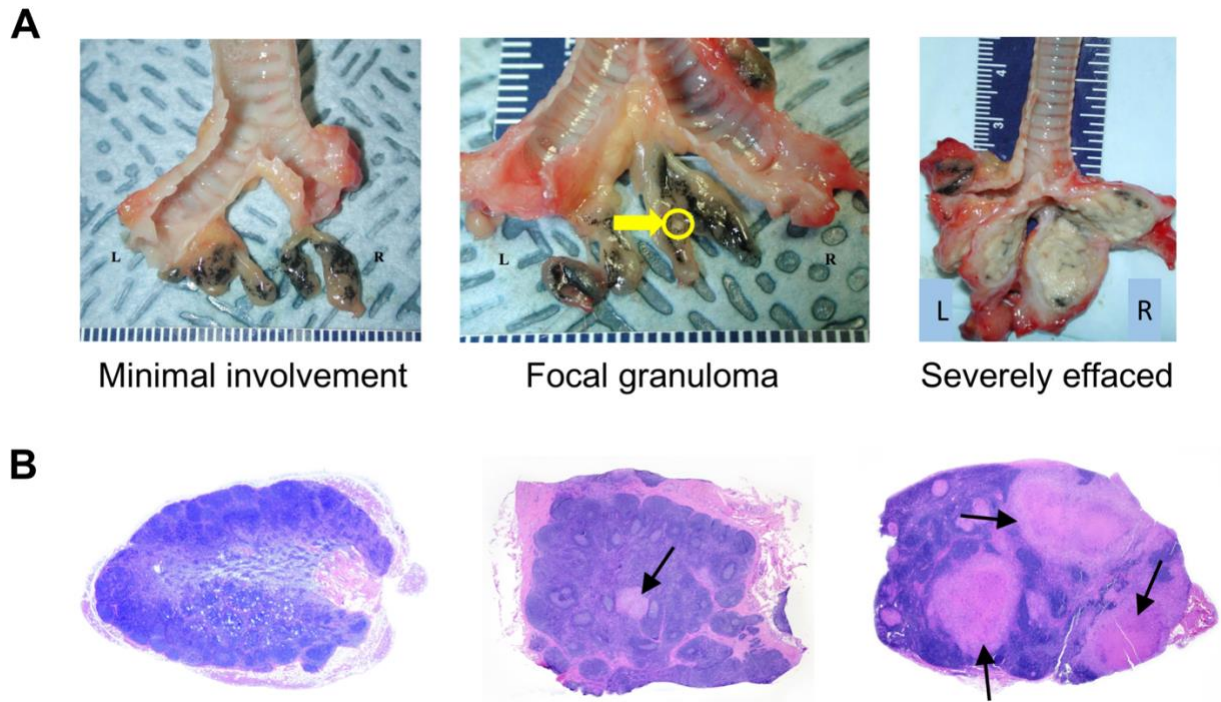


Figure 64. Mtb infection results in granuloma formation and in some instances lymph node effacement.

A. Examples of gross pathology of thoracic lymph nodes from cynomolgus macaques that are minimally involved (left), with focal granuloma (middle) and severely effaced (right). The yellow arrow is pointing to a granuloma. B. Examples of microscopic histopathology of cynomolgus macaque lymph nodes that are not involved (left), with focal granuloma (middle) and severely effaced (right). The arrows are pointing to granulomas.

Mtb-infected thoracic LNs can contain multiple focal non-necrotizing granulomas or large coalescing granulomas that disrupt the LN architecture. We found that even small granulomas (Figure 65B) had large clusters of CD11c+CD68+ macrophages that appeared to push T cells out of these regions and impinged on germinal centers, but also disrupted nearby HEV and lymphatic vessels. Moreover, granulomas and adjacent areas had disorganized coll1 staining instead of the

uniformly-distributed staining associated with the normal conduit network found in uninvolved areas. Large granulomas caused extensive remodeling of LN structure. Effaced LNs (Figure 65C) had coalescing necrotic granulomas with poorly-circumscribed margins and large numbers of CD11c+CD68+ macrophages, and these granulomas displaced T cell- and DC-rich zones in the LN paracortex, destroyed B cell-rich germinal centers, and eliminated the normal vascular elements in their vicinity. The granulomas in these LNs stained positively for coll1, but as with less involved LNs, the staining is disorganized and lacks cohesive conduit-like organization. Interestingly, LN granulomas lack several features that are present in lung granulomas. Although these granulomas are present in B cell and T cell-rich organs, they appear to lack granuloma-adjacent B cell-rich tertiary lymphoid structures [217, 219], and distinct lymphocyte cuff regions. These observations suggest LN granulomas have large populations of potential host cells, but have structural differences that may impair the ability to control bacterial replication. Moreover, the process of granuloma formation in thoracic LNs can destroy important aspects of LN structure that contribute to T cell and B cell priming and may affect overall anti-mycobacterial immunity.

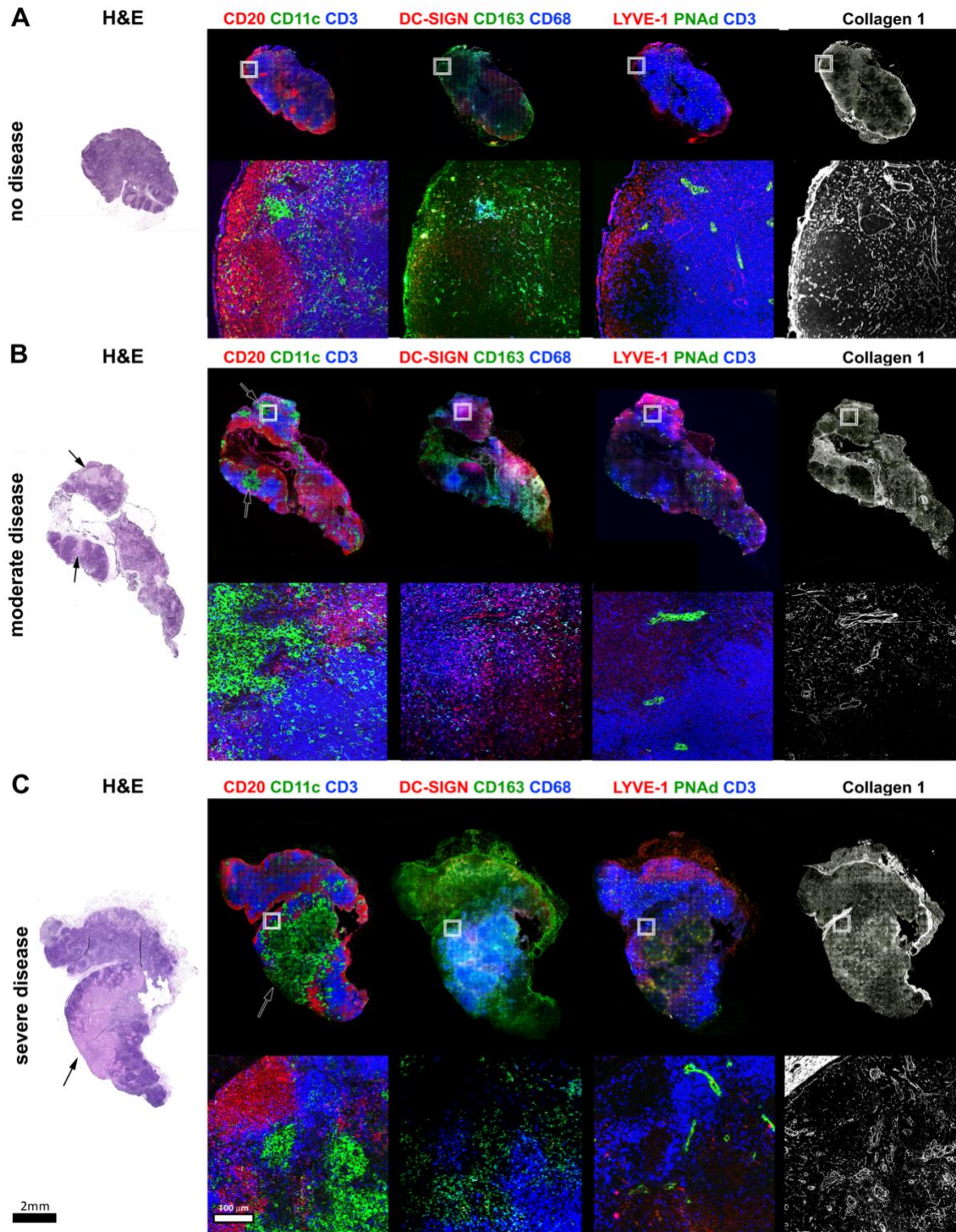


Figure 65. Histologic and immunohistochemical characterization of Mtb-infected macaque lymph nodes with varying levels of disease.

FFPE tissue sections from Mtb-infected macaques were stained with hematoxylin and eosin (H&E) to show the tissue morphology and immunohistochemistry was performed on serial sections to identify the lymph node's cellular, vascular, and structural elements. The box in the full-lymph node image indicates the region for the magnified panels (below) A. Lymph node showing no histologic evidence of disease and normal lymph node architecture. B. Lymph node demonstrating histologically-moderate disease where focal granulomas are present in T cell regions but not yet distorting the overall nodal architecture. Arrow indicates a granuloma. C. Severe lymph node disease showing large-scale disruption of the normal nodal structure in the vicinity of large coalescing granulomas. Arrow indicates a granuloma. Black scale bar (lower left) for the full-scale lymph nodes represents 2 mm. White scale bar (lower left, second column) for magnified image fields, represents 100 μ m.

We hypothesized that effaced LNs (i.e. extensive necrosis) would be an excellent site for Mtb growth so we used auramine-rhodamine (A-R) staining to identify where bacteria localize in LNs. We found that Mtb, visualized as numerous small puncta in A-R stained sections (Figure 66A, A-R inset), were abundant in granulomatous regions but absent from granuloma-free regions suggesting granulomas are foci of bacterial persistence and replication in LNs. When LNs with different levels of effacement were compared for CFU and CEQ, LNs with >50% effacement had significantly higher CFU and CEQ than those with \leq 50% effacement (Figure 66B and 66C) but there was no difference in the killing capacity of LNs with differing degrees of effacement (Figure 66D). The increase in both CEQ and CFU, and lack of killing, suggests that the macrophage populations and necrotic regions associated with effacement are conducive to Mtb persistence and replication.

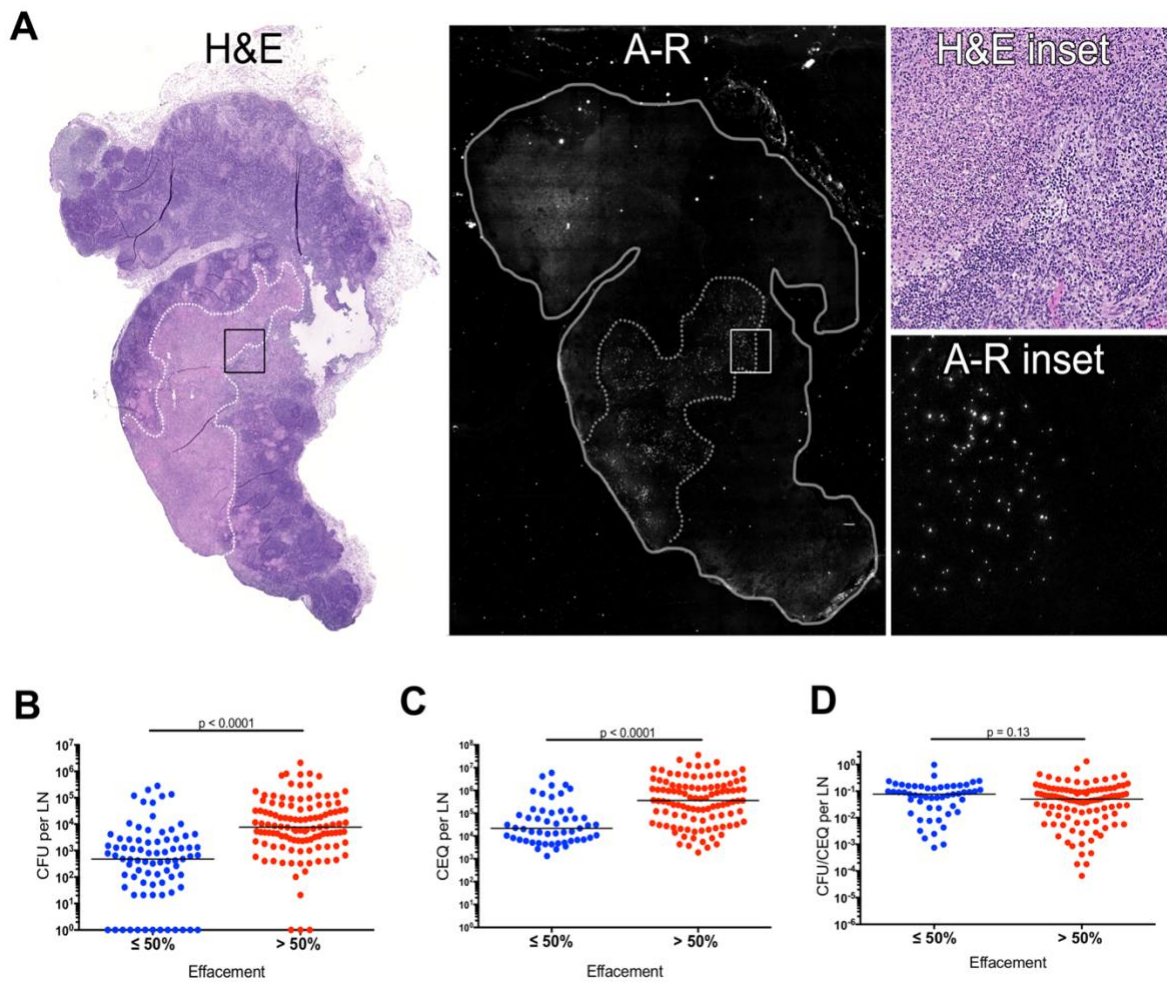


Figure 66. Lymph node effacement promotes Mtb growth.

A. H&E and Auramine-rhodamine (A-R) staining of a severely-effaced thoracic lymph node (previously depicted in Fig. 6C). The location of a large granuloma, indicated by white and grey dashed lines in the H&E and A-R panels, respectively, corresponds with substantial numbers of A-R-stained Mtb. Inset regions (black and white boxes in the H&E and A-R panels, respectively) show the interface between granulomatous and non-granulomatous lymph node regions. B, C. CFU (B) and CEQ (C) of thoracic lymph nodes with $\leq 50\%$ or $> 50\%$ effacement (effacement determined by H&E section). D. Mtb killing capacity (CFU/CEQ) of lymph nodes are not affected

by the degree of effacement. Each data point is one lymph node. The CFU was transformed by adding 1 to reflect sterile but CEQ+ lymph nodes. Statistical test is Mann-Whitney.

5.3.5 Bacterial burden is associated with decreased capacity to induce cytokine production in lymph nodes with granulomas

Cytokine producing cells play important roles in the control of Mtb infection [176]. Although LNs are sites of T cell priming for control of infection in lung granulomas, they also must generate functional cells to control infection within the LNs. We evaluated cytokine expression using multiparameter flow cytometry in thoracic LN cells from 24 cynomolgus macaques (Table 6) included as controls in other studies. We investigated T cell, B cell, and macrophage expression of proinflammatory cytokines: Th1 (IFN α , IL-2, TNF), Th17 (IL-17) and anti-inflammatory cytokine IL-10 following stimulation with peptide pools from Mtb antigens ESAT-6 and CFP-10. LNs with granulomas (identified either by gross pathology or histopathology) were evaluated for this analysis. Uninfected LNs (no granuloma established and no live Mtb) had similar cytokine profile as that of LNs with granuloma that cleared Mtb, however uninfected LNs had significantly higher proportions of CD3 T cells ($p=0.0009$) than LNs with granulomas. The number of LNs for each analysis varied by the panel used in that particular study (Table 7).

Table 7. Cytokine responses in CFU+ and CFU- thoracic LNs.

| Cell Type/Cytokine | Panel A | | | Panel B | | | Panel C | | |
|---------------------|---------------------------------------------------------|------------------------|--------------|----------------------------------------------------------------|------------------------|---------------|---------------------------------------------------------------------------|-----------------|---------------|
| | Thoracic LNs with granuloma: CFU+ vs CFU- (ESAT6+CFP10) | | | Thoracic LNs with granuloma: CFU+ vs CFU- (PDBu and ionomycin) | | | Thoracic LN correlation between CFU burden/LN and variable* (ESAT6+CFP10) | | |
| | CFU+ (Median, n of LN) | CFU- (Median, n of LN) | p value | CFU+ (Median, n of LN) | CFU- (Median, n of LN) | p value | Variable* | Spearman ρ | Prob> p |
| CD3+ | 74.5, n=28 | 77.95, n=20 | 0.1518 | 71.55, n=22 | 75.8, n=14 | 0.1942 | CD3+ | -0.2798 | 0.0541 |
| CD3+ IFN γ | 0.288, n=28 | 0.525, n=20 | 0.3111 | 3.28, n=22 | 7.825, n=14 | 0.0227 | CD3+ IFN γ | -0.1637 | 0.2662 |
| CD3+ IL-2 | 0.3175, n=22 | 0.339, n=20 | 0.6627 | 2.91, n=17 | 7, n=14 | 0.1579 | CD3+ IL-2 | -0.1437 | 0.3639 |
| CD3+ TNF | 0.892, n=28 | 0.551, n=20 | 0.078 | 3.665, n=22 | 9.26, n=14 | 0.0663 | CD3+ TNF | 0.2037 | 0.1649 |
| CD3+ IL-17 | 0.549, n=27 | 0.577, n=18 | 0.4802 | 2.04, n=22 | 3.25, n=13 | 0.3185 | CD3+ IL-17 | -0.1555 | 0.3078 |
| CD3+ IL-10 | 0.958, n=13 | 1.685, n=14 | 0.7564 | 0.725, n=14 | 2.8, n=11 | 0.4342 | CD3+ IL-10 | 0.0201 | 0.9208 |
| CD3+ Ki67 | 1.285, n=6 | 0.614, n=11 | 0.7864 | 0.2785, n=8 | 1.69, n=9 | 0.2766 | CD3+ Ki67 | 0.0201 | 0.939 |
| CD4+ | 61, n=28 | 55.3, n=20 | 0.4872 | 59.75, n=22 | 69.05, n=14 | 0.178 | CD4+ | 0.0915 | 0.5361 |
| CD4+ IFN γ | 0.3165, n=28 | 0.4245, n=20 | 0.7522 | 2.425, n=22 | 4.01, n=14 | 0.0604 | CD4+ IFN γ | -0.069 | 0.6414 |
| CD4+ IL-2 | 0.1495, n=22 | 0.2215, n=20 | 0.3391 | 3.62, n=17 | 8.15, n=14 | 0.1179 | CD4+ IL-2 | -0.2455 | 0.1171 |
| CD4+ TNF | 0.955, n=28 | 0.4025, n=20 | 0.019 | 3.53, n=22 | 10.85, n=14 | 0.0825 | CD4+ TNF | 0.2892 | 0.0462 |
| CD4+ IL-17 | 0.415, n=27 | 0.37, n=18 | 0.959 | 1.915, n=22 | 3.36, n=13 | 0.1055 | CD4+ IL-17 | -0.0493 | 0.7479 |
| CD4+ IL-10 | 0.882, n=13 | 0.2755, n=14 | 0.1408 | 0.3075, n=14 | 2.23, n=11 | 0.2671 | CD4+ IL-10 | 0.2879 | 0.1453 |
| CD4+ Ki67 | 1.24, n=6 | 0.413, n=11 | 0.5908 | 0.2085, n=8 | 1.33, n=9 | 0.1996 | CD4+ Ki67 | 0.1004 | 0.7015 |
| CD8+ | 26.8, n=28 | 25.4, n=20 | 0.9463 | 23.05, n=22 | 20.8, n=14 | 0.6137 | CD8+ | 0.0312 | 0.8333 |
| CD8+ IFN γ | 0.225, n=28 | 0.4115, n=20 | 0.5265 | 5.26, n=21 | 16.5, n=14 | 0.0201 | CD8+ IFN γ | -0.1113 | 0.4513 |
| CD8+ IL-2 | 0.273, n=22 | 0.44, n=20 | 0.7503 | 1.295, n=16 | 5.125, n=14 | 0.0472 | CD8+ IL-2 | -0.1128 | 0.4768 |
| CD8+ TNF | 0.7145, n=28 | 0.5875, n=20 | 0.3136 | 2.69, n=21 | 10.95, n=14 | 0.026 | CD8+ TNF | 0.0999 | 0.4992 |
| CD8+ IL-17 | 0.394, n=27 | 0.345, n=18 | 0.8051 | 0.845, n=21 | 1.19, n=13 | 0.4052 | CD8+ IL-17 | -0.0315 | 0.8374 |
| CD8+ IL-10 | 1.43, n=13 | 0.6015, n=14 | 0.1373 | 0.348, n=13 | 0.695, n=11 | 0.2284 | CD8+ IL-10 | 0.2151 | 0.2813 |
| CD8+ Ki67 | 1.205, n=6 | 0.905, n=11 | 0.3378 | 0.65, n=8 | 2.15, n=9 | 0.2359 | CD8+ Ki67 | 0.2224 | 0.3909 |
| CD20+ | 15.4, n=19 | 19.6, n=11 | 0.3227 | 17.2, n=17 | 24.3, n=8 | 0.0356 | CD20+ | -0.0365 | 0.8481 |
| CD20+ IFN γ | 0.889, n=19 | 0.5, n=11 | 0.545 | 0.483, n=17 | 1.705, n=8 | 0.1527 | CD20+ IFN γ | 0.0598 | 0.7534 |
| CD20+ IL-2 | 0.754, n=13 | 1.12, n=11 | 0.833 | 0.3285, n=12 | 2.455, n=8 | 0.0124 | CD20+ IL-2 | -0.0188 | 0.9307 |
| CD20+ TNF | 1.87, n=19 | 0.943, n=11 | 0.1746 | 2.22, n=17 | 4.085, n=8 | 0.0673 | CD20+ TNF | 0.261 | 0.1636 |
| CD20+ IL-17 | 2.41, n=18 | 2.81, n=9 | 0.7144 | 3.86, n=17 | 4.01, n=7 | 0.2598 | CD20+ IL-17 | 0.0716 | 0.7228 |
| CD20+ IL-10 | 0.958, n=13 | 1.685, n=14 | 0.7564 | 0.725, n=14 | 2.8, n=11 | 0.4342 | CD20+ IL-10 | 0.032 | 0.8876 |
| CD11b+ | 14.7, n=8 | 22.1, n=9 | 0.4807 | 17.55, n=10 | 22.1, n=7 | 0.6691 | CD11b+ | -0.1102 | 0.6737 |
| CD11b+ IFN γ | 11.2, n=8 | 8.13, n=9 | 0.8148 | 11.4, n=9 | 20, n=7 | 0.0229 | CD11b+ IFN γ | -0.0505 | 0.8475 |

Table 7 continued

| | | | | | | | | | |
|--------------|------------------|------------------|---------------|-------------------|------------------|---------------|--------------|----------------|---------------|
| CD11b+ TNF | 12.88, n=8 | 6.44, n=9 | 0.8884 | 9.89, n=9 | 19.5, n=7 | 0.1416 | CD11b+ TNF | -0.2018 | 0.4372 |
| CD11b+ IL-17 | 4.35, n=8 | 14.59, n=4 | 0.1535 | 3.57, n=7 | 15.72, n=4 | 0.2303 | CD11b+ IL-17 | -0.3673 | 0.2402 |
| CD11b+ IL-10 | 3.42, n=8 | 21.8, n=9 | 0.0464 | 0.814, n=9 | 26.5, n=7 | 0.0021 | CD11b+ IL-10 | -0.5046 | 0.0389 |

Panel A shows T cell, B cell and macrophage cytokines in CFU+ and CFU- LNs in response to Mtb-specific antigens, ESAT-6 and CFP-10. Panel B shows T cell, B cell and macrophage cytokines in CFU+ and CFU- LNs in response to non-specific stimulation, PDBu and ionomycin. Panel C shows the correlation between bacterial burden per LN and T cell, B cell and macrophage cytokine responses to Mtb-specific antigens, ESAT-6 and CFP-10.

First, we compared cytokine responses between thoracic LNs with granuloma that had live Mtb (CFU+) and those that cleared Mtb (CFU-). As seen in lung granulomas [121], we found that LN granulomas represent a multi-cytokine environment with the presence of both pro and anti-inflammatory cytokines produced by a variety of cells within a LN. Cytokine responses largely overlapped between CFU+ LNs and CFU- LNs (Table 7). Nevertheless, CFU- LNs with granulomas had significantly higher proportions of CD11b+ cells producing IL-10 (Figure 67A) when compared with CFU+ LNs with granulomas, while CD4+ T cells producing TNF (Figure 67B) were significantly higher in CFU+ LNs (Table 7 Panel A). With the exception of TNF response, there was no significant difference in cytokine producing T, B and CD11b+ cells in CFU+ and CFU- LNs (Table 7 Panel A) in response to Mtb antigens ESAT-6 and CFP-10. Secondly, we questioned whether there was an association between cytokine response and bacterial burden. We found a significant negative correlation between bacterial burden and CD11b+ cells producing IL-10 (Spearman's ρ -0.5046, $p=0.0389$) (Table 7 Panel C), and a positive

correlation with bacterial burden and CD4 T cells producing TNF (ρ 0.2892, $p=0.0462$) (Table 7 Panel C). These data suggest that IL-10 response from macrophages is associated with bacterial clearance while CD4⁺ T cell TNF response could be attributed to ongoing Mtb replication.

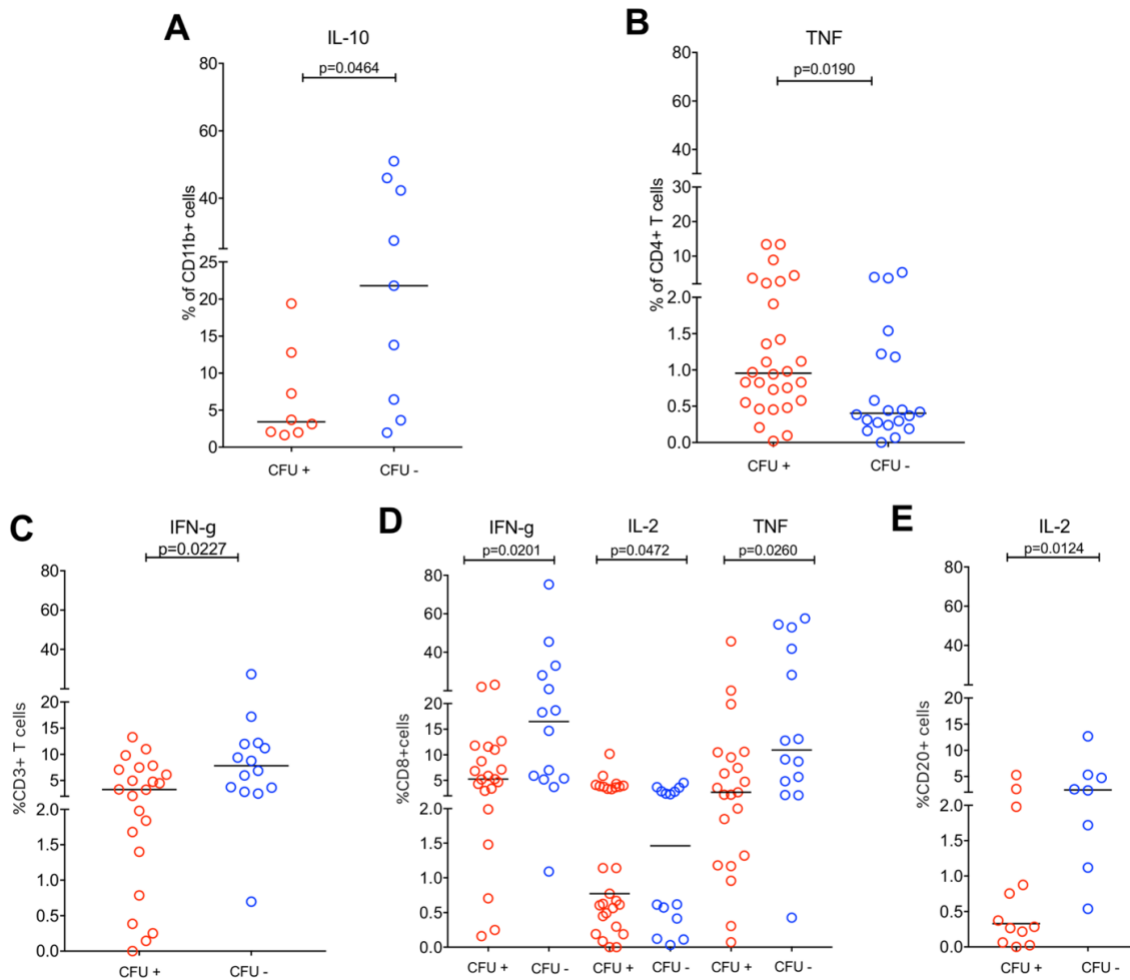


Figure 67. Immune response in thoracic LNs of cynomolgus macaques with granulomas.

Cytokine production in thoracic LN with granuloma in response to ESAT6+CFP10 (A-B) or PDBu and ionomycin (C-E) between LNs with bacterial burden (CFU+, red) and those that cleared (CFU-, blue). A. Frequency of CD11b+ cells producing IL-10 (n=10 macaques; 27 LNs); B. Frequency of CD4+ T cells producing TNF (n=24 macaques; 48 LNs). C. Frequency of CD3+ cells producing IFN γ (n=12 macaques; 35 LNs); D. Frequency of CD8+ cells producing IFN γ (n=12 macaques, 34 LNs) IL-2 (n=10 macaques; 28 LNs) and TNF (n=12 macaques; 34 LNs); E. Frequency of CD20+ cells producing IL-2 (n=11 macaques; 20 LNs). Each symbol represents a LN. Statistical test is Mann-Whitney.

Next, we investigated whether Mtb burden alters the overall capacity of cells in thoracic LNs with granuloma to produce cytokines by stimulating them non-specifically with PDBu and ionomycin. Overall, sterile (CFU-) LNs have a trend towards cells producing higher frequency of cytokines compared to CFU+ LNs. Of note, LNs with granulomas that are sterile had significantly higher frequencies of CD3+ T cells producing IFN γ (Figure 67C); CD8+ cytotoxic T cells producing IFN γ , IL-2 or TNF (Figure 67D) and CD20+ B cells producing IL-2 (Figure 67E) than CFU+ LNs. In addition, we also observed a higher proportion of CD11b+ cells producing IFN γ and IL-10 (Table 7 Panel B) in LNs without bacterial burden under the same conditions, even though PDBu-ionomycin does not induce these cytokine production in CD11b+ cells. These data suggest LN that have sterilized the infection have a higher capacity to produce both pro- and anti-inflammatory cytokines and this may have contributed to its ability to eliminate Mtb.

We extended our investigation to understand whether there are differences in Mtb-specific responses between thoracic and peripheral LNs to determine whether these responses could contribute to protection in the periphery. For this analysis, 14 peripheral LNs and 27 thoracic LNs from 7 animals were evaluated (Table 8). None of the peripheral LNs had any granuloma or grew Mtb from culture, while 14 of thoracic LNs had granulomas and 12 thoracic LNs grew Mtb. Peripheral LNs had significantly higher proportion of CD3+ (Figure 68A) and CD4+ T cells (Figure 68B) than thoracic LNs (Table 8). Irrespective of bacterial burden or granuloma presence, the proliferative capacity of T cells, as measured by Ki67+ CD3+ T cells, especially Ki67+ CD8+ of cytotoxic T cells (Table 8, Figure 68C), was significantly higher in thoracic LNs than in peripheral LNs, suggesting that Mtb induced proliferation might occur in the thoracic LNs. There was no difference in T cell cytokine response or the capacity to induce cytokines response by T cells as determined by PDBu and ionomycin between thoracic and peripheral LNs (Table 8).

Table 8. T cell cytokines and proliferative capacity in response to PDBu and ionomycin in thoracic and peripheral LNs.

| Cell Type/Cytokine | Peripheral LN (Median, n of LN) | Thoracic LN (Median, n of LN) | p value |
|--------------------|---------------------------------|-------------------------------|---------------|
| CD3+ | 79.3, n=14 | 74.5, n=27 | 0.0429 |
| CD3+ IFNg | 0.216, n=14 | 0.249, n=27 | 0.6540 |
| CD3+ IL-2 | 0.712, n=14 | 0.593, n=27 | 0.9293 |
| CD3+ TNF | 0.5135, n=14 | 0.79, n=27 | 0.1586 |
| CD3+ IL-17 | 0.5615, n=14 | 0.363, n=27 | 0.3334 |
| CD3+ IL-10 | 0.258, n=9 | 0.438, n=17 | 0.6340 |
| CD3+ Ki67 | 0.177, n=8 | 0.283, n=18 | 0.0233 |
| CD4+ | 66.35, n=14 | 60.3, n=27 | 0.0343 |
| CD4+ IFNg | 0.195, n=14 | 0.299, n=27 | 0.4840 |
| CD4+ IL-2 | 0.173, n=14 | 0.149, n=27 | 0.5012 |
| CD4+ TNF | 0.4875, n=14 | 0.862, n=27 | 0.1824 |
| CD4+ IL-17 | 0.4655, n=14 | 0.339, n=27 | 0.2161 |
| CD4+ IL-10 | 0.189, n=9 | 0.303, n=17 | 0.4992 |
| CD4+ Ki67 | 0.0638, n=8 | 0.0929, n=15 | 0.0556 |
| CD8+ | 27.95, n=14 | 29.6, n=27 | 0.5362 |
| CD8+ IFNg | 0.2435, n=14 | 0.239, n=27 | 0.7915 |
| CD8+ IL-2 | 1.464, n=14 | 0.772, n=27 | 0.6200 |
| CD8+ TNF | 0.763, n=14 | 1, n=27 | 0.5635 |
| CD8+ IL-17 | 0.507, n=14 | 0.382, n=27 | 0.5962 |
| CD8+ IL-10 | 0.572, n=9 | 0.52, n=17 | >0.9999 |
| CD8+ Ki67 | 0.331, n=8 | 0.676, n=15 | 0.0337 |

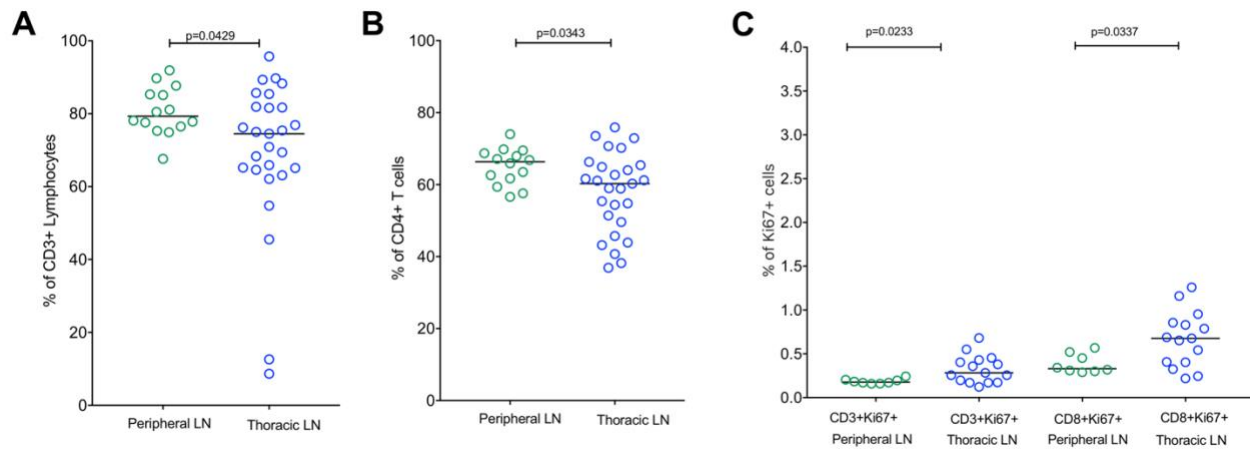


Figure 68. Comparison of immune responses in peripheral and thoracic LNs.

Peripheral (n=14) and thoracic LNs (n=27) from 7 animals were stimulated with ESAT6 and CFP-10 peptides. A. Frequency of CD3+ T cells. B. Frequency of CD4 T cells in peripheral LNs than thoracic LNs. C. Proliferative capacity of T cells measured by Ki67 in CD3+ and CD8+ T cells. Ki67+ T cells are significantly higher in thoracic LNs than in peripheral LNs. Each symbol is a LN. Peripheral LNs are in green and thoracic LNs are in blue. Statistics are Mann-Whitney.

Finally, since we observed that the thoracic LNs with higher bacterial burden had decreased capacity to produce certain cytokines when compared to those with no bacterial burden, we examined whether the degree of LN effacement altered immune cell function in a subset of thoracic LNs where data for degree of effacement (n=55) were available. There was no difference in cytokine responses to Mtb specific antigens, capacity to produce cytokines in LNs without granulomas, $\leq 50\%$ effaced LNs, and $>50\%$ effaced LNs (Table 9) suggesting that LN effacement does not alter the functional capacity of LN cells.

Table 9. T cell cytokines in response to Mtb-specific antigens (ESAT-6 and CFP-10) in differentially effaced LNs.

MCT = multiple comparison test.

| Cell Type/Cytokine | No effacement | | Effacement <50% | | >50% Effacement | | Kruskal Wallis with Dunns MCT |
|----------------------|---------------|----------------|-----------------|----------------|-----------------|----------------|-------------------------------|
| | Mean | Std. Deviation | Mean | Std. Deviation | Mean | Std. Deviation | p value |
| CD3 (of Lymphocytes) | 78.1 | 11.67 | 75.5 | 8.271 | 70.8 | 8.585 | 0.0839 |
| CD3+IFN γ | 1.38 | 3.029 | 0.76 | 0.8869 | 1.65 | 2.715 | 0.8182 |
| CD3+ IL-2 | 1.2 | 1.606 | 1.55 | 1.906 | 1.29 | 2.329 | 0.8494 |
| CD3+ IL-10 | 2.17 | 5.317 | 4.67 | 6.198 | 9.07 | 14.27 | 0.2515 |
| CD3+ IL-17 | 1.93 | 4.723 | 4.41 | 8.153 | 4.29 | 9.848 | 0.7276 |
| CD3+ Ki67 | 0.96 | 1.302 | 2.94 | 3.354 | 0.44 | 0.05873 | 0.7931 |
| CD3+ TNF | 1.3 | 1.484 | 2.2 | 3.774 | 1.18 | 0.9733 | 0.9433 |
| CD4 (of CD3+) | 57.6 | 16.01 | 60.7 | 12.25 | 59.9 | 7.813 | 0.7747 |
| CD4+ IFN γ | 1.3 | 3.045 | 0.68 | 0.9098 | 1.64 | 2.76 | 0.9917 |
| CD4+ IL-2 | 0.84 | 1.745 | 1.21 | 1.999 | 1.12 | 2.495 | 0.6361 |
| CD4+ IL-10 | 2.25 | 5.92 | 4.91 | 8.376 | 9.74 | 16.88 | 0.456 |
| CD4+ IL-17 | 1.81 | 4.849 | 4.22 | 8.232 | 4.47 | 10.45 | 0.5937 |
| CD4+ Ki67 | 0.71 | 1.147 | 2.23 | 2.742 | 0.24 | 0.1443 | 0.5842 |
| CD4+ TNF | 1.38 | 1.537 | 1.98 | 3.742 | 1.19 | 1.051 | 0.5316 |
| CD8 (of CD3+) | 26.5 | 7.585 | 24.4 | 8.817 | 24.3 | 8.507 | 0.7167 |
| CD8+ IFN γ | 1.5 | 3.56 | 0.87 | 0.9963 | 1.71 | 2.775 | 0.64 |
| CD8+ IL-2 | 1.88 | 1.952 | 2.09 | 2.211 | 1.71 | 2.481 | 0.8919 |
| CD8+ IL-10 | 1.21 | 2.662 | 3.06 | 4.768 | 5.05 | 7.011 | 0.841 |
| CD8+ IL-17 | 1.48 | 3.624 | 3.59 | 6.782 | 3.46 | 7.705 | 0.6135 |
| CD8+ Ki67 | 1.38 | 1.51 | 3.62 | 4.054 | 0.77 | 0.1641 | 0.7296 |
| CD8+ TNF | 1.16 | 1.509 | 2.23 | 3.729 | 1.02 | 0.8901 | 0.5074 |

5.3.6 Short course drug treatment is more effective in lung granulomas than in thoracic lymph nodes

Since thoracic LNs are generally poor at killing Mtb, we examined whether there was a relationship between LN involvement and extrapulmonary disease. Greater lymph node involvement, as assessed by gross pathology scoring (which accounts for number of LNs with granulomas, size of LN, and effacement) was associated with more extrapulmonary disease in rhesus (F test, $R_2 = 0.588$, $p < 0.0001$) but not in cynomolgus macaques (Figure 69A). Extrapulmonary score was not related to total LN bacterial burden in either macaque species (Figure 69B). We also examined data from a previous study [338] to determine whether Mtb in thoracic LNs was less effectively killed during a short-course (2 months) linezolid (LZD) treatment relative to lung granulomas. Lung granulomas had a higher proportion of sterility (75% LZD-treated vs. 21.8% control) after drug treatment compared to thoracic LNs (16.7% LZD-treated vs. 2.5% control). The reduction in bacterial burden in LNs (Figure 70A) was lower than the reduction of bacterial burden in lung granulomas (Figure 70B) of LZD-treated macaques (55-fold vs. 181-fold, respectively) compared to untreated control macaques. These data suggest that after 2 months of LZD treatment, Mtb was killed less effectively in thoracic LNs compared to lung granulomas, supporting that LNs are bacterial reservoirs and potential sites of reactivation or relapse. This is consistent with our previously published observation in which short course isoniazid and rifampin treatment for 2 months was more effective in reducing bacterial burden in lung granulomas than in thoracic LN during active disease treatment [268].

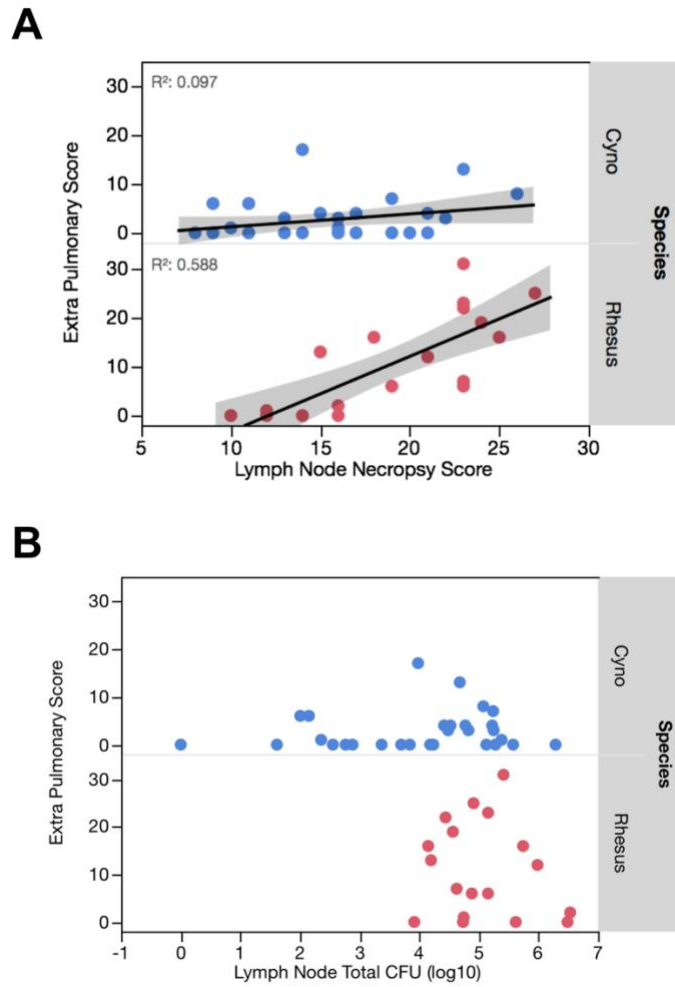


Figure 69. Correlation between extrapulmonary score (extent of extrapulmonary disease at necropsy) and LN necropsy score and bacterial burden.

A. There is a moderate positive correlation between extrapulmonary score and lymph node necropsy score [235] in rhesus macaques but not in cynomolgus macaques. B. No relationship between extrapulmonary score and total LN CFU in cynomolgus and rhesus macaques. Each data point is a macaque. Statistical test is F test.

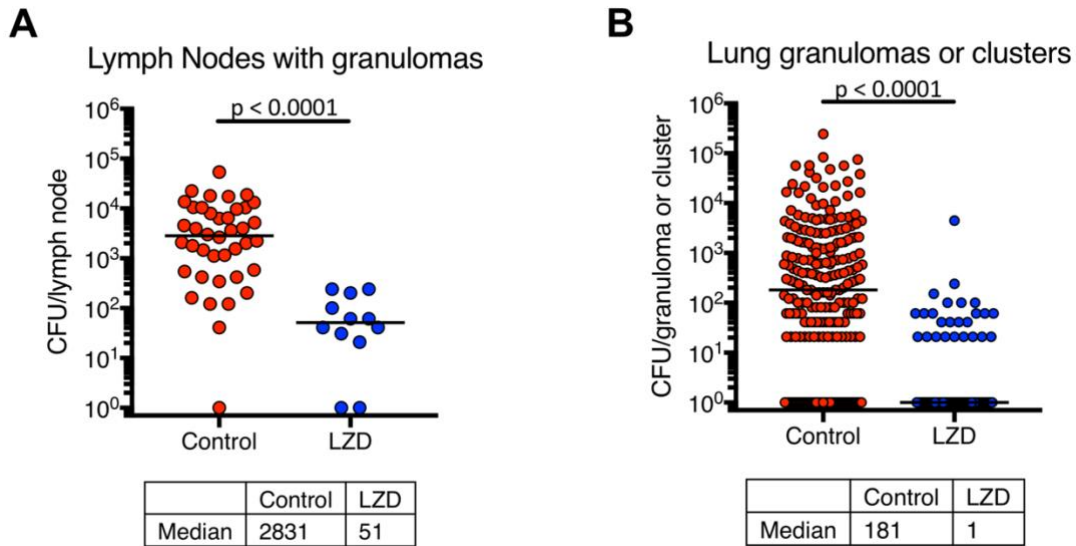


Figure 70. Reduction of bacterial burden in lymph nodes and lung granulomas of cynomolgus macaques after 2 months of linezolid (LZD) therapy (data from study [338]).

A. Lymph nodes with granulomas. B. Lung granulomas or clusters. In box under each graph is the median for each group, used to calculate fold reduction in text. Control n=8, LZD n=5. Each data point is a granuloma or a lymph node. Statistical test is Mann-Whitney.

5.4 Discussion

Traditionally, lung infection has been the primary focus of TB research and treatment, despite evidence that Mtb also infects and persists in LNs. There are unanswered questions regarding the importance of LN infection in the pathogenesis of TB including bacterial replication or killing, and the antimicrobial immune responses in LNs. Here we focused on LN infection in cynomolgus and rhesus macaques, two closely-related nonhuman primate species that replicate the pathology of human TB [230, 232, 233]. We present data supporting that LNs can become

inflamed (FDG-avid) as early as 2 weeks post infection. Starting at 4 weeks post-infection, FDG avidity correlated with the presence of live bacteria in LNs at necropsy. Although thoracic LNs in cynomolgus macaques initiate killing of Mtb by 11 weeks post-infection, with substantially more killing at later time points, LNs from rhesus macaques have impaired killing capacity, likely contributing to the increased susceptibility of this species. We also found that granulomas substantially disrupt the structure of LNs, and can completely efface the organ, which is associated with increased growth of Mtb. Overall, our data support that thoracic LNs are a site of prolonged bacterial persistence, sometimes at quite high levels.

Previous work has demonstrated that LNs are important in reactivation TB [182, 198, 199, 253] but little is known about the interplay of Mtb infection and host responses in LNs. Large human studies by Poulsen in the 1930s and 1940s showed that early after Mtb infection, there was often an initial fever that lasted 2-3 weeks [341, 342]. These subjects presented with enlarged “hilar shadows” by x-ray, assumed to be lymphadenopathy. A large number of subjects also presented with hilar adenitis when they first became tuberculin skin test positive which they ascertained to be ~40 days after infection. To investigate the dynamics of Mtb infection in LNs of macaques, we used PET CT to monitor LNs over the course of infection. In support of Poulsen’s early data, we found increased metabolic activity (FDG uptake) in thoracic LNs as early as 2 weeks post-infection and more LNs became FDG-avid by 4-6 weeks. This increase in FDG uptake is associated with Mtb infection in that nearly all FDG+ LNS are also CFU+ at necropsy, and is likely due to increased metabolic activity of cells during priming of the adaptive immune response as well as the host cells reacting to the presence of Mtb bacilli. However, not all LNs in an individual macaque became infected, and those that were infected could wax and wane in FDG avidity over the course of infection.

Rhesus and cynomolgus macaques are closely related species used in TB research, and we recently performed quantitative analyses of similarities and differences between Mtb infection outcomes in these species [235]. Cynomolgus macaques develop the full range of infection outcomes seen in humans, from clinically latent to severe active TB. In contrast, rhesus macaques are more susceptible, with nearly all animals developing active and often severe TB within several months of experimental low dose infection. One striking feature of TB in rhesus macaques is the often substantial involvement of thoracic LNs with high levels of necrosis; in some cases a LN can grow massively and impinge on the airways causing lobe collapse or erode into a bronchus leading to further dissemination. Certainly, substantial LN involvement can be seen in some cynomolgus macaques, but in general the extent of LN disease is lower in this species [235]. A limitation of comparing these models is that due to the susceptible nature of rhesus macaques, essentially none of these animals present with long term controlled (latent) infection following low dose challenge with virulent Mtb and nearly all succumb before 24 weeks of infection. Thus, LN samples from long term (>26 weeks post-infection) rhesus macaques for comparison with similar time points in cynomolgus macaques are not available.

Here, we show that Mtb grows to the same initial level (with a wide range) in thoracic LNs at 4 weeks post infection in both species, but rhesus lymph nodes were less successful at killing Mtb over time. Remarkably, at 16-29 weeks post-infection, the different disease states (controlling to active disease) of cynomolgus macaques were reflected in the capacities of their LNs to kill Mtb. This further supports our findings that the lungs and LNs are intricately linked during Mtb infection [235]. However, in general, LNs were less bactericidal than lung granulomas in both species [118]. This deficit in bacterial killing at the LN level in part explains the pronounced LN disease and increased susceptibility of rhesus macaques to Mtb infection [235]. Despite the

limitation of CEQ as being simply an estimate of Mtb genomes, it is the only technology at this time that is available to estimate live + dead bacilli and actual killing of Mtb (together with CFU measurement) in vivo. Lung granulomas peak in bacterial burden early in infection with approximately 10^4 - 10^5 CFU per granuloma, followed by substantial killing of bacteria in most granulomas once the adaptive immune response is initiated [118]. In contrast, some thoracic LNs had 100-fold more bacteria than lung granulomas. In cynomolgus macaques, we show that even when granulomas are established, some LNs are able to clear Mtb and these LNs are associated with higher CD11b⁺ cells producing IL-10. LN bacterial burden was inversely correlated with CD11b⁺ cells producing the anti-inflammatory cytokine IL-10 and sterile LNs had significantly higher capacity to produce both pro- and anti- inflammatory cytokines, suggesting this multi-cytokine environment might contribute to bacterial containment in a subset of LNs, similar to our observations in lung TB granulomas [121]. We did not have sufficient samples to conduct a full kinetic analysis of the CD11b⁺IL-10⁺ population; this finding requires further study to understand its significance.

Somewhat surprisingly, we discovered Mtb genomes in peripheral LNs (i.e., axillary and inguinal) that do not drain the lungs, even though most of these LNs were sterile. Although our data suggest that occasionally peripheral LNs can be infected with small numbers of bacteria and are better at killing Mtb than thoracic LNs, we cannot exclude the possibility that genomes detected here were free-floating DNA trapped in these tissues. Histologic analysis did not reveal evidence of pathology in the CEQ⁺ peripheral LNs, even in the few that had viable Mtb. The difference in the cytokine responses and proliferative markers we observed between peripheral and thoracic LNs could be attributed to constant stimuli from Mtb at the thoracic LNs. The improved sterilizing

capacity of peripheral LNs could also be due to the timing of infection in these LNs, which we could not ascertain in our study.

The structure and spatial organization of cells in LNs are critical for their function [343, 344], and may also help explain why LNs have limited abilities to kill Mtb. Even though the killing capacity and immune function of LNs with varying degrees of effacement are similar, the bacterial burden (CEQ and CFU) in >50% effaced LNs was 16-fold higher compared to ≤50% effaced LNs. Our data support that the more extensive the disruption in LN structure is, the more conducive the LN is for Mtb growth and this is likely due to a number of factors. First, the formation of a granuloma recruits a large number of macrophages that can serve as niches for Mtb growth. Moreover, as LN granulomas expand they push out T cells, disrupt B cell follicles, which could interfere in antibody production that could aid in controlling infection [216, 345], and damage LN-associated vasculature, which could potentially change drug availability. This disruption of LN architecture may also affect resident innate immune cells that have been shown to be spatially pre-positioned to provide a cascade of cytokines which promote macrophage antimicrobial resistance limiting pathogen dissemination [325]. In contrast to lung granulomas [217, 336, 346], LN granulomas do not have a well-defined lymphocytic cuff with tertiary lymphoid structures surrounding the epithelioid macrophage region. As the presence of these structures in lung granulomas has been associated with protection in pulmonary TB [205, 219, 347], we speculate that the absence of these structures results in poorly functional granulomas that have limited capacity to restrain or kill Mtb. These observations suggest that granulomas can potently influence aspects of LN architecture that facilitate T cell priming and systemic immunity, while providing an abundance of extra- and intracellular sites for mycobacterial replication.

Early autopsy studies support the idea that LNs serve as long-term reservoirs for Mtb. Viable Mtb bacilli were found in 9.4 - 27% of LNs from autopsies of patients without evidence of TB disease in lungs or anywhere in their bodies [242-244]. Mtb infection of LNs may also have implications in drug treatment. In our study, we found that a short-course LZD therapy was less effective in killing Mtb in LNs compared to Mtb in lung granulomas and this was also observed in short course isoniazid with rifampin [268]. Indeed, in a study that followed 113 patients that relapsed for 30 months, tuberculous lymphadenitis was found as a risk factor for relapse [348]. Of the 12 patients that had both pulmonary and LN TB, 9 (75%) patients had a recurrence exclusively in the LNs, while the remaining 3 patients had recurrence in both lungs and LNs [348]. However, only 1 patient was confirmed by bacterial culture and lymphadenopathy could also be caused by an impaired regulation of the immune system. In HIV+ patients with clinically latent TB, the presence of abnormal FDG uptake in mediastinal LNs was associated with patients showing subclinical TB disease and the likelihood of developing symptomatic TB disease during the 6 month follow up [253]. These studies suggest that Mtb can persist in LNs even after drug treatment, which we observed as well, and increased FDG activity in these tissues are associated with persisting or reactivating TB disease.

This study presents an in-depth investigation into bacterial dynamics and immunity in thoracic LNs during Mtb infection. Our data indicate that LNs can contain large numbers of bacteria and serve as long-term reservoirs of bacterial persistence. Thus, understanding how non-protective LN granulomas differ from protective lung granulomas may lead to strategies that improve TB treatment and outcomes. Moreover, our study identifies LNs and LN infection as important considerations for measuring vaccine and treatment efficacy.

6.0 Summary, implications and future directions

Mycobacterium tuberculosis has been existing with humans for thousands of years. Currently, TB is the leading cause of death from a single microbe in the world. It claimed 1.45 million lives in 2018 alone [2]. BCG was developed almost a hundred years ago and is still the only licensed vaccine against TB. It is effective in protecting infants and children from serious and disseminated disease but has variable efficacy in preventing infection or pulmonary TB in adults, which is the more common form of the disease, highlighting the need for a more effective TB vaccine [19]. The main hindrance to current vaccine development is the lack of biomarkers or immune correlates for protection against TB. Moreover, the protective immune responses to target in vaccine development are largely unknown. Current efforts to study TB mainly focus on the lungs neglecting the contribution of other organs in the disease. A recent NHP Mtb reinfection model [264] showed promising results in protecting against Mtb reinfection, however the mechanism of protection is mostly unexplored. The goal of this dissertation is two-fold: first, to understand the role of lymph nodes in TB and second, to begin dissecting the factors that contribute to the protection a first Mtb infection confers to a secondary Mtb challenge.

6.1 Bacterial viability is not essential but CD4 T cells are important in protection against a second infection

A meta-analysis of early epidemiology studies showed that a person with latent Mtb infection has a 79% lower risk of developing active TB disease compared to an uninfected person

[257]. However, in these early studies, the timing and whether or not the subjects were exposed to or reinfected with Mtb were unknown, since development of active TB was the outcome measure. This limitation has been circumvented by using animal models. A previous study by Cadena et al. [264], established an NHP Mtb reinfection model which demonstrated that a primary Mtb infection protects against the establishment and progression of a secondary Mtb infection. My dissertation is a continuation of that study, focusing on investigating factors that could influence this protection thereby contributing to more effective vaccine design.

The first factor that we investigated is the importance of bacterial viability in the protection against Mtb reinfection. Epidemiology studies showed that the incidence of recurrent TB, either from relapse or reinfection, is 14.6-18x higher in successfully treated individuals compared to initial TB disease in the general population [265, 266]. In Cape Town, South Africa, the incidence rate of recurrent TB due to Mtb reinfection was 4x that of initial TB incidence in the general population [267]. Does this mean that we should stop treating TB patients because they are more at risk of getting reinfected and developing TB disease after successful treatment? Clearly that is not an option. However, in this country and some others, humans with latent TB (infected but without symptoms of disease, LTBI) are offered drug treatment to cure the latent infection and prevent reactivation. Is this a good practice, or might it reduce the protection that a chronic but asymptomatic infection provides? In any event, understanding whether treatment leads to loss of protection against reinfection remains a critical question. While it is difficult to study Mtb reinfection in humans, we can directly answer these questions using an NHP reinfection model.

In my study, a cohort of macaques were infected with DNA barcoded Mtb library A and drug treated 4 months later. After 2-3 months of drug treatment, they were reinfected with Mtb library B. I included controls that followed the same timeline but without drug treatment. Here I

showed that drug treatment did not abolish the protection (ie. formation of fewer new granulomas with lower bacterial burden) a primary infection conferred to a secondary challenge. Although my findings indicate that drug treatment reduced the protection against a secondary infection when compared with the reinfected macaques from the study by Cadena et al. [264], this reduction was not significantly different from the no drug treatment controls. Aside from drug treatment, the main difference between this study and the original study by Cadena et al. is the duration of the primary infection. Cadena et al's reinfected macaques were infected with Mtb library A for 16 weeks before reinfection but the macaques in our study's no drug treatment control were infected with Mtb library A for ~33 weeks before reinfected with Mtb library B. Although drug treatment could be the reason for the reduction in protection, it is also possible that the protection from a primary infection wanes over time. One limitation of this study is the low number of animals in the no drug treatment control. The durability of this protection should be addressed in future studies. Like the 16-week reinfection animals from Cadena et al's study, macaques from both drug treated and non-drug treated groups prevented dissemination of Mtb library B to the lymph nodes when compared to the naïve controls.

No significant difference in the lymphocyte population and function in the BAL was observed between pre- and post-drug treatment time points. The lymphocyte numbers, function and proliferation in the airways were also similar between the two groups 2 weeks before second infection. Interestingly, the no drug treatment control had higher levels of chemokines and cytokines promoting recruitment of immune cells and inflammation. Whether the difference in the chemokine and cytokine environment in the airways between drug treated and non-drug treated groups will have an effect if given more time is currently unknown and should be the subject of future study. Unsurprisingly, given the similar protection between the 2 groups, the immune

response in new granulomas, involved lymph nodes (with granuloma and/or CFU+) and uninvolved lung lobes were not significantly different.

Based on this study, it seems likely that the results from human epidemiology studies were due to selection bias (selection of individuals with predisposition to Mtb infection and TB disease). However, other factors, such as the duration of primary Mtb infection before treatment, treatment duration and timing of second infection, could also have an effect in the rate of developing active TB disease due to Mtb reinfection. This study showed that live Mtb is not strictly necessary in generating protection against Mtb reinfection although the addition of more macaques in the non-drug treated group would give more credence to this conclusion. Nevertheless, this suggests that a successful Mtb vaccine could start out as having live bacteria but then these bacteria could be programmed to kill themselves thereby increasing safety and usage of the vaccine. In addition, the immune response responsible for the protection in 16-week reinfection animals needs to be fully characterized and compared to the immune profile of the animals in this study to give us clues as to the effect of drug treatment and a longer duration of the primary infection in the protection against Mtb reinfection. The role of immune cells, adaptive or innate, as well as antibodies in the Mtb reinfection model is not yet fully elucidated and should be thoroughly examined. This could provide us with a framework of what a protective immune response looks like and strive to achieve that with vaccines or host-directed therapy.

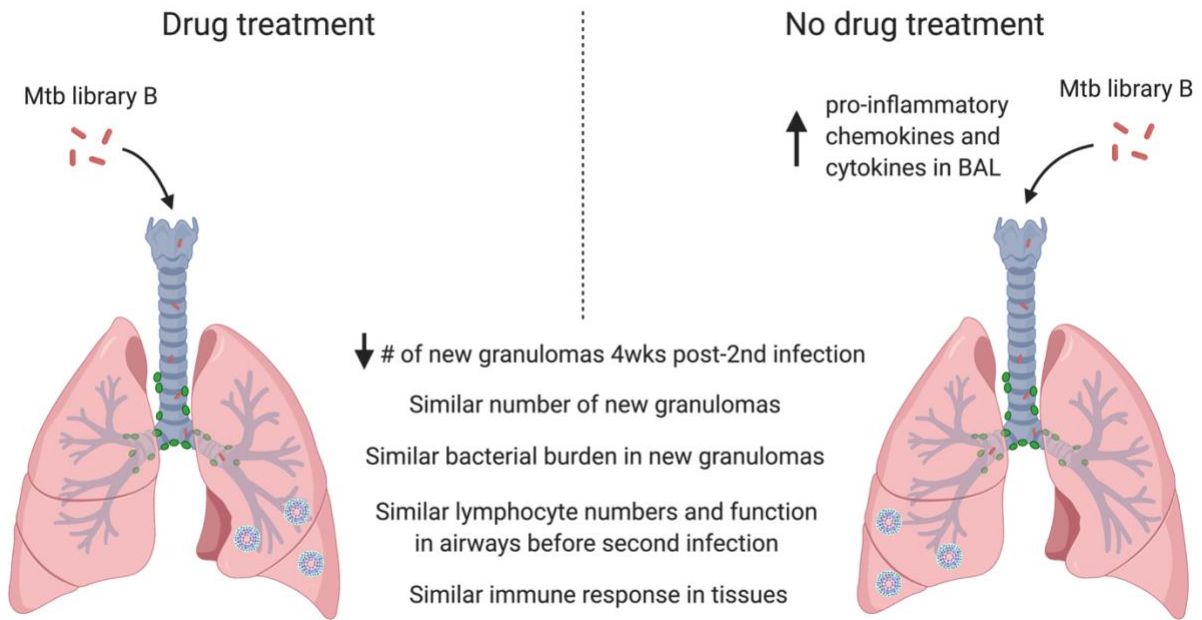


Figure 71. Drug treatment does not abolish protection to secondary Mtb infection.

Both groups had fewer number of granulomas at 4 weeks post-second infection compared to 4 weeks post-first infection. There was no significant difference in the number of new granulomas, bacterial burden of new granulomas, airway lymphocyte numbers and function before second infection and immune responses in tissues examined. Airways of non-drug treated animals had higher levels of proinflammatory cytokines and chemokines that could affect cell recruitment and consequently protection against second infection if given more time.

The next factor I investigated that could be important in the protection against second infection was CD4 T cells. The importance of CD4 T cells in primary Mtb infection and LTBI reactivation is well documented [179-183, 252]. However, this is the first study to interrogate the importance of CD4 T cells in the context of Mtb reinfection. I drug treated macaques 9 weeks after the first infection with Mtb library A to facilitate identification of new granulomas arising from the second infection. Macaques were subsequently divided into 2 groups: (1) α -CD4 group –

received CD4 T cell-depleting antibodies and (2) IgG control group – received IgG control antibodies. A naïve group receiving only Mtb library B (no drug treatment or antibody infusions) and new 16-week reinfection animals similar to those in Cadena et al's study were included as additional controls. Antibody infusions were commenced one week before second infection with Mtb library B. My data showed that CD4 T cells are important in the protection that a primary drug treated Mtb infection confers to a secondary infection. CD4 T cell depletion significantly increased the Mtb burden in new granulomas and lungs compared to the IgG controls. Because the Mtb burden in new granulomas, lungs and thoracic lymph nodes of the α -CD4 group did not reach the level of the naïve group, I concluded that it is likely that other factors are contributing to this protection.

In this study, I showed that macaques previously infected with Mtb library A, regardless of drug treatment, had increased numbers of CD4 and CD8 T cells, but not alveolar macrophages, in their airways before antibody infusion and second infection compared to the naïve controls. In addition, macaques previously infected with Mtb library A, regardless of drug treatment, also showed increased number of CD4 T cells producing IFN γ and TNF in response to stimulation with Mtb-specific proteins ESAT-6/CFP-10 compared to the naïve controls. In contrast, there was no significant difference in the number of cytotoxic and cytokine-producing CD8 T cells in the BAL among the groups. This indicates that a primary Mtb infection-induced recruitment and retention of CD4 and CD8 T cells, in the airways might be protective against Mtb reinfection. Future Mtb vaccines should not only aim to recruit CD4 and CD8 T cells but also aim for the retention of these cells in the airways. The recruitment and retention of Mtb-specific IFN γ and TNF-producing CD4 T cells must also be paid close attention, but there are likely to be other functions of T cells not measured in my study that are important in protection.

CD4 T cell depletion did not affect other cell types in the blood and tissues indicating that the increase in Mtb burden in the α -CD4 group is mainly due to CD4 T cell depletion. Macaques in the α -CD4 group had 10-1000-fold decrease in CD4 T cells in the blood compared to pre-infusion levels, however, the degree of depletion did not correlate with the number of new granulomas and CFU. In tissues, an overall 10-fold decrease in CD4 T cells was achieved compared to IgG control. Similarly, the numbers of the remaining CD4 T cells in the lungs did not correlate with the number of new granulomas and CFU in the α -CD4 group. Although, one caveat in these correlation studies is the low sample size. This suggests a heterogeneous response to CD4 T cell depletion in macaques. The number of cytotoxic and cytokine-producing CD8 T cells were not significantly different among the groups in all tissues examined indicating that CD4 T cells are not essential in CD8 T cell function during a second Mtb infection. Interestingly, CD4 T cell depletion resulted in a decrease in levels of IL-23. Consequently, IL-17A level was also decreased in the α -CD4 group. The importance and roles of IL-23 and IL-17A in the lungs in Mtb reinfection needs to be further studied.

There were 1.6x more live barcodes (from scrapates) in the whole animal (includes granuloma, lung, lymph node and extrapulmonary samples) in both the α -CD4 and naïve groups compared to the IgG group. No significant difference was observed in the median number of live barcodes in the granulomas among all groups. Interestingly, there was significantly more live barcodes in the lymph nodes of α -CD4 group compared to the IgG group. Although, not statistically significant, the median number of barcodes present in both granuloma/lung and lymph nodes was 8x more in the α -CD4 group compared to IgG controls. This indicates that CD4 T cell depletion resulted in greater dissemination of Mtb to the lymph nodes. The mechanism in which

CD4 T cells restrict Mtb dissemination to the lymph nodes must be further studied as this is an important aspect of protection from Mtb infection and progression to disease.

The complexity of Mtb infection and the immune response to it is exemplified in this study. I depleted one cell type – CD4 T cells – and showed an increase in Mtb burden in the lungs. However, the bacterial burden in the α -CD4 group did not reach the levels of the naïve group suggesting other factors contributing to the protection against Mtb reinfection. This demonstrates that the protective immune response to Mtb is multifactorial. One limitation of this study is we were not able to completely deplete CD4 T cells in the tissues and the remaining functional CD4 T cells may have also contributed to the modest protection in the α -CD4 group compared to the naïve controls. Flow cytometry and Luminex analyses performed in this study can only interrogate known variables, thus, an unbiased approach is needed. As such, we are also analyzing new granulomas and uninvolved lung lobes using single cell RNA sequencing. In addition, we are collaborating with Dr. Galit Alter in profiling antibodies in the BAL, lung tissues and blood in both the drug treatment and CD4 T cell depletion studies. The importance of CD8 T cells should also be examined, in similar depletion studies. Aside from interrogating the immune response in the context of Mtb reinfection, another avenue of research could be to determine whether a primary Mtb infection protects against a secondary infection from a different strain with varying virulence profiles. This could probe whether strain-specific epitopes are needed in this protection. Additionally, it will determine whether a second infection with a highly virulent Mtb strain will be able to overcome the protection conferred by a primary infection caused by a less virulent strain and vice versa.

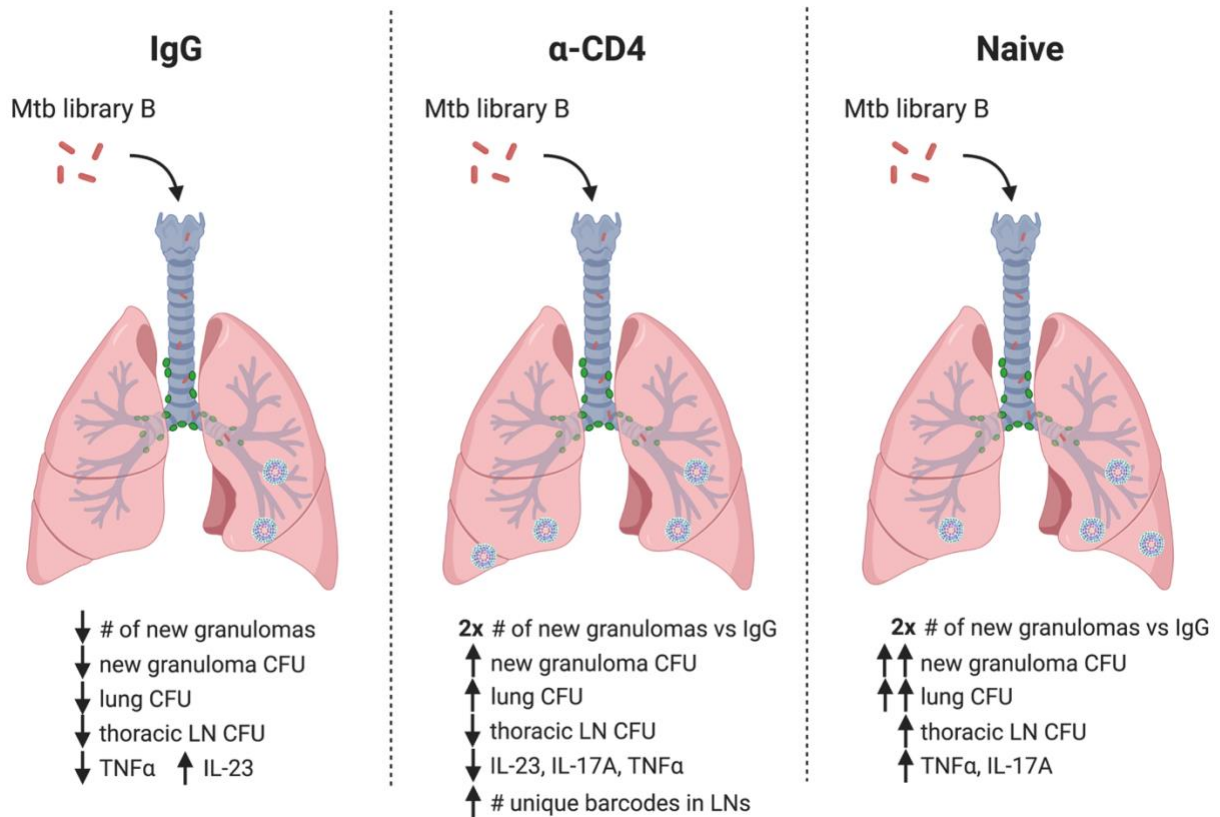


Figure 72. CD4 T cell depletion reduces protection against Mtb reinfection.

CD4 T cell depletion resulted in higher bacterial burden in new granulomas and lungs but not in thoracic lymph nodes. Animals in the α-CD4 group had lower levels of IL-23, IL-17A and TNFα in the lungs. CD4 T cell depletion resulted in greater dissemination of Mtb in the lymph nodes.

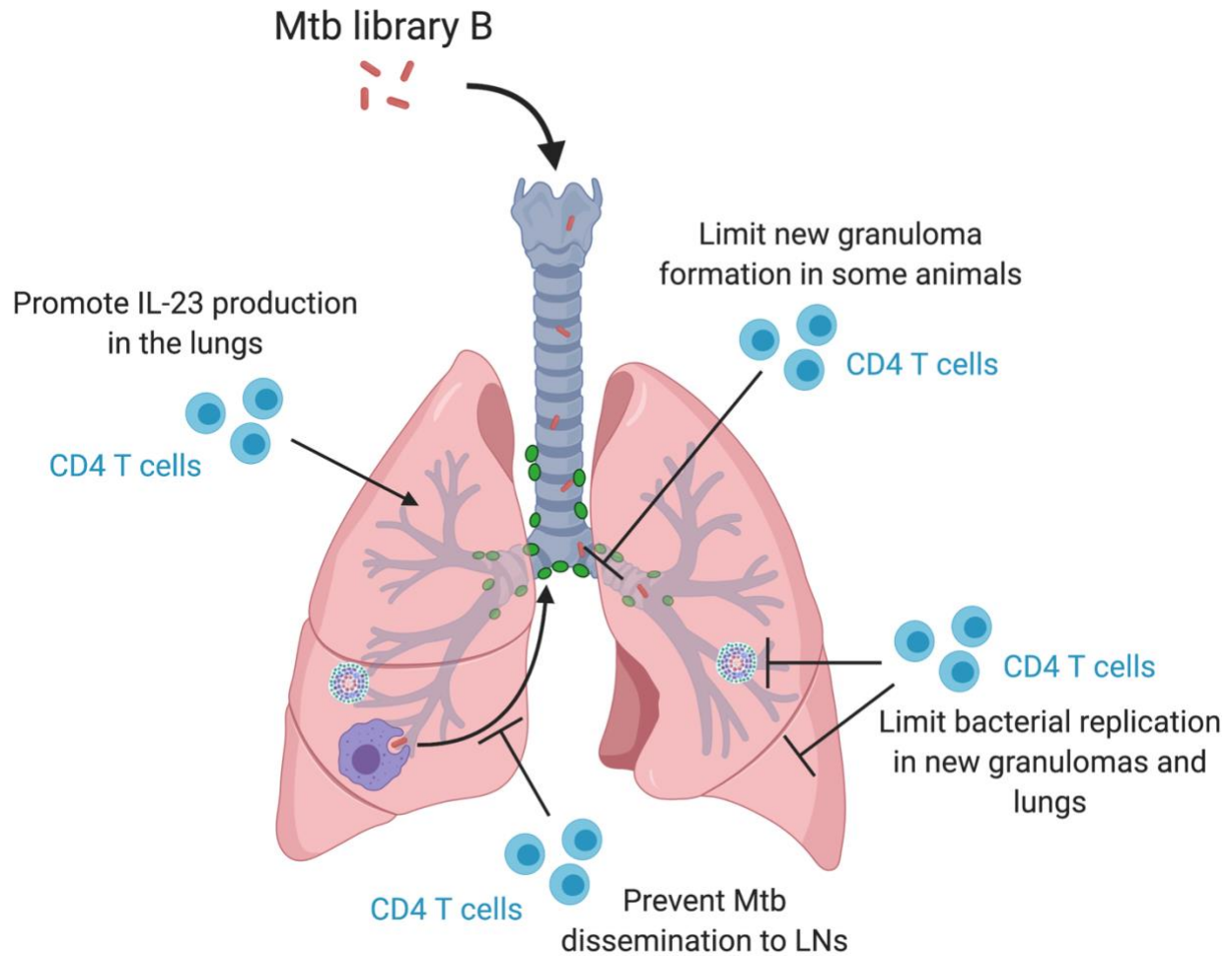


Figure 73. Role of CD4 T cells in Mtb reinfection.

CD4 T cells are important in limiting new granuloma formation in some but not all animals. They also limit bacterial replication in new granulomas and the lungs and prevent dissemination of Mtb to the lymph nodes. IL-23 production is also promoted in the presence of CD4 T cells.

6.2 Lymph nodes are sites of Mtb persistence and growth

Tuberculosis is widely regarded as a lung disease and understandably so, because TB most commonly manifests as a pulmonary disease. However, lymph nodes are the most common site of

extrapulmonary TB [240, 241]. Early autopsies have shown that a granulomatous lesion in the lungs is almost always accompanied by a tuberculous lymph node (Ghon complex) [238, 239] and that lymph nodes can be infected with Mtb without the individual showing any signs of pulmonary disease [242-244]. The goal of one part of my thesis was to probe the dynamics of Mtb infection in the lymph nodes and investigate the role that lymph nodes play in TB. Lymph nodes have been extensively studied as sites of immune activation during an Mtb infection [106, 107] but no one has studied the dynamics of Mtb infection in the lymph nodes themselves. Here, I used two closely-related macaque species (cynomolgus and rhesus) that faithfully recapitulate human TB disease to study Mtb infection in the lymph nodes [231-233]. In addition, macaques have multiple thoracic lymph nodes similar to humans, as opposed to few thoracic lymph nodes present in small animals, making macaques ideal to model Mtb infection in the lymph nodes.

In this study, I showed that 90% of lymph nodes visible by PET CT 1-2 days before necropsy were CFU+. Mtb reached its peak CFU at 4-6 weeks post-infection in cynomolgus macaque lymph nodes which declined as the infection progressed. In contrast, live Mtb burden in rhesus macaque lymph nodes remained unchanged throughout the course of the infection. Estimating total Mtb numbers in lymph nodes by CEQ (Mtb genomes) showed that Mtb reached similar levels in lymph nodes of both macaque species, however cynomolgus macaque lymph nodes were able to kill (CFU/CEQ) Mtb after 4-6 weeks post-infection while there was minimal killing in the lymph nodes of rhesus macaques throughout the examined time points post-infection. This might explain why rhesus macaques develop more severe disease characterized by enlarged lymph nodes impinging on their airways and occasionally resulting in lung lobe collapse and lymph node erosion into the airways [235]. Mtb infection in lymph nodes can result in multiple or coalescing granulomas which disrupt the lymph node's normal architecture and organization

crucial to its function (ie. lymphatic filtration and immune cell trafficking to, from and within the lymph node). I showed that destruction of the lymph node architecture brought about by granulomas was associated with higher bacterial burden. Granulomas in lymph nodes seem to lack adjacent B cell-rich tertiary lymphoid structures found normally in lung granulomas which have been associated with immune control [217, 219]. IL-10-producing macrophages were associated with bacterial clearance while TNF-producing CD4 T cells were associated with bacterial burden. However, it is still not clear why lymph nodes are so poor at killing Mtb, and this needs to be investigated further. Overall, my studies demonstrate that lymph nodes are more than sites of antigen presentation and immune activation—they are critical sites of Mtb persistence and growth.

My work draws much needed attention to the role of lymph nodes in tuberculosis and fills a knowledge gap in the pathogenesis of TB. For years, scientists have focused on Mtb infection in the lungs neglecting the other battlefield where Mtb is silently winning. Lymph nodes can act as Trojan horses secretly cultivating Mtb bacilli, eroding to the airways and thus contributing to transmission or becoming sources of TB reactivation. It is therefore imperative to also examine the efficacy of new vaccines or drug treatments in limiting Mtb dissemination to the lymph nodes or completely sterilizing these organs. A common feature of the robust protection seen in the context of Mtb reinfection and intravenous BCG vaccination is the lack of Mtb dissemination to the lymph nodes. My work supports that preventing infection of lymph nodes is likely to limit the extent of disease overall as well as the chance for reactivation of infection later, and should be included as an important outcome measure for vaccine efficacy. Importantly, I showed that short-course drug treatment was not as successful in killing Mtb in the lymph nodes compared to lung granulomas which could be linked to the lower penetration of drugs in these organs. This has serious ramifications in the development of anti-TB drugs. Careful examination of the lymph

nodes must be performed in testing efficacy of drugs against Mtb. Further investigations as to the reason for the low penetration of drugs in lymph nodes must be considered. Existing knowledge and tools (eg. hydrophobicity, size, nanomaterials) that improve targeting and retention in lymph nodes should be used to design more effective drugs. I also showed that we can identify those lymph nodes that contain live Mtb using PET CT. This will aid in the noninvasive examination of animals or patients when testing vaccines and new anti-TB drugs or regimens. Immune profiling of lymph nodes that were able to sterilize Mtb by bulk/single cell RNA sequencing or by Luminex may prove to be beneficial in characterizing protective immune responses.

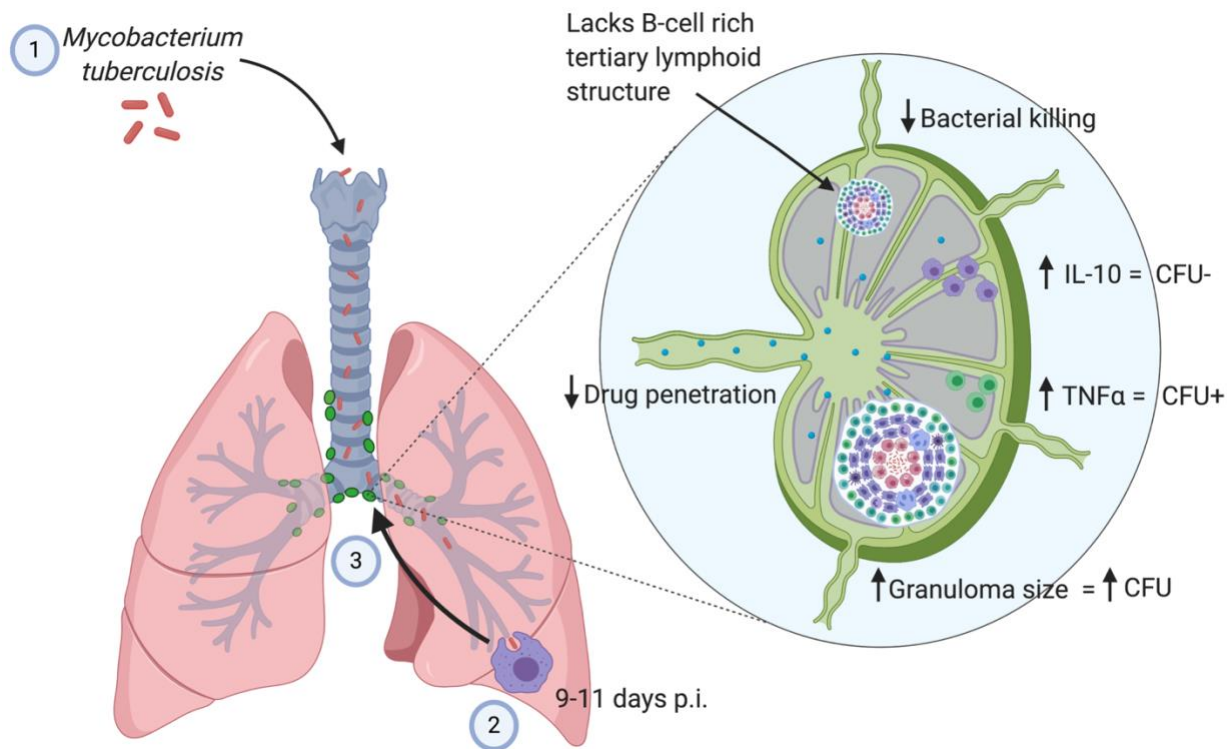


Figure 74. *M. tuberculosis* infection in lymph nodes.

Mtb enters the airways and gets phagocytosed by an alveolar macrophage and transported to the lymph node 9-11 days post-infection. Once Mtb enters the lymph node, it induces the formation of a granuloma that lacks B cell-rich tertiary lymphoid structures and are poor at killing Mtb. The greater the lymph node effacement due to increasing granuloma size, the higher the Mtb burden. Macrophages producing IL-10 are associated with sterilization of lymph nodes while TNF α production of T cells is associated with CFU positivity. Anti-TB drugs have lower penetration in the lymph nodes compared to lung granulomas.

This dissertation elucidated the role of lymph nodes in Mtb infection. It revealed how Mtb uses lymph nodes as niches of growth and persistence making it imperative for vaccine and anti-TB drug development efforts to pay close attention to these organs. Additionally, this dissertation examined 2 unexplored factors that might contribute to the protective immune response to Mtb

reinfection. I showed that bacterial viability is not essential but CD4 T cells are important in the protection a primary Mtb infection confers to a secondary Mtb challenge.

My dissertation provided elements to consider and target when designing and testing vaccines and anti-TB drugs. The world is in dire need of new and more effective TB vaccines. The rise of multidrug and extensively drug resistant Mtb strains also necessitates the development of new anti-TB drugs. This work also gave rise to multiple areas of future research that will advance our knowledge in the crucial factors contributing to the protection against Mtb infection. We are slowly but steadily advancing. I believe the results of my dissertation, along with extensive TB research currently being done around the world, will be able to defeat TB someday. I know we will. Millions of lives depend on it.

7.0 Publication record

Ganchua SKC, Cadena AM, Maiello P, Gideon HP, Myers AJ, Junecko BF, Klein EC, Lin PL, Mattila JT and Flynn JL. 2018. Lymph nodes are sites of prolonged bacterial persistence during *Mycobacterium tuberculosis* infection in macaques. *PLoS Pathogens*. 14(11): e1007337.

Ganchua SKC, White AG, Klein EC and Flynn JL. 2020. Lymph nodes – the neglected battlefield in tuberculosis. *PLoS Pathogens*. 16(8): e1008632.

8.0 Lymph nodes – the neglected battlefield in tuberculosis

This chapter is the full adaptation of the original publication:

Ganchua SKC, White AG, Klein EC and Flynn JL. 2020. Lymph nodes – the neglected battlefield in tuberculosis. *PLoS Pathogens*. In press.

8.1 Introduction

Tuberculosis (TB) is an ancient disease that has plagued humans for thousands of years [349]. It has claimed millions of lives, killing 1.45 million people in 2018 alone, making it the leading cause of death by a single infectious agent. It is caused by bacteria, *Mycobacterium tuberculosis* (Mtb), which are spread in aerosolized droplets expelled from symptomatic individuals, that is those with active TB [2]. Recent estimates suggest approximately 1/4 of the world's human population is currently infected with this microbe without symptomatic and microbiological evidence of disease, which is clinically defined as latent TB [3]. Even though TB most commonly manifests as a pulmonary disease, extrapulmonary TB also occurs. In humans, Mtb infection usually results in a Ghon complex – a tuberculous lung lesion accompanied by a granuloma in a thoracic lymph node [238, 239]. Infected lymph nodes are considered to be extrapulmonary, even if they are within the thoracic cavity, and are the most common sites of extrapulmonary Mtb infection [240, 241]. Lymph nodes are niches for Mtb growth and persistence [350]. Early autopsy studies in humans found live Mtb in lymph nodes without signs of TB disease

anywhere else in the body [242-244]. Even lymph nodes that appeared normal through gross inspection by a trained pathologist could harbor live Mtb [242]. In cattle, lymph nodes are the most common site of *Mycobacterium bovis* infection [245]. In a small study of 15 cattle with evidence of bovine TB in lymph nodes, only 1 had identifiable pulmonary infection [246]. However, some authors as cited by Neill et al [245] believe that a more comprehensive inspection of the bovine lungs should be performed since TB lesions can be small. It is widely accepted that in bovine TB lymph nodes get infected first while pulmonary lesions develop later during the infection [245, 247]. In our experience working with non-human primates, lymph nodes are almost always infected with Mtb along with the lungs [350]. Occasionally, we find lymph nodes with no apparent granuloma also harboring live Mtb bacilli. Given these observations, it is understandable that Behr and Waters proposed TB as a lymphatic disease rather than strictly a pulmonary disease [248].

Reviews of human TB lymphadenitis focusing on epidemiology, clinical manifestations, pathology, diagnosis and treatment have been published [304, 351-354]. Here, we aim to review the pathogenesis of Mtb infection in lymph nodes, drawing on studies from animal models and humans.

8.2 From the air to the lymph nodes

Infection begins when Mtb enters the airways in inhaled droplet nuclei expelled from individuals with active TB disease. Poulsen published two extensive studies in the 1950s detailing the early events in Mtb infection in 517 tuberculin skin test (TST) converters in the Faroe Islands [341, 342]. At the time Poulsen conducted his study, this group of islands just north of the United Kingdom had a population of 30,000 living in isolated villages. A version of TST was done

routinely on all inhabitants and detailed medical histories were recorded. He determined that the incubation period, that is the time from Mtb exposure to the first clinical sign of infection (eg. fever, erythema nodosum (reddish nodules of inflammation on the skin), TST conversion, x-ray showing hilar adenopathy or lung abnormalities), is around 40 days. The first sign of infection was almost always onset of fever [342, 355]. The changes seen in chest radiographs were observed early, often coincident with the initial fever, and these changes consisted mainly of enlarged and dense hilar shadows. The hila is composed of pulmonary arteries and veins, major bronchi and lymph nodes. The common causes of enlarged hila are (1) lymphadenopathy and tumors, (2) arterial or venous hypertension and (3) increase in pulmonary blood flow [356]. Often, these hilar changes remained for 1-2 years before receding. Pulmonary infiltrates were not as common, present only in a little more than 1/3 of children and less than 1/3 in adults [341], although the radiograph technology at the time was unlikely to be sufficient to detect small initial lung lesions. Of the 517 TST converters, 333 (64%) showed hilar lymphadenitis which occurred more in children than in adults (78% of children vs 56% of adults). However, after prolonged observation, only ~10% of the TST converters developed clinically defined active TB, indicating that the early events involving lymph nodes and lungs occur in a large percentage of people following infection, even though only a fraction of these will go on to develop active disease.

The involvement of lymph nodes during the first month of Mtb infection is well established in mouse models of TB. After aerosol infection, Mtb is phagocytosed by alveolar macrophages, myeloid dendritic cells (DC) and neutrophils in the lungs [105]. While other respiratory viral and bacterial pathogens induce DC migration to the lymph nodes to activate the adaptive immune system by 1-3 days post-infection [249-251], this important process is delayed in Mtb infection. Several studies have shown that Mtb-infected DCs do not migrate to the lymph node and prime T

cells until 9-11 days post-infection (Figure 75) [106-108]. This delay in the dissemination of Mtb bacteria to the lymph nodes is thought to play a role in the increased susceptibility of C3H/HeJ mice to Mtb compared to C57BL/6 mice [106]. Wolf and colleagues also showed that the migration of DCs was transient, slowing down after peaking at 21 days post-infection, an interesting observation given the chronic nature of TB. Not only are DC migratory functions dysregulated, but DCs and interstitial macrophages that transport Mtb to the lymph nodes are relatively poor at stimulating T cell responses to Mtb antigens [107].

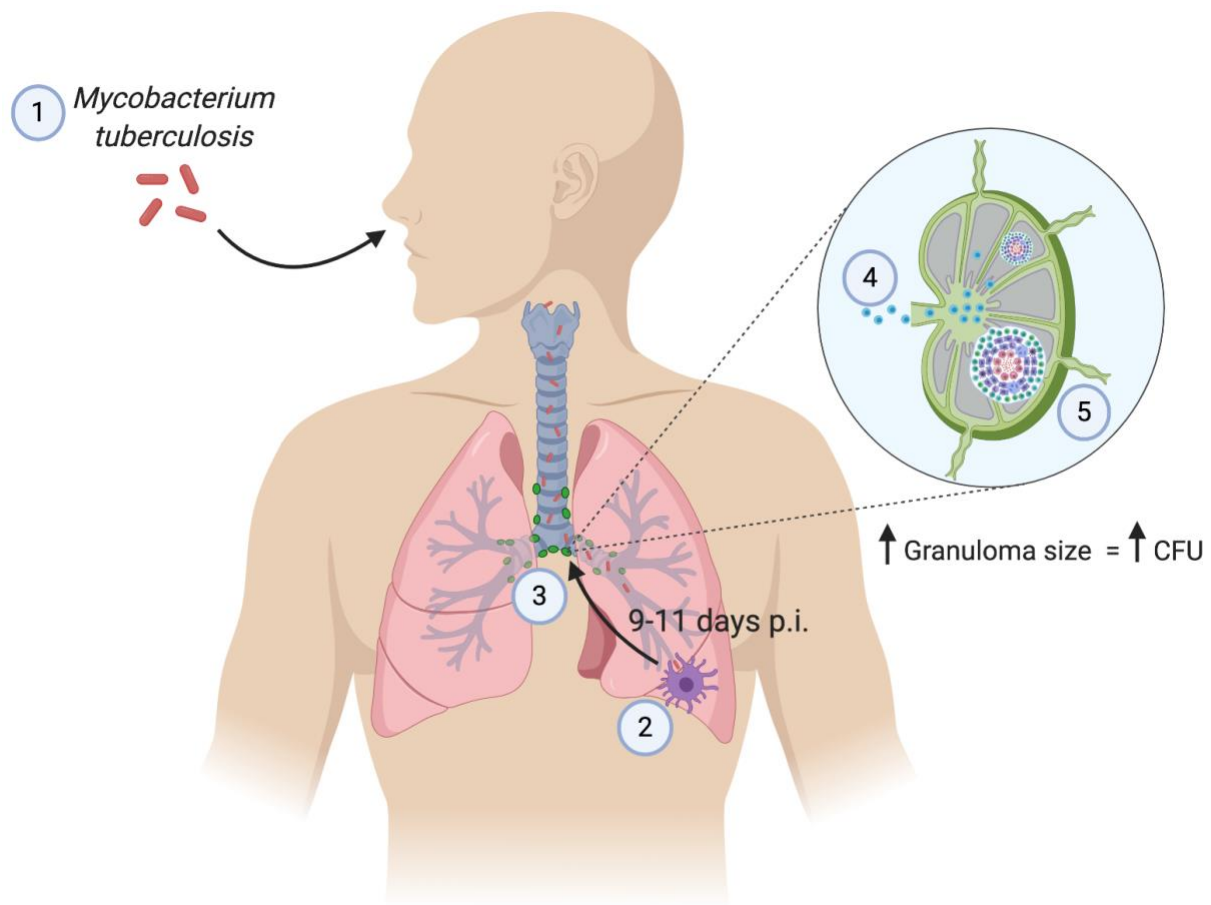


Figure 75. *Mycobacterium tuberculosis* travels to the thoracic lymph nodes from the lungs.

(1) Infection begins when a person inhales aerosolized droplets containing Mtb. (2) Mtb travels into the lungs and is taken up by phagocytic cells. (3) Mtb is then transported to a thoracic lymph node on the same side of the body. Steps 2 and 3 takes 9-11 days in mice. (4) Mtb-containing phagocytic cells present antigen to naïve lymphocytes and generates an immune response. Activated lymphocytes travel back to the lungs to contain Mtb infection. (5) Live Mtb, either shuttled to the lymph nodes by phagocytic cells or carried by lymph fluid, begins to multiply and cause a granuloma to form. Mtb burden increases as the granuloma size increases. Lymph nodes are generally not able to eliminate the infection.

Lymph nodes are a major component of early *Mtb* infection in guinea pigs aerosolly infected with 20 CFU [310, 311, 324]. One of the earliest (5-15 days post-infection) observations in the lungs is inflammation of pulmonary lymphatic vessels [324]. Marked thoracic lymph node enlargement could be seen around 20 days post-infection progressing to severe lymphadenopathy at 30 days post-infection [310, 311]. Lymph node involvement has also been noted in rabbit models [357-359].

Non-human primates (NHP), particularly cynomolgus macaques, are excellent experimental TB models since they present with the full spectrum of human clinical TB (latent to active TB) when challenged with a low dose (≤ 25 CFU) and form granulomas identical to those formed in humans [116, 230-234, 360-362]. Although rhesus macaques are more susceptible and generally develop active TB, their TB pathology also recapitulates that of humans [235, 363, 364]. Macaques also have multiple thoracic lymph nodes that presumably drain different sections of the lungs, just like in humans, as opposed to rodents having only a few lung-draining lymph nodes. NHP provide an excellent model for studying the involvement of thoracic lymph nodes in *Mtb* infection.

By performing serial positron emission tomography coupled with computed tomography (PET CT) scans, we can track *Mtb* infection in the lungs and lymph nodes of NHPs over the course of infection [119, 199, 235, 236, 276, 338, 339]. We used a radiolabeled glucose analog, ^{18}F -fluorodeoxyglucose (FDG), as our PET probe which is taken up and retained by metabolically active cells. FDG avidity is a surrogate marker for inflammation in lung granulomas and lymph nodes [119, 199, 235, 236, 276, 338, 339]. In contrast to lung granulomas, lymph nodes can be difficult to detect by PET CT unless they are enlarged or FDG avid (metabolically active) [119, 235]. In macaques, one or more thoracic lymph nodes start to become FDG avid 2-4 weeks post-

infection, as do the lung granulomas [119, 276, 350]. These FDG avid thoracic lymph nodes could reflect immune cell activation or proliferation in response to priming, as well as an active site of Mtb infection. Combining PET CT data with quantitative bacterial burden assessments in NHP, we reported that when thoracic lymph nodes were “hot” (SUVR or maximum standard uptake ratio normalized to muscle ≥ 5), 96.3% contained culturable Mtb bacilli, however only 50% of “warm” thoracic lymph nodes (SUVR ≥ 2.3 but < 5) had live Mtb. Interestingly, 40 of 240 lymph nodes that were not detectable by PET (SUVR < 2.3) also had culturable Mtb [276, 350]. In a previous study examining the early events of Mtb infection in cynomolgus macaques, granulomas assessed grossly were observed to form first in the thoracic lymph nodes before being detectable in the lungs [231]. Macaques euthanized at 3 weeks post-infection had bilaterally enlarged hilar lymph nodes, however no gross nor microscopic granuloma were seen in the thoracic lymph nodes or lungs of these animals. Macaques euthanized at 4 weeks post-infection had bilaterally enlarged hilar lymph nodes but only 1 of 2 macaques had a small granuloma grossly visible in the enlarged hilar lymph node. At this time point, multiple thoracic lymph nodes showed evidence of infection ranging from early (i.e. aggregates of epithelioid macrophages, sometimes with multinucleated giant cells) to more advanced (i.e. multifocal and coalescing areas of inflammation with central necrosis). One macaque had 1 granuloma in the lungs that was seen microscopically. By 5 to 6 weeks post-infection, macaques exhibited greater pathology in both thoracic lymph nodes and lungs. Caseous granulomas were visible in both lungs and thoracic lymph nodes by gross assessment. T cell responses in thoracic lymph nodes to mycobacterial proteins [culture filtrate protein (CFP)] can be detected by ELISPOT at 3-4 weeks post-infection and this generally preceded responses in the blood and lungs. These observations suggest that pathology may progress from the thoracic lymph nodes to the lungs and this coincides with the adaptive immune

response being activated in the lymph nodes first before trafficking to the lungs [231]. However, it should be noted that this early study was done without the benefit of PET CT imaging, and it is very possible that early small granulomas in lungs were missed during necropsy.

Once Mtb enters the airways and the lungs, only a fraction (9/98, 9.2%) gets transported to one or more thoracic lymph nodes and successfully infects them. By using DNA barcoded Mtb strains that allow discrimination of individual bacteria, Martin and colleagues [120] tracked infection dynamics in lungs and thoracic lymph nodes of cynomolgus macaques. While the majority of lung granulomas were formed by a single bacterium (only 1 barcode was found per granuloma), most lymph nodes were infected with multiple bacteria (≥ 2 barcodes). However, only a fraction (9/98, 9.2%) of the barcodes found in lung granulomas were also identified in culturable bacteria from lymph nodes. This suggests that after replicating in the lungs, either not all of Mtb that seeded granulomas were also able to disseminate to the lymph nodes and successfully replicate there, or they were transported to the lymph nodes but did not establish a productive infection.

8.3 Bacterial dynamics in the lymph nodes

To the authors' knowledge, there is currently limited existing comprehensive analysis of Mtb bacterial dynamics in lymph nodes of small animal models. The reports indicate that Mtb gets shuttled into the lymph nodes mostly by dendritic cells and interstitial macrophages around 9-11 days post-infection [106-108], but since most of these studies were focused on the early events of T cell priming, mice were sacrificed at around day 28 and the fate of Mtb in these lymph nodes during long term infection is unknown. In these T cell priming studies, mice were infected at varying doses (<15 to 555 CFU) and the peak CFU was detected around days 14-21 post-infection

at $\sim 10^5$ - 10^6 numbers [105-108, 308]. The degree and timing of peak CFU was correlated to the magnitude of the inoculation dose. A longer-term study on the effect of BCG on Mtb burden in various tissues found that Mtb inoculated into the ear reaches peak CFU in ear-draining lymph nodes around 28 days post-infection in unvaccinated C57BL/6 mice and remains relatively constant at 10^3 CFU until 120 days post-infection [365]. Another study that followed Mtb infection in resistant (B10.MBR) and susceptible (B10.SM) strains of mice showed a rapid increase of Mtb to $\sim 10^4$ CFU in the thoracic lymph node 3 weeks post-infection which increased to 10^4 - 10^5 CFU by 10 weeks post-infection [366]. In guinea pigs, Mtb can be cultured from lymph nodes in very low numbers (~ 100 CFU) as early as 5 days post-infection, reaching a peak at 20 days post-infection (10^6 CFU) before decreasing and stabilizing by 60 days at 10^5 CFU [312]. These studies suggest that in mice and guinea pigs, once Mtb enters the lymph node, the host is unable to eliminate it, making the lymph node a bacterial reservoir.

Studying Mtb bacterial dynamics in human lymph nodes is extremely difficult since the timing of Mtb infection is usually unknown and thoracic lymph node biopsies are invasive. However, NHP models provide an opportunity to dissect the dynamics of lung and lymph node infections since infection timing and dose are known, and necropsies can be performed at various time points post-infection. The two species of macaques most commonly used to model TB respond differently to Mtb infection. Following low dose infection, about half the cynomolgus macaques develop active TB disease and the other half develop latent Mtb infection (defined as no clinical signs of disease and negative Mtb cultures from bronchoalveolar lavage and gastric aspirate over 6 months) [232]. Rhesus macaques, on the other hand, are more susceptible to Mtb infection, always developing active TB disease when infected with a fully virulent strain of Mtb [235]. One difference between the two species is how their lymph nodes respond to Mtb infection.

Rhesus macaque lymph nodes present with more extensive pathology and greater increases in size such that the lymph nodes can impinge on the airways, sometimes leading to lobe collapse. A recent publication from our group showed that live Mtb burden reaches its peak at 4-6 weeks post-infection in both cynomolgus and rhesus macaques [350]. In cynomolgus macaques, this Mtb burden is reduced 100-fold by 11-14 weeks post-infection and remains constant until 16-29 weeks. In cynomolgus macaques that had latent Mtb infection (34-54 weeks post-infection), one or a few lymph nodes had Mtb bacilli and the bacterial numbers were significantly fewer compared to earlier time points post-infection. In contrast, although rhesus macaque lymph nodes had ~10-fold lower Mtb burden at 4 weeks post-infection compared to cynomolgus macaques, this level of bacteria is maintained until 16-28 weeks post-infection. We determined the chromosomal equivalents (CEQ; Mtb genomes quantified by qPCR) in each lymph node as an approximation of the total number of bacteria (counting both live and dead Mtb) and found equivalent numbers in both macaque species at nearly all time points post-infection. The ratio of live Mtb (CFU) to CEQ can be used to determine the killing capacity of each lymph node [118]. For both macaque species, there was minimal Mtb killing in the lymph nodes at 4-6 weeks post-infection, however cynomolgus macaque lymph nodes were able to kill at least a portion of Mtb at later time points post-infection. The killing capacity of rhesus macaque lymph nodes never improved even at 16-28 weeks post-infection. Thus, Mtb grew to the same level in the lymph nodes of both macaque species, however rhesus macaque lymph nodes were not successful at killing Mtb, contributing to the more severe disease in the lymph nodes of these animals. We also found Mtb DNA in peripheral lymph nodes (axillary and inguinal) which do not drain the lungs. Since most of these lymph nodes were sterile and did not have granulomas apparent by histopathology, it seems that they have a high capacity for killing Mtb. However, trafficking of dead Mtb or Mtb genomes to

these lymph nodes is also possible. In general, lymph nodes are poor killers of Mtb compared to lung granulomas [118, 350].

8.4 Immune response of lymph nodes to Mtb

Once Mtb has reached the lymph nodes and an adaptive immune response is generated, the lymph node needs to contain or kill the growing number of Mtb bacteria inside it. Otherwise, the lymph node can be destroyed by necrosis. The primary mechanism to achieve bacterial killing is likely through the production of cytokines, chemokines, cytolytic and other effector molecules by cells in the lymph nodes [129, 176]. Although our study showed limited to no killing in the majority of thoracic lymph nodes in cynomolgus and rhesus macaques, we still found sterile lymph nodes with granulomas, albeit small in number [16 out of 200 (8%) lymph nodes with granulomas by microscopic histopathology were sterile]. Thus, some lymph nodes are successful in killing Mtb however this is a rare occurrence. Comparing successful and unsuccessful immune response of lymph nodes may provide clues to immune control of TB.

Human studies investigating the immune response in Mtb-infected lymph nodes compared biopsied cervical lymph nodes of patients with TB lymphadenitis (TBLN) with either healthy controls, patients with only pulmonary TB and patients with other lymph node disease (e.g. cancer, non-TB-specific reactive lymphadenitis) [367-370]. All studies obtained transcription profiles but only one study examined protein levels. Moreover, only one study obtained data on bacterial burden in the lymph node samples from the TBLN patients. With these caveats in mind, we can only view these findings as the lymph node's response to Mtb infection without knowing whether that response was successful in killing the bacteria. In general, unstimulated cervical lymph nodes

from patients with TBLN exhibited upregulated transcripts related to viral defense, inflammatory response, TLR- and TNF-signaling and Th1-associated pathways compared to lymph nodes from healthy controls or patients with pulmonary TB only, TB meningitis or lymph node cancer [367, 368]. Downregulation of Th2 pathways was also observed [368]. When stimulated with Mtb-specific antigens, CFU+ lymph nodes had higher IL-10, Th1, Th17, and GM-CSF protein levels compared to CFU- lymph nodes from TBLN patients. No difference in levels of Th2 cytokines (IL-4, IL-5 and IL-13), IL-1 β or IL-18 was observed [369]. In contrast to other studies, Rahman and colleagues [370] showed that lymph nodes from children with TBLN had lower IFN α , TNF and IL-17 expression compared to non-TB-specific reactive lymph nodes and healthy tonsil controls. However, Foxp3, TGF β , and IL-13 mRNA were increased in lymph nodes from TBLN children. No changes in IL-4 or IL-10 were detected. Different experimental measures (mRNA vs. protein), technique (microarray vs. qPCR), samples and controls (TBLN patients vs. variety of samples used as controls) and patients (adults vs. children) could all contribute to variability in findings. The aggregate data support that lymph nodes respond to Mtb infection in a variety of ways but whether these responses promote growth or killing of Mtb is unknown.

We examined Th1 (IFN- γ , TNF, IL-2), Th17 (IL-17) and IL-10 cytokine expression from T cells, B cells and CD11b+ cells in thoracic lymph nodes of 24 cynomolgus macaques in response to Mtb antigen (ESAT-6 and CFP-10) stimulation [350]. Uninfected lymph nodes (no granuloma by gross inspection or histopathology and no live Mtb) had higher proportions of CD3+ T cells than lymph nodes with granulomas. This is likely due to the destruction of lymph node architecture by granulomas. When compared to lymph nodes with live Mtb (CFU+), lymph nodes that were able to clear Mtb (with granulomas but CFU negative) had a significantly higher proportion of CD11b+ cells producing IL-10. On the other hand, CFU positive lymph nodes had a higher

proportion of CD4⁺ T cells producing TNF. A significant negative correlation was found between IL-10-producing CD11b⁺ cells and bacterial burden while a weak but significant positive correlation was found between CD4⁺ T cells producing TNF and bacterial burden. These data suggest that bacterial clearance is associated with CD11b⁺ macrophages producing IL-10 while TNF-producing CD4 T cells is associated with Mtb replication. The presence of IL-10 can be beneficial to lymph nodes as a balance of pro-inflammatory and anti-inflammatory signals and is associated with bacterial clearance in lung granulomas [121]. Neutralizing IL-10 in cynomolgus macaques also resulted in higher Mtb burden in lymph nodes at 4 weeks post-infection [212].

8.5 Mtb remodels lymph node structure

Lymph nodes are organs whose function is tightly linked to their architecture. Different types of cells have predetermined spaces they call “home” (e.g. B cells in follicles, T cells in paracortex, macrophages distributed throughout the cortex, subcapsular sinus and medullary region) (Figure 76A). Antigen presenting cells interact with T and B cells in set locations and this facilitates initiation of the adaptive immune response [314-317, 344]. Mtb infection of lymph nodes result in formation of granulomas, either in separate foci or coalescing, that destroy the lymph node’s architecture (Figure 76B-D). We provided evidence that in lymph nodes where $\geq 50\%$ of the area is occupied by a granuloma or coalescing granulomas Mtb burden is higher compared to lymph nodes with granuloma(s) occupying $< 50\%$. This is true whether we examined live Mtb burden (CFU) or total Mtb burden (live and dead Mtb; CEQ). Minimal killing (CFU/CEQ) was observed irrespective of extent of granuloma involvement. Even a small granuloma composed of clusters of macrophages can push T cells out of their normal spatial

arrangement, impinge on germinal centers, and disrupt the normal vasculature in these organs [350]. Similar disruption of lymph node architecture has been shown in humans with TB lymphadenitis [370]. Granulomas that form in lymph nodes are structurally distinct from granulomas that form in the lungs. We showed that even though lymph node granulomas form in the T cell and B cell regions of the lymph node, they lack B cell-rich tertiary lymphoid structures that form in the periphery of a lung granuloma. Distinct lymphocyte cuff regions found in lung granulomas are also negligible in lymph node granulomas. These observations suggest that the structural and compositional differences between lymph node and lung granulomas could be related to the poor Mtb killing potential of lymph nodes [350].

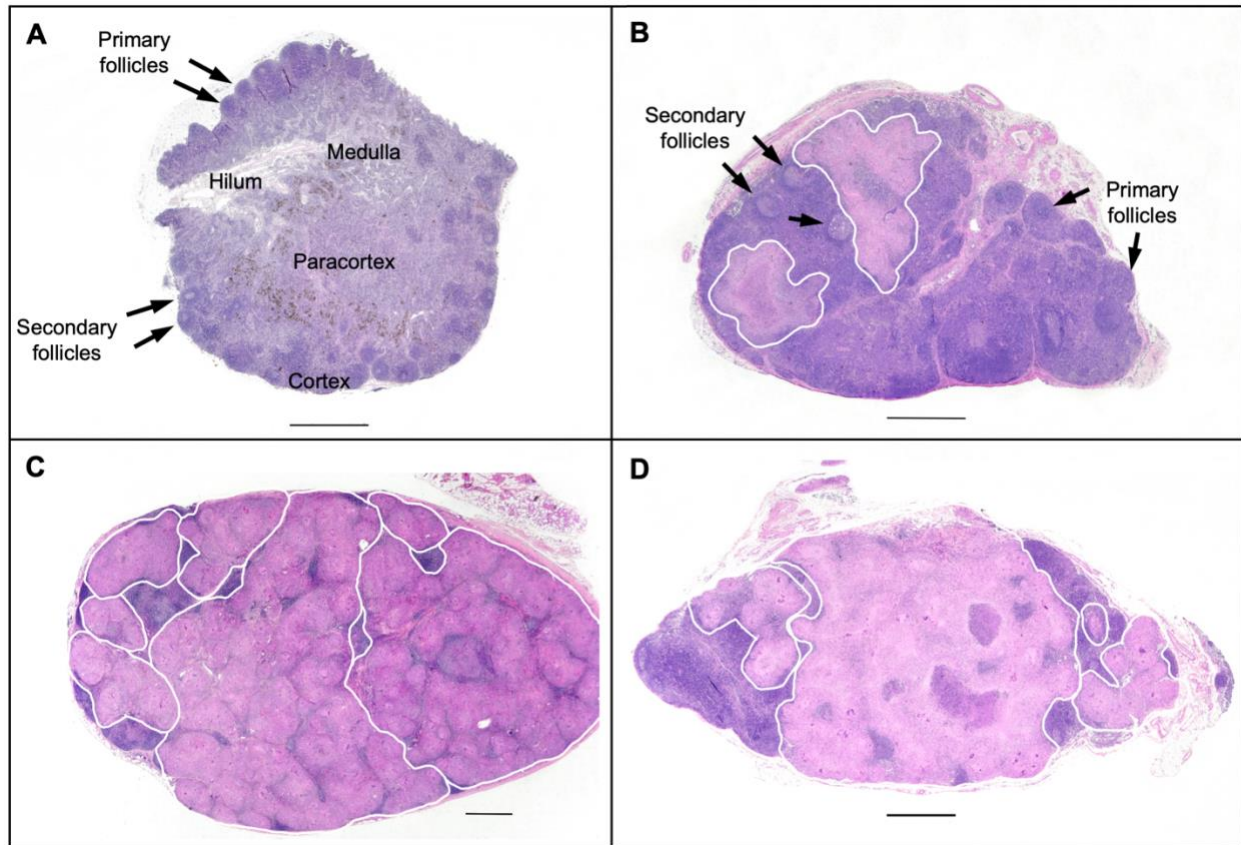


Figure 76. Mtb infection results in granuloma formation that disrupts the normal lymph node architecture.

(A) Lymph node showing normal architecture without granuloma formation. (B) Lymph node with partially effacing granulomas. (C) Total nodal effacement by multiple coalescing non-necrotizing granulomas. (D) Near total nodal effacement by multiple coalescing caseous granulomas. Granulomas are outlined with a white line. Measuring bar = 1 mm.

We compared the cytokine response (Th1, Th17, IL-10) and proliferation (Ki67) of CD4⁺ and CD8⁺ T cells to Mtb-specific antigens in lymph nodes without granulomas, with <50% granuloma involvement and with >50% involvement. There was no difference in any of the cytokines or Ki67 measured among all groups suggesting that the size of the granuloma inside a

lymph node does not affect the overall function of the lymph node T cells [350]. Using immunohistochemistry, lymph nodes of human patients with TB lymphadenitis also displayed extensive remodeling and enrichment of macrophages and DCs, with relatively stable T cell proportions, while the number of B cells were reduced compared to patients with non-TB-specific reactive lymph nodes [370].

8.6 Mtb disseminates ipsilaterally from lungs to lymph nodes

To determine the pattern of Mtb dissemination from lungs to lymph nodes, we examined whether macaques that formed lung granulomas in the right lung lobes had live Mtb in thoracic lymph nodes on the right side (ipsilateral), left side (contralateral), or both sides (bilateral) of the airways. We assessed the presence of granulomas in each lung lobe and bacterial burden in each lymph node obtained during necropsy from 74 cynomolgus macaques 10-55 weeks post-infection. The majority of macaques that formed granulomas on one side of the lungs (~75%) had CFU+ lymph nodes on the same side of the airways (Figure 77). Most macaques that had granulomas on both sides of the lungs also had CFU+ lymph nodes on both sides of the airways (Figure 77). Only a small proportion (~20%) of macaques that had granulomas in only one side of the lungs had bilateral lymph involvement. This suggests that Mtb primarily travels ipsilaterally (same side) from the lungs to the lymph nodes. Variability in draining of the lungs by lymph nodes, airway involvement, and lymph node to lymph node spread could explain the bilateral lymph node involvement in macaques with unilateral lung granulomas.

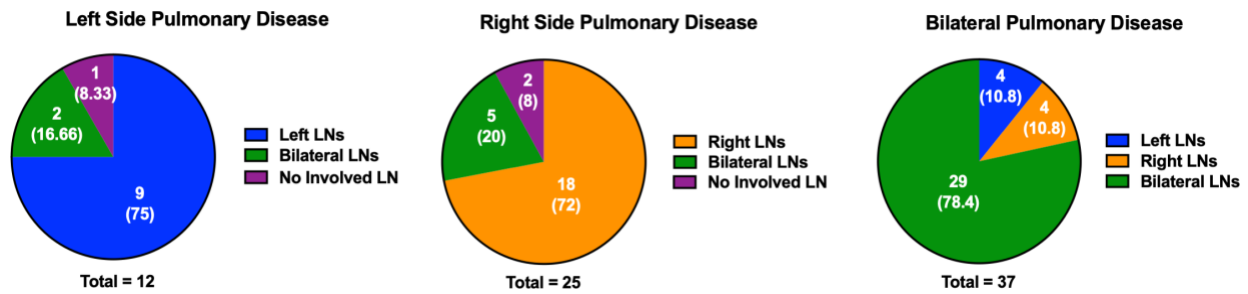


Figure 77. Mtb is spread ipsilaterally from the lungs to the thoracic lymph nodes in macaques.

Cynomolgus macaques infected with low dose Mtb necropsied from 10 to 55 weeks post-infection were assessed for lung disease by gross pathology during necropsy. Lymph node involvement was determined by quantitative culture for Mtb. The pie charts show the lymph node counts. The proportion is in parenthesis. N = 74 monkeys.

These NHP data are consistent with human data from an early study on 283 autopsies of children [238] and is consistent with the anatomy of the lymphatic system draining the lungs. In general, the right lung drains to the lymph nodes on the right side and the left lung drains to the lymph nodes on the left with the exception of the left lower lobe that might cross over to the right via the lower tracheobronchial lymph nodes [371, 372].

8.7 Lymph nodes are sites of TB reactivation

Since true latency and reactivation models are either non-existent or not well studied in small animal models, especially in relation to lymph nodes, we did not include them in this section. Based on human and macaque studies, lymph nodes can play a major role in reactivation of latent

TB caused by immunosuppression. In NHPs, we define reactivation TB as a positive culture in bronchoalveolar lavage and/or gastric aspirate, increase in erythrocyte sedimentation rate, signs of disease such as coughing or weight loss, or the formation of a new granuloma by PET CT after latent Mtb infection was established [182, 183, 198, 199, 252]. In CD4 T cell-depleted cynomolgus macaques, lower CD4+ T cell levels in hilar lymph nodes was associated with reactivation [182]. In TNF-neutralized macaques, early signs of reactivation (ie. non-necrotizing granuloma formation adjacent to established and often mineralized granulomas) were observed microscopically in the lymph nodes [198]. Latently Mtb-infected macaques with a high risk of reactivating after TNF neutralization had a smaller proportion of sterile thoracic lymph nodes, highly metabolically active (by PET CT) lymph nodes and increased live Mtb burden in lymph nodes compared to low risk animals [199]. In a separate study [183], DNA barcoded Mtb bacteria, which allows for the discrimination of individual bacteria, was used to track Mtb dissemination during reactivation of latent TB (latent TB defined in our laboratory as animals with no clinical signs or culturable bronchoalveolar lavage or gastric aspirate and normal erythrocyte sedimentation rate up to 6 months post-Mtb infection [198, 231, 233]) in cynomolgus macaques induced by SIV co-infection. New lung granulomas that arose during reactivation were assessed for DNA barcodes and compared to the DNA barcoded bacilli found in old granulomas (those present prior to SIV infection) or in thoracic lymph nodes. Almost 50% of the DNA barcodes in new granulomas matched DNA barcodes from bacteria only found in lymph nodes and not in the old granulomas. Moreover, Mtb recovered from extrapulmonary sites (eg. liver and spleen) had the same barcodes as Mtb from the lymph nodes. This suggests that Mtb dissemination during reactivation can originate from the lymph nodes dispersing to the lungs and other organs (Figure 78). In antiretroviral-naïve humans with latent TB co-infected with HIV, abnormal FDG uptake in

lymph nodes was associated with reactivation. Ten participants determined to have subclinical TB pathology were more likely to develop abnormal uptake of FDG in thoracic lymph nodes compared to participants without subclinical TB disease. Participants with subclinical TB pathology were also significantly more likely to develop active TB disease (4/10) during the 6-month follow-up period compared the 25 participants with no subclinical pathology of which none developed active TB disease [253]. These data suggest that reactivation of latent TB, whether by SIV/HIV infection, CD4 depletion or TNF neutralization, can start in the lymph nodes and can be predicted by visualizing the metabolic activity of lymph nodes by PET CT.

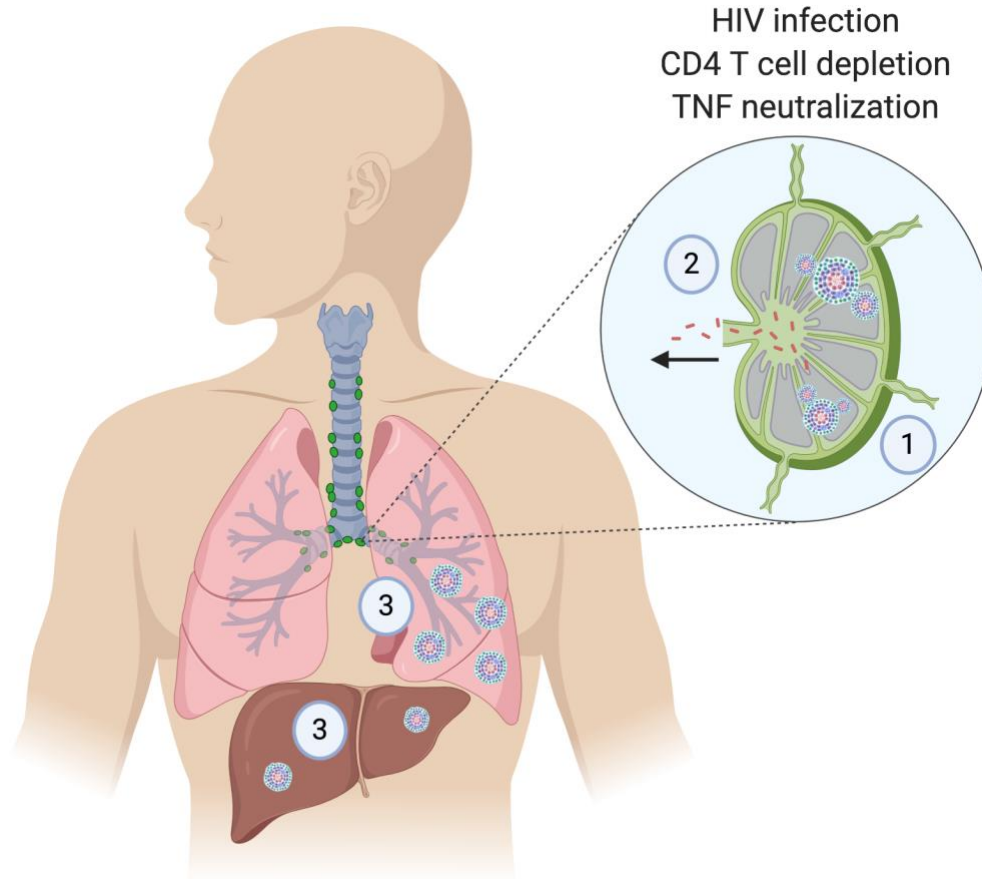


Figure 78. Latent TB reactivation can start in the lymph nodes.

Mtb resides undetected in lymph nodes during latent Mtb infection or as a result of inadequate drug concentration in lymph nodes during treatment. (1) After latent TB reactivation is induced by HIV infection, CD4 depletion or TNF neutralization, non-necrotizing granulomas form adjacent to established and often mineralized granulomas in the lymph nodes. (2) Mtb exits lymph nodes through unknown mechanisms, probably carried by lymph into the subclavian vein and then spreading hematogenously or when the lymph node structure breaks down and delivers bacilli to the airways. (3) Mtb travels to and forms new granulomas in the lungs and other organs (extrapulmonary TB).

8.8 Lymph nodes influence effectiveness of BCG vaccine

Bacillus Calmette-Guerin, or BCG, is a live attenuated *M. bovis* strain and the only licensed vaccine for TB. It is effective at protecting infants and children against the more serious forms of the disease such as miliary disease or TB meningitis, but variable in efficacy in protecting against pulmonary TB in adults [19]. For a vaccine to successfully elicit an immune response, it is required to reach secondary lymphoid organs such as the lymph nodes. A study in C57BL/6 mice compared the efficacy of three BCG vaccination routes [intradermal, subcutaneous (s.c.) and intralymphatic injection] in eliciting a robust immune response and protection from Mtb challenge [254]. Direct injection of BCG to the inguinal lymph nodes resulted in tremendous transient swelling of not just the injected lymph nodes but all the other lymph nodes as well (eg. mesenteric, axillary, brachial, thoracic and cervical nodes). This is in contrast to subcutaneous and intradermal vaccination which caused minimal swelling of any of the lymph nodes examined. Lymph nodes from intralymphatically vaccinated mice harbored greater numbers of BCG by Ziehl-Neelsen staining compared to s.c. vaccinated animals. Intralymphatic vaccination also elicited a more robust immune response compared to s.c. vaccinated animals. Significantly more proliferation and stronger TNF, IL-2, IL-17 and IFN γ responses up to 40 days post-vaccination were observed in PPD-stimulated splenocytes from intralymphatic vaccinated animals compared to s.c. vaccinated animals. Direct vaccination of lymph nodes also resulted in significantly reduced Mtb burden (up to 12 weeks post-infection) against Mtb challenge in the lungs and spleen compared to s.c. and unvaccinated control mice [254]. These data suggest that direct vaccination of lymph nodes could improve the efficacy of BCG in eliciting an immune response and protection against Mtb challenge.

Since lymph nodes are sites of Mtb infection and persistence [350], it is worth considering protection against Mtb infection in lymph nodes in pre-clinical vaccine studies. Two vaccination strategies have shown protection in both lungs and lymph nodes in macaques after Mtb infection. Vaccination with attenuated Mtb [347] and a cytomegalovirus vector encoding Mtb-specific antigens [62] in rhesus macaques have shown that macaques protected against Mtb challenge (e.g. mild disease and significantly lower Mtb burden in lungs) also showed a ~100-fold decrease in culturable Mtb in lung-draining lymph nodes. Complete protection against Mtb infection (i.e. no lung granuloma formation or formation of sterile granulomas) was best achieved in the context of Mtb reinfection in cynomolgus macaques [264] and intravenous BCG vaccination in rhesus macaques [63]. Using DNA barcoded Mtb libraries, cynomolgus macaques were infected with Mtb library A and after 16 weeks, rechallenged with Mtb library B. Macaques initially infected with Mtb library A developed significantly fewer library B lung granulomas, most of them sterile, compared to macaques only infected with Mtb library B (naïve controls). Importantly, Mtb library B only disseminated to the lymph nodes in 1 of 8 Mtb library A-infected macaques and this was only in 1 lymph node. In contrast, 5 out of 6 naïve controls had one or more CFU+ lymph nodes [264]. Intravenous (IV) BCG vaccination protected 6 out of 10 rhesus macaques from forming lung granulomas after Mtb challenge. Three of the remaining IV-BCG vaccinated macaques were protected and formed ≤ 3 granulomas and had significantly lower lung CFU compared to the standard intradermal (ID) vaccination route. Overall, IV-BCG macaques had a 100,000-fold reduction in thoracic bacterial burden compared to the ID BCG group. Similar to the Mtb reinfection study, 9 out of 10 rhesus macaques in the IV-BCG vaccinated group did not grow Mtb in any of their lymph nodes examined. Based on these studies, a successful vaccine should induce rapid killing of Mtb when it enters the lungs and prevent Mtb from reaching the lymph nodes.

When macaques were analyzed only four weeks after BCG vaccination (without Mtb challenge), only IV-BCG vaccinated animals had BCG in bronchoalveolar lavage (BAL), spleen, lung lobes, peripheral and thoracic lymph nodes, while ID vaccinated animals only harbored BCG in skin and draining axillary lymph nodes. Aerosol vaccinated animals had BCG in lung lobes and BAL. At 2-4 weeks post-IV BCG vaccination, increased inflammation (FDG avidity) in lung-draining lymph nodes, lung lobes and spleen was observed by PET CT; this was not seen in the other routes. IV-BCG vaccinated animals also had transient enlargement of the spleen and enlarged lymph nodes that contained non-necrotizing granulomas and increased proliferation in the B cell region, often with active germinal centers [63]. It seems that BCG infiltration and metabolic activity (probably activation of immune response) in thoracic lymph nodes and spleen sets IV-BCG vaccinated macaques apart from other vaccination routes and may be important contributors to the astounding protection that IV-BCG vaccination conferred against Mtb challenge. In both mice and NHP studies, BCG colonization of lung-draining lymph nodes is correlated with protection against Mtb challenge [63, 254]. In addition, prevention of Mtb infection in lymph nodes and not just the lungs should also be targeted when designing a vaccine. The role of lymph nodes in vaccine efficacy is worthy of additional study.

8.9 Lower drug penetration in lymph nodes

Lymph nodes are sites where Mtb can persist, disseminate and reactivate [182, 183, 198, 199, 253]. Therefore, it is imperative that anti-TB drugs be tested for their ability to eliminate Mtb bacteria in the lymph nodes. Short-course drug treatment studies in cynomolgus macaques show that reduction in Mtb burden in lymph nodes is significantly impaired compared to lung

granulomas (55-fold reduction in lymph nodes vs 181-fold reduction in lung granulomas [350]) in drug-treated versus untreated controls. Thus, anti-TB drugs are more effective in killing Mtb in lung granulomas compared to lymph nodes [268, 350]. There is only one study that the authors are aware of that examined concentrations of rifampicin (RIF) and isoniazid (INH), both first-line anti-TB drugs, in the blood, lungs, granulomas and lymph nodes in humans [255, 256]. Rifampicin had the highest concentration in the blood (6.95 $\mu\text{g/ml}$) followed by tuberculous foci (2.43 $\mu\text{g/g}$) and healthy lung tissue (2.22 $\mu\text{g/g}$). Thoracic lymph nodes (1.41 $\mu\text{g/g}$) had lower RIF concentration compared to blood and lung granulomas. Interestingly, the lowest RIF concentration was found in caseous lymph nodes (0.03 $\mu\text{g/g}$). In contrast, although INH concentration was also highest in the blood (4.11 $\mu\text{g/ml}$), its concentration in healthy lungs (0.58 $\mu\text{g/g}$), bronchopulmonary lymph nodes (0.53 $\mu\text{g/g}$), cavities (0.59 $\mu\text{g/g}$), tuberculous foci (0.6 $\mu\text{g/g}$) and caseous lymph nodes (0.21 $\mu\text{g/g}$) were all relatively similar [255, 256]. Remarkably, caseous lymph nodes had once again the lowest INH concentration. No information about Mtb burden in the different tissues were provided. Although this is just one study, it provides a glimpse of lower RIF and INH penetration in lymph nodes compared to lung granulomas. This lower drug penetration in lymph nodes could explain the reduced efficacy of anti-TB drugs in killing Mtb in the lymph node compartment.

HIV also uses lymph nodes as latent reservoirs. Similar to the findings above, studies of drug penetration in lymph nodes in HIV patients show that concentrations of antiretroviral drugs in lymph nodes are significantly lower compared to the blood [373-375]. By sequencing HIV DNA and RNA from blood and inguinal lymph nodes of HIV-infected patients at different time intervals post-anti-retroviral treatment), Lorenzo-Redondo and colleagues discovered that despite undetectable levels of viral RNA in plasma during treatment, low-level viral replication still occurs in lymph nodes and this phenomenon was attributed to low antiretroviral drug penetration in these

organs [373, 374]. Similar findings were reported in a study of 12 HIV-infected patients after antiretroviral drug initiation. Fletcher and colleagues showed that the antiretroviral drug concentrations in lymph nodes were significantly lower compared to the blood and this correlated with continuous HIV replication [375]. Thus, lower drug penetration in lymph nodes is not unique to tuberculosis.

8.10 Concluding Remarks

Lymph nodes are underappreciated in the study of TB. It is clear that aside from their main function of initiating and shaping adaptive immune responses, lymph nodes also serve as niches for Mtb growth and persistence. Although lymph nodes mount an immune response to Mtb infection, data support that they are poor killers of Mtb [350]. In addition, latent TB reactivation can originate from lymph nodes [182, 183, 198, 199, 253]. As such, eliminating Mtb in these organs requires closer attention. Current anti-TB drug regimens are less efficient in reducing Mtb burden in the lymph nodes compared to lung granulomas, which may be attributed to poor penetration of drugs in the involved lymph nodes. Vaccine and anti-TB drug trials should examine efficacy of preventing Mtb infection or eliminating Mtb in lymph nodes and not just the lungs. Tools (e.g. nanomaterials) and efficient antigen or drug design can also be used to target anti-TB drugs and vaccines to the lymph nodes. Further studies in improving vaccine and drug delivery to the lymph nodes is warranted.

8.11 Methodology

8.11.1 Mtb dissemination from lungs to lymph nodes analysis

Cynomolgus macaques (*Macaca fascicularis*) (n=74) that served as controls (no vaccine or drug treatment) for other studies from 2011 to 2018 were selected for this study. These macaques were infected with 2-92 CFU (median = 8 CFU) of *M. tuberculosis* Erdman using a bronchoscope. Existing records were reviewed for the location of granulomas in the lungs and CFU positivity of lymph nodes in the same animal. Data were graphed using GraphPad Prism v8 (GraphPad Software, San Diego, CA). All procedures and protocols were approved by the University of Pittsburgh's Institutional Animal Care and Use Committee.

8.11.2 Histology

Histological examination was performed by an experienced veterinary pathologist (E. Klein) as previously described [231]. Lymph nodes obtained during necropsy were cut (4-6mm) and stained with hematoxylin and eosin. Characteristics of granulomas, such as, size, type (caseous, non-necrotizing, suppurative, or mixed), distribution pattern (focal, multifocal, coalescing, focally extensive and locally invasive), and cellular composition were noted.

8.11.3 Ethics Statement

All experimental manipulations, protocols, and care of the animals were approved by the University of Pittsburgh School of Medicine Institutional Animal Care and Use Committee

(IACUC). The protocol assurance number for our IACUC is A3187-01. Our specific protocol approval numbers for this project are: 1105870, 11090030, 11110045, 12060181, 12080653, 12090832, 13122856, 14023305, 14043492, 15055811, 15066174, 15126588, 16017370, 17029987, 17060529. The IACUC adheres to national guidelines established in the Animal Welfare Act (7 U.S.C. Sections 2131–2159) and the Guide for the Care and Use of Laboratory Animals (8th Edition) as mandated by the U.S. Public Health Service Policy.

All macaques used in this study were housed at the University of Pittsburgh in rooms with autonomously controlled temperature, humidity, and lighting. Animals were singly housed in caging at least 2 square meters apart that allowed visual and tactile contact with neighboring conspecifics. The macaques were fed twice daily with biscuits formulated for nonhuman primates, supplemented at least 4 days/week with large pieces of fresh fruits or vegetables. Animals had access to water *ad libitem*. Because our macaques were singly housed due to the infectious nature of these studies, an enhanced enrichment plan was designed and overseen by our nonhuman primate enrichment specialist. This plan has 3 components. First, species-specific behaviors are encouraged. All animals have access to toys and other manipulata, some of which will be filled with food treats (e.g. frozen fruit, peanut butter, etc.). These are rotated on a regular basis. Puzzle feeders foraging boards, and cardboard tubes containing small food items also are placed in the cage to stimulate foraging behaviors. Adjustable mirrors accessible to the animals stimulate interaction between animals. Second, routine interaction between humans and macaques are encouraged. These interactions occur daily and consist mainly of small food objects offered as enrichment and adhere to established safety protocols. Animal caretakers are encouraged to interact with the animals (by talking or with facial expressions) while performing tasks in the housing area. Routine procedures (e.g. feeding, cage cleaning, etc) are done on a strict schedule to

allow the animals to acclimate to a routine daily schedule. Third, all macaques are provided with a variety of visual and auditory stimulation. Housing areas contain either radios or TV/video equipment that play cartoons or other formats designed for children for at least 3 hours each day. The videos and radios are rotated between animal rooms so that the same enrichment is not played repetitively for the same group of animals.

All animals are checked at least twice daily to assess appetite, attitude, activity level, hydration status, etc. Following *M. tuberculosis* infection, the animals are monitored closely for evidence of disease (e.g., anorexia, weight loss, tachypnea, dyspnea, coughing). Physical exams, including weights, are performed on a regular basis. Animals are sedated prior to all veterinary procedures (e.g. blood draws, etc.) using ketamine or other approved drugs. Regular PET CT imaging is conducted on most of our macaques following infection and has proved very useful for monitoring disease progression. Our veterinary technicians monitor animals especially closely for any signs of pain or distress. If any are noted, appropriate supportive care (e.g. dietary supplementation, rehydration) and clinical treatments (analgesics) are given. Any animal considered to have advanced disease or intractable pain or distress from any cause is sedated with ketamine and then humanely euthanatized using sodium pentobarbital.

8.12 Acknowledgements

We thank the members of the Flynn and Lin laboratories, as well as Dr. Charles Scanga, for helpful discussions. In particular, we thank our veterinary and research technical staff for their expertise and commitment to these studies.

Bibliography

1. Pai M, Behr MA, Dowdy D, Dheda K, Divangahi M, Boehme CC, et al. Tuberculosis. *Nat Rev Dis Primers*. 2016;2:16076. Epub 2016/10/28. doi: 10.1038/nrdp.2016.76. PubMed PMID: 27784885.
2. WHO. Global tuberculosis report 2019. Geneva2019. Available from: https://www.who.int/tb/publications/global_report/en/.
3. Houben RM, Dodd PJ. The Global Burden of Latent Tuberculosis Infection: A Re-estimation Using Mathematical Modelling. *PLoS Med*. 2016;13(10):e1002152. Epub 2016/10/26. doi: 10.1371/journal.pmed.1002152. PubMed PMID: 27780211; PubMed Central PMCID: PMC5079585.
4. Banuls AL, Sanou A, Van Anh NT, Godreuil S. Mycobacterium tuberculosis: ecology and evolution of a human bacterium. *J Med Microbiol*. 2015;64(11):1261-9. Epub 2015/09/20. doi: 10.1099/jmm.0.000171. PubMed PMID: 26385049.
5. Brosch R, Gordon SV, Pym A, Eiglmeier K, Garnier T, Cole ST. Comparative genomics of the mycobacteria. *Int J Med Microbiol*. 2000;290(2):143-52. Epub 2000/10/25. doi: 10.1016/S1438-4221(00)80083-1. PubMed PMID: 11045919.
6. Sreevatsan S, Pan X, Stockbauer KE, Connell ND, Kreiswirth BN, Whittam TS, et al. Restricted structural gene polymorphism in the Mycobacterium tuberculosis complex indicates evolutionarily recent global dissemination. *Proc Natl Acad Sci U S A*. 1997;94(18):9869-74. Epub 1997/09/02. doi: 10.1073/pnas.94.18.9869. PubMed PMID: 9275218; PubMed Central PMCID: PMC23284.
7. Cole ST, Brosch R, Parkhill J, Garnier T, Churcher C, Harris D, et al. Deciphering the biology of Mycobacterium tuberculosis from the complete genome sequence. *Nature*. 1998;393(6685):537-44. Epub 1998/06/20. doi: 10.1038/31159. PubMed PMID: 9634230.
8. Gordon SV, Parish T. Microbe Profile: Mycobacterium tuberculosis: Humanity's deadly microbial foe. *Microbiology*. 2018;164(4):437-9. Epub 2018/02/22. doi: 10.1099/mic.0.000601. PubMed PMID: 29465344.
9. Gagneux S. Ecology and evolution of Mycobacterium tuberculosis. *Nat Rev Microbiol*. 2018;16(4):202-13. Epub 2018/02/20. doi: 10.1038/nrmicro.2018.8. PubMed PMID: 29456241.
10. Gagneux S, Small PM. Global phylogeography of Mycobacterium tuberculosis and implications for tuberculosis product development. *Lancet Infect Dis*. 2007;7(5):328-37. Epub 2007/04/24. doi: 10.1016/S1473-3099(07)70108-1. PubMed PMID: 17448936.

11. Jackson M. The mycobacterial cell envelope-lipids. *Cold Spring Harb Perspect Med*. 2014;4(10). Epub 2014/08/12. doi: 10.1101/cshperspect.a021105. PubMed PMID: 25104772; PubMed Central PMCID: PMC4200213.
12. Brennan PJ, Besra GS. Structure, function and biogenesis of the mycobacterial cell wall. *Biochem Soc Trans*. 1997;25(1):188-94. Epub 1997/02/01. doi: 10.1042/bst0250188. PubMed PMID: 9056869.
13. Minnikin DE. Chemical principles in the organization of lipid components in the mycobacterial cell envelope. *Res Microbiol*. 1991;142(4):423-7. Epub 1991/05/01. doi: 10.1016/0923-2508(91)90114-p. PubMed PMID: 1871427.
14. Ortalo-Magne A, Lemassu A, Laneelle MA, Bardou F, Silve G, Gounon P, et al. Identification of the surface-exposed lipids on the cell envelopes of *Mycobacterium tuberculosis* and other mycobacterial species. *J Bacteriol*. 1996;178(2):456-61. Epub 1996/01/01. doi: 10.1128/jb.178.2.456-461.1996. PubMed PMID: 8550466; PubMed Central PMCID: PMC177678.
15. Smith T, Wolff KA, Nguyen L. Molecular biology of drug resistance in *Mycobacterium tuberculosis*. *Curr Top Microbiol Immunol*. 2013;374:53-80. Epub 2012/11/28. doi: 10.1007/82_2012_279. PubMed PMID: 23179675; PubMed Central PMCID: PMC3982203.
16. Vasanthakumari R, Jagannath K, Rajasekaran S. A cold staining method for acid-fast bacilli. *Bull World Health Organ*. 1986;64(5):741-3. Epub 1986/01/01. PubMed PMID: 2433067; PubMed Central PMCID: PMC2490969.
17. Chen P, Shi M, Feng GD, Liu JY, Wang BJ, Shi XD, et al. A highly efficient Ziehl-Neelsen stain: identifying de novo intracellular *Mycobacterium tuberculosis* and improving detection of extracellular *M. tuberculosis* in cerebrospinal fluid. *J Clin Microbiol*. 2012;50(4):1166-70. Epub 2012/01/13. doi: 10.1128/JCM.05756-11. PubMed PMID: 22238448; PubMed Central PMCID: PMC3318527.
18. Liu J, Tran V, Leung AS, Alexander DC, Zhu B. BCG vaccines: their mechanisms of attenuation and impact on safety and protective efficacy. *Hum Vaccin*. 2009;5(2):70-8. Epub 2009/01/24. doi: 10.4161/hv.5.2.7210. PubMed PMID: 19164935.
19. Mangtani P, Abubakar I, Ariti C, Beynon R, Pimpin L, Fine PE, et al. Protection by BCG vaccine against tuberculosis: a systematic review of randomized controlled trials. *Clin Infect Dis*. 2014;58(4):470-80. Epub 2013/12/18. doi: 10.1093/cid/cit790. PubMed PMID: 24336911.
20. Behr MA, Wilson MA, Gill WP, Salamon H, Schoolnik GK, Rane S, et al. Comparative genomics of BCG vaccines by whole-genome DNA microarray. *Science*. 1999;284(5419):1520-3. Epub 1999/05/29. doi: 10.1126/science.284.5419.1520. PubMed PMID: 10348738.

21. Hsu T, Hingley-Wilson SM, Chen B, Chen M, Dai AZ, Morin PM, et al. The primary mechanism of attenuation of bacillus Calmette-Guerin is a loss of secreted lytic function required for invasion of lung interstitial tissue. *Proc Natl Acad Sci U S A*. 2003;100(21):12420-5. Epub 2003/10/15. doi: 10.1073/pnas.1635213100. PubMed PMID: 14557547; PubMed Central PMCID: PMCPMC218773.
22. Lewis KN, Liao R, Guinn KM, Hickey MJ, Smith S, Behr MA, et al. Deletion of RD1 from *Mycobacterium tuberculosis* mimics bacille Calmette-Guerin attenuation. *J Infect Dis*. 2003;187(1):117-23. Epub 2003/01/01. doi: 10.1086/345862. PubMed PMID: 12508154; PubMed Central PMCID: PMCPMC1458498.
23. Guinn KM, Hickey MJ, Mathur SK, Zakel KL, Grotzke JE, Lewinsohn DM, et al. Individual RD1-region genes are required for export of ESAT-6/CFP-10 and for virulence of *Mycobacterium tuberculosis*. *Mol Microbiol*. 2004;51(2):359-70. Epub 2004/02/06. doi: 10.1046/j.1365-2958.2003.03844.x. PubMed PMID: 14756778; PubMed Central PMCID: PMCPMC1458497.
24. Berthet FX, Rasmussen PB, Rosenkrands I, Andersen P, Gicquel B. A *Mycobacterium tuberculosis* operon encoding ESAT-6 and a novel low-molecular-mass culture filtrate protein (CFP-10). *Microbiology*. 1998;144 (Pt 11):3195-203. Epub 1998/12/10. doi: 10.1099/00221287-144-11-3195. PubMed PMID: 9846755.
25. Conrad WH, Osman MM, Shanahan JK, Chu F, Takaki KK, Cameron J, et al. Mycobacterial ESX-1 secretion system mediates host cell lysis through bacterium contact-dependent gross membrane disruptions. *Proc Natl Acad Sci U S A*. 2017;114(6):1371-6. Epub 2017/01/26. doi: 10.1073/pnas.1620133114. PubMed PMID: 28119503; PubMed Central PMCID: PMCPMC5307465.
26. Simeone R, Bobard A, Lippmann J, Bitter W, Majlessi L, Brosch R, et al. Phagosomal rupture by *Mycobacterium tuberculosis* results in toxicity and host cell death. *PLoS Pathog*. 2012;8(2):e1002507. Epub 2012/02/10. doi: 10.1371/journal.ppat.1002507. PubMed PMID: 22319448; PubMed Central PMCID: PMCPMC3271072.
27. van der Wel N, Hava D, Houben D, Fluitsma D, van Zon M, Pierson J, et al. *M. tuberculosis* and *M. leprae* translocate from the phagolysosome to the cytosol in myeloid cells. *Cell*. 2007;129(7):1287-98. Epub 2007/07/03. doi: 10.1016/j.cell.2007.05.059. PubMed PMID: 17604718.
28. Houben D, Demangel C, van Ingen J, Perez J, Baldeon L, Abdallah AM, et al. ESX-1-mediated translocation to the cytosol controls virulence of mycobacteria. *Cell Microbiol*. 2012;14(8):1287-98. Epub 2012/04/25. doi: 10.1111/j.1462-5822.2012.01799.x. PubMed PMID: 22524898.
29. Tan T, Lee WL, Alexander DC, Grinstein S, Liu J. The ESAT-6/CFP-10 secretion system of *Mycobacterium marinum* modulates phagosome maturation. *Cell Microbiol*. 2006;8(9):1417-29. Epub 2006/08/23. doi: 10.1111/j.1462-5822.2006.00721.x. PubMed PMID: 16922861.

30. Pathak SK, Basu S, Basu KK, Banerjee A, Pathak S, Bhattacharyya A, et al. Direct extracellular interaction between the early secreted antigen ESAT-6 of *Mycobacterium tuberculosis* and TLR2 inhibits TLR signaling in macrophages. *Nat Immunol.* 2007;8(6):610-8. Epub 2007/05/09. doi: 10.1038/ni1468. PubMed PMID: 17486091.
31. Welin A, Eklund D, Stendahl O, Lerm M. Human macrophages infected with a high burden of ESAT-6-expressing *M. tuberculosis* undergo caspase-1- and cathepsin B-independent necrosis. *PLoS One.* 2011;6(5):e20302. Epub 2011/06/04. doi: 10.1371/journal.pone.0020302. PubMed PMID: 21637850; PubMed Central PMCID: PMC3102687.
32. Gao LY, Guo S, McLaughlin B, Morisaki H, Engel JN, Brown EJ. A mycobacterial virulence gene cluster extending RD1 is required for cytolysis, bacterial spreading and ESAT-6 secretion. *Mol Microbiol.* 2004;53(6):1677-93. Epub 2004/09/03. doi: 10.1111/j.1365-2958.2004.04261.x. PubMed PMID: 15341647.
33. Samten B, Wang X, Barnes PF. *Mycobacterium tuberculosis* ESX-1 system-secreted protein ESAT-6 but not CFP10 inhibits human T-cell immune responses. *Tuberculosis (Edinb).* 2009;89 Suppl 1:S74-6. Epub 2009/12/17. doi: 10.1016/S1472-9792(09)70017-4. PubMed PMID: 20006311.
34. Shiloh MU. Mechanisms of mycobacterial transmission: how does *Mycobacterium tuberculosis* enter and escape from the human host. *Future Microbiol.* 2016;11:1503-6. Epub 2016/11/11. doi: 10.2217/fmb-2016-0185. PubMed PMID: 27831741; PubMed Central PMCID: PMC3491170.
35. Yang H, Kruh-Garcia NA, Dobos KM. Purified protein derivatives of tuberculin--past, present, and future. *FEMS Immunol Med Microbiol.* 2012;66(3):273-80. Epub 2012/07/06. doi: 10.1111/j.1574-695X.2012.01002.x. PubMed PMID: 22762692; PubMed Central PMCID: PMC3491170.
36. Huebner RE, Schein MF, Bass JB, Jr. The tuberculin skin test. *Clin Infect Dis.* 1993;17(6):968-75. Epub 1993/12/01. doi: 10.1093/clinids/17.6.968. PubMed PMID: 8110954.
37. Farhat M, Greenaway C, Pai M, Menzies D. False-positive tuberculin skin tests: what is the absolute effect of BCG and non-tuberculous mycobacteria? *Int J Tuberc Lung Dis.* 2006;10(11):1192-204. Epub 2006/11/30. PubMed PMID: 17131776.
38. Wang L, Turner MO, Elwood RK, Schulzer M, FitzGerald JM. A meta-analysis of the effect of Bacille Calmette Guerin vaccination on tuberculin skin test measurements. *Thorax.* 2002;57(9):804-9. Epub 2002/08/30. doi: 10.1136/thorax.57.9.804. PubMed PMID: 12200526; PubMed Central PMCID: PMC1746436.
39. van Ingen J, de Zwaan R, Dekhuijzen R, Boeree M, van Soolingen D. Region of difference 1 in nontuberculous *Mycobacterium* species adds a phylogenetic and taxonomical character. *J Bacteriol.* 2009;191(18):5865-7. Epub 2009/07/21. doi: 10.1128/JB.00683-09. PubMed PMID: 19617365; PubMed Central PMCID: PMC2737943.

40. Pai M, Denkinger CM, Kik SV, Rangaka MX, Zwerling A, Oxlade O, et al. Gamma interferon release assays for detection of Mycobacterium tuberculosis infection. *Clin Microbiol Rev.* 2014;27(1):3-20. Epub 2014/01/08. doi: 10.1128/CMR.00034-13. PubMed PMID: 24396134; PubMed Central PMCID: PMC3910908.
41. Al-Orainey IO. Diagnosis of latent tuberculosis: Can we do better? *Ann Thorac Med.* 2009;4(1):5-9. Epub 2009/06/30. doi: 10.4103/1817-1737.44778. PubMed PMID: 19561914; PubMed Central PMCID: PMC3910908.
42. Furin J, Cox H, Pai M. Tuberculosis. *Lancet.* 2019;393(10181):1642-56. Epub 2019/03/25. doi: 10.1016/S0140-6736(19)30308-3. PubMed PMID: 30904262.
43. WHO. Latent TB Infection: Updated and consolidated guidelines for programmatic management. Geneva2018. Available from: <https://www.who.int/tb/publications/2018/latent-tuberculosis-infection/en/>.
44. Diagnostic Standards and Classification of Tuberculosis in Adults and Children. This official statement of the American Thoracic Society and the Centers for Disease Control and Prevention was adopted by the ATS Board of Directors, July 1999. This statement was endorsed by the Council of the Infectious Disease Society of America, September 1999. *Am J Respir Crit Care Med.* 2000;161(4 Pt 1):1376-95. Epub 2000/04/14. doi: 10.1164/ajrccm.161.4.16141. PubMed PMID: 10764337.
45. Ryu YJ. Diagnosis of pulmonary tuberculosis: recent advances and diagnostic algorithms. *Tuberc Respir Dis (Seoul).* 2015;78(2):64-71. Epub 2015/04/11. doi: 10.4046/trd.2015.78.2.64. PubMed PMID: 25861338; PubMed Central PMCID: PMC3910902.
46. Steingart KR, Ramsay A, Pai M. Optimizing sputum smear microscopy for the diagnosis of pulmonary tuberculosis. *Expert Rev Anti Infect Ther.* 2007;5(3):327-31. Epub 2007/06/06. doi: 10.1586/14787210.5.3.327. PubMed PMID: 17547496.
47. WHO. Fluorescent light-emitting diode (LED) microscopy for diagnosis of tuberculosis: policy statement2011. Available from: <https://apps.who.int/iris/handle/10665/44602>.
48. Lawn SD, Nicol MP. Xpert(R) MTB/RIF assay: development, evaluation and implementation of a new rapid molecular diagnostic for tuberculosis and rifampicin resistance. *Future Microbiol.* 2011;6(9):1067-82. Epub 2011/10/01. doi: 10.2217/fmb.11.84. PubMed PMID: 21958145; PubMed Central PMCID: PMC3910901.
49. CDC. Tuberculosis: Signs & Symptoms 2016. Available from: <https://www.cdc.gov/tb/topic/basics/signsandSYMPTOMS.htm>.
50. Lin PL, Flynn JL. CD8 T cells and Mycobacterium tuberculosis infection. *Semin Immunopathol.* 2015;37(3):239-49. Epub 2015/04/29. doi: 10.1007/s00281-015-0490-8. PubMed PMID: 25917388; PubMed Central PMCID: PMC3910900.

51. Lin PL, Flynn JL. Understanding latent tuberculosis: a moving target. *J Immunol.* 2010;185(1):15-22. Epub 2010/06/22. doi: 10.4049/jimmunol.0903856. PubMed PMID: 20562268; PubMed Central PMCID: PMCPMC3311959.
52. Selwyn PA, Alcabes P, Hartel D, Buono D, Schoenbaum EE, Klein RS, et al. Clinical manifestations and predictors of disease progression in drug users with human immunodeficiency virus infection. *N Engl J Med.* 1992;327(24):1697-703. Epub 1992/12/10. doi: 10.1056/NEJM199212103272401. PubMed PMID: 1359411.
53. Barry CE, 3rd, Boshoff HI, Dartois V, Dick T, Ehrt S, Flynn J, et al. The spectrum of latent tuberculosis: rethinking the biology and intervention strategies. *Nat Rev Microbiol.* 2009;7(12):845-55. Epub 2009/10/27. doi: 10.1038/nrmicro2236. PubMed PMID: 19855401; PubMed Central PMCID: PMCPMC4144869.
54. Lin PL, Flynn JL. The End of the Binary Era: Revisiting the Spectrum of Tuberculosis. *J Immunol.* 2018;201(9):2541-8. Epub 2018/10/24. doi: 10.4049/jimmunol.1800993. PubMed PMID: 30348659; PubMed Central PMCID: PMCPMC6217958.
55. Houk VN. Spread of tuberculosis via recirculated air in a naval vessel: the Byrd study. *Ann N Y Acad Sci.* 1980;353:10-24. Epub 1980/01/01. doi: 10.1111/j.1749-6632.1980.tb18901.x. PubMed PMID: 6939378.
56. Ma N, Zalwango S, Malone LL, Nsereko M, Wampande EM, Thiel BA, et al. Clinical and epidemiological characteristics of individuals resistant to *M. tuberculosis* infection in a longitudinal TB household contact study in Kampala, Uganda. *BMC Infect Dis.* 2014;14:352. Epub 2014/06/28. doi: 10.1186/1471-2334-14-352. PubMed PMID: 24970328; PubMed Central PMCID: PMCPMC4091673.
57. Stein CM, Zalwango S, Malone LL, Thiel B, Mupere E, Nsereko M, et al. Resistance and Susceptibility to *Mycobacterium tuberculosis* Infection and Disease in Tuberculosis Households in Kampala, Uganda. *Am J Epidemiol.* 2018;187(7):1477-89. Epub 2018/01/06. doi: 10.1093/aje/kwx380. PubMed PMID: 29304247; PubMed Central PMCID: PMCPMC6031055.
58. Hill PC, Brookes RH, Fox A, Jackson-Sillah D, Jeffries DJ, Lugos MD, et al. Longitudinal assessment of an ELISPOT test for *Mycobacterium tuberculosis* infection. *PLoS Med.* 2007;4(6):e192. Epub 2007/06/15. doi: 10.1371/journal.pmed.0040192. PubMed PMID: 17564487; PubMed Central PMCID: PMCPMC1891317.
59. Hochberg NS, Rekhtman S, Burns J, Ganley-Leal L, Helbig S, Watts NS, et al. The complexity of diagnosing latent tuberculosis infection in older adults in long-term care facilities. *Int J Infect Dis.* 2016;44:37-43. Epub 2016/01/24. doi: 10.1016/j.ijid.2016.01.007. PubMed PMID: 26802447.
60. Tait DR, Hatherill M, Van Der Meeren O, Ginsberg AM, Van Brakel E, Salaun B, et al. Final Analysis of a Trial of M72/AS01E Vaccine to Prevent Tuberculosis. *N Engl J Med.* 2019;381(25):2429-39. Epub 2019/10/30. doi: 10.1056/NEJMoa1909953. PubMed PMID: 31661198.

61. Nemes E, Geldenhuys H, Rozot V, Rutkowski KT, Ratangee F, Bilek N, et al. Prevention of *M. tuberculosis* Infection with H4:IC31 Vaccine or BCG Revaccination. *N Engl J Med*. 2018;379(2):138-49. Epub 2018/07/12. doi: 10.1056/NEJMoa1714021. PubMed PMID: 29996082; PubMed Central PMCID: PMC5937161.
62. Hansen SG, Zak DE, Xu G, Ford JC, Marshall EE, Malouli D, et al. Prevention of tuberculosis in rhesus macaques by a cytomegalovirus-based vaccine. *Nat Med*. 2018;24(2):130-43. Epub 2018/01/16. doi: 10.1038/nm.4473. PubMed PMID: 29334373; PubMed Central PMCID: PMC5909823.
63. Darrah PA, Zeppa JJ, Maiello P, Hackney JA, Wadsworth MH, 2nd, Hughes TK, et al. Prevention of tuberculosis in macaques after intravenous BCG immunization. *Nature*. 2020;577(7788):95-102. Epub 2020/01/03. doi: 10.1038/s41586-019-1817-8. PubMed PMID: 31894150; PubMed Central PMCID: PMC7015856.
64. Tiemersma EW, van der Werf MJ, Borgdorff MW, Williams BG, Nagelkerke NJ. Natural history of tuberculosis: duration and fatality of untreated pulmonary tuberculosis in HIV negative patients: a systematic review. *PLoS One*. 2011;6(4):e17601. Epub 2011/04/13. doi: 10.1371/journal.pone.0017601. PubMed PMID: 21483732; PubMed Central PMCID: PMC3070694.
65. Nahid P, Dorman SE, Alipanah N, Barry PM, Brozek JL, Cattamanchi A, et al. Official American Thoracic Society/Centers for Disease Control and Prevention/Infectious Diseases Society of America Clinical Practice Guidelines: Treatment of Drug-Susceptible Tuberculosis. *Clin Infect Dis*. 2016;63(7):e147-e95. Epub 2016/08/16. doi: 10.1093/cid/ciw376. PubMed PMID: 27516382; PubMed Central PMCID: PMC6590850.
66. Zumla A, Nahid P, Cole ST. Advances in the development of new tuberculosis drugs and treatment regimens. *Nat Rev Drug Discov*. 2013;12(5):388-404. Epub 2013/05/01. doi: 10.1038/nrd4001. PubMed PMID: 23629506.
67. Barry CE. Lessons from seven decades of antituberculosis drug discovery. *Curr Top Med Chem*. 2011;11(10):1216-25. Epub 2011/03/16. doi: 10.2174/156802611795429158. PubMed PMID: 21401509; PubMed Central PMCID: PMC6380367.
68. STREPTOMYCIN treatment of pulmonary tuberculosis. *Br Med J*. 1948;2(4582):769-82. Epub 1948/10/30. PubMed PMID: 18890300; PubMed Central PMCID: PMC2091872.
69. Lehmann J. Para-aminosalicylic acid in the treatment of tuberculosis. *Lancet*. 1946;1(6384):15. Epub 1946/01/05. doi: 10.1016/s0140-6736(46)91185-3. PubMed PMID: 21008766.
70. TREATMENT of pulmonary tuberculosis with streptomycin and para-aminosalicylic acid; a Medical Research Council investigation. *Br Med J*. 1950;2(4688):1073-85. Epub 1950/11/11. PubMed PMID: 14772553; PubMed Central PMCID: PMC2039351.

71. Unissa AN, Subbian S, Hanna LE, Selvakumar N. Overview on mechanisms of isoniazid action and resistance in *Mycobacterium tuberculosis*. *Infect Genet Evol.* 2016;45:474-92. Epub 2016/09/11. doi: 10.1016/j.meegid.2016.09.004. PubMed PMID: 27612406.
72. Bardou F, Raynaud C, Ramos C, Laneelle MA, Laneelle G. Mechanism of isoniazid uptake in *Mycobacterium tuberculosis*. *Microbiology.* 1998;144 (Pt 9):2539-44. Epub 1998/10/23. doi: 10.1099/00221287-144-9-2539. PubMed PMID: 9782502.
73. Zhang Y, Heym B, Allen B, Young D, Cole S. The catalase-peroxidase gene and isoniazid resistance of *Mycobacterium tuberculosis*. *Nature.* 1992;358(6387):591-3. Epub 1992/08/13. doi: 10.1038/358591a0. PubMed PMID: 1501713.
74. Timmins GS, Deretic V. Mechanisms of action of isoniazid. *Mol Microbiol.* 2006;62(5):1220-7. Epub 2006/11/01. doi: 10.1111/j.1365-2958.2006.05467.x. PubMed PMID: 17074073.
75. Winder FG, Collins P, Rooney SA. Effects of isoniazid on mycolic acid synthesis in *Mycobacterium tuberculosis* and on its cell envelope. *Biochem J.* 1970;117(2):27P. Epub 1970/04/01. doi: 10.1042/bj1170027pa. PubMed PMID: 4986870; PubMed Central PMCID: PMC1178907.
76. Takayama K, Wang L, David HL. Effect of isoniazid on the in vivo mycolic acid synthesis, cell growth, and viability of *Mycobacterium tuberculosis*. *Antimicrob Agents Chemother.* 1972;2(1):29-35. Epub 1972/07/01. doi: 10.1128/aac.2.1.29. PubMed PMID: 4208567; PubMed Central PMCID: PMC1178907.
77. Timmins GS, Master S, Rusnak F, Deretic V. Nitric oxide generated from isoniazid activation by KatG: source of nitric oxide and activity against *Mycobacterium tuberculosis*. *Antimicrob Agents Chemother.* 2004;48(8):3006-9. Epub 2004/07/27. doi: 10.1128/AAC.48.8.3006-3009.2004. PubMed PMID: 15273113; PubMed Central PMCID: PMC1178907.
78. Jagielski T, Bakula Z, Roeske K, Kaminski M, Napiorkowska A, Augustynowicz-Kopec E, et al. Detection of mutations associated with isoniazid resistance in multidrug-resistant *Mycobacterium tuberculosis* clinical isolates. *J Antimicrob Chemother.* 2014;69(9):2369-75. Epub 2014/05/24. doi: 10.1093/jac/dku161. PubMed PMID: 24855126.
79. Cardoso RF, Cooksey RC, Morlock GP, Barco P, Cecon L, Forestiero F, et al. Screening and characterization of mutations in isoniazid-resistant *Mycobacterium tuberculosis* isolates obtained in Brazil. *Antimicrob Agents Chemother.* 2004;48(9):3373-81. Epub 2004/08/26. doi: 10.1128/AAC.48.9.3373-3381.2004. PubMed PMID: 15328099; PubMed Central PMCID: PMC1178907.
80. Gopal P, Gruber G, Dartois V, Dick T. Pharmacological and Molecular Mechanisms Behind the Sterilizing Activity of Pyrazinamide. *Trends Pharmacol Sci.* 2019;40(12):930-40. Epub 2019/11/11. doi: 10.1016/j.tips.2019.10.005. PubMed PMID: 31704175; PubMed Central PMCID: PMC1178907.

81. Solotorovsky M, Gregory FJ, Ironson EJ, Bugie EJ, O'Neill RC, Pfister R, 3rd. Pyrazinoic acid amide; an agent active against experimental murine tuberculosis. *Proc Soc Exp Biol Med.* 1952;79(4):563-5. Epub 1952/04/01. doi: 10.3181/00379727-79-19447. PubMed PMID: 14920496.
82. Konno K, Feldmann FM, McDermott W. Pyrazinamide susceptibility and amidase activity of tubercle bacilli. *Am Rev Respir Dis.* 1967;95(3):461-9. Epub 1967/03/01. doi: 10.1164/arrd.1967.95.3.461. PubMed PMID: 4225184.
83. Leonardi R, Jackowski S. Biosynthesis of Pantothenic Acid and Coenzyme A. *EcoSal Plus.* 2007;2(2). Epub 2007/04/01. doi: 10.1128/ecosalplus.3.6.3.4. PubMed PMID: 26443589; PubMed Central PMCID: PMCPMC4950986.
84. Sun Q, Li X, Perez LM, Shi W, Zhang Y, Sacchettini JC. The molecular basis of pyrazinamide activity on *Mycobacterium tuberculosis* PanD. *Nat Commun.* 2020;11(1):339. Epub 2020/01/19. doi: 10.1038/s41467-019-14238-3. PubMed PMID: 31953389; PubMed Central PMCID: PMCPMC6969166.
85. Spry C, Kirk K, Saliba KJ. Coenzyme A biosynthesis: an antimicrobial drug target. *FEMS Microbiol Rev.* 2008;32(1):56-106. Epub 2008/01/05. doi: 10.1111/j.1574-6976.2007.00093.x. PubMed PMID: 18173393.
86. Jureen P, Werngren J, Toro JC, Hoffner S. Pyrazinamide resistance and *pncA* gene mutations in *Mycobacterium tuberculosis*. *Antimicrob Agents Chemother.* 2008;52(5):1852-4. Epub 2008/03/05. doi: 10.1128/AAC.00110-08. PubMed PMID: 18316515; PubMed Central PMCID: PMCPMC2346646.
87. Sreevatsan S, Pan X, Zhang Y, Kreiswirth BN, Musser JM. Mutations associated with pyrazinamide resistance in *pncA* of *Mycobacterium tuberculosis* complex organisms. *Antimicrob Agents Chemother.* 1997;41(3):636-40. Epub 1997/03/01. PubMed PMID: 9056006; PubMed Central PMCID: PMCPMC163764.
88. Zhang S, Chen J, Shi W, Liu W, Zhang W, Zhang Y. Mutations in *panD* encoding aspartate decarboxylase are associated with pyrazinamide resistance in *Mycobacterium tuberculosis*. *Emerg Microbes Infect.* 2013;2(6):e34. Epub 2013/06/01. doi: 10.1038/emi.2013.38. PubMed PMID: 26038471; PubMed Central PMCID: PMCPMC3697303.
89. Werngren J, Alm E, Mansjo M. Non-*pncA* Gene-Mutated but Pyrazinamide-Resistant *Mycobacterium tuberculosis*: Why Is That? *J Clin Microbiol.* 2017;55(6):1920-7. Epub 2017/04/14. doi: 10.1128/JCM.02532-16. PubMed PMID: 28404681; PubMed Central PMCID: PMCPMC5442549.
90. Goude R, Amin AG, Chatterjee D, Parish T. The arabinosyltransferase *EmbC* is inhibited by ethambutol in *Mycobacterium tuberculosis*. *Antimicrob Agents Chemother.* 2009;53(10):4138-46. Epub 2009/07/15. doi: 10.1128/AAC.00162-09. PubMed PMID: 19596878; PubMed Central PMCID: PMCPMC2764220.

91. Forbes M, Kuck NA, Peets EA. Mode of action of ethambutol. *J Bacteriol.* 1962;84:1099-103. Epub 1962/11/01. PubMed PMID: 13958686; PubMed Central PMCID: PMCPMC278016.
92. Kilburn JO, Greenberg J. Effect of ethambutol on the viable cell count in *Mycobacterium smegmatis*. *Antimicrob Agents Chemother.* 1977;11(3):534-40. Epub 1977/03/01. doi: 10.1128/aac.11.3.534. PubMed PMID: 856004; PubMed Central PMCID: PMCPMC352017.
93. Takayama K, Kilburn JO. Inhibition of synthesis of arabinogalactan by ethambutol in *Mycobacterium smegmatis*. *Antimicrob Agents Chemother.* 1989;33(9):1493-9. Epub 1989/09/01. doi: 10.1128/aac.33.9.1493. PubMed PMID: 2817850; PubMed Central PMCID: PMCPMC172689.
94. Alcaide F, Pfyffer GE, Telenti A. Role of *embB* in natural and acquired resistance to ethambutol in mycobacteria. *Antimicrob Agents Chemother.* 1997;41(10):2270-3. Epub 1997/10/23. PubMed PMID: 9333060; PubMed Central PMCID: PMCPMC164105.
95. Sreevatsan S, Stockbauer KE, Pan X, Kreiswirth BN, Moghazeh SL, Jacobs WR, Jr., et al. Ethambutol resistance in *Mycobacterium tuberculosis*: critical role of *embB* mutations. *Antimicrob Agents Chemother.* 1997;41(8):1677-81. Epub 1997/08/01. PubMed PMID: 9257740; PubMed Central PMCID: PMCPMC163984.
96. Telenti A, Philipp WJ, Sreevatsan S, Bernasconi C, Stockbauer KE, Wieles B, et al. The *emb* operon, a gene cluster of *Mycobacterium tuberculosis* involved in resistance to ethambutol. *Nat Med.* 1997;3(5):567-70. Epub 1997/05/01. doi: 10.1038/nm0597-567. PubMed PMID: 9142129.
97. Campbell EA, Korzheva N, Mustaev A, Murakami K, Nair S, Goldfarb A, et al. Structural mechanism for rifampicin inhibition of bacterial rna polymerase. *Cell.* 2001;104(6):901-12. Epub 2001/04/06. doi: 10.1016/s0092-8674(01)00286-0. PubMed PMID: 11290327.
98. A controlled trial of six months chemotherapy in pulmonary tuberculosis. Second report: results during the 24 months after the end of chemotherapy. British Thoracic Association. *Am Rev Respir Dis.* 1982;126(3):460-2. Epub 1982/09/01. doi: 10.1164/arrd.1982.126.3.460. PubMed PMID: 6751175.
99. Short-course chemotherapy in pulmonary tuberculosis. A controlled trial by the British Thoracic and Tuberculosis Association. *Lancet.* 1976;2(7995):1102-4. Epub 1976/11/20. PubMed PMID: 62946.
100. Hartmann G, Honikel KO, Knusel F, Nuesch J. The specific inhibition of the DNA-directed RNA synthesis by rifamycin. *Biochim Biophys Acta.* 1967;145(3):843-4. Epub 1967/01/01. doi: 10.1016/0005-2787(67)90147-5. PubMed PMID: 4863911.
101. Zaw MT, Emran NA, Lin Z. Mutations inside rifampicin-resistance determining region of *rpoB* gene associated with rifampicin-resistance in *Mycobacterium tuberculosis*. *J Infect*

- Public Health. 2018;11(5):605-10. Epub 2018/05/01. doi: 10.1016/j.jiph.2018.04.005. PubMed PMID: 29706316.
102. Prasad R, Singh A, Gupta N. Adverse drug reactions in tuberculosis and management. *Indian J Tuberc.* 2019;66(4):520-32. Epub 2019/12/10. doi: 10.1016/j.ijtb.2019.11.005. PubMed PMID: 31813444.
 103. Rendon A, Tiberi S, Scardigli A, D'Ambrosio L, Centis R, Caminero JA, et al. Classification of drugs to treat multidrug-resistant tuberculosis (MDR-TB): evidence and perspectives. *J Thorac Dis.* 2016;8(10):2666-71. Epub 2016/11/22. doi: 10.21037/jtd.2016.10.14. PubMed PMID: 27867538; PubMed Central PMCID: PMC5107456.
 104. Sotgiu G, Centis R, D'Ambrosio L, Migliori GB. Tuberculosis treatment and drug regimens. *Cold Spring Harb Perspect Med.* 2015;5(5):a017822. Epub 2015/01/13. doi: 10.1101/cshperspect.a017822. PubMed PMID: 25573773; PubMed Central PMCID: PMC4448591.
 105. Wolf AJ, Linas B, Trevejo-Nunez GJ, Kincaid E, Tamura T, Takatsu K, et al. Mycobacterium tuberculosis infects dendritic cells with high frequency and impairs their function in vivo. *J Immunol.* 2007;179(4):2509-19. Epub 2007/08/07. doi: 10.4049/jimmunol.179.4.2509. PubMed PMID: 17675513.
 106. Chackerian AA, Alt JM, Perera TV, Dascher CC, Behar SM. Dissemination of Mycobacterium tuberculosis Is Influenced by Host Factors and Precedes the Initiation of T-Cell Immunity. *Infection and Immunity.* 2002;70(8):4501-9. doi: 10.1128/iai.70.8.4501-4509.2002.
 107. Wolf AJ, Desvignes L, Linas B, Banaiee N, Tamura T, Takatsu K, et al. Initiation of the adaptive immune response to Mycobacterium tuberculosis depends on antigen production in the local lymph node, not the lungs. *J Exp Med.* 2008;205(1):105-15. doi: 10.1084/jem.20071367. PubMed PMID: 18158321; PubMed Central PMCID: PMC2234384.
 108. Reiley WW, Calayag MD, Wittmer ST, Huntington JL, Pearl JE, Fountain JJ, et al. ESAT-6-specific CD4 T cell responses to aerosol Mycobacterium tuberculosis infection are initiated in the mediastinal lymph nodes. *Proc Natl Acad Sci U S A.* 2008;105(31):10961-6. doi: 10.1073/pnas.0801496105. PubMed PMID: 18667699; PubMed Central PMCID: PMC2504808.
 109. Ramakrishnan L. Revisiting the role of the granuloma in tuberculosis. *Nat Rev Immunol.* 2012;12(5):352-66. Epub 2012/04/21. doi: 10.1038/nri3211. PubMed PMID: 22517424.
 110. Russell DG, Cardona PJ, Kim MJ, Allain S, Altare F. Foamy macrophages and the progression of the human tuberculosis granuloma. *Nat Immunol.* 2009;10(9):943-8. Epub 2009/08/21. doi: 10.1038/ni.1781. PubMed PMID: 19692995; PubMed Central PMCID: PMC2759071.

111. Saunders BM, Cooper AM. Restraining mycobacteria: role of granulomas in mycobacterial infections. *Immunol Cell Biol.* 2000;78(4):334-41. Epub 2000/08/18. doi: 10.1046/j.1440-1711.2000.00933.x. PubMed PMID: 10947857.
112. Algood HM, Lin PL, Flynn JL. Tumor necrosis factor and chemokine interactions in the formation and maintenance of granulomas in tuberculosis. *Clin Infect Dis.* 2005;41 Suppl 3:S189-93. Epub 2005/06/29. doi: 10.1086/429994. PubMed PMID: 15983898.
113. Roach DR, Bean AG, Demangel C, France MP, Briscoe H, Britton WJ. TNF regulates chemokine induction essential for cell recruitment, granuloma formation, and clearance of mycobacterial infection. *J Immunol.* 2002;168(9):4620-7. Epub 2002/04/24. doi: 10.4049/jimmunol.168.9.4620. PubMed PMID: 11971010.
114. Silva Miranda M, Breiman A, Allain S, Deknuydt F, Altare F. The tuberculous granuloma: an unsuccessful host defence mechanism providing a safety shelter for the bacteria? *Clin Dev Immunol.* 2012;2012:139127. Epub 2012/07/20. doi: 10.1155/2012/139127. PubMed PMID: 22811737; PubMed Central PMCID: PMC3395138.
115. Davis JM, Ramakrishnan L. The role of the granuloma in expansion and dissemination of early tuberculous infection. *Cell.* 2009;136(1):37-49. Epub 2009/01/13. doi: 10.1016/j.cell.2008.11.014. PubMed PMID: 19135887; PubMed Central PMCID: PMC3134310.
116. Cadena AM, Fortune SM, Flynn JL. Heterogeneity in tuberculosis. *Nat Rev Immunol.* 2017;17(11):691-702. Epub 2017/07/25. doi: 10.1038/nri.2017.69. PubMed PMID: 28736436.
117. Flynn JL, Klein EC. Pulmonary Tuberculosis in Monkeys. In: Leong FJ, Dartois V, Thomas D, editors. *A Color Atlas of Comparative Pathology of Pulmonary Tuberculosis.* Boca Raton, FL: CRC Press; 2011. p. 83-105.
118. Lin PL, Ford CB, Coleman MT, Myers AJ, Gawande R, Ioerger T, et al. Sterilization of granulomas is common in active and latent tuberculosis despite within-host variability in bacterial killing. *Nat Med.* 2014;20(1):75-9. doi: 10.1038/nm.3412. PubMed PMID: 24336248; PubMed Central PMCID: PMC3947310.
119. Coleman MT, Maiello P, Tomko J, Frye LJ, Fillmore D, Janssen C, et al. Early Changes by (18)Fluorodeoxyglucose positron emission tomography coregistered with computed tomography predict outcome after Mycobacterium tuberculosis infection in cynomolgus macaques. *Infect Immun.* 2014;82(6):2400-4. doi: 10.1128/IAI.01599-13. PubMed PMID: 24664509; PubMed Central PMCID: PMC4019174.
120. Martin CJ, Cadena AM, Leung VW, Lin PL, Maiello P, Hicks N, et al. Digitally Barcoding Mycobacterium tuberculosis Reveals In Vivo Infection Dynamics in the Macaque Model of Tuberculosis. *MBio.* 2017;8(3). doi: 10.1128/mBio.00312-17. PubMed PMID: 28487426; PubMed Central PMCID: PMC5424202.

121. Gideon HP, Phuah J, Myers AJ, Bryson BD, Rodgers MA, Coleman MT, et al. Variability in tuberculosis granuloma T cell responses exists, but a balance of pro- and anti-inflammatory cytokines is associated with sterilization. *PLoS Pathog.* 2015;11(1):e1004603. doi: 10.1371/journal.ppat.1004603. PubMed PMID: 25611466; PubMed Central PMCID: PMC4303275.
122. Whitsett JA, Alenghat T. Respiratory epithelial cells orchestrate pulmonary innate immunity. *Nat Immunol.* 2015;16(1):27-35. Epub 2014/12/19. doi: 10.1038/ni.3045. PubMed PMID: 25521682; PubMed Central PMCID: PMC4318521.
123. Li Y, Wang Y, Liu X. The role of airway epithelial cells in response to mycobacteria infection. *Clin Dev Immunol.* 2012;2012:791392. Epub 2012/05/10. doi: 10.1155/2012/791392. PubMed PMID: 22570668; PubMed Central PMCID: PMC3337601.
124. Scordo JM, Knoell DL, Torrelles JB. Alveolar Epithelial Cells in Mycobacterium tuberculosis Infection: Active Players or Innocent Bystanders? *J Innate Immun.* 2016;8(1):3-14. Epub 2015/09/19. doi: 10.1159/000439275. PubMed PMID: 26384325; PubMed Central PMCID: PMC4724319.
125. Bermudez LE, Goodman J. Mycobacterium tuberculosis invades and replicates within type II alveolar cells. *Infect Immun.* 1996;64(4):1400-6. Epub 1996/04/01. PubMed PMID: 8606107; PubMed Central PMCID: PMC173932.
126. Garcia-Perez BE, Mondragon-Flores R, Luna-Herrera J. Internalization of Mycobacterium tuberculosis by macropinocytosis in non-phagocytic cells. *Microb Pathog.* 2003;35(2):49-55. Epub 2003/08/07. doi: 10.1016/s0882-4010(03)00089-5. PubMed PMID: 12901843.
127. Mehta PK, King CH, White EH, Murtagh JJ, Jr., Quinn FD. Comparison of in vitro models for the study of Mycobacterium tuberculosis invasion and intracellular replication. *Infect Immun.* 1996;64(7):2673-9. Epub 1996/07/01. PubMed PMID: 8698494; PubMed Central PMCID: PMC174125.
128. Ryndak MB, Singh KK, Peng Z, Laal S. Transcriptional profile of Mycobacterium tuberculosis replicating in type II alveolar epithelial cells. *PLoS One.* 2015;10(4):e0123745. Epub 2015/04/07. doi: 10.1371/journal.pone.0123745. PubMed PMID: 25844539; PubMed Central PMCID: PMC4386821.
129. de Martino M, Lodi L, Galli L, Chiappini E. Immune Response to Mycobacterium tuberculosis: A Narrative Review. *Front Pediatr.* 2019;7:350. Epub 2019/09/12. doi: 10.3389/fped.2019.00350. PubMed PMID: 31508399; PubMed Central PMCID: PMC6718705.
130. Vieira OV, Botelho RJ, Grinstein S. Phagosome maturation: aging gracefully. *Biochem J.* 2002;366(Pt 3):689-704. Epub 2002/06/14. doi: 10.1042/BJ20020691. PubMed PMID: 12061891; PubMed Central PMCID: PMC1222826.

131. Philips JA. Mycobacterial manipulation of vacuolar sorting. *Cell Microbiol.* 2008;10(12):2408-15. Epub 2008/09/12. doi: 10.1111/j.1462-5822.2008.01239.x. PubMed PMID: 18783482.
132. Fratti RA, Chua J, Vergne I, Deretic V. Mycobacterium tuberculosis glycosylated phosphatidylinositol causes phagosome maturation arrest. *Proc Natl Acad Sci U S A.* 2003;100(9):5437-42. Epub 2003/04/19. doi: 10.1073/pnas.0737613100. PubMed PMID: 12702770; PubMed Central PMCID: PMCPMC154363.
133. Indrigo J, Hunter RL, Actor JK. Cord factor trehalose 6,6'-dimycolate (TDM) mediates trafficking events during mycobacterial infection of murine macrophages. *Microbiology.* 2003;149(Pt 8):2049-59. Epub 2003/08/09. doi: 10.1099/mic.0.26226-0. PubMed PMID: 12904545.
134. Herbst S, Schaible UE, Schneider BE. Interferon gamma activated macrophages kill mycobacteria by nitric oxide induced apoptosis. *PLoS One.* 2011;6(5):e19105. Epub 2011/05/12. doi: 10.1371/journal.pone.0019105. PubMed PMID: 21559306; PubMed Central PMCID: PMCPMC3085516.
135. Gutierrez MG, Master SS, Singh SB, Taylor GA, Colombo MI, Deretic V. Autophagy is a defense mechanism inhibiting BCG and Mycobacterium tuberculosis survival in infected macrophages. *Cell.* 2004;119(6):753-66. Epub 2004/12/21. doi: 10.1016/j.cell.2004.11.038. PubMed PMID: 15607973.
136. Neyrolles O, Wolschendorf F, Mitra A, Niederweis M. Mycobacteria, metals, and the macrophage. *Immunol Rev.* 2015;264(1):249-63. Epub 2015/02/24. doi: 10.1111/imr.12265. PubMed PMID: 25703564; PubMed Central PMCID: PMCPMC4521620.
137. Queval CJ, Brosch R, Simeone R. The Macrophage: A Disputed Fortress in the Battle against Mycobacterium tuberculosis. *Front Microbiol.* 2017;8:2284. Epub 2017/12/09. doi: 10.3389/fmicb.2017.02284. PubMed PMID: 29218036; PubMed Central PMCID: PMCPMC5703847.
138. Aderem A, Ulevitch RJ. Toll-like receptors in the induction of the innate immune response. *Nature.* 2000;406(6797):782-7. Epub 2000/08/30. doi: 10.1038/35021228. PubMed PMID: 10963608.
139. Mortaz E, Adcock IM, Tabarsi P, Masjedi MR, Mansouri D, Velayati AA, et al. Interaction of Pattern Recognition Receptors with Mycobacterium Tuberculosis. *J Clin Immunol.* 2015;35(1):1-10. Epub 2014/10/15. doi: 10.1007/s10875-014-0103-7. PubMed PMID: 25312698; PubMed Central PMCID: PMCPMC4306732.
140. Hossain MM, Norazmi MN. Pattern recognition receptors and cytokines in Mycobacterium tuberculosis infection--the double-edged sword? *Biomed Res Int.* 2013;2013:179174. Epub 2013/12/19. doi: 10.1155/2013/179174. PubMed PMID: 24350246; PubMed Central PMCID: PMCPMC3844256.

141. Brightbill HD, Libraty DH, Krutzik SR, Yang RB, Belisle JT, Bleharski JR, et al. Host defense mechanisms triggered by microbial lipoproteins through toll-like receptors. *Science*. 1999;285(5428):732-6. Epub 1999/07/31. doi: 10.1126/science.285.5428.732. PubMed PMID: 10426995.
142. Underhill DM, Ozinsky A, Smith KD, Aderem A. Toll-like receptor-2 mediates mycobacteria-induced proinflammatory signaling in macrophages. *Proc Natl Acad Sci U S A*. 1999;96(25):14459-63. Epub 1999/12/10. doi: 10.1073/pnas.96.25.14459. PubMed PMID: 10588727; PubMed Central PMCID: PMCPMC24458.
143. Liu PT, Stenger S, Li H, Wenzel L, Tan BH, Krutzik SR, et al. Toll-like receptor triggering of a vitamin D-mediated human antimicrobial response. *Science*. 2006;311(5768):1770-3. Epub 2006/02/25. doi: 10.1126/science.1123933. PubMed PMID: 16497887.
144. Kim K, Sohn H, Kim JS, Choi HG, Byun EH, Lee KI, et al. Mycobacterium tuberculosis Rv0652 stimulates production of tumour necrosis factor and monocytes chemoattractant protein-1 in macrophages through the Toll-like receptor 4 pathway. *Immunology*. 2012;136(2):231-40. Epub 2012/03/06. doi: 10.1111/j.1365-2567.2012.03575.x. PubMed PMID: 22385341; PubMed Central PMCID: PMCPMC3403266.
145. Jung SB, Yang CS, Lee JS, Shin AR, Jung SS, Son JW, et al. The mycobacterial 38-kilodalton glycolipoprotein antigen activates the mitogen-activated protein kinase pathway and release of proinflammatory cytokines through Toll-like receptors 2 and 4 in human monocytes. *Infect Immun*. 2006;74(5):2686-96. Epub 2006/04/20. doi: 10.1128/IAI.74.5.2686-2696.2006. PubMed PMID: 16622205; PubMed Central PMCID: PMCPMC1459749.
146. Means TK, Jones BW, Schromm AB, Shurtleff BA, Smith JA, Keane J, et al. Differential effects of a Toll-like receptor antagonist on Mycobacterium tuberculosis-induced macrophage responses. *J Immunol*. 2001;166(6):4074-82. Epub 2001/03/10. doi: 10.4049/jimmunol.166.6.4074. PubMed PMID: 11238656.
147. Bafica A, Scanga CA, Feng CG, Leifer C, Cheever A, Sher A. TLR9 regulates Th1 responses and cooperates with TLR2 in mediating optimal resistance to Mycobacterium tuberculosis. *J Exp Med*. 2005;202(12):1715-24. Epub 2005/12/21. doi: 10.1084/jem.20051782. PubMed PMID: 16365150; PubMed Central PMCID: PMCPMC2212963.
148. Ferguson JS, Weis JJ, Martin JL, Schlesinger LS. Complement protein C3 binding to Mycobacterium tuberculosis is initiated by the classical pathway in human bronchoalveolar lavage fluid. *Infect Immun*. 2004;72(5):2564-73. Epub 2004/04/23. doi: 10.1128/iai.72.5.2564-2573.2004. PubMed PMID: 15102764; PubMed Central PMCID: PMCPMC387845.
149. Schlesinger LS, Bellinger-Kawahara CG, Payne NR, Horwitz MA. Phagocytosis of Mycobacterium tuberculosis is mediated by human monocyte complement receptors and complement component C3. *J Immunol*. 1990;144(7):2771-80. Epub 1990/04/01. PubMed PMID: 2108212.

150. Kang PB, Azad AK, Torrelles JB, Kaufman TM, Beharka A, Tibesar E, et al. The human macrophage mannose receptor directs Mycobacterium tuberculosis lipoarabinomannan-mediated phagosome biogenesis. *J Exp Med*. 2005;202(7):987-99. Epub 2005/10/06. doi: 10.1084/jem.20051239. PubMed PMID: 16203868; PubMed Central PMCID: PMCPMC2213176.
151. Schlesinger LS. Macrophage phagocytosis of virulent but not attenuated strains of Mycobacterium tuberculosis is mediated by mannose receptors in addition to complement receptors. *J Immunol*. 1993;150(7):2920-30. Epub 1993/04/01. PubMed PMID: 8454864.
152. Pedrosa J, Saunders BM, Appelberg R, Orme IM, Silva MT, Cooper AM. Neutrophils play a protective nonphagocytic role in systemic Mycobacterium tuberculosis infection of mice. *Infect Immun*. 2000;68(2):577-83. Epub 2000/01/20. doi: 10.1128/iai.68.2.577-583.2000. PubMed PMID: 10639420; PubMed Central PMCID: PMCPMC97179.
153. Sugawara I, Udagawa T, Yamada H. Rat neutrophils prevent the development of tuberculosis. *Infect Immun*. 2004;72(3):1804-6. Epub 2004/02/24. doi: 10.1128/iai.72.3.1804-1806.2004. PubMed PMID: 14977991; PubMed Central PMCID: PMCPMC356015.
154. Petrofsky M, Bermudez LE. Neutrophils from Mycobacterium avium-infected mice produce TNF-alpha, IL-12, and IL-1 beta and have a putative role in early host response. *Clin Immunol*. 1999;91(3):354-8. Epub 1999/06/17. doi: 10.1006/clim.1999.4709. PubMed PMID: 10370382.
155. Fulton SA, Reba SM, Martin TD, Boom WH. Neutrophil-mediated mycobacteriocidal immunity in the lung during Mycobacterium bovis BCG infection in C57BL/6 mice. *Infect Immun*. 2002;70(9):5322-7. Epub 2002/08/17. doi: 10.1128/iai.70.9.5322-5327.2002. PubMed PMID: 12183593; PubMed Central PMCID: PMCPMC128293.
156. Eruslanov EB, Lyadova IV, Kondratieva TK, Majorov KB, Scheglov IV, Orlova MO, et al. Neutrophil responses to Mycobacterium tuberculosis infection in genetically susceptible and resistant mice. *Infect Immun*. 2005;73(3):1744-53. Epub 2005/02/26. doi: 10.1128/IAI.73.3.1744-1753.2005. PubMed PMID: 15731075; PubMed Central PMCID: PMCPMC1064912.
157. Marzo E, Vilaplana C, Tapia G, Diaz J, Garcia V, Cardona PJ. Damaging role of neutrophilic infiltration in a mouse model of progressive tuberculosis. *Tuberculosis (Edinb)*. 2014;94(1):55-64. Epub 2013/12/03. doi: 10.1016/j.tube.2013.09.004. PubMed PMID: 24291066.
158. Berry MP, Graham CM, McNab FW, Xu Z, Bloch SA, Oni T, et al. An interferon-inducible neutrophil-driven blood transcriptional signature in human tuberculosis. *Nature*. 2010;466(7309):973-7. Epub 2010/08/21. doi: 10.1038/nature09247. PubMed PMID: 20725040; PubMed Central PMCID: PMCPMC3492754.
159. Zhang X, Majlessi L, Deriaud E, Leclerc C, Lo-Man R. Coactivation of Syk kinase and MyD88 adaptor protein pathways by bacteria promotes regulatory properties of

- neutrophils. *Immunity*. 2009;31(5):761-71. Epub 2009/11/17. doi: 10.1016/j.immuni.2009.09.016. PubMed PMID: 19913447.
160. Mattila JT, Maiello P, Sun T, Via LE, Flynn JL. Granzyme B-expressing neutrophils correlate with bacterial load in granulomas from *Mycobacterium tuberculosis*-infected cynomolgus macaques. *Cell Microbiol*. 2015;17(8):1085-97. Epub 2015/02/06. doi: 10.1111/cmi.12428. PubMed PMID: 25653138; PubMed Central PMCID: PMC4570831.
 161. Barnes PF, Leedom JM, Chan LS, Wong SF, Shah J, Vachon LA, et al. Predictors of short-term prognosis in patients with pulmonary tuberculosis. *J Infect Dis*. 1988;158(2):366-71. Epub 1988/08/01. doi: 10.1093/infdis/158.2.366. PubMed PMID: 3403993.
 162. Lyadova IV. Neutrophils in Tuberculosis: Heterogeneity Shapes the Way? *Mediators Inflamm*. 2017;2017:8619307. Epub 2017/06/20. doi: 10.1155/2017/8619307. PubMed PMID: 28626346; PubMed Central PMCID: PMC4570831.
 163. Lowe DM, Redford PS, Wilkinson RJ, O'Garra A, Martineau AR. Neutrophils in tuberculosis: friend or foe? *Trends Immunol*. 2012;33(1):14-25. Epub 2011/11/19. doi: 10.1016/j.it.2011.10.003. PubMed PMID: 22094048.
 164. Denis M. Human neutrophils, activated with cytokines or not, do not kill virulent *Mycobacterium tuberculosis*. *J Infect Dis*. 1991;163(4):919-20. Epub 1991/04/01. doi: 10.1093/infdis/163.4.919. PubMed PMID: 1901338.
 165. Corleis B, Korbel D, Wilson R, Bylund J, Chee R, Schaible UE. Escape of *Mycobacterium tuberculosis* from oxidative killing by neutrophils. *Cell Microbiol*. 2012;14(7):1109-21. Epub 2012/03/13. doi: 10.1111/j.1462-5822.2012.01783.x. PubMed PMID: 22405091.
 166. Gideon HP, Phuah J, Junecko BA, Mattila JT. Neutrophils express pro- and anti-inflammatory cytokines in granulomas from *Mycobacterium tuberculosis*-infected cynomolgus macaques. *Mucosal Immunol*. 2019;12(6):1370-81. Epub 2019/08/23. doi: 10.1038/s41385-019-0195-8. PubMed PMID: 31434990; PubMed Central PMCID: PMC6824993.
 167. Reis e Sousa C, Hieny S, Scharon-Kersten T, Jankovic D, Charest H, Germain RN, et al. In vivo microbial stimulation induces rapid CD40 ligand-independent production of interleukin 12 by dendritic cells and their redistribution to T cell areas. *J Exp Med*. 1997;186(11):1819-29. Epub 1998/01/07. doi: 10.1084/jem.186.11.1819. PubMed PMID: 9382881; PubMed Central PMCID: PMC2199158.
 168. Wu T, Guo S, Wang J, Li L, Xu L, Liu P, et al. Interaction between mannosylated lipoarabinomannan and dendritic cell-specific intercellular adhesion molecule-3 grabbing nonintegrin influences dendritic cells maturation and T cell immunity. *Cell Immunol*. 2011;272(1):94-101. Epub 2011/10/22. doi: 10.1016/j.cellimm.2011.09.001. PubMed PMID: 22014390.

169. Henderson RA, Watkins SC, Flynn JL. Activation of human dendritic cells following infection with *Mycobacterium tuberculosis*. *J Immunol*. 1997;159(2):635-43. Epub 1997/07/15. PubMed PMID: 9218578.
170. Mihret A, Mamo G, Tafesse M, Hailu A, Parida S. Dendritic Cells Activate and Mature after Infection with *Mycobacterium tuberculosis*. *BMC Res Notes*. 2011;4:247. Epub 2011/07/23. doi: 10.1186/1756-0500-4-247. PubMed PMID: 21777464; PubMed Central PMCID: PMC3148562.
171. Vankayalapati R, Wizel B, Weis SE, Safi H, Lakey DL, Mandelboim O, et al. The NKp46 receptor contributes to NK cell lysis of mononuclear phagocytes infected with an intracellular bacterium. *J Immunol*. 2002;168(7):3451-7. Epub 2002/03/22. doi: 10.4049/jimmunol.168.7.3451. PubMed PMID: 11907104.
172. Vankayalapati R, Garg A, Porgador A, Griffith DE, Klucar P, Safi H, et al. Role of NK cell-activating receptors and their ligands in the lysis of mononuclear phagocytes infected with an intracellular bacterium. *J Immunol*. 2005;175(7):4611-7. Epub 2005/09/24. doi: 10.4049/jimmunol.175.7.4611. PubMed PMID: 16177106.
173. Dhiman R, Indramohan M, Barnes PF, Nayak RC, Paidipally P, Rao LV, et al. IL-22 produced by human NK cells inhibits growth of *Mycobacterium tuberculosis* by enhancing phagolysosomal fusion. *J Immunol*. 2009;183(10):6639-45. Epub 2009/10/30. doi: 10.4049/jimmunol.0902587. PubMed PMID: 19864591.
174. Vankayalapati R, Klucar P, Wizel B, Weis SE, Samten B, Safi H, et al. NK cells regulate CD8+ T cell effector function in response to an intracellular pathogen. *J Immunol*. 2004;172(1):130-7. Epub 2003/12/23. doi: 10.4049/jimmunol.172.1.130. PubMed PMID: 14688318.
175. Roy S, Barnes PF, Garg A, Wu S, Cosman D, Vankayalapati R. NK cells lyse T regulatory cells that expand in response to an intracellular pathogen. *J Immunol*. 2008;180(3):1729-36. Epub 2008/01/23. doi: 10.4049/jimmunol.180.3.1729. PubMed PMID: 18209070.
176. O'Garra A, Redford PS, McNab FW, Bloom CI, Wilkinson RJ, Berry MP. The immune response in tuberculosis. *Annu Rev Immunol*. 2013;31:475-527. Epub 2013/03/23. doi: 10.1146/annurev-immunol-032712-095939. PubMed PMID: 23516984.
177. Cooper AM. Cell-mediated immune responses in tuberculosis. *Annu Rev Immunol*. 2009;27:393-422. Epub 2009/03/24. doi: 10.1146/annurev.immunol.021908.132703. PubMed PMID: 19302046; PubMed Central PMCID: PMC314298253.
178. Aaron L, Saadoun D, Calatroni I, Launay O, Memain N, Vincent V, et al. Tuberculosis in HIV-infected patients: a comprehensive review. *Clin Microbiol Infect*. 2004;10(5):388-98. Epub 2004/04/29. doi: 10.1111/j.1469-0691.2004.00758.x. PubMed PMID: 15113314.
179. Leveton C, Barnass S, Champion B, Lucas S, De Souza B, Nicol M, et al. T-cell-mediated protection of mice against virulent *Mycobacterium tuberculosis*. *Infect Immun*.

- 1989;57(2):390-5. Epub 1989/02/01. PubMed PMID: 2492259; PubMed Central PMCID: PMC313109.
180. Flory CM, Hubbard RD, Collins FM. Effects of in vivo T lymphocyte subset depletion on mycobacterial infections in mice. *J Leukoc Biol.* 1992;51(3):225-9. Epub 1992/03/01. doi: 10.1002/jlb.51.3.225. PubMed PMID: 1347311.
 181. Mogue T, Goodrich ME, Ryan L, LaCourse R, North RJ. The relative importance of T cell subsets in immunity and immunopathology of airborne *Mycobacterium tuberculosis* infection in mice. *J Exp Med.* 2001;193(3):271-80. Epub 2001/02/07. doi: 10.1084/jem.193.3.271. PubMed PMID: 11157048; PubMed Central PMCID: PMC2195922.
 182. Lin PL, Rutledge T, Green AM, Bigbee M, Fuhrman C, Klein E, et al. CD4 T cell depletion exacerbates acute *Mycobacterium tuberculosis* while reactivation of latent infection is dependent on severity of tissue depletion in cynomolgus macaques. *AIDS Res Hum Retroviruses.* 2012;28(12):1693-702. doi: 10.1089/AID.2012.0028. PubMed PMID: 22480184; PubMed Central PMCID: PMC3505050.
 183. Diedrich CR, Rutledge T, Maiello P, Baranowski TM, White AG, Borish HJ, et al. SIV and *Mycobacterium tuberculosis* synergy within the granuloma accelerates the reactivation pattern of latent tuberculosis. *bioRxiv.* 2020. doi: 10.1101/2020.02.21.959353.
 184. Kumar P. IFN γ -producing CD4(+) T lymphocytes: the double-edged swords in tuberculosis. *Clin Transl Med.* 2017;6(1):21. Epub 2017/06/25. doi: 10.1186/s40169-017-0151-8. PubMed PMID: 28646367; PubMed Central PMCID: PMC5482791.
 185. Green AM, Difazio R, Flynn JL. IFN- γ from CD4 T cells is essential for host survival and enhances CD8 T cell function during *Mycobacterium tuberculosis* infection. *J Immunol.* 2013;190(1):270-7. Epub 2012/12/13. doi: 10.4049/jimmunol.1200061. PubMed PMID: 23233724; PubMed Central PMCID: PMC3683563.
 186. Flynn JL, Goldstein MM, Triebold KJ, Koller B, Bloom BR. Major histocompatibility complex class I-restricted T cells are required for resistance to *Mycobacterium tuberculosis* infection. *Proc Natl Acad Sci U S A.* 1992;89(24):12013-7. Epub 1992/12/15. doi: 10.1073/pnas.89.24.12013. PubMed PMID: 1465432; PubMed Central PMCID: PMC50688.
 187. Behar SM, Dascher CC, Grusby MJ, Wang CR, Brenner MB. Susceptibility of mice deficient in CD1D or TAP1 to infection with *Mycobacterium tuberculosis*. *J Exp Med.* 1999;189(12):1973-80. Epub 1999/06/22. doi: 10.1084/jem.189.12.1973. PubMed PMID: 10377193; PubMed Central PMCID: PMC2192974.
 188. Stenger S, Hanson DA, Teitelbaum R, Dewan P, Niazi KR, Froelich CJ, et al. An antimicrobial activity of cytolytic T cells mediated by granulysin. *Science.* 1998;282(5386):121-5. Epub 1998/10/02. doi: 10.1126/science.282.5386.121. PubMed PMID: 9756476.

189. Chen CY, Huang D, Wang RC, Shen L, Zeng G, Yao S, et al. A critical role for CD8 T cells in a nonhuman primate model of tuberculosis. *PLoS Pathog.* 2009;5(4):e1000392. Epub 2009/04/22. doi: 10.1371/journal.ppat.1000392. PubMed PMID: 19381260; PubMed Central PMCID: PMCPMC2663842.
190. Cooper AM, Dalton DK, Stewart TA, Griffin JP, Russell DG, Orme IM. Disseminated tuberculosis in interferon gamma gene-disrupted mice. *J Exp Med.* 1993;178(6):2243-7. Epub 1993/12/01. doi: 10.1084/jem.178.6.2243. PubMed PMID: 8245795; PubMed Central PMCID: PMCPMC2191280.
191. Flynn JL, Chan J, Triebold KJ, Dalton DK, Stewart TA, Bloom BR. An essential role for interferon gamma in resistance to *Mycobacterium tuberculosis* infection. *J Exp Med.* 1993;178(6):2249-54. Epub 1993/12/01. doi: 10.1084/jem.178.6.2249. PubMed PMID: 7504064; PubMed Central PMCID: PMCPMC2191274.
192. Cooper AM, Magram J, Ferrante J, Orme IM. Interleukin 12 (IL-12) is crucial to the development of protective immunity in mice intravenously infected with *mycobacterium tuberculosis*. *J Exp Med.* 1997;186(1):39-45. Epub 1997/07/07. doi: 10.1084/jem.186.1.39. PubMed PMID: 9206995; PubMed Central PMCID: PMCPMC2198958.
193. Sullivan BM, Jobe O, Lazarevic V, Vasquez K, Bronson R, Glimcher LH, et al. Increased susceptibility of mice lacking T-bet to infection with *Mycobacterium tuberculosis* correlates with increased IL-10 and decreased IFN-gamma production. *J Immunol.* 2005;175(7):4593-602. Epub 2005/09/24. doi: 10.4049/jimmunol.175.7.4593. PubMed PMID: 16177104.
194. Rosain J, Kong XF, Martinez-Barricarte R, Oleaga-Quintas C, Ramirez-Alejo N, Markle J, et al. Mendelian susceptibility to mycobacterial disease: 2014-2018 update. *Immunol Cell Biol.* 2019;97(4):360-7. Epub 2018/09/29. doi: 10.1111/imcb.12210. PubMed PMID: 30264912; PubMed Central PMCID: PMCPMC6438774.
195. Bustamante J, Boisson-Dupuis S, Abel L, Casanova JL. Mendelian susceptibility to mycobacterial disease: genetic, immunological, and clinical features of inborn errors of IFN-gamma immunity. *Semin Immunol.* 2014;26(6):454-70. Epub 2014/12/03. doi: 10.1016/j.smim.2014.09.008. PubMed PMID: 25453225; PubMed Central PMCID: PMCPMC4357480.
196. Flynn JL, Goldstein MM, Chan J, Triebold KJ, Pfeffer K, Lowenstein CJ, et al. Tumor necrosis factor-alpha is required in the protective immune response against *Mycobacterium tuberculosis* in mice. *Immunity.* 1995;2(6):561-72. Epub 1995/06/01. doi: 10.1016/1074-7613(95)90001-2. PubMed PMID: 7540941.
197. Keane J, Gershon S, Wise RP, Mirabile-Levens E, Kasznica J, Schwiertman WD, et al. Tuberculosis associated with infliximab, a tumor necrosis factor alpha-neutralizing agent. *N Engl J Med.* 2001;345(15):1098-104. Epub 2001/10/13. doi: 10.1056/NEJMoa011110. PubMed PMID: 11596589.

198. Lin PL, Myers A, Smith L, Bigbee C, Bigbee M, Fuhrman C, et al. Tumor necrosis factor neutralization results in disseminated disease in acute and latent *Mycobacterium tuberculosis* infection with normal granuloma structure in a cynomolgus macaque model. *Arthritis Rheum.* 2010;62(2):340-50. doi: 10.1002/art.27271. PubMed PMID: 20112395; PubMed Central PMCID: PMCPMC3047004.
199. Lin PL, Maiello P, Gideon HP, Coleman MT, Cadena AM, Rodgers MA, et al. PET CT Identifies Reactivation Risk in Cynomolgus Macaques with Latent *M. tuberculosis*. *PLoS Pathog.* 2016;12(7):e1005739. doi: 10.1371/journal.ppat.1005739. PubMed PMID: 27379816; PubMed Central PMCID: PMCPMC4933353.
200. Chen YC, Chin CH, Liu SF, Wu CC, Tsen CC, Wang YH, et al. Prognostic values of serum IP-10 and IL-17 in patients with pulmonary tuberculosis. *Dis Markers.* 2011;31(2):101-10. Epub 2011/09/08. doi: 10.3233/DMA-2011-0808. PubMed PMID: 21897004; PubMed Central PMCID: PMCPMC3826581.
201. Scriba TJ, Kalsdorf B, Abrahams DA, Isaacs F, Hofmeister J, Black G, et al. Distinct, specific IL-17- and IL-22-producing CD4+ T cell subsets contribute to the human anti-mycobacterial immune response. *J Immunol.* 2008;180(3):1962-70. Epub 2008/01/23. doi: 10.4049/jimmunol.180.3.1962. PubMed PMID: 18209095; PubMed Central PMCID: PMCPMC2219462.
202. Heidarneshad F, Asnaashari A, Rezaee SA, Ghezelsouf R, Ghazvini K, Valizadeh N, et al. Evaluation of Interleukin17 and Interleukin 23 expression in patients with active and latent tuberculosis infection. *Iran J Basic Med Sci.* 2016;19(8):844-50. Epub 2016/10/18. PubMed PMID: 27746865; PubMed Central PMCID: PMCPMC5048119.
203. Dheda K, Chang JS, Lala S, Huggett JF, Zumla A, Rook GA. Gene expression of IL17 and IL23 in the lungs of patients with active tuberculosis. *Thorax.* 2008;63(6):566-8. Epub 2008/05/31. doi: 10.1136/thx.2007.092205. PubMed PMID: 18511642.
204. Jurado JO, Pasquinelli V, Alvarez IB, Pena D, Rovetta AI, Tateosian NL, et al. IL-17 and IFN-gamma expression in lymphocytes from patients with active tuberculosis correlates with the severity of the disease. *J Leukoc Biol.* 2012;91(6):991-1002. Epub 2012/03/15. doi: 10.1189/jlb.1211619. PubMed PMID: 22416258; PubMed Central PMCID: PMCPMC3360475.
205. Gopal R, Monin L, Slight S, Uche U, Blanchard E, Fallert Junecko BA, et al. Unexpected role for IL-17 in protective immunity against hypervirulent *Mycobacterium tuberculosis* HN878 infection. *PLoS Pathog.* 2014;10(5):e1004099. doi: 10.1371/journal.ppat.1004099. PubMed PMID: 24831696; PubMed Central PMCID: PMCPMC4022785.
206. Khader SA, Bell GK, Pearl JE, Fountain JJ, Rangel-Moreno J, Cilley GE, et al. IL-23 and IL-17 in the establishment of protective pulmonary CD4+ T cell responses after vaccination and during *Mycobacterium tuberculosis* challenge. *Nat Immunol.* 2007;8(4):369-77. Epub 2007/03/14. doi: 10.1038/ni1449. PubMed PMID: 17351619.

207. O'Leary S, O'Sullivan MP, Keane J. IL-10 blocks phagosome maturation in mycobacterium tuberculosis-infected human macrophages. *Am J Respir Cell Mol Biol.* 2011;45(1):172-80. Epub 2010/10/05. doi: 10.1165/rcmb.2010-0319OC. PubMed PMID: 20889800.
208. Gong JH, Zhang M, Modlin RL, Linsley PS, Iyer D, Lin Y, et al. Interleukin-10 downregulates Mycobacterium tuberculosis-induced Th1 responses and CTLA-4 expression. *Infect Immun.* 1996;64(3):913-8. Epub 1996/03/01. PubMed PMID: 8641800; PubMed Central PMCID: PMCPMC173856.
209. Redford PS, Boonstra A, Read S, Pitt J, Graham C, Stavropoulos E, et al. Enhanced protection to Mycobacterium tuberculosis infection in IL-10-deficient mice is accompanied by early and enhanced Th1 responses in the lung. *Eur J Immunol.* 2010;40(8):2200-10. Epub 2010/06/03. doi: 10.1002/eji.201040433. PubMed PMID: 20518032; PubMed Central PMCID: PMCPMC3378704.
210. Turner J, Gonzalez-Juarrero M, Ellis DL, Basaraba RJ, Kipnis A, Orme IM, et al. In vivo IL-10 production reactivates chronic pulmonary tuberculosis in C57BL/6 mice. *J Immunol.* 2002;169(11):6343-51. Epub 2002/11/22. doi: 10.4049/jimmunol.169.11.6343. PubMed PMID: 12444141.
211. Beamer GL, Flaherty DK, Assogba BD, Stromberg P, Gonzalez-Juarrero M, de Waal Malefyt R, et al. Interleukin-10 promotes Mycobacterium tuberculosis disease progression in CBA/J mice. *J Immunol.* 2008;181(8):5545-50. Epub 2008/10/04. doi: 10.4049/jimmunol.181.8.5545. PubMed PMID: 18832712; PubMed Central PMCID: PMCPMC2728584.
212. Wong EA, Evans S, Kraus CR, Engelman KD, Maiello P, Flores WJ, et al. IL-10 Impairs Local Immune Response in Lung Granulomas and Lymph Nodes during Early Mycobacterium tuberculosis Infection. *J Immunol.* 2020;204(3):644-59. Epub 2019/12/22. doi: 10.4049/jimmunol.1901211. PubMed PMID: 31862711; PubMed Central PMCID: PMCPMC6981067.
213. Andersen P, Woodworth JS. Tuberculosis vaccines--rethinking the current paradigm. *Trends Immunol.* 2014;35(8):387-95. Epub 2014/05/31. doi: 10.1016/j.it.2014.04.006. PubMed PMID: 24875637.
214. Glatman-Freedman A, Casadevall A. Serum therapy for tuberculosis revisited: reappraisal of the role of antibody-mediated immunity against Mycobacterium tuberculosis. *Clin Microbiol Rev.* 1998;11(3):514-32. Epub 1998/07/17. PubMed PMID: 9665981; PubMed Central PMCID: PMCPMC88894.
215. Achkar JM, Casadevall A. Antibody-mediated immunity against tuberculosis: implications for vaccine development. *Cell Host Microbe.* 2013;13(3):250-62. Epub 2013/03/19. doi: 10.1016/j.chom.2013.02.009. PubMed PMID: 23498951; PubMed Central PMCID: PMCPMC3759397.
216. Lu LL, Chung AW, Rosebrock TR, Ghebremichael M, Yu WH, Grace PS, et al. A Functional Role for Antibodies in Tuberculosis. *Cell.* 2016;167(2):433-43 e14. Epub

- 2016/09/27. doi: 10.1016/j.cell.2016.08.072. PubMed PMID: 27667685; PubMed Central PMCID: PMC5526202.
217. Phuah JY, Mattila JT, Lin PL, Flynn JL. Activated B cells in the granulomas of nonhuman primates infected with Mycobacterium tuberculosis. *Am J Pathol.* 2012;181(2):508-14. doi: 10.1016/j.ajpath.2012.05.009. PubMed PMID: 22721647; PubMed Central PMCID: PMC3409439.
 218. Phuah J, Wong EA, Gideon HP, Maiello P, Coleman MT, Hendricks MR, et al. Effects of B Cell Depletion on Early Mycobacterium tuberculosis Infection in Cynomolgus Macaques. *Infect Immun.* 2016;84(5):1301-11. Epub 2016/02/18. doi: 10.1128/IAI.00083-16. PubMed PMID: 26883591; PubMed Central PMCID: PMC4862708.
 219. Slight SR, Rangel-Moreno J, Gopal R, Lin Y, Fallert Junecko BA, Mehra S, et al. CXCR5(+) T helper cells mediate protective immunity against tuberculosis. *J Clin Invest.* 2013;123(2):712-26. Epub 2013/01/03. doi: 10.1172/JCI65728. PubMed PMID: 23281399; PubMed Central PMCID: PMC3561804.
 220. Chackerian AA, Behar SM. Susceptibility to Mycobacterium tuberculosis: lessons from inbred strains of mice. *Tuberculosis (Edinb).* 2003;83(5):279-85. Epub 2003/09/16. doi: 10.1016/s1472-9792(03)00017-9. PubMed PMID: 12972341.
 221. Singh AK, Gupta UD. Animal models of tuberculosis: Lesson learnt. *Indian J Med Res.* 2018;147(5):456-63. Epub 2018/08/08. doi: 10.4103/ijmr.IJMR_554_18. PubMed PMID: 30082569; PubMed Central PMCID: PMC6094516.
 222. Miyazaki E, Chaisson RE, Bishai WR. Analysis of rifapentine for preventive therapy in the Cornell mouse model of latent tuberculosis. *Antimicrob Agents Chemother.* 1999;43(9):2126-30. Epub 1999/09/03. PubMed PMID: 10471552; PubMed Central PMCID: PMC89434.
 223. Kupz A, Zedler U, Staber M, Kaufmann SH. A Mouse Model of Latent Tuberculosis Infection to Study Intervention Strategies to Prevent Reactivation. *PLoS One.* 2016;11(7):e0158849. Epub 2016/07/09. doi: 10.1371/journal.pone.0158849. PubMed PMID: 27391012; PubMed Central PMCID: PMC4938611.
 224. Subbian S, Tsenova L, Yang G, O'Brien P, Parsons S, Peixoto B, et al. Chronic pulmonary cavitary tuberculosis in rabbits: a failed host immune response. *Open Biol.* 2011;1(4):110016. Epub 2012/05/31. doi: 10.1098/rsob.110016. PubMed PMID: 22645653; PubMed Central PMCID: PMC3352086.
 225. Gong W, Liang Y, Wu X. Animal Models of Tuberculosis Vaccine Research: An Important Component in the Fight against Tuberculosis. *Biomed Res Int.* 2020;2020:4263079. Epub 2020/02/07. doi: 10.1155/2020/4263079. PubMed PMID: 32025519; PubMed Central PMCID: PMC6984742 conflict of interest.
 226. Sugawara I, Udagawa T, Aoki T, Mizuno S. Establishment of a guinea pig model of latent tuberculosis with GFP-introduced Mycobacterium tuberculosis. *Tohoku J Exp Med.*

- 2009;219(3):257-62. Epub 2009/10/24. doi: 10.1620/tjem.219.257. PubMed PMID: 19851055.
227. Subbian S, Tsenova L, O'Brien P, Yang G, Kushner NL, Parsons S, et al. Spontaneous latency in a rabbit model of pulmonary tuberculosis. *Am J Pathol.* 2012;181(5):1711-24. Epub 2012/09/11. doi: 10.1016/j.ajpath.2012.07.019. PubMed PMID: 22960076; PubMed Central PMCID: PMC3483799.
228. Manabe YC, Kesavan AK, Lopez-Molina J, Hatem CL, Brooks M, Fujiwara R, et al. The aerosol rabbit model of TB latency, reactivation and immune reconstitution inflammatory syndrome. *Tuberculosis (Edinb).* 2008;88(3):187-96. Epub 2007/12/11. doi: 10.1016/j.tube.2007.10.006. PubMed PMID: 18068491; PubMed Central PMCID: PMC4477206.
229. van Leeuwen LM, van der Sar AM, Bitter W. Animal models of tuberculosis: zebrafish. *Cold Spring Harb Perspect Med.* 2014;5(3):a018580. Epub 2014/11/22. doi: 10.1101/cshperspect.a018580. PubMed PMID: 25414379; PubMed Central PMCID: PMC4355259.
230. Scanga CA, Flynn JL. Modeling tuberculosis in nonhuman primates. *Cold Spring Harb Perspect Med.* 2014;4(12):a018564. doi: 10.1101/cshperspect.a018564. PubMed PMID: 25213189; PubMed Central PMCID: PMC4292094.
231. Lin PL, Pawar S, Myers A, Pegu A, Fuhrman C, Reinhart TA, et al. Early events in *Mycobacterium tuberculosis* infection in cynomolgus macaques. *Infect Immun.* 2006;74(7):3790-803. doi: 10.1128/IAI.00064-06. PubMed PMID: 16790751; PubMed Central PMCID: PMC1489679.
232. Lin PL, Rodgers M, Smith L, Bigbee M, Myers A, Bigbee C, et al. Quantitative comparison of active and latent tuberculosis in the cynomolgus macaque model. *Infect Immun.* 2009;77(10):4631-42. doi: 10.1128/IAI.00592-09. PubMed PMID: 19620341; PubMed Central PMCID: PMC2747916.
233. Capuano SV, 3rd, Croix DA, Pawar S, Zinovik A, Myers A, Lin PL, et al. Experimental *Mycobacterium tuberculosis* infection of cynomolgus macaques closely resembles the various manifestations of human *M. tuberculosis* infection. *Infect Immun.* 2003;71(10):5831-44. PubMed PMID: 14500505; PubMed Central PMCID: PMC201048.
234. Flynn JL, Gideon HP, Mattila JT, Lin PL. Immunology studies in non-human primate models of tuberculosis. *Immunol Rev.* 2015;264(1):60-73. Epub 2015/02/24. doi: 10.1111/imr.12258. PubMed PMID: 25703552; PubMed Central PMCID: PMC4339213.
235. Maiello P, DiFazio RM, Cadena AM, Rodgers MA, Lin PL, Scanga CA, et al. Rhesus macaques are more susceptible to progressive tuberculosis than cynomolgus macaques: A quantitative comparison. *Infect Immun.* 2017. doi: 10.1128/IAI.00505-17. PubMed PMID: 28947646.

236. White AG, Maiello P, Coleman MT, Tomko JA, Frye LJ, Scanga CA, et al. Analysis of 18FDG PET/CT Imaging as a Tool for Studying Mycobacterium tuberculosis Infection and Treatment in Non-human Primates. *J Vis Exp.* 2017;(127). doi: 10.3791/56375. PubMed PMID: 28930979.
237. Esposito S, Tagliabue C, Bosis S. Tuberculosis in children. *Mediterr J Hematol Infect Dis.* 2013;5(1):e2013064. Epub 2013/12/24. doi: 10.4084/MJHID.2013.064. PubMed PMID: 24363879; PubMed Central PMCID: PMC3867258.
238. Blacklock JW. The Primary Lung Focus of Tuberculosis in Children. *Proc R Soc Med.* 1932;25(5):725-33. PubMed PMID: 19988654; PubMed Central PMCID: PMC2183650.
239. Myers JA. The natural history of tuberculosis in the human body; forty-five years of observation. *JAMA.* 1965;194(10):1086-92. PubMed PMID: 5294688.
240. Prakasha SR, Suresh G, D'Sa I P, Shetty SS, Kumar SG. Mapping the pattern and trends of extrapulmonary tuberculosis. *J Glob Infect Dis.* 2013;5(2):54-9. doi: 10.4103/0974-777X.112277. PubMed PMID: 23853432; PubMed Central PMCID: PMC3703211.
241. Peto HM, Pratt RH, Harrington TA, LoBue PA, Armstrong LR. Epidemiology of extrapulmonary tuberculosis in the United States, 1993-2006. *Clin Infect Dis.* 2009;49(9):1350-7. doi: 10.1086/605559. PubMed PMID: 19793000.
242. Loomis HP. Some facts in the etiology of tuberculosis, evidenced by thirty autopsies and experiments upon animals. *Medical Record.* 1890;38(25):689.
243. Wang CY. An experimental study of latent tuberculosis. *Lancet.* 1916;188(4853):417-9.
244. Dutta NK, Karakousis PC. Latent tuberculosis infection: myths, models, and molecular mechanisms. *Microbiol Mol Biol Rev.* 2014;78(3):343-71. Epub 2014/09/04. doi: 10.1128/MMBR.00010-14. PubMed PMID: 25184558; PubMed Central PMCID: PMC4187682.
245. Neill SD, Bryson DG, Pollock JM. Pathogenesis of tuberculosis in cattle. *Tuberculosis (Edinb).* 2001;81(1-2):79-86. Epub 2001/07/21. doi: 10.1054/tube.2000.0279. PubMed PMID: 11463227.
246. Whipple DL, Bolin CA, Miller JM. Distribution of lesions in cattle infected with *Mycobacterium bovis*. *J Vet Diagn Invest.* 1996;8(3):351-4. doi: 10.1177/104063879600800312. PubMed PMID: 8844579.
247. Van Rhijn I, Godfroid J, Michel A, Rutten V. Bovine tuberculosis as a model for human tuberculosis: advantages over small animal models. *Microbes Infect.* 2008;10(7):711-5. Epub 2008/06/10. doi: 10.1016/j.micinf.2008.04.005. PubMed PMID: 18538612.

248. Behr MA, Waters WR. Is tuberculosis a lymphatic disease with a pulmonary portal? *Lancet Infect Dis.* 2014;14(3):250-5. doi: 10.1016/S1473-3099(13)70253-6. PubMed PMID: 24268591.
249. Moltedo B, Li W, Yount JS, Moran TM. Unique type I interferon responses determine the functional fate of migratory lung dendritic cells during influenza virus infection. *PLoS Pathog.* 2011;7(11):e1002345. Epub 2011/11/11. doi: 10.1371/journal.ppat.1002345. PubMed PMID: 22072965; PubMed Central PMCID: PMC3207893.
250. Kim TS, Braciale TJ. Respiratory dendritic cell subsets differ in their capacity to support the induction of virus-specific cytotoxic CD8+ T cell responses. *PLoS One.* 2009;4(1):e4204. Epub 2009/01/16. doi: 10.1371/journal.pone.0004204. PubMed PMID: 19145246; PubMed Central PMCID: PMC2615220.
251. Rosendahl A, Bergmann S, Hammerschmidt S, Goldmann O, Medina E. Lung dendritic cells facilitate extrapulmonary bacterial dissemination during pneumococcal pneumonia. *Front Cell Infect Microbiol.* 2013;3:21. Epub 2013/06/27. doi: 10.3389/fcimb.2013.00021. PubMed PMID: 23802100; PubMed Central PMCID: PMC3689026.
252. Diedrich CR, Mattila JT, Klein E, Janssen C, Phuah J, Sturgeon TJ, et al. Reactivation of latent tuberculosis in cynomolgus macaques infected with SIV is associated with early peripheral T cell depletion and not virus load. *PLoS One.* 2010;5(3):e9611. Epub 2010/03/13. doi: 10.1371/journal.pone.0009611. PubMed PMID: 20224771; PubMed Central PMCID: PMC2835744.
253. Esmail H, Lai RP, Lesosky M, Wilkinson KA, Graham CM, Coussens AK, et al. Characterization of progressive HIV-associated tuberculosis using 2-deoxy-2-[18F]fluoro-D-glucose positron emission and computed tomography. *Nat Med.* 2016;22(10):1090-3. doi: 10.1038/nm.4161. PubMed PMID: 27595321; PubMed Central PMCID: PMC5055809.
254. Waeckerle-Men Y, Bruffaerts N, Liang Y, Jurion F, Sander P, Kundig TM, et al. Lymph node targeting of BCG vaccines amplifies CD4 and CD8 T-cell responses and protection against *Mycobacterium tuberculosis*. *Vaccine.* 2013;31(7):1057-64. Epub 2013/01/01. doi: 10.1016/j.vaccine.2012.12.034. PubMed PMID: 23273509.
255. Kislitsyna NA. [Comparative evaluation of rifampicin and isoniazid penetration into the pathological foci of the lungs in tuberculosis patients]. *Probl Tuberk.* 1985;(4):55-7. Epub 1985/01/01. PubMed PMID: 4001111.
256. Dartois V, Barry CE. Clinical pharmacology and lesion penetrating properties of second- and third-line antituberculous agents used in the management of multidrug-resistant (MDR) and extensively-drug resistant (XDR) tuberculosis. *Curr Clin Pharmacol.* 2010;5(2):96-114. Epub 2010/02/17. doi: 10.2174/157488410791110797. PubMed PMID: 20156156; PubMed Central PMCID: PMC344931.
257. Andrews JR, Noubary F, Walensky RP, Cerda R, Losina E, Horsburgh CR. Risk of progression to active tuberculosis following reinfection with *Mycobacterium tuberculosis*.

- Clin Infect Dis. 2012;54(6):784-91. Epub 2012/01/24. doi: 10.1093/cid/cir951. PubMed PMID: 22267721; PubMed Central PMCID: PMCPMC3284215.
258. Cohen T, van Helden PD, Wilson D, Colijn C, McLaughlin MM, Abubakar I, et al. Mixed-strain mycobacterium tuberculosis infections and the implications for tuberculosis treatment and control. *Clin Microbiol Rev.* 2012;25(4):708-19. Epub 2012/10/05. doi: 10.1128/CMR.00021-12. PubMed PMID: 23034327; PubMed Central PMCID: PMCPMC3485752.
 259. Kanai K, Yanagisawa K. Studies on the reinfection in experimental tuberculosis of rats. *Jpn J Med Sci Biol.* 1955;8(2):129-34. Epub 1955/04/01. doi: 10.7883/yoken1952.8.129. PubMed PMID: 13278106.
 260. Kanai K, Yanagisawa K. Studies on the reinfection in experimental tuberculosis of guinea pigs. *Jpn J Med Sci Biol.* 1955;8(2):115-27. Epub 1955/04/01. doi: 10.7883/yoken1952.8.115. PubMed PMID: 13278105.
 261. Ratcliffe HL, Wells WF. Tuberculosis of rabbits induced by droplet nuclei infection; response to reinfection. *J Exp Med.* 1948;87(6):585-94. Epub 1948/06/01. doi: 10.1084/jem.87.6.585. PubMed PMID: 18858647; PubMed Central PMCID: PMCPMC2135791.
 262. Lurie MB. The Fate of Tubercle Bacilli in the Organs of Reinfected Rabbits. *J Exp Med.* 1929;50(6):747-65. Epub 1929/11/30. doi: 10.1084/jem.50.6.747. PubMed PMID: 19869661; PubMed Central PMCID: PMCPMC2131660.
 263. Henao-Tamayo M, Obregon-Henao A, Ordway DJ, Shang S, Duncan CG, Orme IM. A mouse model of tuberculosis reinfection. *Tuberculosis (Edinb).* 2012;92(3):211-7. Epub 2012/03/21. doi: 10.1016/j.tube.2012.02.008. PubMed PMID: 22429719.
 264. Cadena AM, Hopkins FF, Maiello P, Carey AF, Wong EA, Martin CJ, et al. Concurrent infection with Mycobacterium tuberculosis confers robust protection against secondary infection in macaques. *PLoS Pathog.* 2018;14(10):e1007305. Epub 2018/10/13. doi: 10.1371/journal.ppat.1007305. PubMed PMID: 30312351; PubMed Central PMCID: PMCPMC6200282.
 265. Shen X, Yang C, Wu J, Lin S, Gao X, Wu Z, et al. Recurrent tuberculosis in an urban area in China: Relapse or exogenous reinfection? *Tuberculosis (Edinb).* 2017;103:97-104. Epub 2017/02/27. doi: 10.1016/j.tube.2017.01.007. PubMed PMID: 28237039; PubMed Central PMCID: PMCPMC5638046.
 266. Millet JP, Orcau A, de Olalla PG, Casals M, Rius C, Cayla JA. Tuberculosis recurrence and its associated risk factors among successfully treated patients. *J Epidemiol Community Health.* 2009;63(10):799-804. Epub 2009/01/31. doi: 10.1136/jech.2008.077560. PubMed PMID: 19179367.
 267. Verver S, Warren RM, Beyers N, Richardson M, van der Spuy GD, Borgdorff MW, et al. Rate of reinfection tuberculosis after successful treatment is higher than rate of new

- tuberculosis. *Am J Respir Crit Care Med.* 2005;171(12):1430-5. Epub 2005/04/16. doi: 10.1164/rccm.200409-1200OC. PubMed PMID: 15831840.
268. Lin PL, Dartois V, Johnston PJ, Janssen C, Via L, Goodwin MB, et al. Metronidazole prevents reactivation of latent *Mycobacterium tuberculosis* infection in macaques. *Proc Natl Acad Sci U S A.* 2012;109(35):14188-93. Epub 2012/07/25. doi: 10.1073/pnas.1121497109. PubMed PMID: 22826237; PubMed Central PMCID: PMC3435210.
269. Condos R, Rom WN, Liu YM, Schluger NW. Local immune responses correlate with presentation and outcome in tuberculosis. *Am J Respir Crit Care Med.* 1998;157(3 Pt 1):729-35. Epub 1998/03/28. doi: 10.1164/ajrccm.157.3.9705044. PubMed PMID: 9517583.
270. Ainslie GM, Solomon JA, Bateman ED. Lymphocyte and lymphocyte subset numbers in blood and in bronchoalveolar lavage and pleural fluid in various forms of human pulmonary tuberculosis at presentation and during recovery. *Thorax.* 1992;47(7):513-8. Epub 1992/07/01. doi: 10.1136/thx.47.7.513. PubMed PMID: 1412093; PubMed Central PMCID: PMC463860.
271. Luzze H, Johnson DF, Dickman K, Mayanja-Kizza H, Okwera A, Eisenach K, et al. Relapse more common than reinfection in recurrent tuberculosis 1-2 years post treatment in urban Uganda. *Int J Tuberc Lung Dis.* 2013;17(3):361-7. Epub 2013/02/15. doi: 10.5588/ijtld.11.0692. PubMed PMID: 23407224; PubMed Central PMCID: PMC6623981.
272. Marx FM, Dunbar R, Enarson DA, Williams BG, Warren RM, van der Spuy GD, et al. The temporal dynamics of relapse and reinfection tuberculosis after successful treatment: a retrospective cohort study. *Clin Infect Dis.* 2014;58(12):1676-83. Epub 2014/03/22. doi: 10.1093/cid/ciu186. PubMed PMID: 24647020.
273. Uys P, Brand H, Warren R, van der Spuy G, Hoal EG, van Helden PD. The Risk of Tuberculosis Reinfection Soon after Cure of a First Disease Episode Is Extremely High in a Hyperendemic Community. *PLoS One.* 2015;10(12):e0144487. Epub 2015/12/10. doi: 10.1371/journal.pone.0144487. PubMed PMID: 26649422; PubMed Central PMCID: PMC4674135.
274. Lawn SD, Myer L, Edwards D, Bekker LG, Wood R. Short-term and long-term risk of tuberculosis associated with CD4 cell recovery during antiretroviral therapy in South Africa. *AIDS.* 2009;23(13):1717-25. Epub 2009/05/23. doi: 10.1097/QAD.0b013e32832d3b6d. PubMed PMID: 19461502; PubMed Central PMCID: PMC3801095.
275. Wessler T, Joslyn LR, Borish HJ, Gideon HP, Flynn JL, Kirschner DE, et al. A computational model tracks whole-lung *Mycobacterium tuberculosis* infection and predicts factors that inhibit dissemination. *PLoS Comput Biol.* 2020;16(5):e1007280. Epub 2020/05/21. doi: 10.1371/journal.pcbi.1007280. PubMed PMID: 32433646; PubMed Central PMCID: PMC7239387.

276. Lin PL, Coleman T, Carney JP, Lopresti BJ, Tomko J, Fillmore D, et al. Radiologic Responses in Cynomolgus Macaques for Assessing Tuberculosis Chemotherapy Regimens. *Antimicrob Agents Chemother.* 2013;57(9):4237-44. doi: 10.1128/AAC.00277-13. PubMed PMID: 23796926; PubMed Central PMCID: PMC3754323.
277. Laidlaw BJ, Craft JE, Kaech SM. The multifaceted role of CD4(+) T cells in CD8(+) T cell memory. *Nat Rev Immunol.* 2016;16(2):102-11. Epub 2016/01/20. doi: 10.1038/nri.2015.10. PubMed PMID: 26781939; PubMed Central PMCID: PMC4860014.
278. Serbina NV, Lazarevic V, Flynn JL. CD4(+) T cells are required for the development of cytotoxic CD8(+) T cells during Mycobacterium tuberculosis infection. *J Immunol.* 2001;167(12):6991-7000. Epub 2001/12/12. doi: 10.4049/jimmunol.167.12.6991. PubMed PMID: 11739519.
279. Novy P, Quigley M, Huang X, Yang Y. CD4 T cells are required for CD8 T cell survival during both primary and memory recall responses. *J Immunol.* 2007;179(12):8243-51. Epub 2007/12/07. doi: 10.4049/jimmunol.179.12.8243. PubMed PMID: 18056368.
280. Zhang S, Zhang H, Zhao J. The role of CD4 T cell help for CD8 CTL activation. *Biochem Biophys Res Commun.* 2009;384(4):405-8. Epub 2009/05/05. doi: 10.1016/j.bbrc.2009.04.134. PubMed PMID: 19410556.
281. Bold TD, Ernst JD. CD4+ T cell-dependent IFN-gamma production by CD8+ effector T cells in Mycobacterium tuberculosis infection. *J Immunol.* 2012;189(5):2530-6. Epub 2012/07/28. doi: 10.4049/jimmunol.1200994. PubMed PMID: 22837486; PubMed Central PMCID: PMC3424308.
282. Sun JC, Bevan MJ. Defective CD8 T cell memory following acute infection without CD4 T cell help. *Science.* 2003;300(5617):339-42. Epub 2003/04/12. doi: 10.1126/science.1083317. PubMed PMID: 12690202; PubMed Central PMCID: PMC3424308.
283. Janssen EM, Lemmens EE, Wolfe T, Christen U, von Herrath MG, Schoenberger SP. CD4+ T cells are required for secondary expansion and memory in CD8+ T lymphocytes. *Nature.* 2003;421(6925):852-6. Epub 2003/02/21. doi: 10.1038/nature01441. PubMed PMID: 12594515.
284. Shedlock DJ, Shen H. Requirement for CD4 T cell help in generating functional CD8 T cell memory. *Science.* 2003;300(5617):337-9. Epub 2003/04/12. doi: 10.1126/science.1082305. PubMed PMID: 12690201.
285. Gallegos AM, van Heijst JW, Samstein M, Su X, Pamer EG, Glickman MS. A gamma interferon independent mechanism of CD4 T cell mediated control of M. tuberculosis infection in vivo. *PLoS Pathog.* 2011;7(5):e1002052. Epub 2011/06/01. doi: 10.1371/journal.ppat.1002052. PubMed PMID: 21625591; PubMed Central PMCID: PMC3098235.

286. Khader SA, Pearl JE, Sakamoto K, Gilmartin L, Bell GK, Jelley-Gibbs DM, et al. IL-23 compensates for the absence of IL-12p70 and is essential for the IL-17 response during tuberculosis but is dispensable for protection and antigen-specific IFN-gamma responses if IL-12p70 is available. *J Immunol.* 2005;175(2):788-95. Epub 2005/07/09. doi: 10.4049/jimmunol.175.2.788. PubMed PMID: 16002675.
287. Wilson NJ, Boniface K, Chan JR, McKenzie BS, Blumenschein WM, Mattson JD, et al. Development, cytokine profile and function of human interleukin 17-producing helper T cells. *Nat Immunol.* 2007;8(9):950-7. Epub 2007/08/07. doi: 10.1038/ni1497. PubMed PMID: 17676044.
288. Oppmann B, Lesley R, Blom B, Timans JC, Xu Y, Hunte B, et al. Novel p19 protein engages IL-12p40 to form a cytokine, IL-23, with biological activities similar as well as distinct from IL-12. *Immunity.* 2000;13(5):715-25. Epub 2000/12/15. doi: 10.1016/s1074-7613(00)00070-4. PubMed PMID: 11114383.
289. Aggarwal S, Ghilardi N, Xie MH, de Sauvage FJ, Gurney AL. Interleukin-23 promotes a distinct CD4 T cell activation state characterized by the production of interleukin-17. *J Biol Chem.* 2003;278(3):1910-4. Epub 2002/11/06. doi: 10.1074/jbc.M207577200. PubMed PMID: 12417590.
290. Stockinger B, Veldhoen M. Differentiation and function of Th17 T cells. *Curr Opin Immunol.* 2007;19(3):281-6. Epub 2007/04/17. doi: 10.1016/j.coi.2007.04.005. PubMed PMID: 17433650.
291. Lockhart E, Green AM, Flynn JL. IL-17 production is dominated by gammadelta T cells rather than CD4 T cells during *Mycobacterium tuberculosis* infection. *J Immunol.* 2006;177(7):4662-9. Epub 2006/09/20. doi: 10.4049/jimmunol.177.7.4662. PubMed PMID: 16982905.
292. Chackerian AA, Chen SJ, Brodie SJ, Mattson JD, McClanahan TK, Kastelein RA, et al. Neutralization or absence of the interleukin-23 pathway does not compromise immunity to mycobacterial infection. *Infect Immun.* 2006;74(11):6092-9. Epub 2006/08/23. doi: 10.1128/IAI.00621-06. PubMed PMID: 16923792; PubMed Central PMCID: PMC1695481.
293. Happel KI, Lockhart EA, Mason CM, Porretta E, Keoshkerian E, Odden AR, et al. Pulmonary interleukin-23 gene delivery increases local T-cell immunity and controls growth of *Mycobacterium tuberculosis* in the lungs. *Infect Immun.* 2005;73(9):5782-8. Epub 2005/08/23. doi: 10.1128/IAI.73.9.5782-5788.2005. PubMed PMID: 16113296; PubMed Central PMCID: PMC1231058.
294. Okamoto Yoshida Y, Umemura M, Yahagi A, O'Brien RL, Ikuta K, Kishihara K, et al. Essential role of IL-17A in the formation of a mycobacterial infection-induced granuloma in the lung. *J Immunol.* 2010;184(8):4414-22. Epub 2010/03/10. doi: 10.4049/jimmunol.0903332. PubMed PMID: 20212094.

295. Lombard R, Doz E, Carreras F, Epardaud M, Le Vern Y, Buzoni-Gatel D, et al. IL-17RA in Non-Hematopoietic Cells Controls CXCL-1 and 5 Critical to Recruit Neutrophils to the Lung of Mycobacteria-Infected Mice during the Adaptive Immune Response. *PLoS One*. 2016;11(2):e0149455. Epub 2016/02/13. doi: 10.1371/journal.pone.0149455. PubMed PMID: 26871571; PubMed Central PMCID: PMC4752258.
296. Foreman TW, Mehra S, LoBato DN, Malek A, Alvarez X, Golden NA, et al. CD4+ T-cell-independent mechanisms suppress reactivation of latent tuberculosis in a macaque model of HIV coinfection. *Proc Natl Acad Sci U S A*. 2016;113(38):E5636-44. Epub 2016/09/08. doi: 10.1073/pnas.1611987113. PubMed PMID: 27601645; PubMed Central PMCID: PMC45035858.
297. Netea MG, van Crevel R. BCG-induced protection: effects on innate immune memory. *Semin Immunol*. 2014;26(6):512-7. Epub 2014/12/03. doi: 10.1016/j.smim.2014.09.006. PubMed PMID: 25444548.
298. Choreno-Parra JA, Weinstein LI, Yunis EJ, Zuniga J, Hernandez-Pando R. Thinking Outside the Box: Innate- and B Cell-Memory Responses as Novel Protective Mechanisms Against Tuberculosis. *Front Immunol*. 2020;11:226. Epub 2020/03/03. doi: 10.3389/fimmu.2020.00226. PubMed PMID: 32117325; PubMed Central PMCID: PMC7034257.
299. WHO. Global Tuberculosis Report 20172017.
300. Talmi YP, Finkelstein Y, Tov YS, Zohar Y, Laurian N. Scrofula revisited. *J Laryngol Otol*. 1988;102(4):387-8. PubMed PMID: 3290370.
301. German JL, Black TC, Chapman JS. Tuberculosis of superficial lymph nodes. *Dis Chest*. 1956;30(3):326-37. PubMed PMID: 13356734.
302. Grzybowski S, Allen EA. History and importance of scrofula. *Lancet*. 1995;346(8988):1472-4. PubMed PMID: 7490997.
303. Krishna M, Gole SG. Comparison of Conventional Ziehl-Neelsen Method of Acid Fast Bacilli with Modified Bleach Method in Tuberculous Lymphadenitis. *J Cytol*. 2017;34(4):188-92. doi: 10.4103/JOC.JOC_84_16. PubMed PMID: 29118472; PubMed Central PMCID: PMC5655654.
304. Fontanilla JM, Barnes A, von Reyn CF. Current diagnosis and management of peripheral tuberculous lymphadenitis. *Clin Infect Dis*. 2011;53(6):555-62. Epub 2011/08/26. doi: 10.1093/cid/cir454. PubMed PMID: 21865192.
305. Diedrich CR, O'Hern J, Gutierrez MG, Allie N, Papier P, Meintjes G, et al. Relationship Between HIV Coinfection, Interleukin 10 Production, and Mycobacterium tuberculosis in Human Lymph Node Granulomas. *J Infect Dis*. 2016;214(9):1309-18. doi: 10.1093/infdis/jiw313. PubMed PMID: 27462092; PubMed Central PMCID: PMC5079364.

306. Heysell SK, Thomas TA, Sifri CD, Rehm PK, Houtp ER. 18-Fluorodeoxyglucose positron emission tomography for tuberculosis diagnosis and management: a case series. *BMC Pulm Med.* 2013;13:14. doi: 10.1186/1471-2466-13-14. PubMed PMID: 23514625; PubMed Central PMCID: PMC3637578.
307. Ghesani N, Patrawalla A, Lardizabal A, Salgame P. Increased Cellular Activity in Thoracic Lymph Nodes in Early Human Latent Tuberculosis Infection. *Am J Respir Crit Care Med.* 2014;189(6):748-50.
308. Myers AJ, Marino S, Kirschner DE, Flynn JL. Inoculation dose of Mycobacterium tuberculosis does not influence priming of T cell responses in lymph nodes. *J Immunol.* 2013;190(9):4707-16. doi: 10.4049/jimmunol.1203465. PubMed PMID: 23547119; PubMed Central PMCID: PMC3674545.
309. Zhan L, Tang J, Sun M, Qin C. Animal Models for Tuberculosis in Translational and Precision Medicine. *Front Microbiol.* 2017;8:717. Epub 2017/05/20. doi: 10.3389/fmicb.2017.00717. PubMed PMID: 28522990; PubMed Central PMCID: PMC5415616.
310. Basaraba RJ, Dailey DD, McFarland CT, Shanley CA, Smith EE, McMurray DN, et al. Lymphadenitis as a major element of disease in the guinea pig model of tuberculosis. *Tuberculosis (Edinb).* 2006;86(5):386-94. Epub 2006/02/14. doi: 10.1016/j.tube.2005.11.003. PubMed PMID: 16473044.
311. Kraft SL, Dailey D, Kovach M, Stasiak KL, Bennett J, McFarland CT, et al. Magnetic resonance imaging of pulmonary lesions in guinea pigs infected with Mycobacterium tuberculosis. *Infect Immun.* 2004;72(10):5963-71. Epub 2004/09/24. doi: 10.1128/IAI.72.10.5963-5971.2004. PubMed PMID: 15385500; PubMed Central PMCID: PMC517538.
312. Ordway D, Palanisamy G, Henao-Tamayo M, Smith EE, Shanley C, Orme IM, et al. The cellular immune response to Mycobacterium tuberculosis infection in the guinea pig. *J Immunol.* 2007;179(4):2532-41. Epub 2007/08/07. PubMed PMID: 17675515.
313. Cassidy JP, Bryson DG, Pollock JM, Evans RT, Forster F, Neill SD. Early lesion formation in cattle experimentally infected with Mycobacterium bovis. *J Comp Pathol.* 1998;119(1):27-44. Epub 1998/08/26. PubMed PMID: 9717125.
314. Bajenoff M, Granjeaud S, Guerder S. The strategy of T cell antigen-presenting cell encounter in antigen-draining lymph nodes revealed by imaging of initial T cell activation. *J Exp Med.* 2003;198(5):715-24. doi: 10.1084/jem.20030167. PubMed PMID: 12953093; PubMed Central PMCID: PMC362194192.
315. Chtanova T, Han SJ, Schaeffer M, van Dooren GG, Herzmark P, Striepen B, et al. Dynamics of T cell, antigen-presenting cell, and pathogen interactions during recall responses in the lymph node. *Immunity.* 2009;31(2):342-55. doi: 10.1016/j.immuni.2009.06.023. PubMed PMID: 19699173; PubMed Central PMCID: PMC3704215.

316. Hickman HD, Takeda K, Skon CN, Murray FR, Hensley SE, Loomis J, et al. Direct priming of antiviral CD8+ T cells in the peripheral interfollicular region of lymph nodes. *Nat Immunol.* 2008;9(2):155-65. doi: 10.1038/ni1557. PubMed PMID: 18193049.
317. Junt T, Moseman EA, Iannacone M, Massberg S, Lang PA, Boes M, et al. Subcapsular sinus macrophages in lymph nodes clear lymph-borne viruses and present them to antiviral B cells. *Nature.* 2007;450(7166):110-4. doi: 10.1038/nature06287. PubMed PMID: 17934446.
318. Bajenoff M, Egen JG, Koo LY, Laugier JP, Brau F, Glaichenhaus N, et al. Stromal cell networks regulate lymphocyte entry, migration, and territoriality in lymph nodes. *Immunity.* 2006;25(6):989-1001. doi: 10.1016/j.immuni.2006.10.011. PubMed PMID: 17112751; PubMed Central PMCID: PMCPMC2692293.
319. Gray EE, Cyster JG. Lymph node macrophages. *J Innate Immun.* 2012;4(5-6):424-36. doi: 10.1159/000337007. PubMed PMID: 22488251; PubMed Central PMCID: PMCPMC3574571.
320. Roozendaal R, Mempel TR, Pitcher LA, Gonzalez SF, Verschoor A, Mebius RE, et al. Conduits mediate transport of low-molecular-weight antigen to lymph node follicles. *Immunity.* 2009;30(2):264-76. doi: 10.1016/j.immuni.2008.12.014. PubMed PMID: 19185517; PubMed Central PMCID: PMCPMC2699624.
321. Sixt M, Kanazawa N, Selg M, Samson T, Roos G, Reinhardt DP, et al. The conduit system transports soluble antigens from the afferent lymph to resident dendritic cells in the T cell area of the lymph node. *Immunity.* 2005;22(1):19-29. doi: 10.1016/j.immuni.2004.11.013. PubMed PMID: 15664156.
322. Gretz JE, Norbury CC, Anderson AO, Proudfoot AE, Shaw S. Lymph-borne chemokines and other low molecular weight molecules reach high endothelial venules via specialized conduits while a functional barrier limits access to the lymphocyte microenvironments in lymph node cortex. *J Exp Med.* 2000;192(10):1425-40. PubMed PMID: 11085745; PubMed Central PMCID: PMCPMC2193184.
323. Lerner TR, de Souza Carvalho-Wodarz C, Repnik U, Russell MR, Borel S, Diedrich CR, et al. Lymphatic endothelial cells are a replicative niche for *Mycobacterium tuberculosis*. *J Clin Invest.* 2016;126(3):1093-108. doi: 10.1172/JCI83379. PubMed PMID: 26901813; PubMed Central PMCID: PMCPMC4767353.
324. Basaraba RJ, Smith EE, Shanley CA, Orme IM. Pulmonary lymphatics are primary sites of *Mycobacterium tuberculosis* infection in guinea pigs infected by aerosol. *Infect Immun.* 2006;74(9):5397-401. doi: 10.1128/IAI.00332-06. PubMed PMID: 16926435; PubMed Central PMCID: PMCPMC1594862.
325. Kastenmuller W, Torabi-Parizi P, Subramanian N, Lammermann T, Germain RN. A spatially-organized multicellular innate immune response in lymph nodes limits systemic pathogen spread. *Cell.* 2012;150(6):1235-48. doi: 10.1016/j.cell.2012.07.021. PubMed PMID: 22980983; PubMed Central PMCID: PMCPMC3514884.

326. Voedisch S, Koenecke C, David S, Herbrand H, Forster R, Rhen M, et al. Mesenteric lymph nodes confine dendritic cell-mediated dissemination of *Salmonella enterica* serovar Typhimurium and limit systemic disease in mice. *Infect Immun*. 2009;77(8):3170-80. doi: 10.1128/IAI.00272-09. PubMed PMID: 19506012; PubMed Central PMCID: PMCPMC2715677.
327. Iannacone M, Moseman EA, Tonti E, Bosurgi L, Junt T, Henrickson SE, et al. Subcapsular sinus macrophages prevent CNS invasion on peripheral infection with a neurotropic virus. *Nature*. 2010;465(7301):1079-83. doi: 10.1038/nature09118. PubMed PMID: 20577213; PubMed Central PMCID: PMCPMC2892812.
328. Mustafa T, Wiker HG, Mfinanga SG, Morkve O, Sviland L. Immunohistochemistry using a *Mycobacterium tuberculosis* complex specific antibody for improved diagnosis of tuberculous lymphadenitis. *Mod Pathol*. 2006;19(12):1606-14. doi: 10.1038/modpathol.3800697. PubMed PMID: 16980944.
329. Knox J, Lane G, Wong JS, Trevan PG, Karunajeewa H. Diagnosis of tuberculous lymphadenitis using fine needle aspiration biopsy. *Intern Med J*. 2012;42(9):1029-36. doi: 10.1111/j.1445-5994.2012.02748.x. PubMed PMID: 22372860.
330. Tadesse M, Abebe G, Abdissa K, Aragaw D, Abdella K, Bekele A, et al. GeneXpert MTB/RIF Assay for the Diagnosis of Tuberculous Lymphadenitis on Concentrated Fine Needle Aspirates in High Tuberculosis Burden Settings. *PLoS One*. 2015;10(9):e0137471. doi: 10.1371/journal.pone.0137471. PubMed PMID: 26366871; PubMed Central PMCID: PMCPMC4569183.
331. Kirwan DE, Ugarte-Gil C, Gilman RH, Caviedes L, Rizvi H, Ticona E, et al. Microscopic Observation Drug Susceptibility Assay for Rapid Diagnosis of Lymph Node Tuberculosis and Detection of Drug Resistance. *J Clin Microbiol*. 2016;54(1):185-9. doi: 10.1128/JCM.02227-15. PubMed PMID: 26511739; PubMed Central PMCID: PMCPMC4702711.
332. Samstein M, Schreiber HA, Leiner IM, Susac B, Glickman MS, Pamer EG. Essential yet limited role for CCR2(+) inflammatory monocytes during *Mycobacterium tuberculosis*-specific T cell priming. *Elife*. 2013;2:e01086. doi: 10.7554/eLife.01086. PubMed PMID: 24220507; PubMed Central PMCID: PMCPMC3820971.
333. Marino S, Gideon HP, Gong C, Mankad S, McCrone JT, Lin PL, et al. Computational and Empirical Studies Predict *Mycobacterium tuberculosis*-Specific T Cells as a Biomarker for Infection Outcome. *PLoS Comput Biol*. 2016;12(4):e1004804. Epub 2016/04/12. doi: 10.1371/journal.pcbi.1004804. PubMed PMID: 27065304; PubMed Central PMCID: PMCPMC4827839.
334. Gideon HP, Skinner JA, Baldwin N, Flynn JL, Lin PL. Early Whole Blood Transcriptional Signatures Are Associated with Severity of Lung Inflammation in *Cynomolgus* Macaques with *Mycobacterium tuberculosis* Infection. *J Immunol*. 2016;197(12):4817-28. Epub 2016/11/12. doi: 10.4049/jimmunol.1601138. PubMed PMID: 27837110; PubMed Central PMCID: PMCPMC5289749.

335. Thompson EG, Shankar S, Gideon HP, Braun J, Valvo J, Skinner JA, et al. Prospective Discrimination of Controllers From Progressors Early After Low-Dose Mycobacterium tuberculosis Infection of Cynomolgus Macaques using Blood RNA Signatures. *J Infect Dis.* 2018;217(8):1318-22. Epub 2018/01/13. doi: 10.1093/infdis/jiy006. PubMed PMID: 29325117.
336. Mattila JT, Ojo OO, Kepka-Lenhart D, Marino S, Kim JH, Eum SY, et al. Microenvironments in tuberculous granulomas are delineated by distinct populations of macrophage subsets and expression of nitric oxide synthase and arginase isoforms. *J Immunol.* 2013;191(2):773-84. doi: 10.4049/jimmunol.1300113. PubMed PMID: 23749634; PubMed Central PMCID: PMC3746594.
337. Gong C, Mattila JT, Miller M, Flynn JL, Linderman JJ, Kirschner D. Predicting lymph node output efficiency using systems biology. *J Theor Biol.* 2013;335:169-84. doi: 10.1016/j.jtbi.2013.06.016. PubMed PMID: 23816876; PubMed Central PMCID: PMC3783027.
338. Coleman MT, Chen RY, Lee M, Lin PL, Dodd LE, Maiello P, et al. PET/CT imaging reveals a therapeutic response to oxazolidinones in macaques and humans with tuberculosis. *Sci Transl Med.* 2014;6(265):265ra167. doi: 10.1126/scitranslmed.3009500. PubMed PMID: 25473035.
339. Mattila JT, Beaino W, Maiello P, Coleman MT, White AG, Scanga CA, et al. Positron Emission Tomography Imaging of Macaques with Tuberculosis Identifies Temporal Changes in Granuloma Glucose Metabolism and Integrin alpha4beta1-Expressing Immune Cells. *J Immunol.* 2017;199(2):806-15. doi: 10.4049/jimmunol.1700231. PubMed PMID: 28592427; PubMed Central PMCID: PMC5520654.
340. Munoz-Elias EJ, Timm J, Botha T, Chan WT, Gomez JE, McKinney JD. Replication dynamics of Mycobacterium tuberculosis in chronically infected mice. *Infect Immun.* 2005;73(1):546-51. doi: 10.1128/IAI.73.1.546-551.2005. PubMed PMID: 15618194; PubMed Central PMCID: PMC538940.
341. Poulsen A. Some clinical features of tuberculosis. *Acta Tuberc Scand.* 1957;33(1-2):37-92; concl. PubMed PMID: 13424392.
342. Poulsen A. Some clinical features of tuberculosis. 1. Incubation period. *Acta Tuberc Scand.* 1950;24(3-4):311-46. PubMed PMID: 14783027.
343. Gasteiger G, Ataide M, Kastenmuller W. Lymph node - an organ for T-cell activation and pathogen defense. *Immunol Rev.* 2016;271(1):200-20. doi: 10.1111/imr.12399. PubMed PMID: 27088916.
344. Willard-Mack CL. Normal structure, function, and histology of lymph nodes. *Toxicol Pathol.* 2006;34(5):409-24. doi: 10.1080/01926230600867727. PubMed PMID: 17067937.

345. Lu LL, Suscovich TJ, Fortune SM, Alter G. Beyond binding: antibody effector functions in infectious diseases. *Nat Rev Immunol.* 2018;18(1):46-61. Epub 2017/10/25. doi: 10.1038/nri.2017.106. PubMed PMID: 29063907.
346. Kauffman KD, Sallin MA, Sakai S, Kamenyeva O, Kabat J, Weiner D, et al. Defective positioning in granulomas but not lung-homing limits CD4 T-cell interactions with *Mycobacterium tuberculosis*-infected macrophages in rhesus macaques. *Mucosal Immunol.* 2017. doi: 10.1038/mi.2017.60. PubMed PMID: 28745326.
347. Kaushal D, Foreman TW, Gautam US, Alvarez X, Adekambi T, Rangel-Moreno J, et al. Mucosal vaccination with attenuated *Mycobacterium tuberculosis* induces strong central memory responses and protects against tuberculosis. *Nat Commun.* 2015;6:8533. doi: 10.1038/ncomms9533. PubMed PMID: 26460802; PubMed Central PMCID: PMC4608260.
348. Chang KC, Leung CC, Yew WW, Ho SC, Tam CM. A nested case-control study on treatment-related risk factors for early relapse of tuberculosis. *Am J Respir Crit Care Med.* 2004;170(10):1124-30. Epub 2004/09/18. doi: 10.1164/rccm.200407-905OC. PubMed PMID: 15374844.
349. Daniel TM. The history of tuberculosis. *Respir Med.* 2006;100(11):1862-70. Epub 2006/09/05. doi: 10.1016/j.rmed.2006.08.006. PubMed PMID: 16949809.
350. Ganchua SKC, Cadena AM, Maiello P, Gideon HP, Myers AJ, Junecko BF, et al. Lymph nodes are sites of prolonged bacterial persistence during *Mycobacterium tuberculosis* infection in macaques. *PLoS Pathog.* 2018;14(11):e1007337. Epub 2018/11/02. doi: 10.1371/journal.ppat.1007337. PubMed PMID: 30383808; PubMed Central PMCID: PMC6211753.
351. Handa U, Mundi I, Mohan S. Nodal tuberculosis revisited: a review. *J Infect Dev Ctries.* 2012;6(1):6-12. Epub 2012/01/14. doi: 10.3855/jidc.2090. PubMed PMID: 22240421.
352. Catano JC, Robledo J. Tuberculous Lymphadenitis and Parotitis. *Microbiol Spectr.* 2016;4(6). Epub 2017/01/14. doi: 10.1128/microbiolspec.TNMI7-0008-2016. PubMed PMID: 28084205.
353. Mohapatra PR, Janmeja AK. Tuberculous lymphadenitis. *J Assoc Physicians India.* 2009;57:585-90. Epub 2010/03/10. PubMed PMID: 20209720.
354. Jawahar MS. Scrofula revisited: an update on the diagnosis and management of tuberculosis of superficial lymph nodes. *Indian J Pediatr.* 2000;67(2 Suppl):S28-33. Epub 2000/12/29. PubMed PMID: 11129904.
355. Wallgren A. The time-table of tuberculosis. *Tubercle.* 1948;29(11):245-51. Epub 1948/11/01. doi: 10.1016/s0041-3879(48)80033-4. PubMed PMID: 18101320.
356. Sarkar S, Jash D, Maji A, Patra A. Approach to unequal hilum on chest x-ray. *The Journal of Association of Chest Physicians.* 2013;1(2):32-7.

357. Converse PJ, Dannenberg AM, Jr., Estep JE, Sugisaki K, Abe Y, Schofield BH, et al. Cavitory tuberculosis produced in rabbits by aerosolized virulent tubercle bacilli. *Infect Immun*. 1996;64(11):4776-87. Epub 1996/11/01. PubMed PMID: 8890239; PubMed Central PMCID: PMCPMC174445.
358. Nedeltchev GG, Raghunand TR, Jassal MS, Lun S, Cheng QJ, Bishai WR. Extrapulmonary dissemination of *Mycobacterium bovis* but not *Mycobacterium tuberculosis* in a bronchoscopic rabbit model of cavitory tuberculosis. *Infect Immun*. 2009;77(2):598-603. Epub 2008/12/10. doi: 10.1128/IAI.01132-08. PubMed PMID: 19064634; PubMed Central PMCID: PMCPMC2632025.
359. Dorman SE, Hatem CL, Tyagi S, Aird K, Lopez-Molina J, Pitt ML, et al. Susceptibility to tuberculosis: clues from studies with inbred and outbred New Zealand White rabbits. *Infect Immun*. 2004;72(3):1700-5. Epub 2004/02/24. doi: 10.1128/iai.72.3.1700-1705.2004. PubMed PMID: 14977978; PubMed Central PMCID: PMCPMC356026.
360. Zhang J, Guo M, Rao Y, Wang Y, Xian Q, Yu Q, et al. *Mycobacterium tuberculosis* Erdman infection of cynomolgus macaques of Chinese origin. *J Thorac Dis*. 2018;10(6):3609-21. Epub 2018/08/03. doi: 10.21037/jtd.2018.05.189. PubMed PMID: 30069358; PubMed Central PMCID: PMCPMC6051865.
361. Sharpe S, White A, Gleeson F, McIntyre A, Smyth D, Clark S, et al. Ultra low dose aerosol challenge with *Mycobacterium tuberculosis* leads to divergent outcomes in rhesus and cynomolgus macaques. *Tuberculosis (Edinb)*. 2016;96:1-12. Epub 2016/01/21. doi: 10.1016/j.tube.2015.10.004. PubMed PMID: 26786648.
362. Walsh GP, Tan EV, dela Cruz EC, Abalos RM, Villahermosa LG, Young LJ, et al. The Philippine cynomolgus monkey (*Macaca fascicularis*) provides a new nonhuman primate model of tuberculosis that resembles human disease. *Nat Med*. 1996;2(4):430-6. Epub 1996/04/01. doi: 10.1038/nm0496-430. PubMed PMID: 8597953.
363. Dijkman K, Vervenne RAW, Sombroek CC, Boot C, Hofman SO, van Meijgaarden KE, et al. Disparate Tuberculosis Disease Development in Macaque Species Is Associated With Innate Immunity. *Front Immunol*. 2019;10:2479. Epub 2019/11/19. doi: 10.3389/fimmu.2019.02479. PubMed PMID: 31736945; PubMed Central PMCID: PMCPMC6838139.
364. Zhang J, Xian Q, Guo M, Huang Z, Rao Y, Wang Y, et al. *Mycobacterium tuberculosis* Erdman infection of rhesus macaques of Chinese origin. *Tuberculosis (Edinb)*. 2014;94(6):634-43. Epub 2014/09/17. doi: 10.1016/j.tube.2014.08.005. PubMed PMID: 25224753.
365. Sathkumara HD, Pai S, Aceves-Sanchez MJ, Ketheesan N, Flores-Valdez MA, Kupz A. BCG Vaccination Prevents Reactivation of Latent Lymphatic Murine Tuberculosis Independently of CD4(+) T Cells. *Front Immunol*. 2019;10:532. Epub 2019/04/06. doi: 10.3389/fimmu.2019.00532. PubMed PMID: 30949177; PubMed Central PMCID: PMCPMC6437071.

366. Mischenko VV, Kapina MA, Eruslanov EB, Kondratieva EV, Lyadova IV, Young DB, et al. Mycobacterial dissemination and cellular responses after 1-lobe restricted tuberculosis infection of genetically susceptible and resistant mice. *J Infect Dis.* 2004;190(12):2137-45. Epub 2004/11/20. doi: 10.1086/425909. PubMed PMID: 15551212.
367. Zhang Z, Liu Y, Wang W, Xing Y, Jiang N, Zhang H, et al. Identification of Differentially Expressed Genes Associated with Lymph Node Tuberculosis by the Bioinformatic Analysis Based on a Microarray. *J Comput Biol.* 2020;27(1):121-30. Epub 2019/08/29. doi: 10.1089/cmb.2019.0161. PubMed PMID: 31460784.
368. Maji A, Misra R, Kumar Mondal A, Kumar D, Bajaj D, Singhal A, et al. Expression profiling of lymph nodes in tuberculosis patients reveal inflammatory milieu at site of infection. *Sci Rep.* 2015;5:15214. Epub 2015/10/16. doi: 10.1038/srep15214. PubMed PMID: 26469538; PubMed Central PMCID: PMC4606593.
369. Kathamuthu GR, Moideen K, Sridhar R, Baskaran D, Babu S. Enhanced Mycobacterial Antigen-Induced Pro-Inflammatory Cytokine Production in Lymph Node Tuberculosis. *Am J Trop Med Hyg.* 2019;100(6):1401-6. Epub 2019/04/18. doi: 10.4269/ajtmh.18-0834. PubMed PMID: 30994092; PubMed Central PMCID: PMC6553923.
370. Rahman S, Gudetta B, Fink J, Granath A, Ashenafi S, Aseffa A, et al. Compartmentalization of immune responses in human tuberculosis: few CD8+ effector T cells but elevated levels of FoxP3+ regulatory t cells in the granulomatous lesions. *Am J Pathol.* 2009;174(6):2211-24. Epub 2009/05/14. doi: 10.2353/ajpath.2009.080941. PubMed PMID: 19435796; PubMed Central PMCID: PMC2684186.
371. Richter E, Feyerabend T. Normal lymph node topography : CT-atlas. Berlin ; New York: Springer-Verlag; 1991. xiii, 153 p. p.
372. Marais BJ, Gie RP, Schaaf HS, Hesselning AC, Obihara CC, Starke JJ, et al. The natural history of childhood intra-thoracic tuberculosis: a critical review of literature from the pre-chemotherapy era. *Int J Tuberc Lung Dis.* 2004;8(4):392-402. Epub 2004/05/15. PubMed PMID: 15141729.
373. Lorenzo-Redondo R, Fryer HR, Bedford T, Kim EY, Archer J, Pond SLK, et al. Persistent HIV-1 replication maintains the tissue reservoir during therapy. *Nature.* 2016;530(7588):51-6. Epub 2016/01/28. doi: 10.1038/nature16933. PubMed PMID: 26814962; PubMed Central PMCID: PMC4865637.
374. Licht A, Alter G. A Drug-Free Zone--Lymph Nodes as a Safe Haven for HIV. *Cell Host Microbe.* 2016;19(3):275-6. Epub 2016/03/11. doi: 10.1016/j.chom.2016.02.018. PubMed PMID: 26962938.
375. Fletcher CV, Staskus K, Wietgreffe SW, Rothenberger M, Reilly C, Chipman JG, et al. Persistent HIV-1 replication is associated with lower antiretroviral drug concentrations in lymphatic tissues. *Proc Natl Acad Sci U S A.* 2014;111(6):2307-12. Epub 2014/01/29. doi: 10.1073/pnas.1318249111. PubMed PMID: 24469825; PubMed Central PMCID: PMC3926074.